Municipal Solid Waste Incineration (MSWI) Bottom Ash - from waste to value

Characterization, treatments and application

Pei Tang

/ Department of the Built Environment

bouwstenen 234

Municipal solid waste incineration (MSWI) bottom ash - from waste to value

Characterization, treatments and application

Pei Tang

De promotiecommissie is als volgt samengesteld:

Voorzitter:	Prof. ir. E.S.M. Nelissen
Promotor:	Prof. dr. ir. H.J.H. Brouwers
Co-promotor:	Dr. Dipl. Eng. M.V.A. Florea
Leden:	Prof. dr. H. Justnes (Norwegian University of Science and Technology)
	Prof. dr. W. Chen (Wuhan University of Technology)
	Prof. dr. dr. H. Pöllmann (Martin Luther University of Halle-Wittenberg)
	Prof. dr. ir. N. De Belie (Ghent University)
	Prof. dr. ir. D.M.J. Smeulders

TU/e Technische Universiteit Eindhoven University of Technology

CIP-DATA LIBRARY TECHNISCHE UNIVERSITEIT EINDHOVEN

Municipal solid waste incineration (MSWI) bottom ash - from waste to value: Characterization, treatments and application/ by Pei Tang

A catalogue record is available from the Eindhoven University of Technology Library

ISBN: 978-90-386-4386-1

Bouwstenen 234

NUR 955

Ph.D. Thesis, Eindhoven University of Technology, the Netherlands

Cover design: Pei Tang

Cover photographs supplied by Attero b.v.

Printed by: ProefschriftMaken || Vianen

Municipal solid waste incineration (MSWI) bottom ash - from waste to value

characterization, treatments and application

PROEFSCHRIFT

ter verkrijging van de graad van doctor aan de Technische Universiteit Eindhoven, op gezag van de rector magnificus prof.dr.ir. F.P.T. Baaijens, voor een commissie aangewezen door het College voor Promoties, in het openbaar te verdedigen op donderdag 14 december 2017 om 14:00 uur

door

Pei Tang

geboren te Henan, China

Dit proefschrift is goedgekeurd door de promotoren en de samenstelling van de promotiecommissie is als volgt:

voorzitter:	prof.ir. E.S.M. Nelissen
promotor:	prof.dr.ir. H.J.H. Brouwers
copromotor(en):	dr.dipl.eng. M.V.A. Florea
leden:	prof.dr. H. Justnes (Norwegian University of Science and Technology)
	prof.dr. W. Chen (Wuhan University of Technology)
	prof.dr.dr. H. Pöllmann (Martin Luther University of Halle-Wittenberg)
	prof.dr.ir. N. De Belie (Ghent University)
	prof.dr.ir. D.M.J. Smeulders

Het onderzoek of ontwerp dat in dit proefschrift wordt beschreven is uitgevoerd in overeenstemming met de TU/e Gedragscode Wetenschapsbeoefening.

Preface

When I started to write the preface of this thesis, I felt one more step close to the end of my PhD period, all the memory rushed into my mind. It feels like just happened on yesterday, I cannot believe that I have left the Netherlands, the group and the University for more than half-year already. I remember clearly the night when I arrived at Eindhoven, the Netherlands, on 19th November 2011 and since then I studied and performed research in the Building Materials group of prof.dr.ir. H.J.H. (Jos) Brouwers in Eindhoven University of Technology until 31st, October 2016. It is a place where I stayed the longest besides my hometown. During the five-year PhD journey, there were happiness, challenges, struggles, pressure and motivations which fulfilled my life and work. To be honest, it was not easy at all for me to go through this period, no matter in life or in work. I never thought there would be that many challenges and difficulties to do research as a PhD candidate, it was completely different from knowledge learning as a student. This period gives me an impressive experience which will benefit the rest of my life. Fortunately, with the accompany and encouragement from the colleagues, friends and families, I am still motivated to try hard to reach the destination on pursuing a PhD degree. Therefore, I want to express my sincere acknowledgement to all these people.

First of all, I want to express my great thanks to my supervisor and promoter, prof.dr.ir. H.J.H. (Jos) Brouwers, who provided me the precious chance to join the Building Materials group in Eindhoven University of Technology to do my PhD research. It was deeply remembered in my mind of the first-time meeting in Wuhan in October 2010. How times flies. During the five-years PhD study under your supervision, you have paid great effort, time and energy to guide me how to be professional in research study. Your suggestions, comments and discussions promote the finishing of PhD research and my thesis, many thanks for your patience and help. I was so grateful that you spent such long time reading my thesis carefully, even during your traveling in Wuhan; and the comments you provided really improve the quality of my thesis. The discussion of the thesis page by page with you in Wuhan was so valuable. Furthermore, thank you for recommending me to prof. Poon Chi-sun in The Hong Kong Polytechnic University to continue my research after my PhD contract finished in October 2016.

My thanks also go to my daily supervisor and co-promoter, dr.dipl. Eng. M.V.A. (Miruna) Florea, for her effort and contribution during my PhD study. You have spent a lot of your time correcting my English and leading me into the research field of solid wastes, which significantly promotes the writing of my thesis. I can imagine that it was also not easy for you to supervise me when I had little background about solid waste at the beginning. Especially in the first year, I had so many questions to ask you and you were so patient to explain. I really appreciate what you have done and contributed during my PhD period, which has deep effect in my life. In addition, I would also like to thank dr. Qingliang Yu and dr.ir. P. Spiesz, who once co-supervised me, even though it was a short duration.

Within the two-weeks co-supervision, dr. Qingliang Yu helped to build up the first complete version of my thesis outline, and the suggestion on way of thinking for doing research really helped me a lot. Dr.ir. P. Spiesz gave very useful comments on the modification of my paper draft which were finally accepted and published. With the help, guidance, and suggestions from these three persons in daily work, I gained many useful skills related to research work.

My great appreciation goes to the Promotion Committee, prof.dr. H. Justnes (Norwegian University of Science and Technology), prof.dr. W. Chen (Wuhan University of Technology), prof.dr.dr. H. Pöllmann (Martin Luther University of Halle-Wittenberg), prof.dr.ir. N. De Belie (Ghent University), prof.dr.ir. D.M.J. Smeulders (Eindhoven University of Technology) for accepting to be members in my PhD committee. Their research outcomes and contributions in the fields of building materials and solid wastes provide valuable information and guidance during my PhD research, and I am grateful to have you as advisors in this stage.

I would also like to thank prof. Zhe'an Lu as my master supervisor and prof. dr. Wei Chen in Wuhan University of Technology. It was prof. Lu who advised me to do PhD in abroad and then brought me in contact with prof.dr.ir. H.J.H. (Jos) Brouwers, this suggestion opened a door to contact with completely new things and world. The encouragement prof. Lu have given motivated me to continue and overcame the difficulties I met in those years. I really appreciate the attitude you always told me: be happy and it is the most important thing in life. I start to understand what you mean and try to follow it to make life simple, easier and joyful. The talks with prof.dr. Wei Chen each time when we met in the Netherlands or Wuhan were so meaningful and enjoyable, I learned from you the manners of dealing things in work and life, which are very helpful.

I also appreciate the financial support of the Chinese Scholarship Council (CSC) and the sponsors of Building Materials group chaired by prof.dr.ir. H.J.H. (Jos) Brouwers in Eindhoven University of Technology. Furthermore, I would like to thank the additional support from Attero b.v. and Smals b.v., especially the partial financial and technical support in the fifth year of my research. There was a very nice cooperation on the project with Abdullah Cakir and Bas Nauts from Attero b.v., and Daphne Sijtsma, Maarten Smals and Harry Kouwenhoven from Smals b.v. The kindly help from Abdullah, Daphne, Maarten and Harry on the project significantly speeded up the finishing of my research on pelletization of solid wastes, the relevant work and outcomes make up one of the important parts of the thesis.

During my PhD research, all the technicians in the laboratory provided so much professional help, guidance and suggestion making my experiments efficient and successful, especially from ing. A.C.A. (Anneke) Delsing, H.L.W. (Harrie) Smulders, G.A.H. (Geert-Jan) Maas, P.H. Cappon, ir. H.M. (Hans) Lamers, ing. M.A.C.M. (Martien)

Ceelen, and ing. J.J.P. (Johan) van den Oever, who gave a lot of support in the lab in the last year when I had so many samples to test every day.

The building Materials group is such as large and international group, and is moving forwards rapidly under the leading of prof.dr.ir. H.J.H. (Jos) Brouwers. It is my great honour to be one member of it, and spent five years with my colleagues. The time we spent playing Frisbee and volleyball, charting at the coffee corner, sky bar and joining the conference, is a great memory for me. I still remember the first group dinner organized in my apartment, it was such a joyful party. These colleagues are: Alberto, Ariën, Arno, Azee, Bo, Chris, Florent, Gang, George, Guillaume, Hoss, Kaja, Kate, Katerina, Katrin, Miruna, Peipeng, Perry, Przemek, Qadeer, Qingliang, Rui, Štěpán, Veronica, Xu, Yuri, and Zhengyao. I also want to thank our BPS secretaries: Ginny, Léontine and Moniek. I am hoping to keep in touch with all of you in the future.

Part of this thesis work was finished with the assistance of the master student - Tamizhselvan Munuswamy, thank you for your help in this research. I hope my supervision was useful for your future career.

I would like to express my appreciations to all my friends in the Netherlands, Chinese and the Mrs. 'crazy', with who we had travelled around Europe, played sports and had parties. Some of you gave me a lot of support and encouragement when I was suffering, I appreciate a lot. Due to the very long list, I will not mention all the names here, to all of you: thank you so much and wish you all the best.

Finally, and the most importantly, my sincere thanks goes to my family, my parents and brother, and my aunts and uncles. Thanks for always supporting and encouraging me to go through the tough time in life, and being on my side. My every forward step and success, as well as this thesis, I dedicate to you.

Pei Tang

September 2017

Hong Kong, China

Contents

Chapter 1

1 Introduction

1.1 Municipal solid waste (MSW) management

Municipal solid waste (MSW) is a type of wastes consisting of daily items discarded as unwanted matter from human activities, which can be generally divided into several categories according to its source - domestic solid waste from households and public areas, commercial solid waste from restaurants, offices, and markets, etc., and industrial solid waste, such as sewage sludge from wastewater treatment plants and construction and demolition waste (CDW) (GovHK, 2015; Shekdar, 2009). Generally, the MSW consists of a compostable fraction (such as food waste), a combustible fraction (such as glass, plastics, paper and textiles), an inert fraction (such as stones, metals, glass and ceramics), as well as a water content which normally exists in the compostable fraction (Preda, 2007). The disposal of these solid wastes and their management have drawn attention widely, and awareness on the development of systematic recycling of these solid wastes has been risen recent years all over the word due to the following reasons. Firstly, these wastes contain recyclable materials, such as plastic, metals, etc. The direct disposal or landfill of these wastes is a wasting of potential resources to a certain extent. Secondly, the improper management of these wastes may cause the pollution of the natural environment, soil and water, etc., and consequently harm human beings. Thirdly but not last, the cost for the remediation of the pollution or unexpected damage of environment related to the waste disposal can be reduced significantly. Hence, proper waste management is of great need. In the Netherlands, pre-separations of glass, paper and plastic wastes are required by the government and then well conducted by the householders before they dispose their household wastes, which significantly enlarges the recycling of reusable resource. Some organic wastes are used for generating biogas through anaerobic digestion or gasification technology (EBA, 2017), and some wastes containing heavy metals which are harmful to environment are treated or sent for landfill, etc. The left municipal solid wastes are then sent to the relevant plants for further treatment and recycling in proper ways, such as being incinerated, which will be addressed in Section 1.2.

Regarding the management of the MSW, the main guiding principle is reduce, reuse and recycle (3R) which became executed gradually since the 20th century in European countries (Preda, 2007). Due to the early and fast development of the economy and then lack of resource and space in many European countries, the waste management system also has been first developed in EU countries (EPA, 2017; EEA, 2013). The way of managing these wastes includes landfill, composting, incineration, etc. The main management types of

solid wastes in the 28 EU member states since 1995 to 2015 were collected and published, and the changes of managements have been summarized and shown in Figure 1.1 (Eurostat, 2017). It depicts that landfilling was the dominant way to manage these solid in 1995 in these countries, however, this is in continuous decrease since then, while the incineration and composing as waste management have a dramatic increase, with a great growth of recycling of wastes. As landfilling of solid wastes can only store waste temporarily, meanwhile, the generation of harmful gas and leachate also generates secondary pollution to the surroundings (Calder & Stark, 2010). Moreover, the land space in most countries is limited, such as in many EU countries, and also in Singapore, Japan, Hong Kong, etc. Hence, the landfilling of wastes is generally avoided, only used when there is no other option (Karanjekar et al., 2015). Beside landfilling, the wastes containing high organic content could be treated through waste composting technique, which is a biological process mainly used to deal with organic wastes for anaerobic or aerobic decomposition and the resulted product can be used as soil fertilizer (Soares et al., 2016; Woon & Lo, 2016; Zhang et al., 2013), or co-generated biogas which can be used as fuel.

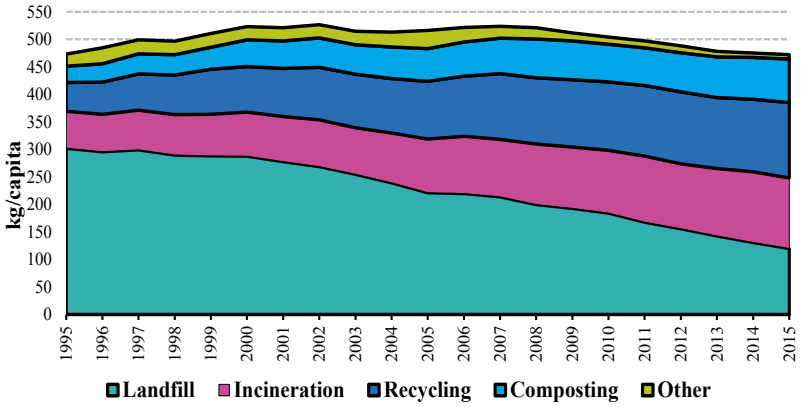

Figure 1.1: Municipal waste treatments in 1995-2015 (Eurostat, 2017)

The recycling of solid wastes is a direct way to minimize their amount and cost spent on the solid waste management, which meanwhile could enlarge the resource conservation. The recyclable wastes include glass and metals (Kaya, 2016), plastics (Pivnenko et al., 2016; Vazquez & Barbosa, 2016), paper (Pivnenko et al., 2015), etc. and relevant sorting techniques (Gundupalli et al., 2017) are developed in order to recycle these wastes effectively, which on one hand enlarge the recycling level, and on the other hand reduce the labour needed, especially for developed countries.

The incineration of MSW is used widely nowadays as a waste-to-energy (WtE) technique, and is well developed, particularly in developed countries. The MSW incineration (MSWI) can reduce the volume and mass of solid wastes by around 80-90% which reduce the need for landfill significantly; moreover, heat can be generated during the incineration process

which can be used to produce electricity (Brunner & Rechberger, 2015). The MSWI is adapted as a dominant treatment of solid waste in most of the developed countries, and in recent years, in the developing countries as well (Abd Kadir et al., 2013; Li et al., 2015). It was reported that the number of incinerators is around 220 in mainland China until 2015, which has increased by 1.4 times since 2009 (NBS, 2015).

1.2 Municipal solid waste incineration (MSWI)

As mentioned above, MSW incineration (MSWI) is widely used and is considered as an effective way to deal with the municipal solid wastes on reducing waste mass and volume. In addition, during the incineration of MSW, energy in the form of heat is produced which can be used for heating or electricity production; hence, MSWI is also called Waste-to-Energy (WtE) technique. However, it is not a complete win-to-win strategy due to the generation of the by-products in the incineration plants, such as MSWI bottom ash, fly ash, air pollution control ash, etc. (Van der Sloot et al., 2001). As shown in Figure 1.1, the number of incinerators is increasing in developed countries; similar trend is now found in developing countries (NBS, 2015), and the importance of MSWI also generated increasing awareness in recent years in developing countries. Subsequently, the amount of incineration residues grows dramatically and the management of these by-products is becoming a challenge on the sustainable development of resources and energy.

The Netherlands is far ahead on the municipal solid waste management and incineration system, where MSWI residues are classified according to its national legislation (SQD-Soil Quality Decree, 2013) based on its leaching behaviours and requirements of environmental protection. Moreover, the residues are disposed in proper ways, such as landfilling or using in road base. The MSWI bottom ash as the dominating by-product in WtE plants is mainly used in road base covered with the isolation layers to avoid its pollution potential to the surrounding environment (Born & Veelenturf, 1997). However, the intensively recycling and use of MSWI residues are in great demand nowadays, especially in the Netherlands. This is attributed to the raising awareness of environmental protecting and circular development of resources, particularly in developed countries. Hence, in the Netherlands, the government is promoting the further research on the MSWI residues for better application and deeper recycling by increasing the tax fee for landfilling of solid wastes and eventually forbidding landfill completely; meanwhile, a ‘greendeals’ (GD 076, 2010) program was established to help the implement of the sustainable plans. Therefore, an intensive research on the MSWI bottom ash is started on the purpose of its further recycling and application than the current low-grade way.

1.3 Mortar and concrete

Mortar and concrete are composite materials consist cementitious binders, additives and aggregates, and are widely used for construction elements (Sandor, 1992). Figure 1.2 shows the ingredients used for concrete and their size classifications (Hüsken, 2010).

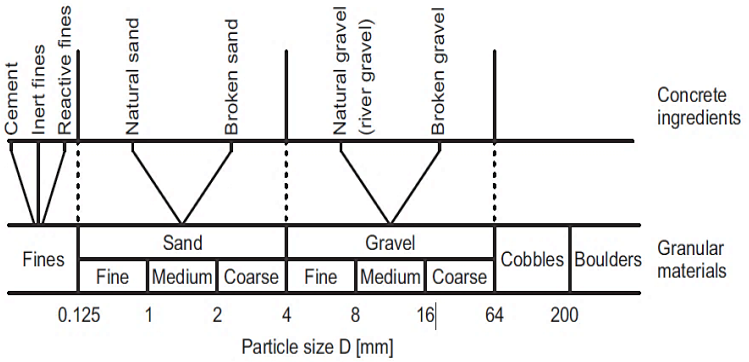

Figure 1.2: Size classes used for the denomination of granular materials and concrete ingredients (Hüsken, 2010)

The cementitious binder is a powdered material with the ability to bind the other composites (such as sand and gravel) to form a hardened element in the designed shape. Ordinary Portland cement (OPC) is the most common cement type in building construction; it is reported that around 4180 million tonnes of cement was produced worldwide in 2014 (Hendrik, 2015). The production of cement starts with the burning of limestone and clay at 1450 ºC in a kiln to obtain clinker, followed by a grounding process of the clinker until the desirable particle sizes of powder is obtained. This process is high energy consumption and CO_2 emission, which is causing environmental pollution (Wilson, 1993). The reactive fines are normally added to cement as supplementary cementing materials (SCMs) to provide additional contribution to the properties of the mortar or concrete, such as silica fume which is a by-product from silicon alloys production and mainly contains amorphous silicon dioxide, ground granulated blast furnace slag (GGBS) from steel factory and pulverized fly ash (PFA) from power plant burning coal (Taylor, 1997). Filler materials which have no hydration properties are also added to mortar or concrete mix as binder substitute in a certain amount to lower the cost of product. The proper application of these SCMs in mortar and concrete can reduce the amount cement used without causing significant effect on their properties. Aggregate is a particular material bound by cement to form mortar or concrete, which normally makes up around 60-80% of the mortar or concrete mix. It can be divided as fine aggregate (sand fraction, below 4 mm) and coarse aggregates (above 4 mm, gravel) according to its particle size in EN 12620 (2002). The mostly used aggregate in concrete field is from natural source after the crushing, washing and sieving procedure in factory. Nowadays, the application of recycled aggregates from mining industry, recycling industry of demolished construction materials, etc. as natural aggregates replacement in mortar or concrete have been widely investigated, considering the sustainable development of environment and resource (Kou et al., 2011).

1.4 Research aim and strategy

Currently, studies on MSWI residues are widely reported; however, the research is mainly focused on the coarse fraction including treatments and applications, while the fine fractions which have more issues are not so thoroughly investigated. The aim of this study is to have a systematic and in-depth study on the MSWI bottom ash from two WtE plants in the Netherlands, especially the fine fraction (0-2 mm), and to find a proper recycling way based on its application purpose as ingredients of building materials (such as binder, sand, gravel, etc.). The main work is divided into the following steps:

(1) The stability of MSWI bottom ash properties are evaluated by analysing 7 years' historical data.
(2) The potential application fields for MSWI fine bottom ash are estimated experimentally.
(3) Treatments on MSWI fine bottom ash are carried out focusing on increasing its reactivity and reducing its leaching properties.
(4) The integral recycling of MSWI fine bottom ash combining of its application and treatment are investigated.

Eventually, the integral treatments on MSWI fine bottom ash on the purposes of improving its mechanic properties and reducing its negative environmental impact are provided, and a granular artificial lightweight aggregate using MSWI fine bottom ash is produced which can be used as supplementary aggregates in concrete. Subsequently, a closed recycling loop of MSWI fine bottom ash is obtained.

1.5 Outline of the Thesis

To conduct an in-depth and systematic study on the MSWI bottom ashes from WtE plants in the Netherlands for guiding their application in future, several series of experimental work have been carried out, including the characterization, treatments and application of MSWI bottom ash. Subsequently, part of this thesis focuses on the small MSWI bottom ash fraction (0-2 mm), which has more issue compared with big MSWI bottom ash fraction. The relevant research results are summarized and presented in this thesis, and the research outline is shown in Figure 1.3. An explanation of the content in each chapter is given in the following paragraphs.

Chapter 2 summaries the research studies which have been performed on municipal solid waste (MSWI) bottom ash, including characteristics, treatments and application conditions in the construction field. Moreover, the two waste-to-energy plants involved in this research are described.

Chapter 3 describes the experimental methods used in this study for the characterization of the MSWI bottom ashes, including particle size distribution (PSD), water content and water absorption, densities, loss on ignition (LOI), metal content determination, as well as tests

for determination of chemical properties, such as chemical composition by X-ray fluorescence (XRF) and crystalline phases detection by X-ray diffraction (XRD). The environmental impact of the MSWI bottom ashes were evaluated by column leaching test according to the Dutch standards NEN 7383 (2004) and 7 years' leaching data on MSWI bottom ashes are collected and summarized. The fine MSWI bottom ashes are used as sand and binder replacement in mortar. The aim of this chapter is to evaluate the stability of the properties of the MSWI bottom ashes from the two WtE plants and to estimate the application potential of fine bottom ashes in mortars.

Chapter 4 presents the thermal treatment on fine MSWI bottom ash combined with low speed milling. The treated fine bottom ashes are used as binder substitute in mortars. Then, the influence of the treated fine bottom ashes on the binder hydration are evaluated. The leaching properties of the treated fine bottom ashes are estimated and compared with the Dutch legislation. The aim of this chapter is to investigate the influence of thermal treatment on the fine bottom ash with regard to increasing activity, separating metallic aluminium and improving leaching properties.

Chapter 5 shows the leaching behaviour of fine bottom ash originally and after milling into powder. The binding capacity of blended binders (Ordinary Portland cement, ground granulate blast furnace slag, and coal fly ash) of chlorides and heavy metals are investigated. This can be divided into two parts: (1) the binding capacity of chloride from adding NaCl in mortars or binder pastes; (2) the binding capacity of blended binder in mortars when fine bottom ash is used as sand. The main aim of this chapter is to qualify and quantify the leaching behaviours of bottom ash regarding its application purposes and the bind capacity of blended binders on fine bottom ash during its application in mortars.

Chapter 6 describes an integral method to recycle fine MSWI bottom ash, in combination of the other industrial solid wastes through a pelletizing technique. As a trial study, the compatibility of using mixed industrial solid wastes to produce cold bonded artificial aggregates (CBLAs) by pelletization is investigated. The aim of this chapter is to evaluate the possibility of recycling fine MSWI bottom ash by pelletization combined with the function of stabilization of binders.

Chapter 7 addresses several methods to improve the properties of the produced CBLAs. The parameters including binder content, industrial solid wastes combinations, fibre reinforcement, etc. on the CBLAs' properties are evaluated. Finally, CBLA with higher crushing resistance and lower bulk density can be obtained.

Chapter 8 shows the concrete properties containing CBLAs. Three types of CBLAs are used as natural aggregate replacement in self compacting concrete, and the fresh and hardened properties of the concretes are tested. The influence of CBLAs on the durability of concretes are evaluated using freeze thaw resistance tests.

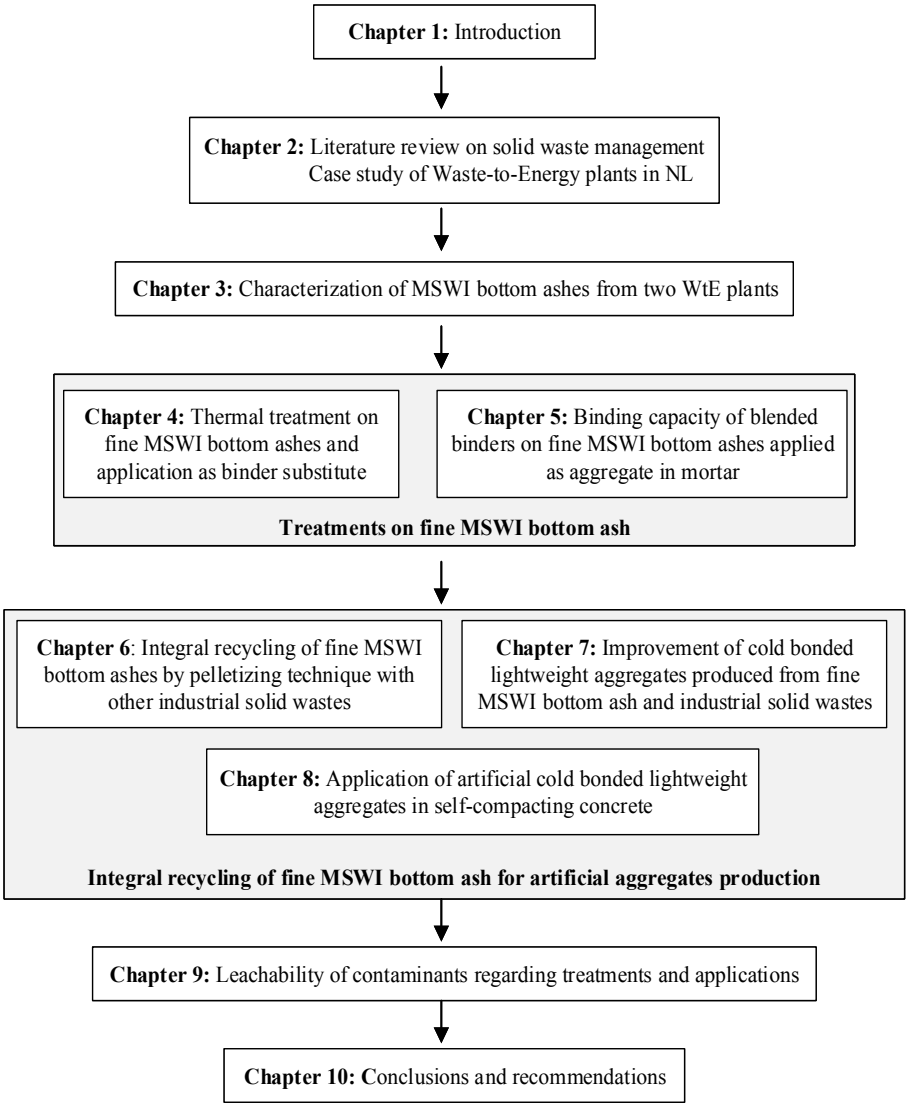

Figure 1.3: Outline of the thesis

Chapter 9 assesses the leachability of contaminants (Sb, Cu, Mo, chloride and sulphate) of fine MSWI bottom ash, regarding the influence of treatments and application methods, such as thermal and washing treatments, application as binder and sand replacement in mortar, use for artificial aggregate production and application of artificial aggregates in concrete.

Chapter 10 summarizes the conclusions of the current thesis and recommendations for future research as continuation of the present work.

Chapter 2

2 Solid residues from MSWI and their management

2.1 Introduction

In recent years, the Waste-to-Energy (WtE) technique in the form of incineration is reported to be an efficient way to deal with the increasing amount of municipal solid wastes (MSWs) worldwide (Leckner, 2015; Stehlík, 2009). The incineration reduces the mass and volume of the solid waste dramatically (Wiles, 1996), thus the requirement for landfilling is decreased (Bosmans et al., 2013). Moreover, energy in the form of heat, electricity, etc. can be recovered from incineration (Cimpan & Wenzel, 2013), which can bring financial benefits. Therefore, it is widely applied and used, especially in developed countries. More and more municipal solid waste incinerators have been and are going to be built world-wide, especially in developing countries where the generation of MSW had a rapid increase in recent years. However, despite the benefits WtE bring, one of the downsides is the considerable amount of solid residues generated, typically incineration bottom ash (IBA), incineration fly ash (IFA), boiler ash, etc., of which IBA accounts for about 80% of the total solid by-products in a WtE plant (Chimenos et al., 1999).

The traditional disposal method for these solid residues from incineration is landfilling, during which the leachate and gas generation need to be monitored for environmental protection (Klein et al., 2001). However, the disadvantages from the landfilling of incineration residues are gradually getting attention. Firstly, the incineration residues contain contaminants which are considered harmful when leaching into the environment (Meima & Comans, 1999); secondly, the degradation of organic matter and the reaction of metals in an alkaline environment may generate gas and eventually cause the expansion and collapse of the landfill sites (Kowalski et al., 2016; He et al., 2015); thirdly, from the sustainable development point of view, it is a waste of potential resource, due to the fact that these residues have very similar properties as building materials, such as aggregates (Van der Sloot et al., 2001); and last but not least, the available space for landfill is getting less with the expansion of economic development all over the world, and governments are trying to reduce landfilling by increasing tax and establishing new legislation (Abd Kadir et al., 2013; Liu et al., 2015). For instance, the Dutch government is planning to prohibit the landfilling of IBA completely by 2020, which means new disposal methods for the incineration residues is urgent and necessary (Greendeals GD 076, 2010).

To explore the potential of better disposal methods, plenty of research studies have been done on MSWI residues, including characterization, treatments and applications (Lam et al., 2010). Moreover, the environmental legislation regarding the local requirement of each

country has been established to limit the disposal of these incineration residues on behalf of the environment and human health (Saner et al., 2011).

In this chapter, two WtE plants in the Netherlands, from which the MSW IBAs are obtained in the following research study, are introduced and described briefly. Additionally, to have an in-depth understanding of the current research status on incineration residues, the research studies on MSWI residues, especially bottom ash (IBA), are summarized.

2.2 Two Waste-to-Energy (WtE) plants in the Netherlands

In this study, there are two WtE plants involved, which are located in Wijster and Moerdijk, respectively, in the Netherlands. Figure 2.1 shows the procedure in a typical WtE. The WtE plant in Wijster started to be in operation in 1996, and includes three parallel processing lines with an annual capacity of around 800,000 tonnes of solid waste. The WtE plant in Moerdijk is in operation since 1997 and the incinerator capacity is around 1,000,000 tonnes. Differently from Moerdijk, the Wijster plant has the pre-separation of metals, paper and plastic, while in Moerdijk, the solid waste is mixed and directly incinerated.

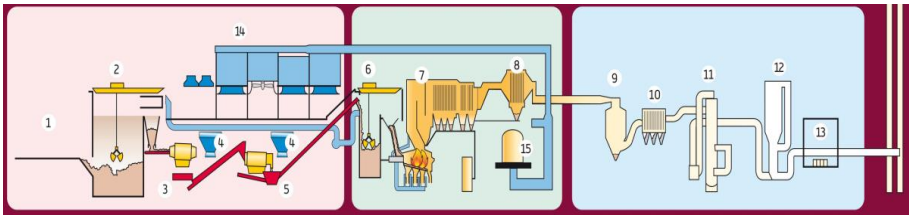

Figure 2.1: The schemic representation of WtE plants in Wijster (1:discharge hall; 2: coarse filling bunker; 3&5: sieve drum; 4: air separator; 6: filling bunker; 7: inicineration boiler; 8: electro filter; 9: spary drier; 10: fabric filter; 11: acidic and neutral washers; 12: oxycat unit; 13: flue gas control; 14: air-cooled condenser; 15: turbine/generator (Attero b.v.)

2.2.1 The WtE plant process

- **Pre-separation of raw solid wastes (only in Wijster)**

The pre-treatment of the collected municipal solid waste starts with the size reduction using rotating sieve drums with holes. The size of holes on the first drum is 190 mm; waste which cannot pass through the holes is blown away by the air separator, so large non-recyclable paper and plastic parts are removed from the waste and then are pressed into big cubes which can be used as fuel for power plants and the cement industry.

The rest of the waste is send to the second drum which has 45 mm holes. There is a rotating drum above the conveyor belt with steel pins called film separator; when the waste from the sieve drum travels on the belt, soft plastics and plastic films can be taken out by the pins. The hard and rigid plastic can be recognized by the infrared equipment fixed above

the belt, which then sends a signal to the computer and the computer controls the action of the blow nozzles at the end of the belt to blow the plastic out of the waste.

These plastics removed from the waste can be used as substitute fuel. The wet part passed from the second drum mainly contains organic matter, sand, stone, and glass. The organic part is sent to the fermentation plants for the generation of green gas and composting. The residue of the waste is sent to the next bunker before being incinerated.

- **Combustion and energy recovery**

The waste is sent to the incinerator by the feeding tube, and air from the storage bunker is pushed into the incinerator in order to reduce the smell in the WtE plants. After burning, the material is transported into a container with water, in which the material is quenched and slag can be removed from the material. After that, the quenched material is stored in the bunker before the separation. The heat in the boiler produces high pressure steam which is used for generating electricity. There are steel tubes around the wall of the boiler with water running inside. The temperature of the boiler is between 1000 and 1300 ºC, which is high enough to turn water into steam with high pressure and temperature because of the closed system. This steam can pass through the turbine blades to generate electricity for the company itself and the public. It can also be used for the heating of the nearby residents.

After the burning of the waste there is still solid matter left, called ash or slag. This material is sent to the treatment of separating the ferrous and non-ferrous parts which can be reused in the metal industry.

- **Separation/recycling of metals from original IBA**

The water-quenched bottom ash contains an unburned fraction, and ferrous and non-ferrous fractions which need to be removed to upgrade the bottom ash. The quenched bottom ash is stored for 6-8 weeks and then sent to the separation line. The material put on the moving belt goes through a magnet which is fixed above the running belt, thus the ferrous fraction in the material is removed and sent to storage before reuse. The belt sends the left material to the eddy current separator to remove the non-ferrous fraction. After the separation of ferrous and non-ferrous metals, the leftover bottom ash is much cleaner and contains fewer metallic parts which are not wanted. The ferrous and non-ferrous materials are stored for further use or sold to recycling companies.

- **Flue gas and waste water cleaning**

There are gas and waste water generated during the incineration procedure from the incinerator and the cleaning of flue gas. They contain contaminants which can be harmful to ground water and air, and therefore need to be cleaned before release back in the environment. The flue gas from the incinerator is blown to the electrostatic filter, where the dust in the gas can be picked up which is named incineration fly ash. The next cleaning step is performed in a huge ‘multi-stage wet scrubber’ where the flue gas is washed by the

water shower; after that hydrochloric acid, heavy metals and sulphur dioxide are left in the water. The treatment setup of gas consists of spray drier, fabric filter, acidic and neutral washers, electrostatic precipitator, and ammonia injecting. The cleaned flue gas is released from the high chimney using a vacuum-draft fan. The gas is continuously tested and monitored. The waste water used during the whole process needs to be treated; during the treatment process gypsum and chemical contaminated filter cakes are obtained. The gypsum can be reused and filter cakes can be sent to special landfills.

2.3 The solid residues from MSWI

2.3.1 The incineration residues

- **Incineration bottom ash (IBA)**

The IBA is generated at the incinerator gate and then send to the water tank for cooling down. After the separation of ferrous and non-ferrous matter, the stony solid left accounts for around 70-80% of the total residues generated in the WtE plant; the other 20-30% of the solid wastes in the WtE plant are fly ash and air pollution control residues. Figure 2.2 shows the MSWI bottom ash received from the WtE plant in Wijster, which has a particle size of 0-31.5 mm. It can be seen that it contains stony granulates, ceramics, unburned matters, and the granulates are covered by a dust layer. Normally, there is also remining metals found in bottom ash, which is not recycled sufficiently by the magnetic and eddy current separators.

Figure 2.2: The MSWI bottom ash

- **Incineration fly ash (IFA)**

Incineration fly ash is collected from the bag separator (Figure 2.1 (8)) which is much finer than bottom ash, and has a particle size under 250 µm. It is reported that this fraction contains very high amounts of heavy metals and in most of the countries it is treated as hazardous materials which cannot be used except in special landfills and treatments (Del Valle-Zermeño et al., 2013).

- **Air pollution control (APC) residues**

The APC residues are produced due to the cleaning of waste gas from the combustion process. They are classified as hazardous materials according to environmental legislation due to their high content of heavy metals (Amutha Rani et al., 2008).

2.3.2 The relevant research studies on MSWI bottom ash

To investigate the potential applications of MSWI bottom ash in the construction field, plenty of research studies have been performed, including the characterization, treatments, related environmental legislations and applications of bottom ashes from different countries.

- **Characterization**

Figure 2.3 summarizes the research aspects performed on the characteristics of the MSWI bottom ash.

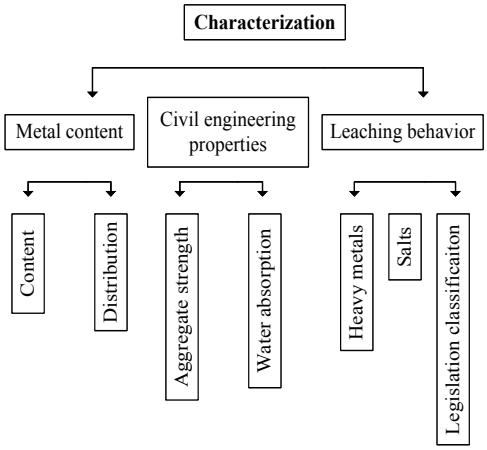

Figure 2.3: The research aspects related to the characterization of MSWI BA

- *Physical and chemical properties*

Chimenos et al. (1999) studied the properties of MSWI bottom ash (> 1 mm) and identified its main components; meanwhile, the distribution of heavy metals in the bottom ash collected in Spain was identified. The relevant MSWI bottom ash studied was a heterogenous stony material, and the metal content was mainly concentrated in fraction 1-6 mm; the heavy metals were concentrated in bottom ash particles under 1 mm, while glass particles were mostly found in fraction 4-6 mm, which was assumed due to the breakage mechanical system or thermal shock. Li et al. (2004) characterized the solid residues from two municipal solid waste incinerators in Shenzhen, mainland China. It was figured out that the bottom ash was more heterogeneous than incineration fly ash, and the leaching of

heavy metals from bottom ash was less than incineration fly ash and it could be landfilled directly.

The study on the chemical and mineralogical properties of one MSWI bottom ash from Germany by Bayuseno & Schmahl (2010) showed that the mineral phases in fresh bottom ash are not stable and they tend to transfer into stable phases during the aging process, and ettringite and a C-S-H (calcium silicate hydrate) phase may form during this process, which help the binding of the heavy metals. Hence, natural weathering is a prospective method to reduce the leaching potential of contaminants from MSWI bottom ash.

- *Metal contents and their recycling*

There are ferrous and non-ferrous metals in the MSWI bottom ashes, which are sources worth to be recycled from both economic and environmental aspects. The ferrous metals in the MSWI bottom ashes in general are recycled by electrical magnetic separators in most of the incineration plants, and eddy current separators are applied to recycle the non-ferrous metals. The distribution and content of the metals in the MSWI bottom ashes vary in different countries, and are related significantly to the life style and recycling conditions of the country. Hence, research studies have been done on the distribution and recycling of metals from MSWI bottom ashes.

Kuo et al. (2007) studied the metal recovery potential from MSWI bottom ash, fly ash, sludge and flue gas from Taiwan, R.O.C., and found that the majority of metals in bottom ash are Fe, Al, Cu, Zn, Cr, and Pb. Xia et al. (2017) investigated the distribution of metals in a MSWI bottom ash from mainland China and evaluated the recovery potential of the metals. It was pointed out that the metal content in the MSWI bottom ash from Shanghai is lower than that from developed countries. The Al was mainly concentrated in particles bigger than 20 mm and in particles 5-20 mm, which originated from aluminium can scrap and around 50-57% wt. of the Al was found in particles under 5 mm. The ferrous metals were found evenly distributed in the bottom ash fractions and lower amount of ferrous metals was in fraction 5-10 mmm, which is around 11-23 g/kg wt. of bottom ash; and around 56-75% of Fe was cumulated in particles under 5 mm. It was also noticed that the Fe exists in the form of hematite (Fe_2O_3), which is difficult to be separated by a general magnetic separator. The content of copper and zinc in the MSWI bottom ash was lower than that of Al, and they were mainly accumulated in fine fractions (such as particles smaller than 5 mm). The Cu in MSWI bottom ash was mostly combined with organic matter and Zn was mainly bound to carbonate fractions, while the content of metallic Zn in bottom ash was rather marginal. It was suggested that the Cu and Zn recovery should rely on advanced separation methods rather than common eddy current separation, such as gravity separation for Cu and acid extraction for Zn, respectively. Even though the content of metals in the MSWI bottom ashes from mainland China is lower than that from other countries, it was suggested to recycle them for saving sources.

Allegrini et al. (2014) carried out a detailed study on the MSWI bottom ash from a full-scale facility in Denmark focusing on the quantification of recoverable resources and the efficiency of the established recovery facility. It was reported that the recycling of non-ferrous metals from the fine bottom ash particles should be more focused on in future studies and the pre-sorting of waste before incineration would be a possible method to recover the metals in bottom ash to avoid the oxidation of metals. The other valuable and critical metals were too low to be further recovered from an economic aspect. Plenty of research has been performed on the recycling of non-ferrous metals such as aluminium, including quantification and qualification (Hu et al., 2011; Grosso et al., 2011; Biganzoli et al., 2012), enhanced recycling technique (Rahman & Bakker, 2013), energy generation potential (Biganzoli et al., 2013; Saffarzadeh et al., 2016), etc. due to the fact that the non-ferrous particles in the MSWI bottom ashes are more difficult to be recycled compared with ferrous ones, and in general they would cause more serious deterioration on the products during application. It was concluded that the oxidation of metallic aluminium during the incineration and water quenching process hinders its recycling efficiency. An enhanced eddy current separator is necessary for the metallic Al recovery from fine bottom ash fractions, or the metallic Al can be used as resource for hydrogen production, while this depends on how much available metallic Al in the bottom ash fractions.

- *Heavy metals and salts*

Yao et al. (2010a) explored the heavy metal content and their distribution in MSWI bottom ashes based on the samples collected from six cites of Zhejiang Province in mainland China. Their results demonstrated that the major heavy metals in these bottom ashes were Zn, Cu, Cr, Mn and Pb, higher than 300 mg/kg; and there was a high variation of the heavy metals contents in bottom ashes, which was attributed to their contents in the input municipal solid wastes. Yao et al. (2013) also studied the heavy metals, such as Cu, Zn and Cd, based on the particle size of the MSWI bottom ash. It was reported that Cu was mainly distributed in particles smaller than 0.45 mm and bigger than 4 mm, while Zn was evenly distributed; Cd had a decreased trend with the increase of particle size. The organic matter bound Cu and carbonate bound Cu increased with the increasing of particle size, and large ash particles had higher contents of unstable Cu.

The leaching behaviours of heavy metals in MSWI bottom ash related to pH and time were investigated (Dijkstra et al., 2006). It was reported that the leaching of Al was significantly related to three minerals which were gibbsite, gypsum and ettringite, while the leaching of Ca at pH 4-8 could be described by the dissolution of gypsum, and by calcite at pH 8-12. Sulphate leaching showed pH independent behaviour, and gypsum solubility controlled the sulphate leaching at pH 4 and 8. Dissolved organic carbon (DOC) was relatively independent of pH and contained mainly humic acid (HA) and fluvic acid. The Cu leaching could be described by the surface complexation to Fe- and Al(hydr)oxides. The leaching of Ni at pH 4 to 8 was time dependent, and Zn leaching could be described by surface

precipitation model under a large range of pH. The long term static immersing leaching test conducted by Liu et al. (2008) showed that the leaching of Pb and Cu was solubility controlled, which was in line with the results reported by others, even though different leaching tests were applied; and the Cu leaching was related to the dissolved organic carbon (DOC) in the bottom ash. The application of MSWI bottom ash as aggregate replacement in hot mixed asphalt and Portland cement concrete (Roessler et al., 2015) demonstrated that the elements in the monolith form had limited mobility and the Portland cement system had better immobilization capacity than hot mixed asphalt.

- **Environmental legislations**

Due to the fact that the MSWI bottom ash contains heavy metals and has the potential to leach into the environment surrounding, the reuse of bottom ash as secondary materials in construction fields is limited. To guide the disposal of MSWI bottom ashes in a safe way, environmental legislation was established according to respective conditions of different countries. The legislation provides disposal suggestions based on the leaching properties of the investigated MSWI bottom ash, and the various leaching tests are used accordingly. The principles of the environmental legislation normally focus on the protection of water, soil, or reducing the amount of waste, etc. (Liu et al., 2015). To qualify the category of a solid waste according to relevant standards, there are two aspects involved - the limit level of leached elements and the testing methods. The dominant leaching tests applied are the shaking test and the column test, with the relevant and required liquid to solid ratio (L/S), pH of solution, testing time, etc. which is a simulation of the real conditions in practice.

Table 2.1 shows the leaching limits in the Dutch legislation. In the Netherlands, the environmental legislation - Soil Quality Decree (SQD, 2013) has the purpose of protecting the soil and groundwater. This legislation specified the requirement for using the stony waste materials in construction. Depending on the leaching behaviours, the investigated materials are divided into three categories - shaped, non-shaped and IMC (Insulation, Management, Control) construction materials.

The MSWI bottom ash undergoes column leaching test according to NEN 7383 (2004), which simulates the leaching of inorganic components from the bottom ash in an aerobic environment as a function of the L/S (0.1-10), and the cumulative leaching for the L/S of 10 l/kg is determined. The sample is firstly dried and crushed to under 4 mm and then put into the vertical column (5 cm diameter and length > 20 cm). Demineralised water (pH≈ 7) flows through the column from bottom to top at a low speed and this procedure may take around three weeks until the L/S 10 is reached. Then the eluate is collected to be tested including pH, electronic conductivity, and concentration of components. If the concentrations of investigated components do not exceed the limit values shown in Table 2.1 (column 3), then the tested materials could be used as non-shaped materials in the construction field; if the concentrations of components do not exceed the values in column

four, then this material could be used, but isolated from the surrounding environment and the monitoring of its leaching during its life cycle is required. The limit values in column 2 are for the moulded and monolithic materials being tested according to the diffusion tested described in NEN 7375 (2004). The tested products are immersed in demineralised water for 64 days, the liquid to volume ratio is 2-5 l/l product volume. The demineralised water is renewed after 6 hours and 1, 2.25, 4, 9, 16, 36 and 64 days after the test started. After 64 days, the pH, electronic conductivity, and concentration of components of the leachate are determined and the leaching result is expressed in mg/m^2.

Table 2.1: The leaching limits according to the Dutch legislation - Soil Quality Decree (2013)

Elements (1)	[1] Shaped [[4] ε_{64} in mg/m^2] (2)	[2] Non-shaped [[5]mg/kg d.m.] (3)	[3]IMC building material [mg/kg d.m.] (4)
Antimony (Sb)	8.7	0.16	0.7
Arsenic (As)	260	0.9	2
Barium (Ba)	1500	22	100
Cadmium (Cd)	3.8	0.04	0.06
Chromium (Cr)	120	0.63	7
Cobalt (Co)	60	0.54	2.4
Copper (Cu)	98	0.9	10
Mercury (Hg)	1.4	0.02	0.08
Lead (Pb)	400	2.3	8.3
Molybdenum (Mo)	144	1	15
Nickel (Ni)	81	0.44	2.1
Selenium (Se)	4.8	0.15	3
Tin (Sn)	50	0.4	2.3
Vanadium (V)	320	1.8	20
Zinc (Zn)	800	4.5	14
Bromide (Br^-)	670	20	34
Chloride (Cl^-)	110000	616	8800
Fluoride (F^-)	2500	55	1500
Sulphate (SO_4^{2-})	165000	1730	20000

1: building material with a minimum volume unit of at least 50 cm^3, and has stable shape under normal conditions;
2: building material that has not been shaped;
3: materials can be used only when isolation, management and control measures are applied; in Dutch called IBC: 'Isoleren-Beheersen-Controleren';
4: the measured cumulative leaching for a component per unit surface area over 64 days, in mg/m^2;
5: mg elements per kg of dry material; d.m.-dry mass.

- **Treatments**

In order to improve the properties of MSWI bottom ash physically or chemically, to obtain a better material for application or to reduce the leaching concentration of contaminants from MSWI bottom ash and lower it environmental risk potential, relevant treatments have been performed and reported as summarized in Figure 2.4.

In general, incinerators are equipped with magnetic separators and non-ferrous separators for the recycling of pure metals, and the major metals recovered are iron and aluminum. For the incinerator plant, the aim is to maximize the recycling of metals, which firstly

provide a financial benefit for the company and secondly a cleaner stony material can be obtained. However, it was reported that the recovery level of metals is related to their oxidation degree and is limited by their particle size (Biganzoli & Grosso, 2013; Biganzoli et al., 2012). Hence, advanced recycle methods were developed, such as modified eddy current separation (Rahman & Bakker, 2013; Settimo et al., 2004), optimized pretreatments (Holm & Simon, 2016), advanced dry recovery (ADR) (De Vries, 2009), etc.

The majority of the research focused on the treatments for leaching of MSWI bottom ash, which include the extraction and immobilization of contaminants. The extraction of contaminants means to pre-leach out the contaminants from bottom ash and reduce the total leachable contents before future application or disposal. The contaminants in the MSWI bottom ashes include salts or heavy metals, and their extraction can be by water or chemical washing. It was reported that the salts in the MSWI bottom ash, such as chlorides, are highly soluble, and could be washed out by simple water washing; however, it was not recommended to wash the MSWI bottom ash due to the large amount of generated waste water (Chen & Chiou, 2007; Lin et al., 2011; Yang et al., 2012). The organic carbon in the bottom ash could be extracted by hydrochloric acid (Guimaraes et al., 2005) and the heavy metals can be extracted by ammonium citrate: Cu (Van Gerven et al., 2007) leaching could be lowered below the limit values after extraction with a 0.2 M ammonium citrate solution followed by three washing steps.

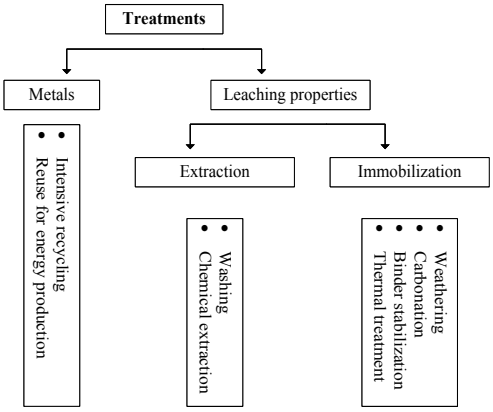

Figure 2.4: The research aspects regarding treatments on MSWIBA

The freshly produced bottom ash from the incinerators is generally dumped into water for cooling down, followed by metals separation and several weeks or months natural weathering. It was reported that the mobility of some metals or elements was reduced during the weathering process (Freyssinet et al., 2002), which was due to the newly formed minerals. It was also addressed that the pH of the bottom ash was stabilized which contributed to the reduced solubility of metal hydroxides (Chimenos et al., 2000; Fléhoc et al., 2006). Therefore, accelerated carbonation was applied as a treatment in order to

accelerate this weathering process to reduce the leaching properties of the MSWI bottom ash.

Rendek et al. (2006) performed accelerated carbonation using pure CO_2 on lab scale on original bottom ash and sieved bottom ash (< 4 mm). Their results displayed that calcite was formed during carbonation and the pH was reduced from 12 to 8; meanwhile, the leaching of Pb, Cr and Cd was reduced. Around 0.023 kg CO_2 per kg of dry bottom ash could be sequestrated; for bottom ash sieved under 4 mm, it was 0.044 kg. By accelerated carbonation, the CO_2 emission from incinerator could be reduced by 0.5-1%. Arickx et al. (2006) conducted carbonation tests under several conditions on the bottom ash fractions, and compared with natural carbonation. It was found that three months ageing was enough for improving the MSWI bottom ash leaching properties considering recycling, while it was still not enough for the sand (0.1-2 mm) and sludge (0-0.1 mm) fractions to meet the requirement. After four weeks of accelerated carbonation, the leaching of Cu reduced dramatically, and the leaching of the other elements could comply with the legislation. The research carried out in (Meima et al., 2002) showed that the leaching of Cu and Mo after carbonation could be decreased by 50% and 3%, respectively; the precipitates found in the carbonated bottom ash were a mixture of Al-rich amorphous material, calcite and maybe gibbsite which may contribute to the decrease of Cu leaching. Lin et al. (2015) reported that the leaching of Cu was influenced by the degree of carbonation, while Cr leaching was more pH dependent. The carbonation conditions, such as time, temperature, moisture content, pH, DOC, IBA properties, etc. will influence the leaching of final treated bottom ash. The research reported in (Baciocchi et al., 2010) revealed that the carbonation of MSWI bottom ash resulted in the decrease of pH which subsequently reduced the solubility of some heavy metals. Cornelis et al. (2006 & 2012) addressed that the Sb leaching from MSWI bottom ash was reduced after a carbonation treatment; the calcium bearing minerals play a significant role controlling Sb leaching at neutral to alkaline pH; when pH > 12, Sb solubility was limited by portlandite and ettringite, when 10.8 < pH < 12, only ettringite influenced Sb leaching; for pH <10, calcite and gypsum played the dominate role for Sb leaching.

The (accelerated) carbonation was suggested as a promising treatment on MSWI bottom ash, which on one hand reduces the leaching of heavy metals, and on the other hand can uptake CO_2.

The stabilization of MSWI bottom ash is a method to immobilize the leachable elements and transfer them into a stable format or absorb/entrap them by the generated mineral phases; this includes stabilization by other solution (Crannell et al., 2000), by binders or alternatives (Van Caneghem et al., 2016; Li et al., 2012), or by chemical activators (Onori et al., 2011; Polettini et al., 2009).

Crannell et al. (2000) used soluble phosphate (PO_4^{3-}) to stabilize heavy metals in MSWI bottom ash; it was found that the Pb, Cu, Zn and Ca in the bottom ash could be effectively stabilized due to the stable phases generated between the bottom ash and the phosphate solution. Ca and Fe containing compounds were used as additives for the immobilization of MSWI bottom ash by Van Caneghem et al. (2016). It reflected that the lower solubility of romeites (calcium antimonate mineral) formed when Ca contained compounds were used contributed to the reduced Sb leaching; co-precipitation of Sb with in-situ formed iron (hydr)oxides under the appearance of Fe salts played a dominant role for the decreased Sb leaching. Li et al. (2012) mixed the MSWI bottom ash with blended cement, and figured out that the heavy metals were immobilized by the hydration products, such as C-S-H and AFt (such as ettringite). Polettini et al. (2009) and Onori et al. (2011) utilized chemical activators, such as NaOH, KOH, $CaCl_2$ or $CaSO_4$, to improve the leaching of MSWI bottom ash in a cement-based system. It was demonstrated that the addition of KOH or $CaCl_2$ could reduce the leaching of heavy metals due to the stability of the main hydration phases, while use of sulphate-based activators was not recommended considering the leaching of metals.

Generally, the treatments on MSWI bottom ash are also matched with their applications, such as use bottom as in concrete and meanwhile, the binders in the concrete have an immobilization effect on the heavy metals in the bottom ash.

- **Applications of MSWI bottom ash**

The application routes of MSWI bottom ash before or after treatment, can be summarized as shown in Figure 2.5. At the early stage, MSWI bottom ash was mostly used as road base due to its physical properties which are similar to normal aggregates, and its leaching behaviors could comply with the legislation established for road construction (Forteza et al., 2004). In the Netherlands, the MSWI bottom ash was used as road base with the isolation layer and monitoring of leaching during service life due to the strict Dutch legislation - SQD (2013). The use of MSWI bottom ash in roads in some countries was successful and the leaching of metals during service life was reported to comply with standards (Dabo et al., 2009; Hjelmar et al., 2007; Izquierdo et al., 2008; Olsson et al., 2006). However, more application potentials for MSWI bottom ash should be explored due to its increasing amount worldwide. Hence, the use of bottom ash was introduced into building construction, such as being used as aggregates, binder alternatives, etc.

Müller & Rübner (2006) used MSWI bottom ash fractions (2-8, 2-32 mm) in concrete to replace natural aggregates. It was found that the metallic Al causes cracks which deteriorate the durability of concrete; the high amount of glass content in bottom ash resulted in alkali-silica reaction (ASR) which contributed to the cracking or spalling of concrete. Hence, it was suggested to reduce the content of Al and glass before use in concrete. The research conducted in (Sorlini et al., 2011) stated that, after a washing treatment on their bottom ash, it could be used in concrete without significant influence on concrete properties.

Ferraris et al. vitrified the MSWI bottom ash at 1450 ºC and a type of dark brown glassy material was obtained (Ferraris et al., 2009). This material could be used as cement replacement for up to 20% wt. and could also be used as sand replacement in low strength mortar.

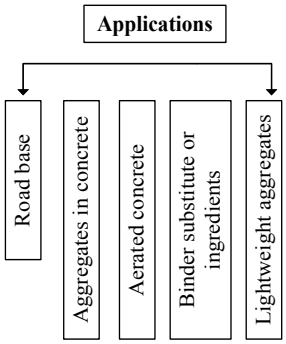

Figure 2.5: The application routes of MSWIBA studied

The MSWI bottom ashes treated by a commercial washing and ADR technique could be used in concrete as aggregates alternatives (Van Dr Wegen et al., 2013), and it was suggested that up to 20% volume of bottom ash for structural concrete can be used to replace aggregates or 50% volume for plain concrete. The washed MSWI bottom ash was used in pervious concrete reported in (Kuo et al., 2013). Their results displayed that the previous concrete with washed coarse bottom ash had higher compressive strength and lower permeability compared with the one with natural aggregate and this concrete could comply with the practical engineering requirement. The MSWI bottom ash treated by enhancing the separation of metals during dry and wet separation in (Keulen et al., 2015) was used as aggregates to produce earth-moist concrete. The results demonstrated that the strength of the concrete was reduced with the increasing amount of treated bottom ash, as well as the freeze thaw resistance. However, the obtained concrete with even 100% treated bottom ash could comply with the standards requirement on curb stone or pavement stone. The leaching of the crushed concrete with 100% treated bottom ash was below the limit emission value defined in the Dutch legislation.

The MSWI bottom ash was used as cement replacement in (Juric et al., 2006); the results showed that the strength of mortar decreased linearly with the increase of IBA amount, and it was recommended that less than 15% of IBA could be used to replace cement. Similar results were reported in (Saikia et al., 2008), where MSWI bottom ash was used as sand replacement in mortar. Li et al. (2012) utilized milled MSWI bottom ash as replacement of blended cement, and addressed that the use of milled bottom ash had very low reactivity and had retardation effect on cement hydration, so up to 30% of milled bottom ash could be used. The leaching of the blended mixture after curing was far below the Chinese standard. The milled bottom ash was used to produce a geopolymerized binder in (Garcia-

Lodeiro et al., 2016) and a type of hybrid cement with a 28-days compressive strength of 33 MPa was obtained. For the application of MSWI bottom ash in concrete, the metal content was recommended to be efficiently separated; the milled bottom ash had a very low reactivity. In general, low-strength concrete could be achieved with the use of MSWI bottom ash. The application of milled MSWI bottom ash as raw material for the production of cold bonded lightweight aggregates could be used to produce concrete blocks (Cioffi et al., 2011). The produced aggregates had lower bulk density and the pellet strength was dramatically influenced by the binder used during the pelletization process. However, no further research work has been conducted in this direction.

It can be summarized that:

(1) There are physical and environmental problems in applying MSWI bottom ash in construction without any pre-treatments - the heavy metals in bottom ash which will leach out as the presence of water will pollute the ground water and are harmful to human health;
(2) The metal content in bottom ash, especially metallic aluminium, will generate hydrogen with alkali content when used in concrete which contribute to the spalling and poor quality of concrete with bottom ash;
(3) Treatments are needed to upgrade the quality of MSWI bottom ash to meet the physical and environmental requirements on building materials;
(4) The economic factor of the treatments and the value of the treated bottom ash for application are the main barrier in practice for bottom ash application.

2.4 Conclusions

In this chapter, the incineration procedure of two WtE plants in the Netherlands was introduced. The considered literature studies included the characteristics, treatments and application of MSWI bottom ashes can be summarized:

(1) The procedures in the WtE plants are very similar worldwide, and generally include solid waste storage, incineration, bottom ash collection and metals separation, fly ash collection and flue gas cleaning. The efficiency of these procedures may be diverse according to the operation conditions based on economic consideration.
(2) There are various environmental legislations on the disposal methods of MSWI bottom ash in different countries and the limit value of leaching concentration from bottom ash and the leaching tests are also different accordingly.
(3) The properties of MSWI bottom ash from different incineration plants vary. Its potential environmental risk and its poor physical properties are the main barriers for the application of MSWI bottom ash. The research in general focuses on the application of MSWI bottom ash in concrete as binder alternatives, aggregates, etc. The metallic aluminium in bottom ash particles which can generate hydrogen, makes it not recommended to be used in concrete, while it could be used in aerated

concrete. The calcite content in fine bottom ash particles suggests a thermal treatment to active the chemical reactivity of bottom ash. The high porosity of bottom ash particles supports the idea of application in lightweight concrete.

(4) The leaching behaviours of heavy metals in the MSWI solid residues are investigated intensively. It is stated that most of the heavy metals are pH dependent during the leaching process. Methods including washing, weathering/carbonation, stabilization, etc. have been used to improve the leaching properties of MSWI bottom ash for its application in the construction field.

(5) In the field of MSWI bottom ash, more effort is needed to focus on the reduction of leaching contaminants, the chemical reactivity of bottom ash, the application of bottom ash in different types of concretes, the upgrading of bottom ash to fit the legislation, the optimization of bottom ash application and the benefit.

From the point of view of construction materials, environment protection and the economy, there is a long way to go for the research on MSWI bottom ash. In this study, the MSWI bottom ashes from different WtE plants in the Netherlands were characterized and evaluated with the purpose of applying as building materials, which is shown in the next chapter.

Chapter 3

3 The characterization of MSWI bottom ashes from two WtE plants*

3.1 Introduction

A very important aspect of the application of MSWI bottom ashes is the stability of their chemical and physical properties (Dabo et al., 2009). It is stated that the properties of the MSWI bottom ashes from different plants and countries vary due to the source of solid waste and incineration process conditions (Ecke et al., 2000; Yao et al., 2010a). Moreover, the environmental legislation, management and application of the MSWI bottom ashes differ from country to country in consideration of the local situation (Van Gerven et al., 2005; Wang & Wang, 2013). In the available literature, studies are seldom focused on the stability of the MSWI bottom ashes properties in relation to the different production period and procedure.

The work in this chapter aims to identify the stability of the properties of two MSWI bottom ashes over a long-time and to classify the type of MSWI bottom ashes in regard to their environmental impact. Additionally, their application potential as a building materials ingredient, such as clinker, cement and sand replacement (Figure 1.2), is analysed. In order to qualify and classify the bottom ashes from these two plants according to the Dutch legislation (SQD, 2013), and then suggest a possible application, their physical and chemical characteristics of the bottom ashes were investigated. The historical test data on MSWI bottom ashes provided by an accredited laboratory was collected and analysed to estimate the change of bottom ash properties in time. The potential of fine bottom ash (< 2 mm, F-BA) to be used as clinker addition and cement replacement after milling was studied through oxide engineering and isothermal calorimetric measurements. Mortars with F-BA were prepared and tested to investigate the influence of bottom ash fines on the mortar properties. The environmental impact of the MSWI bottom ashes was studied by a leaching test, and seven-year leaching data since 2005 was analysed to determine the stability of leachable matter in the analysed bottom ash. Finally, further possible treatment and application methods are suggested.

3.2 Materials collection and test methods

3.2.1 Materials collection

The MSWI bottom ashes investigated in this chapter were provided by the waste-to-energy plants located in Wijster (BAW) and Moerdijk (BAM), as was mentioned in Section 2.2. Since the beginning of the operation of both plants, a periodical bottom ash quality

*Content of this chapter was published elsewhere [Tang, P., Florea, M.V.A., Spiesz, P., and Brouwers, H.J.H., (2015). Construction and Building Material 83, 77-94].

evaluation was conducted. The representative bottom ashes samples were collected from different spots of the large bottom ash piles every 3 weeks and then sealed in plastic buckets before further testing.

3.2.2 Test methods

- **Water content determination**

The received samples after weighting (m_1) was dried in the ventilated oven at 105 °C until a constant mass (m_2) was obtained and the water content (ω) was determined as follows (EN 1097-5 (1999)):

$$\omega = \frac{m_1 - m_2}{m_2} \times 100 \quad (3.1)$$

where ω represents the water content of the investigated samples (%), m_1 is the initial mass of the samples before drying (grams), m_2 is the mass of the tested samples after the drying procedure (grams).

- **Particle size distribution (PSD)**

The particle size distributions (PSDs) of the MSWI bottom ashes, sand and aggregate in the whole research were determined by the sieving method according to EN 933-1 (1997). Meanwhile, the sieving test was also performed on the oven dried bottom ashes to compare with the standard test. The PSDs of powder materials used in this study were measured by laser diffraction (Mastersizer 2000, Malvern).

- **Specific density**

The specific density of the materials in this study was measured using a Micrometrics AccuPyc II 1340 helium pycnometer as described in (Quercia Bianchi, 2014).

- **Water absorption**

The water absorption of the materials was measured according to EN 1097-6 (2013). The sample was firstly saturated in water at room temperature for 24 hours, and then surface dried. After that, the saturated and surface-dried material were further dried in a ventilated oven at 110 ± 5 ºC until a constant mass was reached. The water absorption was expressed as the mass percentage of the absorbed water per a mass unit of the dry material.

$$W_{24} = \frac{m_{wet} - m_d}{m_d} \times 100 \quad (3.2)$$

Where: W is expressed in percentage (%); m_{wet} is the mass of the original investigated material (grams); m_d is the mass of the material cooled after drying following the procedure mentioned above (grams).

- **Chemical compositions and crystalline phases**

The tested materials were firstly dried and then milled into powder under 63 μm. For the materials above 4 mm, they were firstly crushed using a jaw crusher, and then the crushed material was fed into the planetary ball mill for further milling. The tested powders were pressed into plate shape using a hand press tableting machine, and then X-ray fluorescence (XRF) analysis was performed on the tablets using an Epsilon 3 (PANalytical) with Omnian 3 analysing software for determining the chemical compositions. The X-ray diffraction (XRD) measurement was performed on the milled powders using a Rigaku Geigerflex X-ray diffraction spectrometer with Cu-radiation and a detection angle between 3° and 75° or 90°.

- **Total heavy metals content determination**

The milled materials were firstly digested by nitric acid and hydrochloric acid (aqua Regia) according to NEN 6961 (2005) and then the heavy metals in the extracted leachate were determined by inductively coupled plasma-atomic emission spectrometry (ICP-AES) following the procedures given in NEN 6966 (2005).

- **Loss on ignition (LOI) and unburned content determination**

The unburned content in the MSWI bottom ash was measured according to NEN-EN 1744-7 (2010). The bottom ash particles were crushed under 4 mm, and then oven heated at 480 ± 25 ºC for 4 hours. The mass loss after heating is presented as percentage of the dried mass before heating. The LOI of the investigated materials was determined by calculating the mass loss percentage after heating at 950 ºC.

- **Ferrous and non-ferrous content analysis**

The ferrous components in the MSWI bottom ash were separated by a magnet, and the loose metallic iron components (such as cans, screws, nuts, nails, etc.) were picked out manually, and the amount was expressed as mass percentage in the total bottom ash.

- **Metallic aluminium determination**

To quantify the metallic aluminium content in the bottom ash samples, the test method as described in (Qiao et al., 2008a) was applied. According to (Rahman & Bakker, 2013), the separation of metallic Al in coarse bottom ash fractions can be enhanced by using more efficient eddy current separators. However, the enhancement is not sufficient for fine bottom ash particles (Biganzoli et al., 2013). Therefore, prior to the application of fine bottom ash particles, the amount of metallic aluminium should be determined. In this study, the bottom ash fines were milled into powder before the measurement and three samples were tested for each bottom ash sample. The device used for the metallic Al reaction with alkaline solution and the formed H_2 gas collection device used in laboratory is shown in Figure 3.1. The equation used for calculating the amount of metallic Al is described as:

$$2Al + 6H_2O \rightarrow 2Al(OH)_3 + 3H_2 \uparrow \quad (3.3)$$

According to this equation and the ideal gas law, about 1 g of metallic Al can produce 1.336 litre of hydrogen (H_2) at 20ºC. The calculation is shown in Appendix 2.

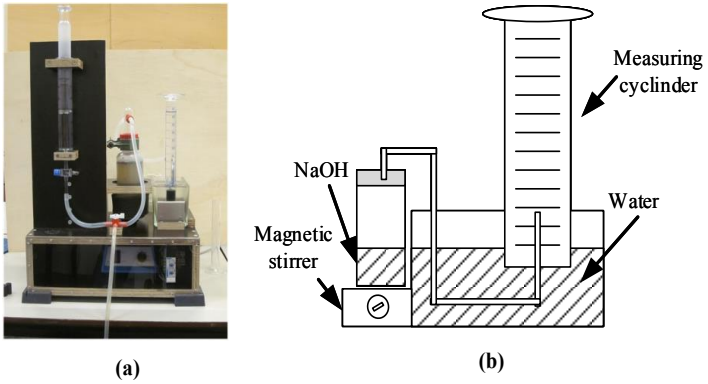

Figure 3.1: The (a) lab set-up and (b) schematic graph to measure the volume of H_2 in IBA

- **Clinker characteristics**

In cement production, the parameters normally used to define clinker characteristics based on the oxide composition are hydraulic ratio (HR), silica ratio (SR), alumina ratio (AR) and lime saturation factor (LSF) (Pan et al., 2008; Taylor, 1997). To evaluate the potential use of MSWI bottom ashes as a raw material for clinker production, the HR, SR, AR and LSF based on the chemical properties of investigated bottom ash samples were calculated as follows (Taylor, 1997):

$$HR = CaO/(SiO_2 + Al_2O_3 + Fe_2O_3) \quad (3.4)$$

$$SR = SiO_2/(Al_2O_3 + Fe_2O_3) \quad (3.5)$$

$$AR = Al_2O_3/Fe_2O_3 \quad (3.6)$$

$$LSF = CaO/(2.8 \times SiO_2 + 1.18 \times Al_2O_3 + 0.65 \times Fe_2O_3) \times 100 \quad (3.7)$$

These parameters calculated for the MSWI were compared with those for cement clinker production, as will be shown later in Table 3.4.

- **Reactivity analyse of waste materials (cement hydration study)**

It is known that during the cement hydration, heat is generated due to chemical reactions which occurs at different stages (Taylor, 1997). The isothermal calorimeter can record the generated heat. By comparing the heat differences detected, the hydration of the sample can be evaluated.

To analyse the reactivity of the bottom ashes, the cement hydration heat development with bottom ash was studied by isothermal calorimetry (eight-channel TAM Air, Thermometric).

The bottom ash sample was milled to under 125 µm using a planetary ball mill and then blended with OPC (CEM I 42.5 N) at various F-BAW or F-BAM ratios (0%, 10%, 20%, 30%, 40% and 100%) and the water to powder ratio was kept constant (w/p = 0.7) for all mixtures. After 5 minutes of manual mixing, the mixture was carefully transferred into the glass ampoule to avoid loading the sample on the upper and side walls. Then the sealed ampule with the sample was loaded into the isothermal calorimeter and the temperature was kept at 23 ºC and the test was stopped after 5 days. The obtained data was analysed and compared with that of plain cement paste.

- **Application of fine MSWI bottom ash in mortars**

To investigate the influence of the fine bottom ash particles (F-BAM and F-BAW) used as sand replacement on the properties of mortar, the mortars were prepared following EN 196-1 (2005). The OPC: water: sand mass ratio was 2: 1: 3 for the reference sample, and then the sand was replaced by fine bottom ash particles by 10%, 20% and 30% by mass. The OPC used in this part of the study was CEM I 42.5 N from ENCI (the Netherlands) and the sand is CEN normalized sand 0 - 2 mm according to EN 196-1 (2005). The water to cement ratio was kept at 0.5. Hardened mortar prisms (40 × 40 × 160 mm^3) were used for the determination of flexural and compressive strengths after 7, 28, and 91 days of water curing.

- **Column leaching test**

To estimate the environmental impact of BAW and BAM resulting from a possible emission of harmful elements, the leaching test following NEN 7383 (2004) was performed and compared with limit leaching values according to the Dutch legislation (SQD, 2013). In order to evaluate the leaching behaviour of the elements in MSWI bottom ash samples from both plants from different production periods, the leaching data from 2005 to 2012 for both BAW and BAM were collected and analysed.

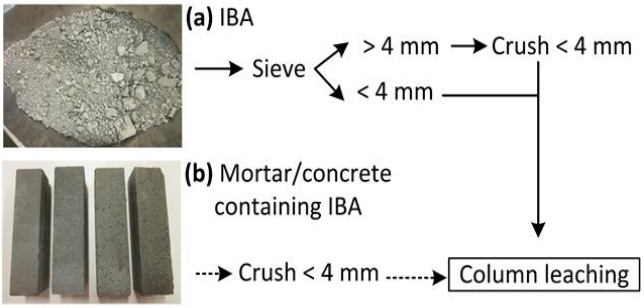

Figure 3.2: The preparation of samples for column leaching test

The leaching tests were performed on two types of samples - MSWI bottom ash and mortar or concrete containing MSWI bottom ash; the preparation of samples for leaching test is shown in Figure 3.2. The prepared sample was placed in the column and water was forced

to flow through the sample from the bottom to top for a certain period, till the water to solid ratio (L/S) of 10 l/kg. The concentration of chemical elements in the eluate was analysed using the ICP-AES according to NEN 6966 (2005), and the amount of chloride and sulphate was determined through HPLC following NEN-EN-ISO 10304-2 (1996). According to the Dutch legislation - SQD (2013), the leaching of the inorganic elements should comply with the limiting values to protect the environment from the potential pollution from emissions from MSWI bottom ash. The leachability of materials is calculated according to the following equation:

$$\text{Leachability (\%)} = \frac{\text{Leached out concentration}}{\text{Total concentration}} \times 100 \tag{3.8}$$

where the total concentrations of elements are determined using ICP-AES after the acid digestion (aqua Regia) of the solid samples.

3.3 Characterization of MSWI bottom ashes

3.3.1 Physical properties

The seven-year average particle size distribution (PSD) data of BAW and BAM are shown in Figure 3.3 together with newly measured data. The PSD curves of both bottom ashes are relatively stable over a period of seven years. Despite the different production processes, the PSD of BAW and BAM are very similar. Approximately 70% of the bottom ash particles are in the range of 0.1 - 11.2 mm, which resembles the commonly used aggregates in concrete (EN 12620, 2002).

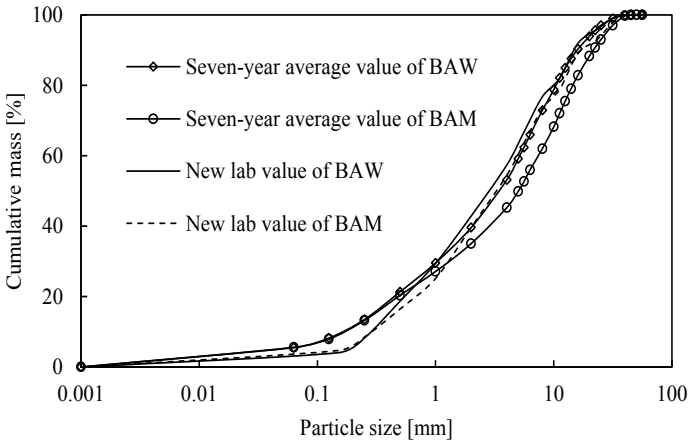

Figure 3.3: The particle size distributions of BAW and BAM

Figure 3.4 depicts that the water content of BAW varies from 13% to 25% and the one of BAM from 12% to 23% in a period of five to seven years. The various water contents of both bottom ashes result from the water quenching and open-air storage.

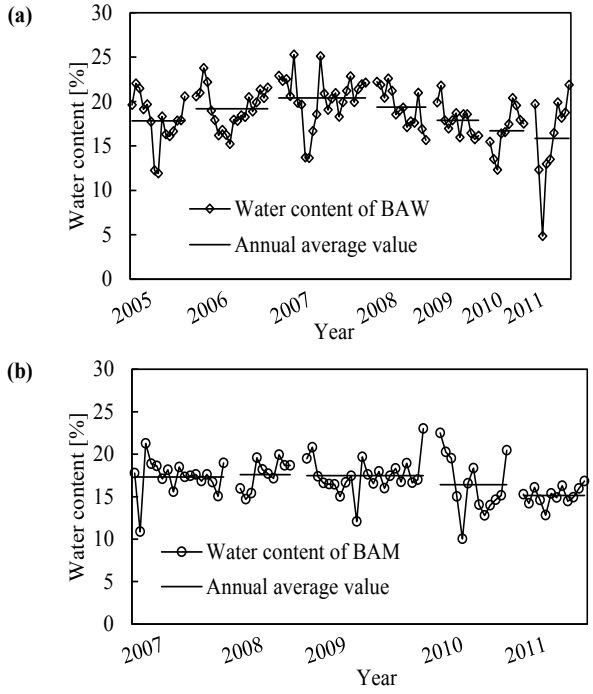

Figure 3.4: The water contents (ω) of (a) BAW and (b) BAM

The annual average water absorption values for both bottom ashes are presented in Table 3.1. The data shows that BAW has a higher water absorption than BAM, which could be caused by the higher porosity of BAW or higher amount of organic matter (Forteza et al., 2004). Compared with natural aggregates (Yang et al., 2011) and recycled aggregates (Kou & Poon, 2012; Zhao et al., 2013) as shown in Table 3.1, the bottom ashes have higher water absorption value.

Table 3.1: The annual average water absorption (W_{24}) of BAW and BAM fractions (4 - 31.5 mm)

24-hours water absorption W_{24} [%]	2006	2007	2008	2010	2011
BAW	-	-	13.23	10.82	11.44
BAM	8.4	7.9	-	8.1	9.8
NA (Yang et al., 2011)	1.4				
RCA (Zhao et al., 2013; Kou & Poon, 2012)	4.1 - 4.26				

NA: natural aggregate; RCA: recycled concrete aggregate; -: not available.

It can be observed from Table 3.2 that the densities of different particle size fractions of BAW and BAM are very comparable. The densities vary between 2.58 and 2.84 g/cm^3, which are lower than that of cement and comparable to the densities of natural aggregates (EN 206-1, 2000). The particle density of each bottom ash fraction is slightly lower than

the incineration bottom ash presented in (Yao et al., 2014), and the variation of the density is very small. The densities of particles between 0.5 - 11.2 mm are higher than other fractions; the possible explanation is the higher amount of remaining metals, which is in line with (Yao et al., 2014).

Table 3.2. The densities of OPC, BAW and BAM fractions

Particle size [mm]	Density [g/cm^3]		Particle size [mm]	Density [g/cm^3]	
	BAW	BAM		BAW	BAM
0 - 0.15	2.61	2.58	4 - 5.66	2.73	2.75
0.15 - 0.25	2.66	2.63	5.66 - 8	2.73	2.84
0.25 - 0.50	2.70	2.67	8 - 11.2	2.75	2.75
0.5 - 1	2.70	2.69	11.2 - 16	2.67	2.67
1 - 2	2.72	2.70	16 - 32	2.66	2.61
2 - 4	2.72	2.68			
IBA (Yao et al., 2014)	2847±159 kg/m^3		CEM I 42.5 N	3.10	

IBA: incineration bottom ash

3.3.2 Chemical properties

- **Chemical compositions**

The total chemical compositions of BAW and BAM are summarized in Figure 3.5. It can be observed that the dominant oxides in both bottom ashes are SiO_2, CaO, Al_2O_3 and Fe_2O_3, which cumulatively account for around 88% of the bottom ash, which is in line with (Bayuseno & Schmahl, 2010; Wei et al., 2011).

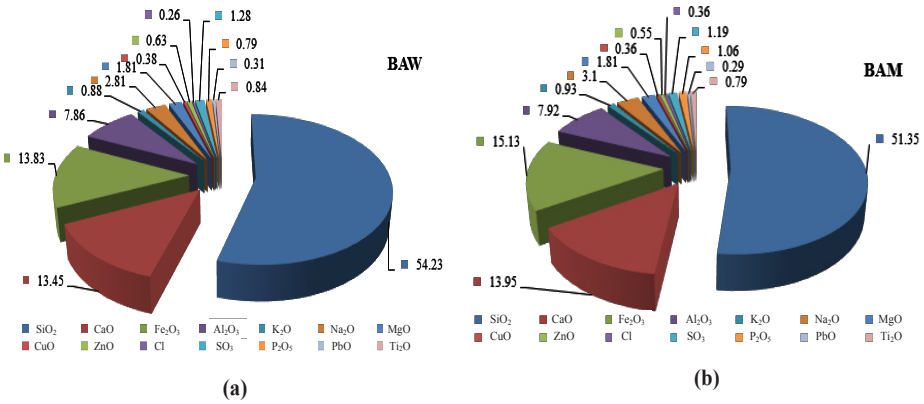

Figure 3.5: The chemical compositions of (a) BAW and (b) BAM

Figure 3.6 shows the SiO_2 distribution in different BAW and BAM size fractions. Other oxides (CaO, Al_2O_3, Fe_2O_3, CuO, SO_3) and chlorine content in the analyzed bottom ashes are presented in Appendix A. The amount of SiO_2 in each bottom ash particle size fraction

was measured and calculated to the proportion of the mass of bottom ash fraction, and also calculated to the total amount of all the bottom ash fractions.

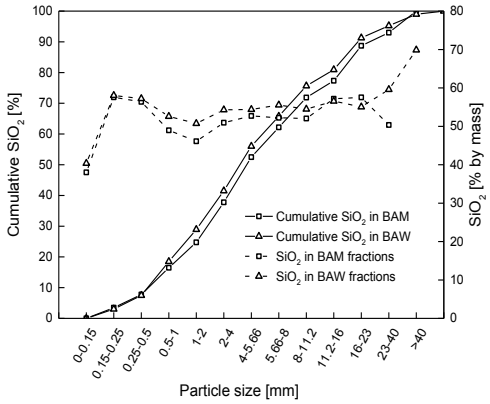

Figure 3.6: The amount of SiO_2 in BAW and BAM fractions

Table 3.3: The dominant chemical compositions of bottom ashes and other materials

Main chemical components	BAW	BAM	CEM I 42.5 N (Deschner et al., 2013)	SF (Saikia et al., 2008)	WBA (Ginés et al., 2009)	Fly ash (Rémond et al., 2002)	CDW (Anastasiou et al., 2014)	HCFA (Qiao et al., 2009a)
SiO_2	54.2	51.4	19.4	41.3	49.4	27.2	38.1	33.1
CaO	13.4	13.9	62.1	16.4	14.7	16.4	29.7	36.2
Fe_2O_3	13.8	15.1	3.6	13.5	8.4	1.8	3.7	5.4
Al_2O_3	7.9	7.9	5.2	9.57	6.6	11.7	6.3	10.8

SF: sand fraction (0.1 - 2 mm) of MSWI bottom ash; WBA: naturally weathered MSWI bottom ash; Fly ash: MSWI fly ash; CDW: construction and demolition waste; HCFA: high calcium fly ash from coal combustion power plant

The finer particles contain higher amount of CaO, Al_2O_3 and Fe_2O_3 and a lower amount of SiO_2. Additionally, the distribution between main oxides of BAW and BAM is very similar. This indicates that the main chemical composition is relatively stable, and is mostly independent of the raw solid waste before the incineration process. Compared with the dominant oxides in OPC (Deschner et al., 2013) and other wastes or secondary materials (Anastasiou et al., 2014; Ginés et al., 2009; Rémond et al., 2002; Saikia et al., 2008) as shown in Table 3.3, the bottom ashes in this study contain higher amounts of SiO_2 and lower amounts of CaO.

Based on the chemical properties of the bottom ash, the parameters for defining clinker characteristics were calculated and the results are shown in Table 3.4. It can be seen that the parameters HR, AR, LSF (defined previously in Section 3.2.2) of the bottom ash particles under 2 mm, as well as the complete bottom ash PSD are under the required values (shown in Table 3.4), except for SR. Therefore, the bottom ash analysed in this study is not suitable to be used as raw material for clinker production. However, the high amount of

SiO_2, Al_2O_3 and Fe_2O_3 indicate its potential to be used as a correction material (Taylor, 1997) for the clinker production. Further research would be needed in order to prove if this potential can be fulfilled; a detailed study of the calcination process in the kiln is necessary in order to verify this possibility.

Table 3.4: The calculated parameters used to define the characteristics of clinker

Parameters	Recommended range (Taylor, 1997)	0 - 2 mm		0 - 31.5 mm	
		F-BAW	F-BAM	BAW	BAM
HR	1.7 - 2.4	0.21	0.22	0.18	0.19
SR	1.7 - 2.7	2.56	2.10	2.50	2.23
AR	1.5 - 3.5	0.66	0.58	0.57	0.52
LSF	≥ 93%	9.36	9.98	7.91	8.56

- **Loss on ignition (LOI)**

The loss on ignition (LOI) of BAW and BAM was measured at 500 ºC to evaluate the amount of unburned organic matter and the results are depicted in Figure 3.7.

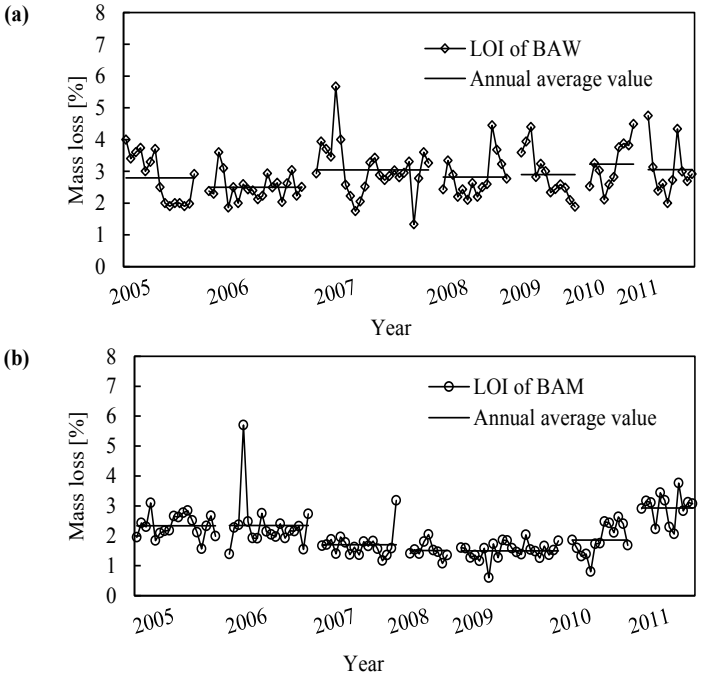

Figure 3.7: The loss on ignition (LOI) of (a) BAW and (b) BAM

It can be noticed that the LOI of BAM is more stable over time than that of BAW. Moreover, BAW has a higher annual average LOI value than BAM, which indicates less organic or burnable matter left in BAM. Interestingly, a pre-separation of paper and plastic from

municipal solid waste was conducted in the waste-to-energy plant of Wijster, so it was expected that BAW would have a lower amount of unburned matter. This discrepancy could be explained by the contribution of paper and plastic to reach a higher incineration temperature and better contact between the heat source and the incinerated mass, which eventually decomposes more organic matter.

- **Mineralogical properties**

The minerals identified in bottom ashes by XRD in literature were mainly quartz (SiO_2), calcite ($CaCO_3$), anhydrite ($CaSO_4$), gehlenite ($Ca_2Al_2SiO_7$) and magnetite (Fe_3O_4) or hematite (Fe_2O_3), in which quartz and calcite were the major crystalline phases (Qiao et al., 2009; Saikia et al., 2008). In this study, the diffractograms of bottom ash particles under 0.15 mm of BAW and BAM are shown in Figure 3.8 as an example and the relative intensities of the relevant peaks of other bottom ash fractions are shown qualitatively in Tables 3.5 and 3.6.

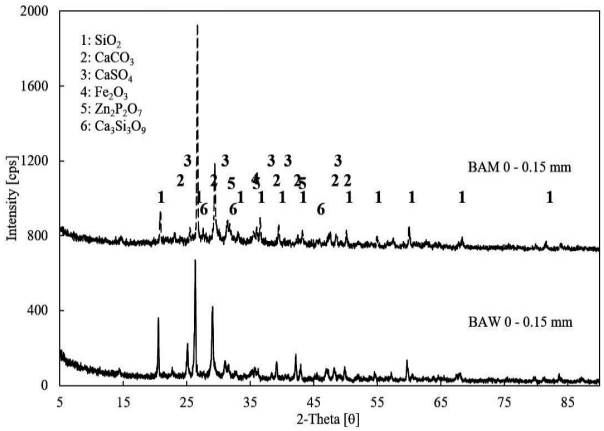

Figure 3.8: The XRD patterns of BAW and BAM particles under 0.15 mm

The analysis of XRD results of BAW shows that the main crystalline phases are quartz (SiO_2), calcite ($CaCO_3$), hematite (Fe_2O_3), zinc pyrophosphate ($Zn_2P_2O_7$) and anhydrite ($CaSO_4$). In all the fractions, SiO_2 as quartz is the main crystalline phase. The particles under 0.15 mm of BAW contain relatively high amounts of $CaCO_3$; Fe_2O_3 can be found in all the fractions of BAW and particles above 5.66 mm contain relatively more Fe_2O_3, while the particles under 2 mm have a higher amount of $CaSO_4$. The main crystalline phases for BAM fractions are SiO_2, $CaCO_3$, Fe_2O_3, $Ca_3Si_3O_9$ (wollastonite), $Zn_2P_2O_7$ and $CaSO_4$. The particles under 2 mm of BAM seem to contain large amounts of $CaCO_3$ and $CaSO_4$. The variation of the same crystals in bottom ash fractions could be attributed to the hardness of the crystalline phases. For instance, the $CaSO_4$ and $CaCO_3$ are softer than SiO_2 and Fe_2O_3, therefore the coarse fractions contain higher amounts of SiO_2 and Fe_2O_3, while gypsum

and limestone can be crushed during storage and transport and will be found mainly in the finer fractions.

Table 3.5: The crystalline phases in BAW fractions (* represents the relative intensity of peaks)

Particles size [mm]	SiO_2	$CaCO_3$	Fe_2O_3	$Ca_3Si_3O_9$	$Zn_2P_2O_7$	$CaSO_4$
0 - 0.15	****	***	*	---	***	***
0.15 - 0.25	****	*	*	***	*	***
0.25 - 0.5	****	*	*	**	*	***
0.5 - 1	****	**	*	*	*	**
1 - 2	****	**	*	*	*	**
2 - 4	****	*	*	*	*	**
4 - 5.66	****	*	*	**	**	*
5.66 - 8	****	*	**	***	**	***
8- 11.2	****	*	**	*	*	*
11.2 - 16	****	--	**	*	*	*
16 - 23	****	*	**	*	*	*
23 - 31.5	****	*	**	*	*	**

Table 3.6: The crystalline phases in BAM fractions (* represents the relative intensity of the peaks)

Particles size [mm]	SiO_2	$CaCO_3$	Fe_2O_3	$Ca_3Si_3O_9$	$Zn_2P_2O_7$	$CaSO_4$
0 - 0.15	****	***	*	***	***	***
0.15 - 0.25	****	***	*	***	***	***
0.25 - 0.5	****	**	*	*	**	***
0.5 - 1	****	**	*	**	**	***
1 - 2	****	***	*	***	***	***
2 - 4	****	*	**	*	*	*
4 - 5.66	****	*	*	**	***	**
5.66 - 8	****	**	**	*	***	**
8 - 11.2	****	**	*	*	**	**
11.2 - 16	****	**	*	*	*	**
16 - 23	****	*	*	*	*	*
23 - 31.5	****	**	*	***	***	**

- **The content of metallic matter**

The annual average amounts of ferrous components and other loose metallic iron in the investigated bottom ashes are shown in Figure 3.9. It can be noticed that the amount, of the ferrous component and loose metallic iron in both BAW and BAM are quite stable in time. The BAM contains a higher amount of both ferrous metals and loose metallic iron than BAW. This result is in line with the chemical compositions as shown in Section 3.3.2 that BAW has a lower amount of equivalent Fe_2O_3 than BAM. The above-mentioned differences between BAW and BAM could be explained as follows: the pre-separation of recyclable materials before incineration in Wijster increases the recycling efficiency of metals. Hence, an enhancement of iron recycling in the Moerdijk plant could also be necessary for improving the quality of the bottom ash.

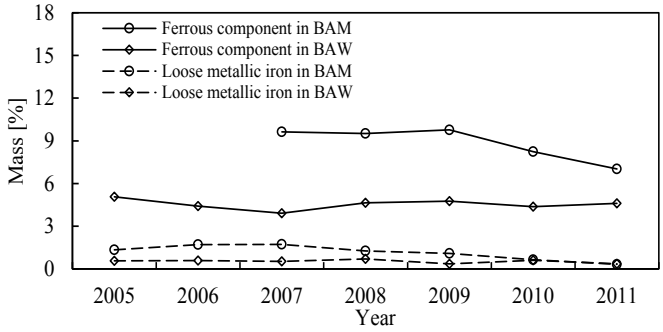

Figure 3.9: The amount of ferrous metals and loose metallic iron in BAW and BAM

The amount of metallic aluminium in fine bottom ash fractions (0-2 mm) of BAW (F-BAW) and BAM (F-BAM) is depicted in Table 3.7. The F-BAW contain more metallic aluminium, around twice as much compared to BAM. However, the XRF results show that F-BAW and F-BAM have quite similar amounts of equivalent Al_2O_3 (Figure 3.5 and Appendix A). Thus, it can be concluded that the aluminium in F-BAW has a lower level of oxidation. Previous research addressed that the oxidation level of metallic aluminium in MSWI bottom ash and the small size of non-ferrous scraps limit the recycling of aluminium; hence, the production of energy from H_2 generated by the chemical reaction between metallic aluminium with a high pH solution is more beneficial (Biganzoli et al., 2012 & 2013). Therefore, how to recover the metallic aluminium from the fine bottom ashes in the form of hydrogen in a practical way might be more important and interesting than enhancing the separation of metallic aluminium by an eddy current separator.

Table 3.7: The amount of metallic aluminum in F-BAW and F-BAM

	Mass [g]	Volume of H_2 [ml]	Amount of metallic Al [mg]	[% wt.]
F-BAW	5.30	44.80	38.64	0.73
	5.54	45.90	39.58	0.71
	6.20	50.30	43.38	0.70
F-BAM	5.01	21.50	18.54	0.37
	5.48	23.00	19.84	0.36
	5.65	24.50	21.09	0.37

3.3.3 Application potential in mortar

The bottom ash particles under 2 mm have a very similar particle size distribution (PSD) and density with sand as shown in Figure 3.10 and Table 3.2. Therefore, in this chapter the bottom ash particles under 2 mm were applied in mortar as sand replacement to investigate their effect on the mortar properties. The flexural and compressive strengths of mortar with various ratios of F-BAW or F-BAM after several periods of curing are shown in Figure

3.11, as well as their reduction percentages compared with the strengths of the reference mortars.

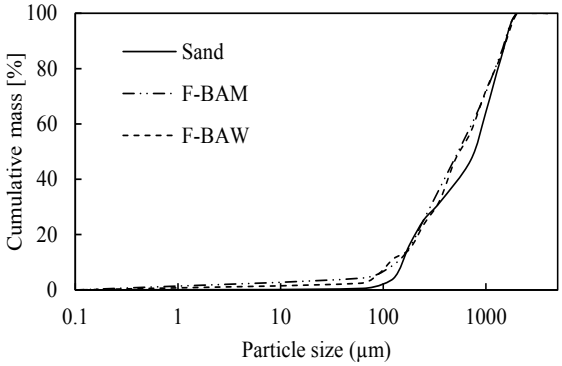

Figure 3.10: The particle size distribution (PSD) of standard sand and fine bottom ashes (0-2 mm)

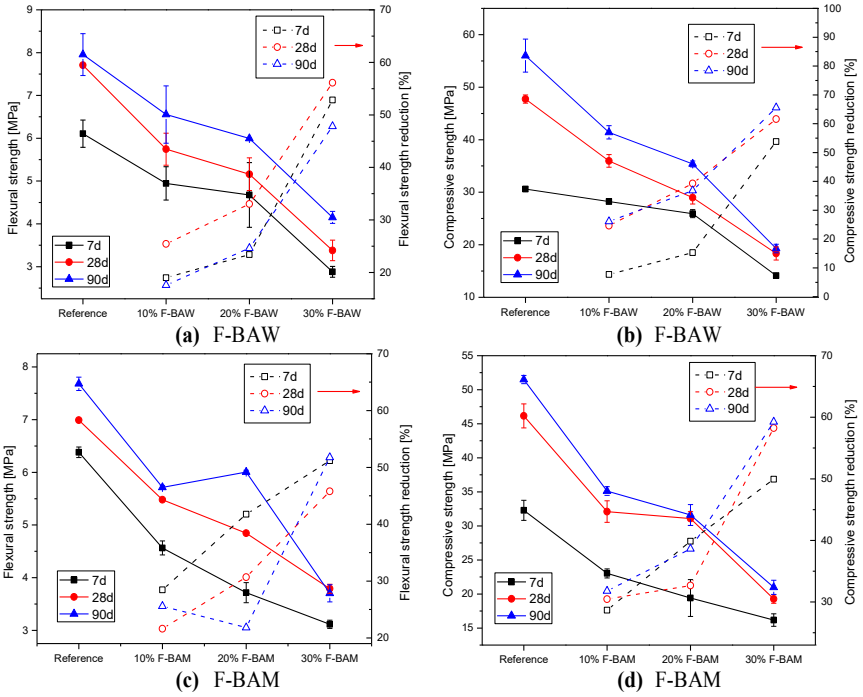

Figure 3.11: The flexural and compressive strengths of mortar with (a, b) F-BAW and (c, d) F-BAM and their reduction percentages compared with the reference, respectively

It can be observed from Figure 3.11 that the use of both bottom ashes decreases the flexural and compressive strengths by around 20%-50%, and the reduction of the strengths increase

with an increasing amount of the bottom ashes. In addition, the strength reductions for mortar with F-BAW is slightly higher than that with F-BAM.

Similar results were reported in (Al-Rawas et al., 2005; Müller & Rübner, 2006). The possible explanation of this phenomenon is that during the mixing of the mortar, part of the water was absorbed by the bottom ash particles due to their high water absorption (as shown in Figure 3.10 the F-BAW and F-BAM have more fine particles under 125 µm than sand). Thus, the cement hydration progressed less, resulting in the reduction of the strength (Tam et al., 2009). Meanwhile, the metallic Al in the F-BAs may react with the alkalis from cement hydration and then generate cracks inside the mortar which in turn lowers the mortar strength, even though no visible cracks or swelling were observed on the surfaces of the samples.

3.3.4 The influence of milled fine bottom ashes (MF-BA) on cement hydration

To study the possibility of using fine bottom ashes as cement replacement, isothermal calorimetry tests were performed. The fine bottom ashes BAM and BAW (0-2 mm) were milled into powder and labelled as MF-BAM and MF-BAW, respectively, and mixed with OPC respectively, as described in Section 3.2.1.

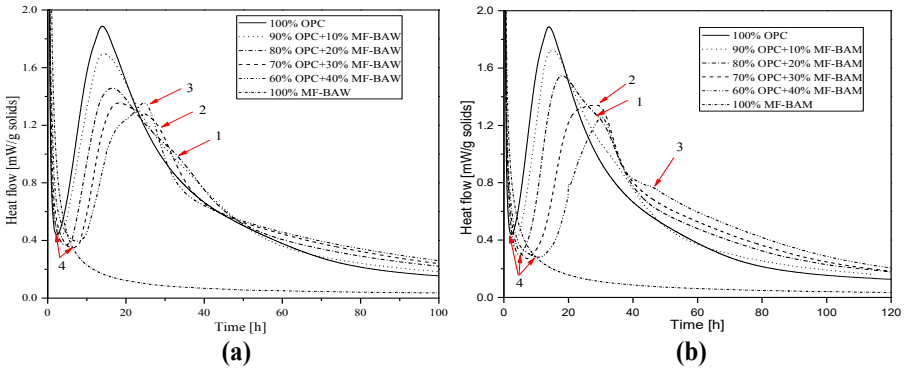

Figure 3.12: Heat flow normalized to total mass of solids

Figure 3.12 shows the development of the heat flow of the hydration of OPC, and OPC with various replacement ratios of MF-BAW and MF-BAM, normalized to the total powder content. As described in (Bullard et al., 2011), the hydration of OPC can be divided into four stages: the initial, the induction, the acceleration, and the deceleration stage. Figure 3.12 (a) and (b) show that the plain MF-BAW and MF-BAM did not show typical hydration curves as OPC, and their heat release rates tended to be stable after 40 hours. This indicates that the MF-BAW and MF-BAM have lower hydraulic activities; this result is in line with the very low HR value shown in Table 3.4. The low hydraulic property of both bottom ashes is due to the existence of the high amount of crystalline phases, such as SiO_2 and $CaCO_3$ (Figure 3.8) (Saikia et al., 2008).

Figure 3.12 shows that the profiles of the heat release rate during cement hydration of samples with cement and MF-BAW or MF-BAM are very similar to each other. For the cement samples mixed with MF-BAW or MF-BAM the last three stages of cement hydration is retarded and each reaction stage is extended. The more MF-BAW or MF-BAM is added, the longer the retardation effect is observed on cement hydration. For samples with 20%, 30% and 40% MF-BAW or MF-BAM, there is a heat release peak observed after about 26 hours of hydration, as shown in Figure 3.12, position 1, 2, 3 on different curves in the deceleration stage of cement hydration. According to (Bullard et al., 2011; Jansen et al., 2012), these peaks refer to the dissolution of C_3A and the precipitation of ettringite, which is defined as "sulphate depletion peak" because of the participation of sulphate to the reaction. Therefore, it can be concluded that adding bottom ash enhances the reaction of sulphate.

The observed influence of bottom ashes on the cement hydration can be explained as follows: (1) the heavy metals such as Cu, Pb, Zn, etc. may disturb the cement hydration (Weeks et al., 2008); (2) the bottom ash contains a certain amount of organic matter, mainly fulvic and humic acids as reported by Arickx et al. (2007), which may have a retardation effect on cement hydration; (3) the high amount of $CaSO_4$ present in bottom ashes enhances the sulphate participation in the deceleration stage of cement hydration.

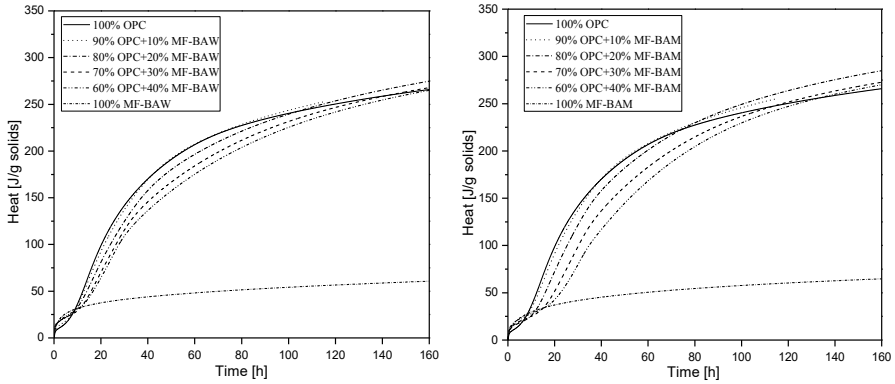

Figure 3.13: Released heat normalized to the total mass of solids

Figure 3.13 shows the cumulative heat released by the samples with MF-BAW or MF-BAM, compared with plain OPC. The cumulative heat generated by the samples was computed starting from the inflexion point when the heat flow starts to rise again after the initial drop, in order to reduce the influence of sample preparation (Florea et al., 2014) (in Figure 3.12, position 4). Figure 3.13 also reveals that the total heat release from the samples with MF-BAW or MF-BAM after the same hydration time is lower than plain OPC and decreases with an increasing amount of bottom ash.

Samples with plain MF-BAW or MF-BAM have the lowest total generated heat. It is known that the reaction of metallic aluminium with alkaline solutions generates 50 - 70 kJ/mol of heat (Porciúncula et al., 2012). Therefore, it can be calculated that the metallic aluminium can produce 13 - 18 J or 7 - 9 J of heat per gram of MF-BAW or MF-BAM, respectively. Thus, there is about 25 - 35% and 13 - 16% of the total heat released from samples of plain MF-BAW or MF-BAM, respectively, due to the reaction of aluminium. The other part of the total heat released can be attributed to the hydraulic reaction of MF-BAW or MF-BAM.

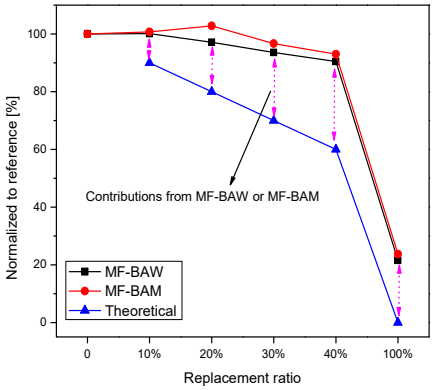

Figure 3.14: The total heat released after 111 hours from the solid mixtures normalized to the reference (100% OPC), and the related to the replacement ratios of OPC by MF-BAW or MF-BAM, and the theoretical total heat released if the added material has no heat contribution

It can be observed in Figure 3.14 that the samples with 10% MF-BAW or MF-BAM and 20% MF-BAM achieve higher cumulative heat than plain OPC, which indicates the contribution of bottom ashes to cement hydration. For samples with 30% and 40% MF-BAW or MF-BAM, the generated heat decreases. However, compared with the replacement level, the reduction of cumulative heat is lower (e.g. 20% MF-BAW with 80% OPC generated relative 97.1% heat of the reference, instead of 80%), which indicates the contribution of bottom ashes.

The calorimetric results show that the MF-BAW and MF-BAM have low hydraulic activities, and their addition to cement leads to the retardation of cement hydration. 10% replacement of cement by bottom ashes can still have comparable or even higher total heat release, hence, future studies can focus on its application in concrete. However, for higher replacement levels, the activity of bottom ashes should be increased in order to reduce its influence on cement hydration. Moreover, proper treatments should be considered in order to reduce the retarding effect of bottom ashes on cement hydration (which is studied in the next chapter).

3.3.5 Leaching behaviour evaluation of MSWI bottom ashes

The total amount of heavy metals from MSWI bottom ashes and their leaching concentrations obtained from historical data are summarized in this section. The total amounts of heavy metals in BAW and BAM are shown in Table 3.8 data obtained from historical tests. The concentration of the heavy metals in BAW and BAM is relatively similar, while BAW has a slightly higher content of antimony (Sb), copper (Cu) and Zinc (Zn) than BAM, and the amount of Mo in BAM is slightly higher than that in BAW.

Table 3.8: The total heavy metal concentration in BAW and BAM

Element	BAW		BAM	
	Range of metal concentration (2005 - 2011)	Average	Range of metal concentration (2005 - 2007)	Average
	mg/kg d.m.		mg/kg d.m.	
Antimony (Sb)	44 - 160	71.3	25 - 56	42.8
Arsenic (As)	5.6 - 10	8.55	4.3 - 8.3	6.68
Cadmium (Cd)	4.6 - 43	11.46	5.6 - 74	21.7
Chromium (Cr)	130 - 250	175	140 - 300	186
Cobalt (Co)	15 - 53	22.2	14 - 28	21
Copper (Cu)	2600 - 11000	4620	2700 - 3900	3280
Lead (Pb)	750 - 2200	1374	990 - 2500	1438
Manganese (Mn)	370 - 1600	744	550 - 990	782.5
Molybdenum (Mo)	5.5 - 9.3	7.8	8 - 11	9.24
Nickel (Ni)	120 - 190	149	110 - 210	162
Vanadium (V)	21 - 27	23.7	21 - 30	24.2
Zinc (Zn)	2300 - 5200	3160	1800 - 3200	2480

The comparison of the historical leaching data with the limit values (in Table 2.1) from SQD (2013) indicates that the BAW and BAM are well under the IMC building material requirements. Hence, both bottom ashes could be potentially used as road base material in combination with insulation layers. Nevertheless, when compared with non-shaped materials emission limit values, the emission of the heavy metals is all well under the limit value of the non-shaped category, except Sb and Cu for BAW and Cu for BAM. In addition, the leaching of chloride and sulphate in both BAW and BAM exceed the relevant limit values. Hereby, the leaching data of these components are illustrated in Figures 3.15- 3.18.

The maximum copper leaching value for non-shaped building materials is 0.9 mg/kg dry matter (d.m.). It can be seen in Figure 3.15 that the leaching of copper from BAW and BAM varies and generally exceeds the limit value most of the time. Furthermore, the copper leaching from BAW is relatively higher than that from BAM. The annual average leaching value of Cu in BAW is approximately 3 - 12 times the limit value, while for BAM is 2.5 - 4 times the limit value.

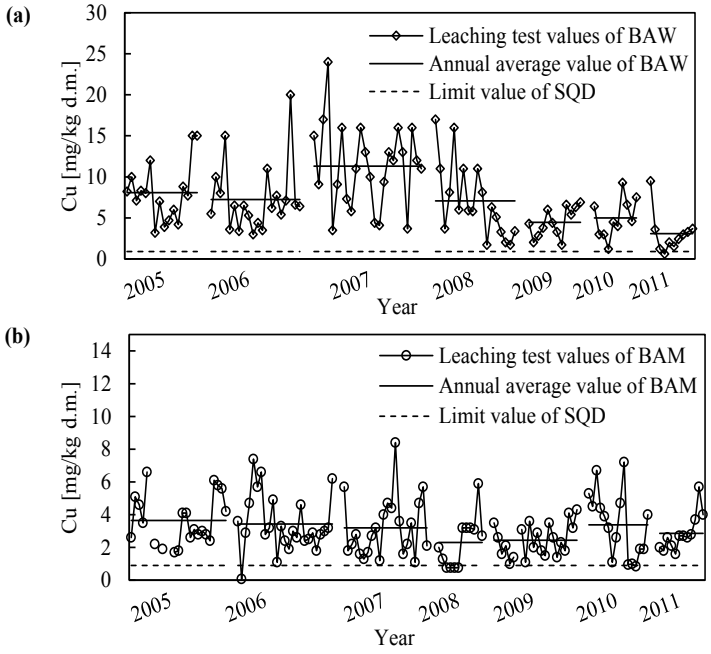

Figure 3.15: The leaching data of copper of (a) BAW and (b) BAM

Figure 3.16 shows the antimony emission from BAW in the column leaching test. The antimony leaching for BAM is always under the limit emission value, hence, only the leaching of BAW is shown here. It can be seen that the antimony leaching in BAW fluctuates along with time and the annual average value has a slight increasing trend since 2005 (around 1 - 3.4 times the limit value).

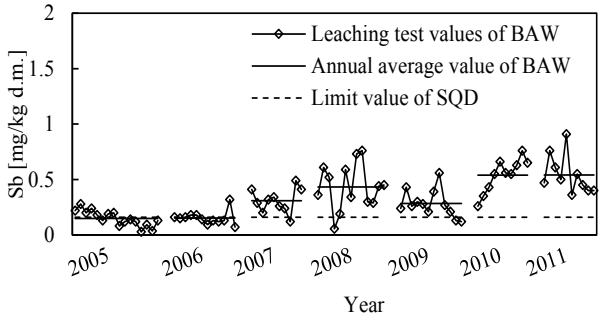

Figure 3.16: The leaching data of antimony of BAW and BAM

The leaching of chloride from BAW frequently exceeds the limit value (Figure 3.17 (a)). The annual average emission value is about 2.4 - 5.5 times the limit value, and since 2008 the value is lower than in previous years. Compared with BAW, BAM has a higher leaching

value of Cl^- and the annual average value is around 4.8 - 6.6 times the limit value (Figure 3.17 (b)).

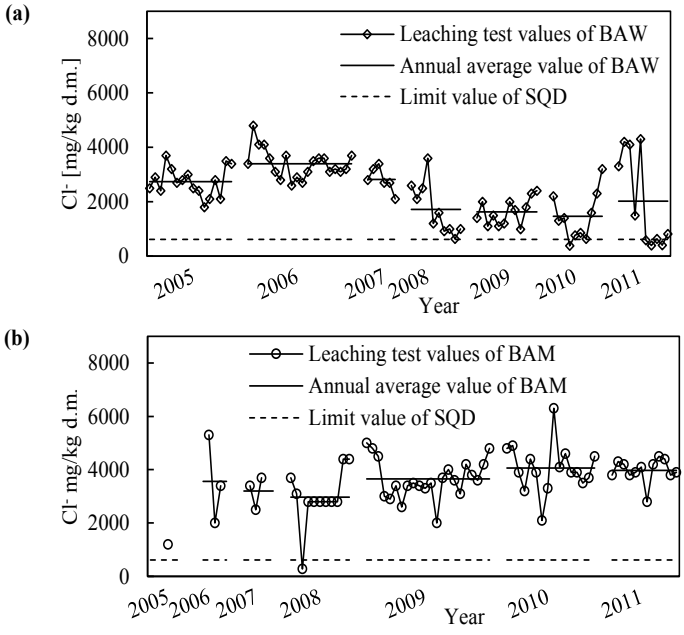

Figure 3.17: The leaching data of chloride of (a) BAW and (b) BAM

The leaching of sulphate from BAW and BAM is shown in Figure 3.18 (a) and (b), respectively. The sulphate emission from BAW always exceeds the limit level, and has an increasing trend since 2006. The annual average value is approximately 1.7 - 5.7 times the limit value. The sulphate leaching of BAM seems lower than that of BAW, and the maximum annual average value is 3.6 times the limit.

It can be noticed from the above analysis that, for using the bottom ashes as non-shaped material, the problematic leaching elements are very similar. Moreover, the emission level of copper, antimony, sulphate of BAW is higher, while BAM has higher chloride emission levels.

To understand the factors contributing to the abovementioned leaching differences between BAW and BAM, and initially provide potential treatments, the leachability of the problematic leaching elements was determined based on their total amount in bottom ashes and the amount released in the leachate using Eq. (3.8) (Table 3.9). It is described in Table 3.9 that BAW contains a higher amount of Sb, and its average value is also higher than that of BAM. The leachability of antimony in BAW is 1.8 times that in BAM, which indicates the antimony in BAW is more leachable than in BAM. Hence, if a water washing treatment is applied to reduce the amount of Sb in bottom ash, it could be expected that BAW would

have a better washing efficiency. According to the previous research, the leaching of copper from MSWI bottom ash is related with the organic matter content (Arickx et al., 2010). Hence, the slightly higher leachability of copper in BAW than in BAM could be explained as a result of a higher amount of organic matter. This is further proved by the higher LOI value of BAW than BAM (Figure 3.7).

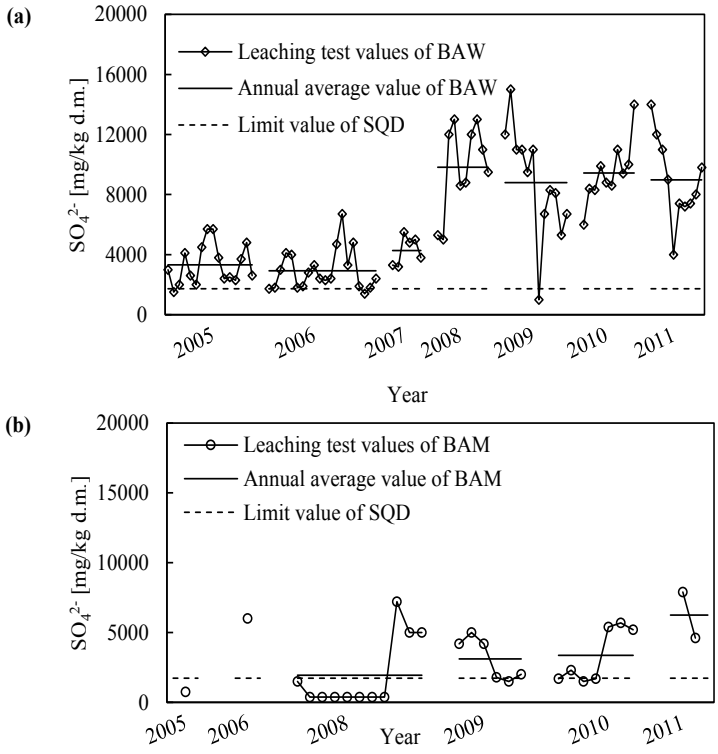

Figure 3.18: The leaching data of sulphate of (a) BAW and (b) BAM

The available data of the total amount of chloride and sulphate in BAW and BAM is limited. However, the data shown in Table 3.9 briefly indicates the extremely high leachability of the chloride and sulphate in both bottom ashes. Hence, the washing efficiency could be expected to be the highest among other leachable elements in bottom ash. This is in line with the findings presented in other studies (Cossu et al., 2012). The leachability of Sb and Cu seems positively related to their total contents in MSWI bottom ash.

The study on the leaching behaviour of BAW and BAM along with time shows that the leaching of most elements is well under the limit value of the legislation, only copper, antimony, chloride and sulphate exceed the limit. For both BAW and BAM, despite the different raw solid waste and different incineration method, the leaching contaminants are the same. Hence, future studies should focus on the investigation of influential factors on

copper, antimony, chloride and sulphate leaching from the bottom ash, and then potential treatments can be suggested.

Table 3.9: The leachability of Sb, Cu, Cl^- and SO_4^{2-} in BAW and BAM

Components	Sb		Cu		Cl^-		SO_4^{2-}	
[mg/kg d.m.]	BAW	BAM	BAW	BAM	BAW	BAM	BAW	BAM
Total amount	44 - 160	25 - 56	2600 - 11000	2700 - 3900	2600 (2400*)	3600	5100 (6100*)	4700
Average Value	71.30	42.80	4620	3280	-	-	-	-
Leaching value	0.055 - 0.76	0.08 - 0.16	1.2 - 20	0.99 - 8.4	380 - 4300 (3000*)	280 - 6300	1000 - 15000 (5700*)	380 - 7900
Average value	0.37	0.12	7.37	4.18	-	-	-	-
Leachability [%]	0.11 - 1	0.19 - 0.52	0.03 - 0.54	0.03 - 0.22	- (1*)	-	- (0.9*)	-
Average value	0.59	0.33	0.18	0.12	-	-	-	-

(*) The data tested in 2005; -: not available.

3.4 Conclusions and recommendations

This chapter presents the characteristics of MSWI bottom ashes from two waste-to-energy plants with different facilities in the Netherlands. The leaching behaviour of both bottom ashes was investigated by analysing seven years of leaching data. The application potential of the bottom ash fines (< 2 mm, MF-BA) was studied experimentally. From the results illustrated in this chapter, the following conclusions can be formulated:

(1) The physical and chemical properties of the bottom ashes from both waste-to-energy plants were stable over time and were very similar with each other, despite different production processes. The coarse bottom ash particles had a higher water absorption than natural aggregate and recycled concrete aggregate.

(2) The dominant oxides found in the bottom ashes are SiO_2, CaO, Al_2O_3 and Fe_2O_3, and the main crystalline phases in BAW are quartz (SiO_2), calcite ($CaCO_3$), hematite (Fe_2O_3), zinc pyrophosphate ($Zn_2P_2O_7$) and anhydrite ($CaSO_4$), and SiO_2 as quartz is the main crystalline phase. And for BAM are SiO_2, $CaCO_3$, Fe_2O_3, $Ca_3Si_3O_9$ (wollastonite), $Zn_2P_2O_7$ and $CaSO_4$. Fine bottom ash particles below 2 mm contain higher amount of calcite and anhydrite. Based on the calculations of relevant parameters, these bottom ashes could possibly be used as correction material for clinker production. This possibility needs further research.

(3) The calorimetry results confirmed that the milled bottom ashes (milled from 0-2 mm to under 125 μm) had very low hydraulic activity and their addition to cement leaded to the retardation of cement hydration. 10% cement replacement by bottom ashes can reach comparable cumulative heat, while more than 20% replacement led to the decrease of total heat release. However, the addition of bottom ashes contributes to the total heat release of cement hydration.

(4) The MSWI bottom ash has a high amount of fine particles (< 125 μm) which leads to higher water absorption and eventually reduces the amount of water available to

react with cement and metallic aluminium in mortar. Hence, the fine bottom ashes (< 2 mm) used as sand replacement reduce the strength of mortars with no visible cracks on the mortar. Thus, zero-slump or roller-compacted concrete with low w/c ratio and higher porosity can be an option for the use of bottom ash as aggregate to avoid cracks.

(5) The leaching behaviour of bottom ashes was relatively stable over time. The leaching contaminants which exceed the legislative limit were copper, antimony, chloride and sulphate. Thus, a future study can be focused on the reduction of these specific contaminants from the investigated bottom ashes

Based on the findings of the present chapter, it can be concluded that the proper treatments are needed to improve the properties of the MSWI bottom ash in order to use it as building materials, which is investigated in the next chapter.

Chapter 4

4 Thermally activated MF-BA applied as binder substitute*

4.1 Introduction

The study in Chapter 3 showed that the milled MSWI fine bottom ash (MF-BA) had low reactivity and contained heavy metals and salts which exceed the leaching limit according to Dutch legislation (SQD, 2013). Hence, in this chapter, treatment was performed to improve the properties of the fine MSWI bottom ash.

Cement clinker production contributes highly to the worldwide CO_2 emission and continuous consumption of raw materials (Schneider et al., 2011; Uwasu et al., 2014). Considering the protection of the environment and sustainable development as a global focus, a reduction of the production and use of cement worldwide is meaningful. In recent years, a significant amount of research has been done on this topic, in which the application of secondary materials as cement replacement attract extensive attention (Antoni et al., 2012; Berryman et al., 2005; Tkaczewska et al., 2012; Xu et al., 2013). Furthermore, the successful use of fly ash and ground blast furnace slag in concrete promotes the research focus on other secondary materials as well, such as incineration wastes (Cheng, 2012; Lee et al., 2011; Lin & Lin, 2006; Siddique & Bennacer, 2012).

Several studies focused on the utilization of municipal solid waste incineration (MSWI) waste as binder, and it is reported that the milled bottom ash contributes very little to the cement hydration because of its low pozzolanic properties. According to the research of Li et al. (Li et al., 2012), 30% of cement replacement by bottom ash reduces the compressive strength of mortars by about 26% after 28 days. However, the leaching properties of the concrete with MSWI bottom ash as binder, performed under the environmental legislation, are well under the limit value of China legislation, which indicates the immobilization of the contaminants in concrete (Shi & Kan, 2009a). Therefore, it is considered that, if the reactivity of the MSWI bottom ash could be increased, its application as binder substitute would be facilitated.

According to previous research, thermal treatment on fine MSWI bottom ash should be an effective way of increasing its reactivity, as well as reducing its leaching concentration of heavy metals. As reported by Qiao et al. (2008b), the milled bottom ash is an inert material and thermal treatment at 800 ˚C decreased the loss on ignition (LOI) and decomposed calcite, subsequently increasing the reactivity of bottom ash by generating new active phases (mayenite - $Ca_{12}Al_{14}O_{33}$ and gehlenite - $Ca_2Al_2SiO_7$). Furthermore, thermal treatments of bottom ash are also proven to be efficient to reduce the leaching of heavy metals (such as Cu and Pb), because of the burning of organic matter, which corresponds

*Content of this chapter was published elsewhere [Tang, P., Florea, M.V.A., Spiesz, P., and Brouwers, H.J.H., (2016) Cem. Concr. Compos., 70, 194–205].

to the leaching of heavy metals (Arickx et al., 2007; Hyks et al., 2011). There are multiple studies on the properties, treatment and application of MSWI wastes (Li et al., 2004; Lin & Lin, 2006; Pera et al., 1997; Van der Sloot et al., 2001; Yao et al., 2010b). However, research focused on the treatment and activation of MSWI bottom ash fines (0 - 2 mm) is scarce.

Hence, this chapter shows the evaluation of the activation of MSWI fine bottom ash (0 - 2 mm) by thermal treatment, and its application as cement substitute in mortar. The characteristics of the treated bottom ash samples are determined and the hydration of the cement with treated bottom ash additions are investigated. Furthermore, the mechanical properties of mortars with treated bottom ash are analysed after different curing times. Finally, the environmental influence of the bottom ash-containing mortar is evaluated through leaching tests.

4.2 Materials and methods

4.2.1 Materials and treatments

The MSWI bottom ash (IBA) used in this chapter is provided by the waste-to-energy plant (Attero) in Wijster, the Netherlands. In this chapter, the bottom ash fines below 2 mm (F-BAW) from the received bottom ash were chosen to be investigated.

The F-BAW was milled into powder to reduce its particle size and make it more homogenous using a planetary ball mill, labelled as MF-BAW. Thermal treatment was performed on the F-BAW and the MF-BAW in the muffle furnace for 24 hours, and the temperatures chosen were 550 ˚C and 750 ˚C, based on the research in (Qiao et al., 2008b; Shi & Kan, 2009a), the heating capacity of the incinerator, and the temperature used to determine the loss on ignition (LOI) (NEN-EN 1744-7, 2010). Thermal treatment at 550 ˚C was performed on the F-BAW before and after milling separately to investigate the influence of treatment order on the bottom ash properties.

It is hypothesized that the IBA particles are covered by dust-like powders, which contain higher amounts of soluble contaminants, and can have a higher reactivity than the particle itself. In order to separate the fine powder attached on the surface of bottom ash particles for investigation, lower speed and short duration of milling were applied during the milling procedure. The treatments procedure is described as follows (Figure 4.1):

- Method 1 is to mill the F-BAW using a planetary ball mill with fixed milling duration and speed in order to reduce the particle size to a maximum 125 μm; the dark-grey powder obtained is labelled as MF-BAW.
- Method 2 and Method 3 are to thermally treat the milled bottom ash after Method 1 at 550 ˚C and 750 ˚C, respectively; reddish-brown powders are obtained, labelled as M5T and M7T, respectively.

- Method 4 is to heat the bottom ash particles at 550 ˚C firstly and then mill them using the same milling procedure as in Method 1, listed as 5TM.
- Method 5 is to mill the thermally treated bottom ash (at 550 ˚C) at shorter duration and lower speed compared to Method 1, followed by a sieving step to select the material below 63 µm (5TMS); particles above 63 µm are labelled as 5TMS^{+}. Due to the fact that the dust or powder attached on the bottom ash particles could not be removed manually one by one or by machine evenly, the lower speed milling procedure was used in order to remove the attached powder from the particle surface using the friction between the particles. The fines bellow 63 µm are chosen to be investigated in order to distinguish the powder from the crushed bigger particles during the milling.

The binder used in the work of this chapter was CEM I 52.5 R (Table 4.1) from ENCI HeidelbergCement (the Netherlands) and the sand was CEN normalized sand 0 - 2 mm according to EN 196-1 (2005).

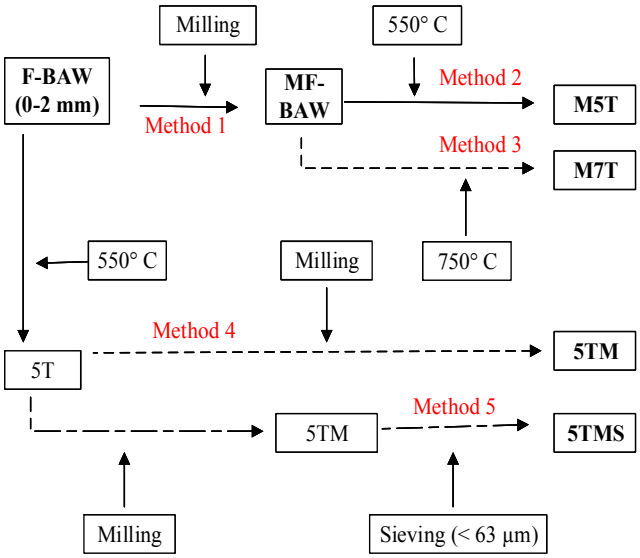

Figure 4.1: The schematic description of treatment procedures on F-BAW and sample preparation

4.2.2 Analysis of material properties

The chemical compositions and crystalline phases of the treated bottom ash and other materials are determined by XRF and XRD, receptively, as described in Section 3.2.2. The particle surface properties of the investigated materials were observed by scanning electron microscope (SEM, Quanta 650 FEG, FEI) and optical microscopy. The particle size distribution (PSD) of all materials considered in this chapter was measured by laser

diffraction (Mastersizer 2000 Malvern), and a helium pycnometer (AccuPyc II 1340) was used to measure the specific densities. The content of metallic aluminium in the bottom ashes are determined using the method described in Section 3.2.2.

4.2.3 Hydration properties study

The effect of the treated bottom ash on the cement hydration was investigated using an isothermal calorimeter (eight-channel TAM Air, Thermometric) as described in Section 3.2.2. Previous studies on the bottom ash show that its use as cement replacement is better to be limited under 30% (Al-Rawas et al., 2005; Juric et al., 2006; Li et al., 2012). Therefore, the treated bottom ash is mixed with cement with the mass ratio of 3:7, and the water to binder ratio is kept at 0.7, considering the loading of the samples into the ampoules. Cement pastes containing different treated bottom ashes were cured in water at 20 ˚C for 7 days, and subsequently small pieces were extracted from the hardened samples and dried with acetone. The 7-days samples were milled and the crystalline phases were investigated by XRD.

4.2.4 Mechanical strength of mortar samples

The treated bottom ash is pre-mixed with cement in a 3:7 ratio, and the mortar samples were prepared according to EN 196-1 (2005). The flowability of the fresh mortars was determined using the flow table test according to EN 1015-3 (2007). The test of compressive and flexural strengths of mortar samples after different curing ages were performed under the same procedure as described in Section 3.2.2. The obtained values were expressed as the averages of three samples.

4.2.5 Leaching behaviour evaluation

The environmental impact of the fine bottom ashes before and after treatment and mortars with these bottom ashes were evaluated by column leaching test with the same methods described in Section 3.2.2.

4.3 Results and discussions

4.3.1 Properties of materials

As presented in Figure 4.2 (a) and according to the study in Chapter 3, the raw F-BAW is a fraction with a similar particle size to sand (Figure 4.3 (a)), and has a dark-grey colour. There are quartz particles, iron, glass particles, as well as heterogeneous particles visually observed in bottom ash. Generally, these F-BAW particles are covered by a dust-like layer. It is noticed that after the thermal treatment the colour changed to reddish and iron oxide particles could be observed. The dust-like layer of particles still exists on the particles' surface, as shown in Figure 4.2 (b).

According to a previous study (Saffarzadeh et al., 2011), after water quenching, the bottom ash particles consist of about 60% particles which were coated by fine particles and other

melted phases. This coat on the bottom ash particles results from the reaction occurred during the rapid water quenching process (Yang et al., 2013), which influences the leaching properties of the bottom ash.

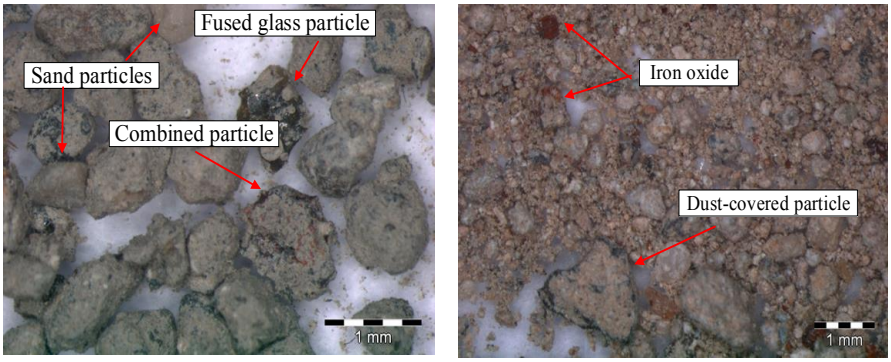

(a) **(b)**

Figure 4.2: MSWI bottom ash particles (a) before and (b) after 550 °C thermal treatment

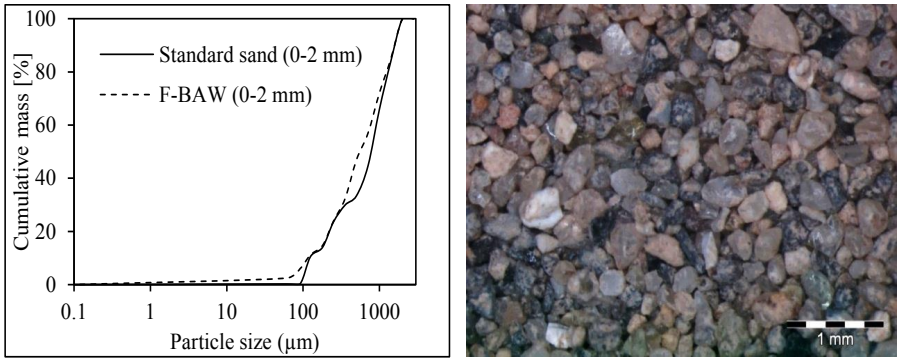

(a) **(b)**

Figure 4.3: (a) Particle size distribution and (b) F-BAW after treatment following Method 5 (particles above 63 µm)

After treatment following Method 5 (Figure 4.1), the bottom ash particles under 63 µm account for 34.7% wt. of the milled bottom ash (compared to the initial 2.4% wt.). The particles above 63 µm shown in Figure 4.3 (b) have a relatively cleaner surface than untreated and thermally treated bottom ashes (Figure 4.2 (a), as the attached dust-like layers on the surface were partially removed due to the friction during milling. Furthermore, these particles are predominantly sand, glass, and iron particles; and some plate-shaped metals were also observed (Figure 4.4 is shown as an example).

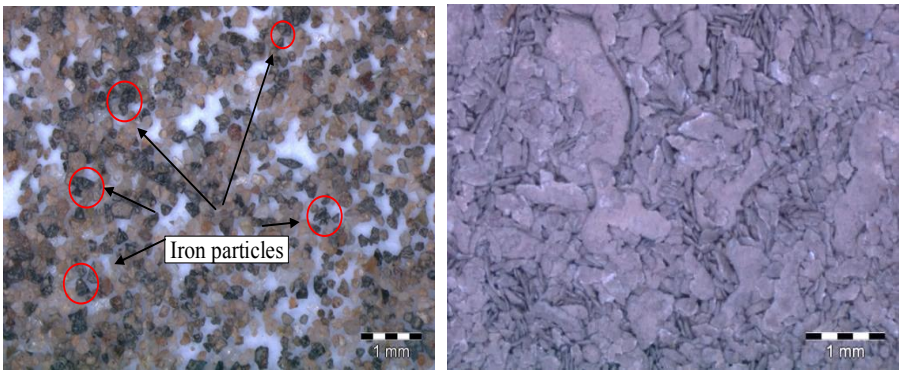

(a) (b)

Figure 4.4: (a) Iron particles and (b) plate-shaped metals sieved out in bottom ash particles above 180 µm after treatment using Method 5

- **Chemical properties**

The chemical compositions of the cement and treated bottom ashes are presented in Table 4.1. The treated bottom ashes consist of the same main oxides as cement (as assumed by XRF), and their main constituents belong to the SiO_2-CaO-Al_2O_3-Fe_2O_3 system, which in total accounts for about 70% - 90% wt. of the bottom ash (Li et al., 2012). However, the treated bottom ashes contain higher amounts of equivalent SiO_2 and less CaO than cement, and the content of Al_2O_3 and Fe_2O_3 is relatively high. A considerable amount of alkali and alkali-earth oxides, such as Na_2O and K_2O, MgO etc. exist in the treated bottom ashes. Similar results are reported elsewhere (Song et al., 2004; Del Valle-Zermeño et al., 2013).

Comparing the samples MF-BAW, M5T and M7T, it can be observed that the content of Cl slightly decreased after the thermal treatment; moreover, a higher temperature leads to a higher decrease of its content. This result is in consistence with the finding shown in (Yang et al., 2013; Yudovich & Ketris, 2006). In addition, this decrease is more noticeable when the thermal treatment is undertaken after the milling of bottom ash. As reported by Yang et al. (Yang et al., 2013) the Cl content is relatively higher in the heterogeneous particles in bottom ash formed during the water quenching procedure, which are unstable under thermal conditions. Therefore, the decomposition of quenched phases in these heterogeneous particles during the heating released the evaporable Cl. Moreover, the organic matter is burnt out during the thermal treatment, thus the organic-associated Cl (Yudovich & Ketris, 2006) is evaporated. Furthermore, the milling increases the particle surface area, leading to the even and efficient heating of the samples, subsequently enhancing the Cl evaporation from the samples.

As expected, due to the larger specific surface area, the pre-milling before heating will increase the thermal treatment efficiency, proved by the lower loss on ignition of M5T and M7T than the one of 5TM. In this chapter, the difference between samples which were pre-

milled and which were directly thermally treated is quantified through metallic Al content determination and mechanical strength of hardened mortars.

Table 4.1: Chemical components and densities of CEM I 52.5 R, MF-BAW, M5T, M7T, 5TM, 5TMS and 5TMS$^+$

Chemical components [% wt.]	CEM I 52.5 R	MF-BAW	M5T	M7T	5TM	5TMS	5TMS$^+$
SiO_2	17.11	35.98	40.55	41.20	35.80	24.49	50.74
CaO	64.99	19.34	19.49	20.03	21.67	28.29	16.02
Al_2O_3	3.80	9.00	9.44	9.82	9.93	11.07	8.64
Fe_2O_3	3.59	11.54	11.74	12.09	12.26	8.99	13.48
MgO	1.56	1.81	1.97	2.09	1.99	2.26	1.92
Na_2O	0.00	1.35	1.49	1.89	1.48	1.37	1.59
K_2O	0.16	1.15	0.94	1.09	1.10	1.22	1.06
CuO	0.02	0.43	0.50	0.53	0.55	0.65	0.48
ZnO	0.15	0.80	0.79	0.82	0.91	1.16	0.71
P_2O_5	0.63	1.02	1.07	1.14	1.13	1.12	1.12
TiO_2	0.27	1.11	1.13	1.16	1.15	1.31	1.14
MnO	0.09	0.16	0.17	0.17	0.18	0.19	0.17
Cl	0.02	0.66	0.64	0.56	0.74	1.06	0.43
SO_3	3.96	4.95	5.24	5.23	5.87	8.82	2.51
Other	2.01	0.69	1.19	0.71	1.31	1.10	*
LOI (550 °C)	0.41	7.37	2.02	1.16	2.86	2.54	*
LOI (950 °C)	1.64	9.99	3.66	1.46	3.93	6.90	*
Density [g/cm^3]	3.10	2.74	2.91	2.97	2.87	2.85	*

*: not detected or tested

Differently from other treated bottom ash samples in this chapter, 5TMS has a relatively higher content of CaO and Al_2O_3, and lower content of SiO_2 and Fe_2O_3. Moreover, its Cl and SO_3 contents are also the highest among all the studied bottom ash samples. According to the literature (Chimenos et al., 2003; Yao et al., 2013), the chemical compositions of MSWI bottom ash differ by size fraction, especially for SiO_2 and CaO. The finer bottom ash particles have higher and lower contents of SiO_2 and CaO, respectively, and this is further confirmed by comparing 5TMS and 5TMS$^+$. Additionally, the content of Cl and SO_3 in 5TMS is almost 1.5 times of that in other treated bottom ash samples in this study. Also, the dust-like layer removed from the bottom ash particles contains a higher amount of Cl than the bottom ash particles themselves, which is in line with the findings in (Chen & Chiou, 2007; Song et al., 2004). The fine bottom ash particles have higher amounts of chlorides and sulphates due to the large specific surface aggregated on the surface of coarse bottom ash particles during the water cooling procedure, as shown in Figure 4.2. As also explained in (Saffarzadeh et al., 2011), the newly formed phases on the surface layer during water cooling and weathering enhanced the absorption sites of chloride and sulphate as well. It is commonly known (Chimenos et al., 2003) that the fine particles contain higher

amount of contaminates due to the large specific area of the particles. However, the comparison of 5TMS and 5TMS^{+} shows that the finer particles or dust layers sticking on the particle surfaces contribute to the higher amount of contaminants in the F-BAW. The same trend is observed for heavy metals (details are discussed in Section 4.3.4). Hence, the prevention of the finer dust sticking on the coarse particle might decrease the content of contaminants in MSWI bottom ash.

Figure 4.5 illustrates the X-ray diffractograms of the investigated samples. The identified predominant crystalline phases are quartz (SiO_2), anhydrite ($CaSO_4$), calcite ($CaCO_3$), hematite (Fe_2O_3) and magnetite (Fe_3O_4). The samples after thermal treatment have a relatively higher peak at about 26.6˚, which represents the main quartz peak. This result is consistent with the investigation of Qiao et al. (2008b). Furthermore, the peak heights corresponding to hematite and magnetite increased, especially in sample M7T. This should be attributed to the fact that heating results in the oxidation of iron in MF-BAW (as shown in Figures 4.2 and 4.4 (b)), and a higher temperature could enhance this oxidation. It is noticed that the calcite peaks decreased after the 550 ˚C thermal treatment, and are not present in sample M7T, which results from the decomposition of calcite at high temperature (Gabrovšek et al., 2006; Qiao et al., 2008c).

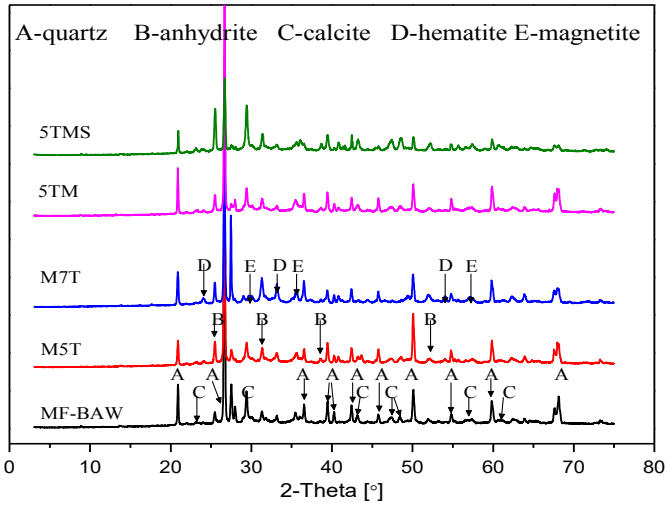

Figure 4.5: XRD diffractograms of the treated bottom ash samples

Qualitatively no significant differences can be observed between 5TMS, 5TM and M5T in the X-ray diffractrograms. Nevertheless, in 5TMS, the quartz peak height is the lowest, this result is in line with the chemical compositions determined in this study (in Table 4.1, where 5TMS is shown to have 24.5% SiO_2, compared to 35.8% and 40.5% for 5TM and M5T, respectively). In addition, the peaks corresponding to anhydrite ($CaSO_4$) and calcite ($CaCO_3$) here are much higher than in other samples. Based on the chemical composition

of this sample, it could be concluded that part of the higher amount of the CaO (about 28% compared to 16-21.7% in other MF-BAW samples in Table 4.1) can be attributed to the anhydrite ($CaSO_4$) and calcite ($CaCO_3$), and the high amount of SO_3 (about 8.8% compared to 2.5-5.9% in other F-BAW samples in Table 4.1) might be related to the amount of anhydrite.

To summarize, the MF-BAW mainly contains crystalline phases like quartz, anhydrite, calcite and hematite, and there is no significant change after 550˚C thermal treatment. However, higher temperatures (around 750˚C) enhance the iron oxidation and decomposition of calcite in MF-BAW. Samples 5TMS, consisting of the fine powder in F-BAW and the dust-like layer on the particles, possess lower quartz and higher calcite and anhydrite contents and they also contain higher concentrations of Cl and SO_3. Hence, the feasible method to prevent or separate the fine powders sticking on the coarse bottom ash particles is an interesting topic.

- **Metallic Al**

The amount of metallic Al in the investigated samples is determined as explained in Section 3.2.2. The results are presented in Table 4.2.

Table 4.2. Metallic aluminum content of bottom ash samples

Sample	MF-BAW	5TM	M7T	5TMS
Metallic Al [% wt.]	0.44	0.48	0.46	< 0.2

It is apparent that the metallic Al content did not change significantly after the thermal treatment. M7T has slightly less metallic Al than 5TM. This should be due to the fact that the higher temperature enhances the oxidation of the metallic Al. 5TMS contains relatively less metallic Al than all the other investigated samples. This can be due to numbers of reasons: (1) the metallic Al in the original bottom ash particles under 63 µm is quite easily oxidized during the heating period; (2) due to the good ductility of the metallic Al, it is deformed into plate-shape particles through the action of the milling balls (as shown in Figure 4.4 (b)), thus enlarging its surface, and consequently making it possible to be sieved out. Therefore, to consider the removal and recovery of metallic Al in the fine bottom ash fraction, special milling equipment should be used, such as an impact mill.

- **Physical properties**

Figure 4.6 illustrates the SEM images of M5T and 5TMS as examples. It can be seen that most of the treated bottom ash particles have irregular shapes, which is a typical characteristic of the milled bottom ash. Moreover, the surface of the particles has flocculent matter attached to the particles, as reported in (Li et al., 2012).

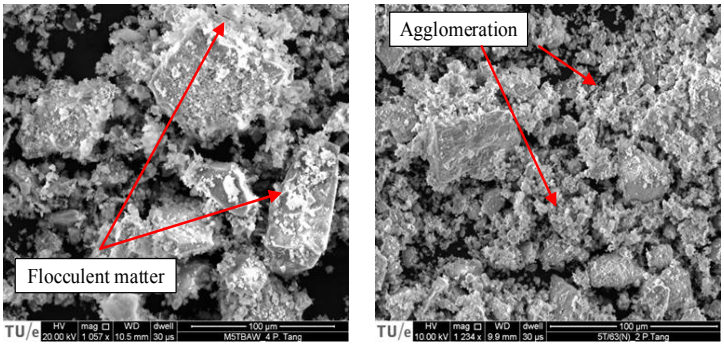

Figure 4.6: SEM images of (a) M5T and (b) 5TMS

The specific densities of the samples are shown in Table 4.1. Sample MF-BAW has a slightly higher density than standard qualified quartz sand, which is about 2.65 g/cm^3. This is due to the fact that, besides other oxides, there are metals and ceramics in the F-BAW which could not be separated completely. The densities of thermally treated bottom ash increased. Moreover, a higher treatment temperature results in a higher density. The variation of the density after thermal treatment can be attributed to the combined effect of two opposing processes: burning out of the organic matter and the oxidation of the metals. The density of 5TMS is lower than other thermally treated samples in this study, which could be due to the removal of iron and quartz particles during sieving (Figure 4.4), as previously explained.

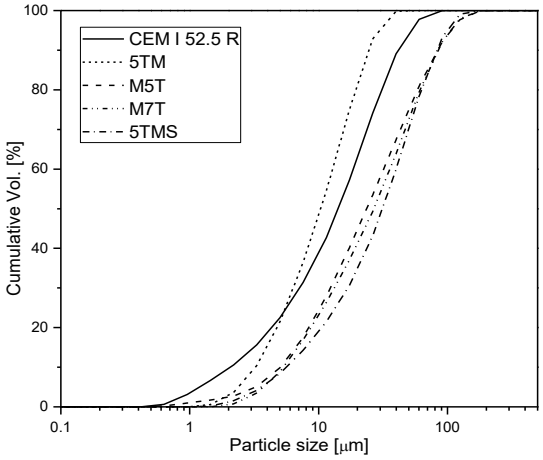

Figure 4.7: The particle size distributions (PSDs) of the investigated materials.

Figure 4.7 presents the particle size distributions of the analysed materials. It can be observed that all the samples are coarser than cement powder, 5TM excepted. Moreover,

the thermal treatment on milled samples results in a coarse particle size, which is due to the agglomeration of fine particles during the thermal treatment (Qiao et al., 2008a). In addition, the flocculent matter on the particles contributes partly to this phenomenon (Figure 4.6 (a)). According to the measured PSD, sample 5TMS has coarser particles compared with other bottom ash samples analysed in this study. However, this is a surprising result, because the 5TMS is composed of particles passing through the 63 µm sieve. This could be because of the agglomeration of the powder (Figure 4.6 (b)), which in turn can be caused by the electrostatic interaction of particles.

To summarize, the order of milling and thermal treatment affects the particle size distribution of the samples. The high temperature of the thermal treatment on MF-BAW contributes to the decomposition of calcite. Moreover, short time and a lower speed milling process, plus sieving, could reduce the metallic aluminium content in the chosen sample.

4.3.2 Hydration properties of bottom ash-cement mixes

In order to evaluate the influence of the thermally treated bottom ash samples and their contribution to cement hydration, the heat development of cement with treated bottom ash (BA) during the hydration process is studied by calorimetry. The heat evaluation of the BA-cement mix, which is calculated based on a unit weight of CEM I 52.5 R, is depicted in Figure 4.8.

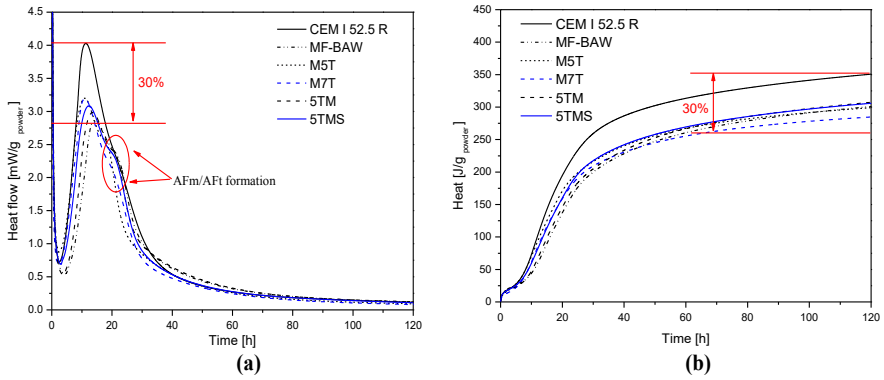

Figure 4.8: The heat evolution of cement with treated bottom ash relative to total solid

The hydration process of cement is typically divided into four periods, namely the initial stage, induction stage, acceleration stage and deceleration stage (Bullard et al., 2011). There is no difference in the aspect of the calorimetric curves of plain cement paste and BA-cement mixes (Figure 4.8 (a)). However, the additions of MF-BAW to cement lead to the retardation of cement hydration, so that the second maximum heat release rate (SMHR) is reached over three hours later than that of the cement paste.

For samples with 5TM, this retardation is reduced by around 48 minutes, and the maximum heat release rate is higher than that of plain cement and cement with sample MF-BAW.

This means that the 5TM has a more beneficial effect on the advancement of cement hydration than the MF-BAW samples. For samples with M5T and M7T, the maximum heat release rate is reached slightly earlier than in the case of plain cement. It can be noticed in Table 4.3 that the time needed for reaching the maximum heat release rate after the acceleration period of cement hydration has a similar trend with that of the loss on ignition of the bottom ash samples at 550 °C. The retardation effect of bottom ash on the cement hydration could be attributed to the organic matter contained in the bottom ash (Gineys et al., 2010; Medina et al., 2013a; Shi & Kan, 2009b). After the thermal treatment at this temperature, the organic matter is burned out, thus the retardation effect is reduced.

During the deceleration stage, there is a 'shoulder' on the hydration curve of samples with bottom ashes at around 17-25 hours. A similar 'shoulder' can also be observed on the net cement hydration curve during the deceleration stage at around 22-27 hours, however, this 'shoulder' is not clearly visible compared to the samples with bottom ashes.

According to (Bullard et al., 2011; Jansen et al., 2012), this 'shoulder' represents to the formation of the AFm phase in plain cement paste. During cement hydration (Bullard et al., 2011), the calcium aluminate (C_3A) reacts with calcium sulphate to form ettringite (AFt); after the calcium sulphate is completely consumed, due to the decrease of sulphate ions in the pore solution, the unstable ettringite converts to monosulphate; this normally occurs after 1 day or 2 after mixing of the cement paste; when a new source of sulphate ions become available in the pore solution, the monosulphate reacts to form ettringite again (Taylor, 1997). Therefore, in Figure 4.8, the shoulder for plain cement at 22-27 h represents the formation of AFm. In the XRD pattern shown in Figure 4.9 on the hydrated cement paste, and AFm phase is found, which also confirms this.

For the samples with ashes, there are several possibilities related to the sulphate consumption reaction. Firstly, the anhydrite in the ashes provides sulphates for the hydration of C_3A in the cement, which may result in more AFt formation (Taylor, 1997); secondly, the sulphate in the ashes does not have an influence on the reaction of C_3A, which means there will be AFm or little AFt found in the cement hydrates; thirdly, the sulphate in the ashes is a new resource for converting the AFm further to form AFt. Hence, the amount, dissolving rate and the type of the sulphate in the ashes are important parameters for its role in the cement reaction (Baur et al., 2004; Tishmack et al., 1999; Shen et al., 2013; Zajac et al., 2014). Therefore, the 'shoulder' for the samples with ashes could be attributed to the formation of AFt or AFm, which is mainly related to sulphate consumption during the cement hydration.

Figure 4.8 (b) and Table 4.3 show that the samples with bottom ashes achieved a higher total heat release after the same hydration duration compared to that of 30% of the total heat released from plain cement; the highest total heat is reached by samples with M5T,

followed by 5TMS, which indicates the extra reaction of samples with ashes compared with plain cement.

Table 4.2. Calorimetric parameters of cement hydration and LOI of the investigated sample

	CEM I 52.5 R	MF-BAW	5TM	M5T	M7T	5TMS
SMHR [hour]	11.32	14.38	13.61	11.00	11.11	12.31
MHR [mW/g_{cem}]	4.03	4.10	4.26	4.57	4.56	4.40
TH [J/g_{cem}]	366.65	453.18	461.62	444.39	422.17	457.15
LOI 550 °C [% wt.]	0.41	7.37	2.86	2.02	1.16	2.54

SMHR: second maximum heat release rate; MHR: maximum heat release rate; TH: Total heat after 168 hours.

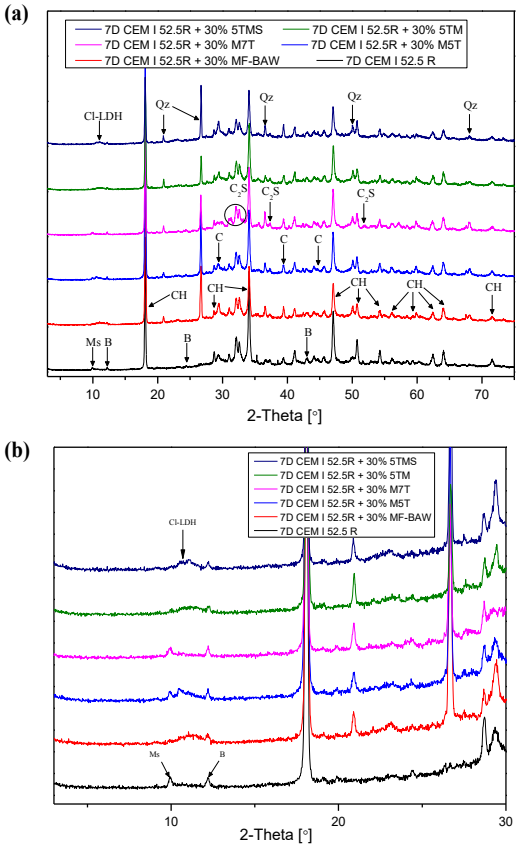

Figure 4.9: XRD diffractograms of the cement pastes with bottom ashes after 7-days hydration (a) 3-75° (b) 3-30° (Ms - monosulphate, B - brownmillite, C - calcite, CH - portlandite, Qz - quartz, C_2S - dicalcium silicate phase, Cl-LDH-chloride layered double hydroxide)

It can be seen from the XRD pattern (Figure 4.9) of the hydrated samples with and without ashes that there is AFm found in the samples of plain cement, M5T and M7T. However, for the other samples with ashes, there is no AFm or AFt found. Considering the calorimetry results together, it can be explained that the samples with M5T and M7T may

provide extra sulphate for cement to form AFm as explained above. For the other samples with ashes, the shoulder can be attributed to the second formation of AFt from AFm because of newly available sulphate; hence, these samples release a higher amount of heat during the cement hydration after 7 days. Also, due to the consumption of the AFm and the poor crystalline structure of AFm (Matschei et al., 2007), there is no AFm or AFt found in the XRD pattern of these samples.

Nevertheless, the hydration of cement is influenced by the organic content, the water to cement ratio, sulphate content, particle size distribution, etc.; thus, the results should not only be explained by a single parameter. However, the total released heat results indicate that the addition of bottom ashes partially contribute to the cement hydration. Moreover, the retardation effect on cement hydration might be reduced by heating the milled bottom ash samples.

4.3.3 Mortar properties

As previous research reported (Filipponi et al., 2003), the lower pozzolanic properties of MF-BAW and its retardation effect on cement hydration limit the amount to be used as cement replacement. Hence, based on literature, the replacement ratio of cement by treated bottom ashes is fixed at 30% in this study. The standard mortars are prepared according to EN 196-1 (2005), and the fresh and hardened states properties are tested. The results are shown in the following section.

- **Flowability of mortars with treated bottom ashes**

The test results show that the flowability of mortar measured by its spread according to the EN 1015-3 (2007) decreases when treated bottom ash is added, except for the sample with MF-BAW (175 mm, compared with 170 mm of the reference). 5TMS leads to the lowest flowability (160 mm), and M7T leads to a higher flowability (169 mm) than M5T (165 mm). However, the quantitative differences on the flowability of the mortars are not significantly affected by adding the treated bottom ashes.

It is commonly known that the particle size distribution, particle shape, and particle texture of the alternative powder influence the water demand and subsequently the flowability of fresh mortar (Jamkar & Rao, 2004; Li et al., 2012). Hence, according to the previous investigations shown in this chapter (Figures 4.5 and 4.6), these complex influential factors contribute to the phenomenon observed here.

- **Compressive and flexural strengths**

The compressive and flexural strengths of mortars containing bottom ash additions after various curing ages are displayed in Figures 4.10 and 4.11. It is demonstrated that both the compressive and flexural strengths of all the samples at all curing ages decrease (Li et al., 2012) when the treated bottom ash is applied. The mortar with 5TMS gains higher strength than other bottom ash-containing samples. Moreover, the decrease of the flexural strength

for all the samples is not as significant compared to the reduction of the compressive strength.

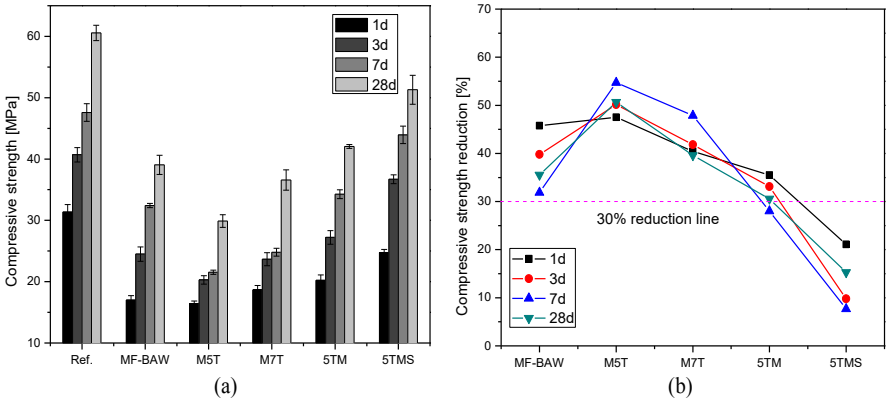

Figure 4.10: (a) Compressive strength of mortars containing bottom ashes after 1, 3, 7, 28 days curing and (b) its reduction percentage compared with reference

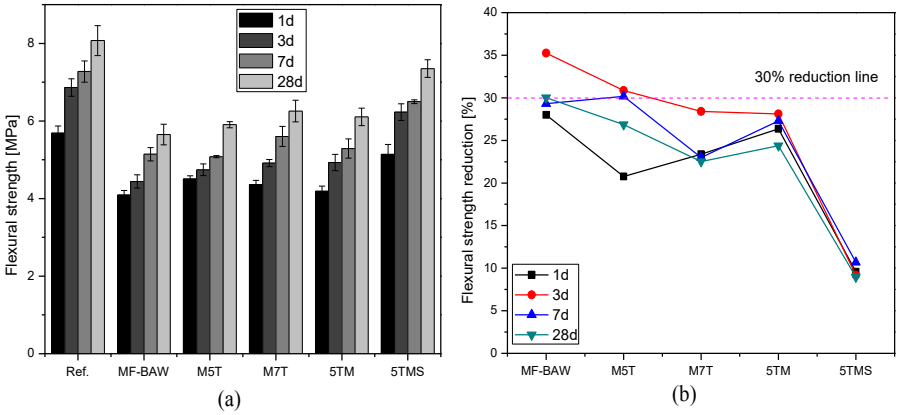

Figure 4.11: (a) Compressive strength of mortars containing bottom ashes after 1, 3, 7, 28 days' curing and (b) its reduction percentage compared with reference

For all the investigated samples, the compressive strength increases with increasing curing age. Furthermore, their differences to the reference are reducing with longer curing age. It is noticed that the mortar with 5TM gains higher compressive strength at all curing ages than the mortar with MF-BAW. This is attributed to the burning of organic matter in the MF-BAW at 550 °C, which decreases the detrimental effect on cement hydration. Additionally, after 28 days curing the decrease of compressive strength of the mortar with MF-BAW is about 36%, while only about 30% decreasing of the mortar with 5TM, indicating the detrimental influence of MF-BAW and 5TM. This is in agreement with the finding presented in Section 4.3.2.

However, the strength test results for the mortar with M5T and M7T are in conflict with the calorimetry results. These mortars have a relatively higher decrease of the compressive strength at all curing ages than other samples. For instance, after 28 days the compressive strength of mortar with M5T and M7T is about 30 MPa and 37 MPa, respectively (51% and 40% decrease compared with reference, respectively). Their strength is even lower than the one of the mortar with MF-BAW. This higher reduction should be due to the inner cracks in mortar (as shown in Figure 4.12) created by the gas generated upon the hardening of mortar. Nevertheless, inner cracks (Yu et al., 2014) are not found in mortar with MF-BAW, 5TM and 5TMS, of which the first two have similar contents of metallic Al. This could be explained as follows: the thermal treatment on the milled bottom ash powder is more efficient on burning out the organic matter, as well as causing the oxidation of metallic aluminium. Hence, after thermal treatment, the surface of the metallic Al particles is oxidized (Biganzoli et al., 2012). Subsequently the reaction between metallic Al and alkalis takes a longer time, and the gas generated later could not be released before the hardening of mortar. Eventually, inner cracks form, which reduce dramatically the strength of mortar.

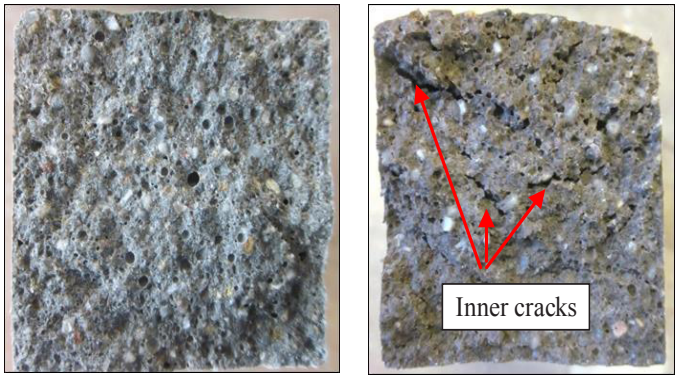

Figure 4.12: The fracture surface of mortars (reference and M5T)

Mortar with 5TMS gains the highest 28-days compressive strength, about 51 MPa, a 15% reduction compared to the reference. This result should be due to the following reasons: (1) the particle size of the 5TMS is controlled under 63 μm, which leads to a denser microstructure of the mortars; (2) it has the lowest metallic Al content in comparison with other treated bottom ash samples, in turn less inner cracks are generated; (3) it has a lower content of SiO_2 and a higher amount of CaO, which may participate in the cement hydration process.

The flexural strength of the mortar decreases after the adding of bottom ash samples; however, the effect of the treated bottom ash on the flexural strength is more complicated than for the compressive strength. The flexural strength is significantly influenced by the cement hydration (Singh & Siddique, 2013), and irregular particle shapes have a positive

effect on flexural strength. As the bottom ash has lower pozzolanic properties and more irregularly-shaped particles, part of the inert particles act as filler in the mortar matrix. Hence, there is a better inter-locking effect between the cement paste and these particles, which contributes to a lower reduction of the flexural strength (Figure 4.11). This finding is consistent with results reported by other researchers (Chen et al., 2011; Sheen et al., 2013).

To summarize, the cement blended with 30% MF-BAW could be used to produce low strength mortar, its compressive strength comparable with that reported previously (Li et al., 2012). The cement with 30% 5TMS could be used to produce a standard mortar which has a 28-day compressive strength of 51 MPa (compared to the 61 MPa reference). The addition of 30% of the treated bottom ashes to replace OPC shows a more than 30% reduction on the mortar strengths, except the use of 30% of sample 5TMS which has only 15% strength reduction, which demonstrates that it might be possible that 15% of 5TMS can be added to replace OPC without deteriorate influence on the mortar strength compared with 100% OPC, as the application of coal fly ash in mortar of concrete (examples shown in Chapter 5).

4.3.4 Leaching behaviour evaluation

- **Leaching properties**

The column leaching test is performed on the treated bottom ash samples, as well as on the mortar with treated samples to evaluate their environmental impact, as detailed in Section 3.2.2. The total amount of investigated components and their leaching concentrations from treated bottom ashes and mortar containing treated bottom ashes are shown in Table 4.4.

It is indicated in Table 4.4 that the leaching of Sb and Cu from the bottom ash without thermal treatment exceeds the limit values (more than 4 times of the limit emission value). However, their leaching concentration reduced significantly after the thermal treatment and is well under the limiting level. This could be due to the burning of the organic matter, which is related to the leaching of copper (Arickx et al., 2010; Meima et al., 1999b; Polettini & Pomi, 2004).

It can be seen that samples MF-BAW and 5TMS have the same amount of Cu, however, MF-BAW has a higher leaching of Cu. This confirms that the thermal treatment decreases the leaching of Cu. Sample 5TM has a higher total amount of Cu than 5TMS, but lower leaching of Cu than 5TMS. This is due to the fact that 5TMS has more soluble Cu, which is mainly absorbed during the quenching process. Nevertheless, the leaching of molybdenum is increased, and 5TMS which concentrated the most contaminated fine powder in MF-BAW has a relatively higher leaching concentration, which further confirms the finding in (Saffarzadeh et al., 2011; Yang et al., 2013) that the dust-layer on the particle surface influences the heavy metal leaching. The chloride leaching of 5TM is lower than that of MF-BAW, which confirms the removal of the highly soluble chlorides by the

thermal treatment (Yang et al., 2013). However, this reduction is not remarkable and the leaching is still above the limit level. The leaching of sulphates from the investigated samples exceeds the limit value of the legislation, and it seems thermal treatment did not influence the leaching of sulphate significantly.

Table 4.3. The Soil Quality Decree (SQD, 2013) limits and leaching properties of treated F-BAW samples and mortar with the treated F-BAW after 28 days curing, and the total amount of certain heavy metals and salts

	SQD limit	Total amount [mg/kg d.m.]			Leaching value [mg/kg d.m.]					
					Treated F-BAW samples			Mortar samples		
		MF-BAW	5TM	5TMS	MF-BAW	5TM	5TMS	MF-BAW	5TM	5TMS
Sb	0.16	75	86	110	0.79	0.037	0.023	< 0.0089	< 0.0059	< 0.0089
Cu	0.9	3100	4000	3100	3.6	< 0.050	0.3	0.17	< 0.050	0.06
Mo	1	11	10	12	0.67	1.4	2.6	0.09	0.11	0.092
Cl^-	616	3800	5300	9200	4400	3300	6600	350	290	450
SO_4^{2-}	1730	18100	24000	45700	16000	20000	23000	180	180	270

The leaching properties of the mortars with treated bottom ash samples are also studied to investigate the immobilization of the contaminants in the samples. It can be seen in Table 4.4 that the leaching of all the investigated heavy metals and the salts is far below the limit leaching level. Hence, the mortars with 30% cement replacement by the treated bottom ash meet the environmental requirement. Moreover, the sulphate is more immobilized than the chloride in the mortar, when comparing their total amount and leached concentration (Table 4.4). This may further prove that the sulphate in bottom ash participates in the cement reaction as explained in Section 4.3.2, hence the leaching of sulphate in the mortar decreases more than that of chloride.

Consequently, in this chapter the leaching of Sb and Cu of the MF-BAW is reduced to values under the limit by thermal treatment. Furthermore, the mortar with treated bottom ash complies with the national environmental legislation considering the leaching of contaminants in future life cycles.

4.4 Conclusions

In this chapter, milling and thermal treatment are applied to upgrade the properties of fine MSWI bottom ash (0-2 mm) from Wijster (F-BAW), and the characteristics of the treated bottom ashes are investigated. Moreover, their effect on cement hydration and mortar properties containing 30% bottom ashes as cement replacement are illustrated. The following conclusions can be drawn:

(1) The main chemical components of the MSWI bottom ash are SiO_2, CaO, Al_2O_3, Fe_2O_3 and the main crystalline phases are quartz, calcite, anhydrite and hematite. After the thermal treatment at 550 ˚C and 750 ˚C, qualitative differences on the chemical compositions are not identified. The higher temperature results in the

decomposition of calcite and enhances the oxidation of iron. The amount of metallic Al is not reduced significantly after the thermal treatment. However, the short time and low speed milling followed by sieving can separate the metallic Al from the fine powder chosen for the investigation. Additionally, this fine powder has a lower amount of SiO_2 and higher amounts of CaO and Al_2O_3.

(2) The hydration of the cement is retarded when milled raw F-BAW is added, which is due to the organic matter and heavy metals. The thermal treatment can reduce the retardation effect of the bottom ash on cement hydration. Furthermore, an efficient thermal treatment on milled bottom ash enhances the contribution of the bottom ash on cement hydration and minimizes its retardation effect. The sulphate content in the bottom ash accelerates the hydration of C_3A and then increases the formation of AFm during the deceleration stage of cement hydration.

(3) The 28-day compressive strength of the mortar with 30% treated bottom ashes replacement is 30-51 MPa, which is less than the reference (61 MPa). The highest strength is obtained in mortars with 5TMS; the 30% cement replacement results in 15% compressive strength and 8% flexural strength reduction. Although an efficient thermal treatment increases the contribution of bottom ash on cement hydration, the oxidation of metallic Al delays the generation of gas. Eventually, the cracks in the hardened mortar reduce its strength.

(4) The thermal treatment efficiently reduces the leaching of Sb and Cu, and slightly decreases the chloride leaching of the bottom ash fines. The mortars with 30% treated bottom ashes are environmentally acceptable according to the Dutch legislation, as the leaching of heavy metals and salts is well under the limit level. The fine dust-layers removed from the bottom ash particles have higher leaching of heavy metals, which confirms that these layers influence the heavy metals leaching of MSWI bottom ash.

(5) The technique for the removal of metallic Al by slow milling (and the formation of metal plates which can be sieved out) was proposed and its applicability was proven.

To further study the influence of treatments on the leaching of contaminants related to the application purpose of MSWI bottom ash, the use of fine MSWI bottom ash (0-2) as sand replacement in mortar is investigated regarding blended binders in the next chapter. The leaching behaviours of contaminants in fine bottom ashes during its application in mortar is also investigated.

Chapter 5

5 Binding capacity of blended binders on contaminants in fine bottom ash (F-BA)*

5.1 Introduction

A number of treatments have been investigated on the MSWI bottom ashes, with the purposes of reducing the leaching of contaminants or immobilizing the contaminants in new products with the addition of additives (Santos et al., 2013). The study in Chapter 4 shows that a thermal treatment could not reduce the leaching of salt from MSWI bottom ash significantly and it was reported by other researchers that the washing of bottom ash was a promising method for salt removal effectively (Cossu et al., 2012; Lin et al., 2011). Furthermore, cementitious materials were widely used to stabilize the contaminants in solid wastes, such as MSWI fly ash, mining wastes, etc. Therefore, based on the application of bottom ashes as aggregates and binder substitutes in concrete (Keulen et al., 2015; Lin & Lin, 2006), the relevant treatments on the bottom ashes (before and after size reduction by milling) were studied. In this chapter, several treatments were conducted on the fine MSWI bottom ash from Moerdijk (F-BAM) and milled BAM (MF-BAM). Washing and the immobilization by blended binders were chosen as treatments. This chapter is divided into the following parts:

(1) Leaching behaviours of heavy metals and salts in F-BAM and MF-BAM during washing, with various liquid to solid ratios;
(2) Hydration study of blended binder with chloride source and waste water addition;
(3) Internal chloride (NaCl) binding in mortars with blended binders;
(4) Immobilization of contaminants in mortars with blended binders when F-BAM is used as sand replacement.

5.2 Materials and methods

5.2.1 Materials

Ordinary Portland Cement (OPC, CEM I 42.5 N) was used as reference binder, and ground granulated blast furnace slag (GGBS) from the steel industry and a coal fly ash (FA) from a power plant were used as supplementary cementitious binders. Their chemical compositions and densities are shown in Table 5.1. The fine MSWI bottom ash (0-2 mm, F-BAM) was provided by the waste-to-energy plant in Moerdijk. The F-BAM was dried at 105 ºC until constant mass was obtained. Then the dried bottom ash (F-BAM) was milled by a planetary ball mill for around 3 hours to obtained a powdered material with a particle

*Part of this chapter was published in a MSc. Thesis [Munuswamy, T., 2016] and in [Tang, P., Munuswamy, T., Florea, M.V.A., and Brouwers, H.J.H., (2015) Proc. 19th Ibausil, Int. Conf. Build. Mater 2-493-2–496].

size under around 125 µm (MF-BAM). The 10% wt. NaCl solution was prepared by mixing pure NaCl with distilled water.

Table 5.1: Material properties

Components [% wt.]	OPC	GGBS	FA	F-BAM
CaO	67.9	40.0	6.2	18.6
SiO_2	14.9	30.2	45.2	39.1
Al_2O_3	3.6	12.7	27.5	7.6
Fe_2O_3	3.3	0.6	6.6	12.9
Na_2O	0	0	1.0	1.0
K_2O	0.8	0.6	2.2	1.1
MgO	1.6	9.1	1.4	1.9
P_2O_5	0.4	0.0	0.8	0.9
TiO_2	0.3	1.4	0.0	0.0
MnO	0.1	0.3	0.1	0.2
CuO	0.0	0.0	0.0	0.4
ZnO	0.1	0.0	0.1	0.7
Cl	0.11	0.1	0.0	0.3
SO_3	4.5	3.6	1.7	4.3
others	0.4	0.3	2.1	1.9
LOI	2.2	1.2	5.3	9.2
Density [g/cm^3]	3.1	2.9	2.3	2.7

5.2.2 Experimental procedure

- ***Water washing of F-BAM and MF-BAM***

A dynamic shaking test was conducted on the F-BAM and MF-BAM using a horizontal shaker at a speed of 250 rpm for 24 hours; the liquid to solid ratios (L/S) chosen was 2, 4, 6, 8 and 10. After the shaking test, the samples were filtered through a 45 µm filter paper and the leachate was collected for the determination of component content.

- ***Binder hydration investigation***

The study in Chapter 4 shows that the chloride in the fine bottom ash is still quite high after thermal treatment and controls the application amount of treated bottom ash in mortar, and the bottom ashes has retardation effect on binder hydration (Chapter 3) which is assumed due to the contaminants in fine bottom ash. Therefore, to further study the influence of contaminants on binder hydration and the binding capacity of blended binders on the contaminants, a salt solution containing 10% sodium chloride (NaCl) (as used for rapid chloride migration test in concrete in NT BUILD 492, (1999)), and waste water from washing of F-BAM were applied as mixing liquid, respectively. The blended binders are OPC (named M1), OPC with 40% GGBS (named M2) and OPC with 15% FA (named M3). The water to binder ratio was 0.5. The waste water from washing of F-BAM with liquid to solid ratios of 2, 4, 6 and 8, respectively, was used.

- ***Mortars with NaCl***

The standard mortar was prepared with the three types of binders above-mentioned according to EN 196-1 (2005) and the water used was the same salt solution used for the calorimetry test. The flexural and compressive strengths were determined after different curing ages. The crushed mortar samples were used for a leaching test with L/S 10 for 24 hours. The chloride content in the leachate was then determined using ion chromatography (IC). The washed samples were milled and then digested using concentrated HNO_3; the chloride extracted in the liquid was then determined using IC.

- ***Mortars with F-BAM* and *MF-BAM***

The F-BAM was used as sand replacement (100%) in standard mortars with three types of blended binders and the MF-BAM was used as binder alternative (30% wt.). The flexural and compressive strengths of the mortars were tested. Shaking testes with L/S of 10 and for 24 hours were performed on the crushed mortar samples with bottom ashes, and the concentrations of heavy metals and salts in the leachate were determined using inductively coupled plasma (ICP) and IC methods, respectively.

5.3 Washing treatment

The total amount of investigated heavy metals and salts in F-BAM are shown in Table 5.2, as well as their leaching concentrations during column leaching test; according to legislation (SQD, 2013) (Chapters 3 and 4), the leaching of Sb, Cu, chloride and sulphate exceed the limits defined for the non-shaped materials.

Table 5.2：The total amount of investigated salts and heavy metals in F-BAM and their leaching concentrations during the column test, and the limit level in SQD (2013)

	Sb	Cu	Mo	Chloride	Sulphate
	[mg/kg d.m.]				
Total amount	83	3100	19	2100	22900
Column leaching	0.47	1.1	0.68	950	11000
Leachability [%]	0.57	0.035	3.6	45	48
SQD limit	0.32	0.9	1.0	616	1730

Figure 5.1 shows the leached-out concentrations of Sb and Cu during the shaking test with various L/S ratios. For both F-BAM and MF-BAM, the leaching of Sb has a linearly increasing trend with the increase of L/S up to L/S 8, while there is a sharp increase when the L/S ratio is 10. The Sb leaching of MF-BAM is around 0.4-1.2 times higher than that of F-BAM, and this factor increases from 0.4 to 1.2 with the L/S ratio increase from 4 to

10. The leaching concentration of Sb from F-BAM during the column leaching test is around 0.47 mg/kg d.m. at a L/S ratio of 10, which is around 80% of that from F-BAM during the shaking test. The concentration of Cu leached out from F-BAM during the shaking test shows a direct correlation with the L/S ratio. For MF-BAM, the leaching concentration of Cu is quite similar with various L/S ratios, and it is much lower than that of F-BAM (around 3 times less). The Cu leaching from F-BAM by shaking test is about 1.6 times higher than that from the column leaching test.

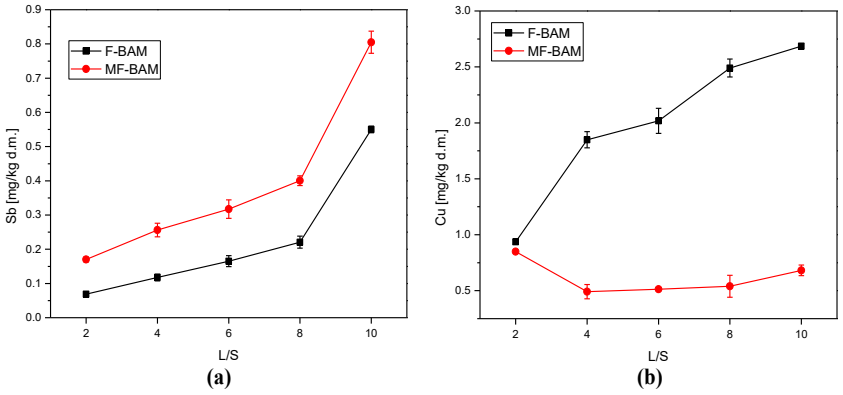

Figure 5.1: The leaching behaviour of (a) Sb and (b) Cu with various L/S ratios in shaking test

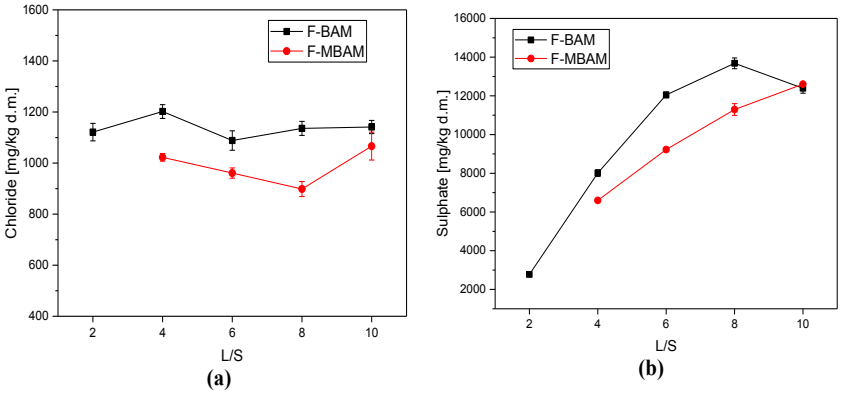

Figure 5.2: The leaching behavior of (a) chloride and (b) sulphate with various L/S ratios in shaking test

It can be seen in Figure 5.2 (a) that the chloride leaching concentration during the shaking test seems not to be influenced by the L/S ratio and also that the MF-BAM has a slightly lower chloride leaching than F-BAM (around 10-30%). The sulphate leaching of both F-BAM and MF-BAM increases when the L/S ratio increases, and the MF-BAM has a slightly lower sulphate leaching (with around 20%). The sulphate leaching during column leaching is approximately 20% lower than the one during the shaking leaching test.

The leaching of Ni, Zn, Pb and Cr of F-BAM in shaking tests all show an increasing trend with the increased L/S ratio, while their leaching from MF-BAM is much lower (even under the detection levels). It seems that the leaching of elements from the MF-BAM is lower than that from F-BAM during the shaking test with various L/S ratios, except for Sb. The leaching of Cu from MF-BAM and chloride from both F-BAM and MF-BAM seem independent of the L/S ratio.

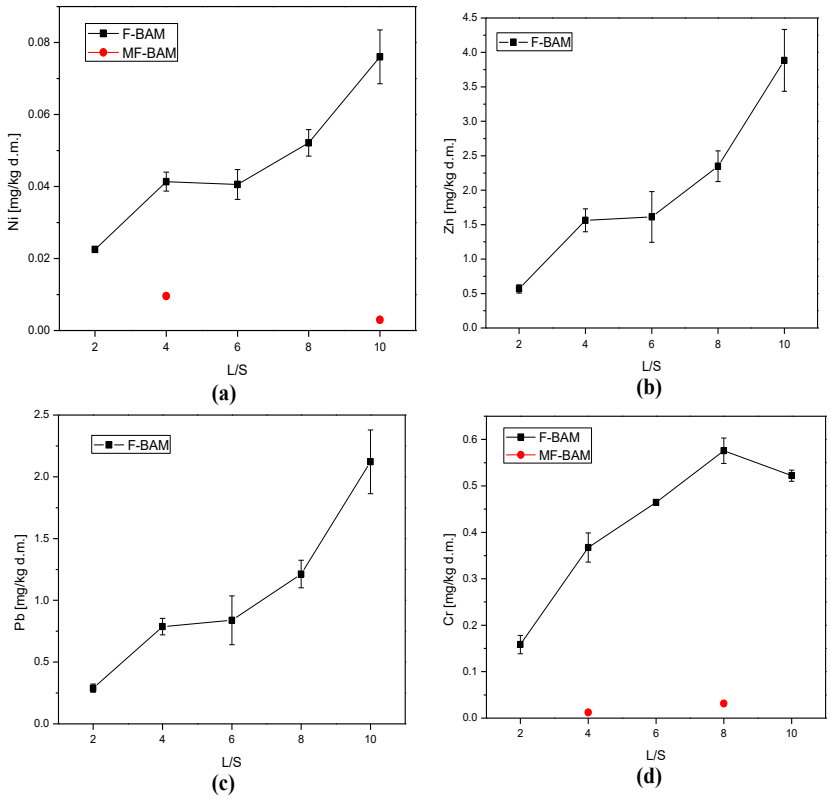

Figure 5.3: The leaching of (a) nickel, (b) zinc, (c) lead and (d) chrome with various L/S ratios in shaking test

It was supposed that the leaching from the MF-BAM would be higher than that of F-BAM, due to the increasing contact surface area with water during shaking, which increases the chance for elements to be washed out. However, the test results show an opposite phenomenon. There are several supposed mechanisms which may contribute to the testing results.

(1) Chloride in MSWI bottom ash is highly soluble, hence, the L/S ratio does not have a significant effect on its leaching, similar as reported in (Alam et al., 2017). Sulphate leaching is related to the solubility of gypsum and other sulphate containing phases in fine bottom ashes, and the increase of L/S ratio results in

higher solubility of these sulphate containing phases. The change of water amount may change the pH of the leachate and then the solubility of alkaline metals will be influenced, which influences the leaching of most metals.

(2) After milling, the increased surface area on one hand can enhance the leaching out of elements, on another hand, it might be possible that the leached ions are absorbed on the surface of the particle during the dynamic shaking due to electric charge, which need further investigation.

5.4 Hydration of blended binders with NaCl and waste water from washing F-BA

5.4.1 Hydration development of blended binders with NaCl

Figure 5.4 depicts the hydration development of blended binders with (M1', M2' and M3') and without (M1, M2 and M3) NaCl solution and the influence from NaCl.

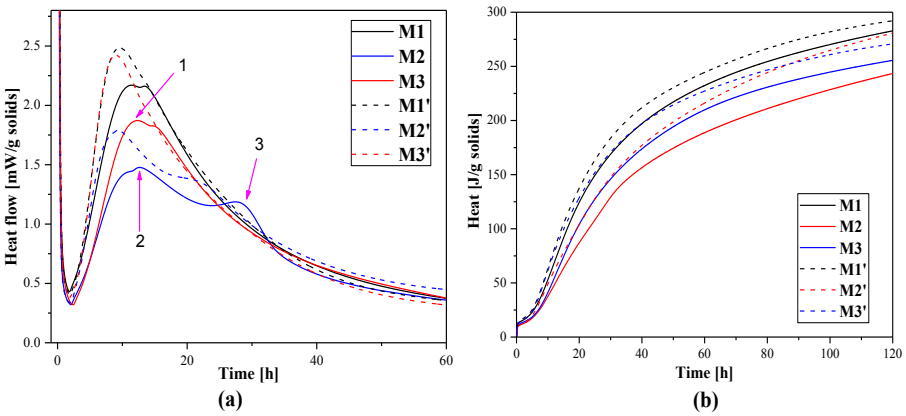

Figure 5.4: The hydration development of blended binders with and without NaCl

It can be seen that samples with GGBS and FA show a different heat flow during the hydration process to plain OPC sample. The sample with GGBS has a lower heat flow (34% less) at the first peak occurring at around 10-11 hours after mixing, as well as the second peak at around 13 hours. There is a 'shoulder' on the heat flow curve at around 28 hours, which is not found in OPC. For the mixture with FA, the heat flow curve is similar to that of OPC, and the maximum heat flow at the first peak is approximately 14% less than that of OPC.

The addition of NaCl to the blended binders results in the change of their heat flow profiles. Firstly, the occurrence of the first heat peak (indicating C_3S reaction) is accelerated for about 1.4-3.4 hours, the second peak (implying C_3A hydration and formation of ettringite) is not distinguished compared with the sample without salt; the third peak for M2 with NaCl occurs 5.4 hours earlier and the heat flow is around 14% higher than M2 without

NaCl. The maximum heat flow of the first peak for samples with NaCl addition increases by 15%, 25% and 30% compared to M1, M2 and M3 without salt, respectively.

The total released heat after 160 hours from samples without salt decreases with the addition of GGBS and FA, M2 (with 40% GGBS to replace OPC) has the lowest total heat (12% less than M1) while M3 has 10% less total heat with 15% FA for OPC replacement. This demonstrates the contribution of GGBS and FA during cement hydration. For samples with NaCl addition, the total heat increases compared with samples without salt addition; the increase is about 1%, 13% and 4% for samples M1', M2' and M3', respectively. From the above results, it can be concluded that the NaCl has more influences on OPC blended with GGBS and FA, at least at the early hydration age. Hence, it can be summarized from the isothermal calorimetry results that the chloride sourced from NaCl accelerates the hydration of C_3S and C_3A, and this effect is more pronounced on blended binders by OPC with GGBS or FA.

Table 5.3：The heat flow and total heat of the mixtures with (M1', M 2' and M3') and without (M1 M2 and M3) NaCl

Samples	Peak 1		Peak 2		Peak 3		Total heat	
	Time	Heat flow	Time	Heat flow	Time	Heat flow	Time	Heat
	[hour]	[mW/g]	[hour]	[mW/g]	[hour]	[mW/g]	[hour]	[J/g]
M1	11.4	2.2	13.4	2.2	*	*		302
M2	10.7	1.4	13.0	1.5	27.5	1.2	160	267
M3	12.4	1.9	15.4	1.8	*	*		273
M1'	9.6	2.5	*	*	*	*		304
M2'	9.3	1.8	*	*	22.0	1.4	160	303
M3'	9.0	2.4	*	*	*	*		283

*: no peak

Figure 5.5 depicts the crystalline phases of the hydrated samples (28 days) with and without NaCl addition. The samples blended by OPC and GGBS or FA shows relatively higher peaks representing hydrotalcite, which is attributed to the higher amount of Al and Mg content in GGBS or FA (Kayali et al., 2012). The XRD pattern of the samples with NaCl addition shows peaks of Friedel's salt (Fs) compared with the ones without chloride source; moreover, the sample blended by OPC and GGBS shows relative higher Hc peak compared with the other two mixtures.

It can be assumed that the generated AFm phases reacted with chloride to form Fs salt, which continuously consume the AFm. Consequently, the transformation of AFt to AFm is promoted, as well as the generation of AFt from the hydration of C_3S.

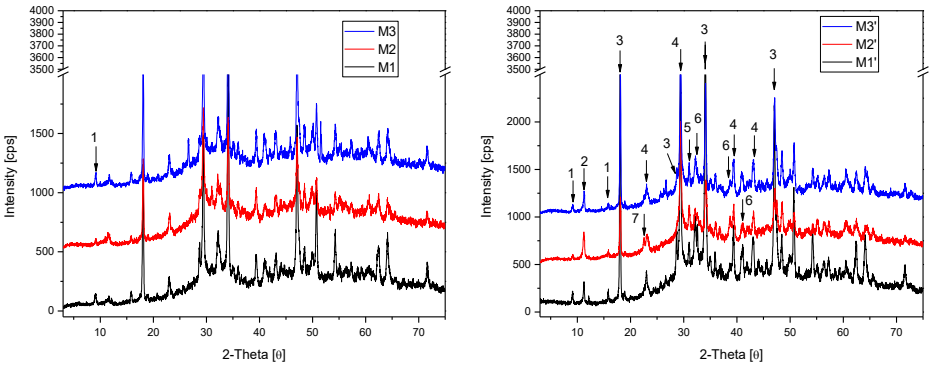

Figure 5.5: The XRD pattern of the hdyrated samples with and without NaCl addition (1-Ettringite; 2-Friedel's salt (Fs)); 3-Portlandite; 4-Calcite; 5-Gypsum/C_2S; 6-C_2S/C_3S; 7-Hydrotalcite (Hc))

5.4.2 Hydration development of blended binders with waste water

The waste water used for washing F-BAM was collected and mixed with cement to investigate the influence of contaminants from F-BAM on the cement hydration; the hydration development of blended binders is investigated through isothermal calorimetry. The calorimeter profiles in Figure 5.6 depict that the waste water from F-BAM has a retardation effect on the hydration of blended binders independent of the L/S ratio for F-BAM washing. Moreover, this retardation effect is enhanced when the L/S ratio used for washing F-BAM increased, and the total heat of the blended binders is higher than the binders mixed with distilled water.

This could be explained by two reasons: (1) the heavy metals washed out from the F-BAM retard the cement hydration and their concentrations increase with the L/S ratios as described in Section 5.3 (Weeks et al., 2008); however, there were also research results indicating that some heavy metals had an accelerating effect on cement hydration, such as Cr, Pb, etc. (Chen et al., 2007); (2) the sulphate content in the waste water participated in the binder hydration, which is demonstrated from the higher second ettringite generation peaks; this has a retardation effect on cement hydration as reported (Zajac et al., 2014); moreover, as shown in the above results on hydration development of blended cement with NaCl, the chloride could accelerate the binder hydration; hence, it could be possible that the chloride washed out from F-BAM in the leachate also has a similar accelerating effect; (3) the organic matter washed out from the F-BAM also had a retardation effect on the cement hydration. For instance, it was reported in (Chen & Wang, 2006) that the humic and fluvic acid content (which were also detected as main organic matter in MSWI bottom ash related to Cu leaching (Guimaraes et al., 2006; Van Zomeren & Comans, 2004)) in the soil had a significant influence on the setting of cement treatment soil; (4) generally, the pH of the leachate from bottom ash is around 9-10, which may also promote the binder hydration.

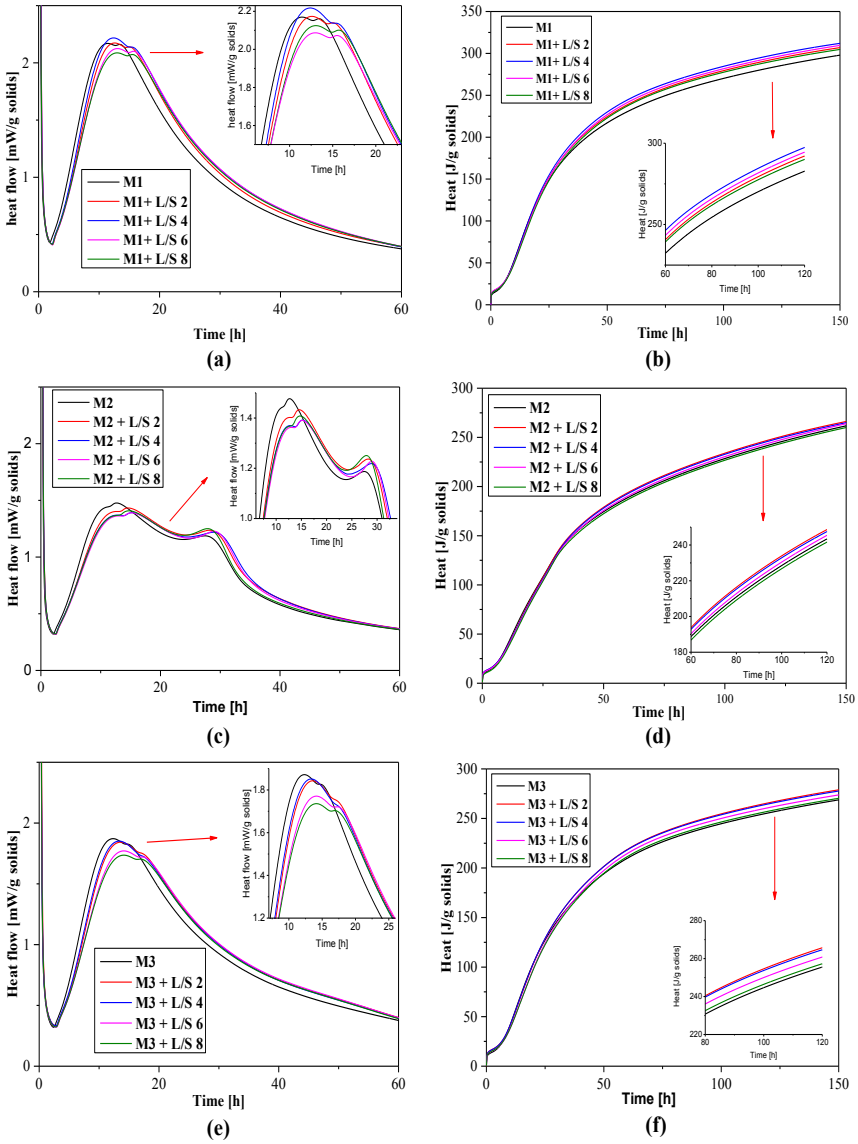

Figure 5.6: The hydration development of blended binders mixed with waste water from F-BAM washed with various L/S ratios in shaking test

Therefore, it can be addressed that the influence of waste washing water from MSWI bottom ash on the blended binder hydration is a combination of several positive and negative factors, including concentration of heavy metals, salts (chloride and sulphate), organic content, and pH of the leachate, etc. It is of interest to qualify and quantify the hydration mechanism of blended binders with waste water from washing of MSWI bottom ash and investigate their immobilization capacity on the contaminants in the leachate,

which may provide indicating information of the integral treatments on MSWI bottom ash, such as combined treatments of water washing and binder stabilization.

5.5 Mortars with NaCl and the chloride binding capacity

Figure 5.7 depicts the flexural and compressive strength of mortars with blended binders and NaCl. It can be seen that the mortar with GGBS has the highest compressive strength and the mortar with FA has the lowest strength, while the compressive strength after 56 days is almost the same as the mortar with OPC. This complies with the calorimetry results shown in Section 5.4.

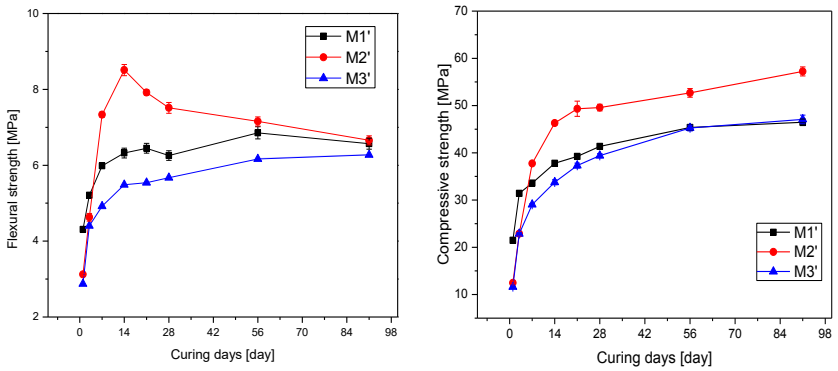

Figure 5.7: The flexural and compressive strengths of the mortar with NaCl addition

Figure 5.8 (a-b) describes the leaching profile of chloride from the crushed mortars with the addition of NaCl and the chloride content left in the washed mortars samples after shaking test. It can be seen that there is a decreasing trend of the concentration of leached out chloride along with curing time for both mortars M1', M2' and M3'. Moreover, the chloride leached out tends to be stable after 7 days curing. Comparing the chloride leaching of M1', M2' and M3', it seems that M1' and M2' have less chloride leached out during most of the tests; however, due to the fact there are too many influencing parameters on the leaching results, it is hard to quantify their differences.

Hence, the total chloride content of the unwashed and washed mortars was tested (Figure 5.8 (c-d)). It was noticed that the total chloride in the unwashed mortars has a decreasing trend with the curing age, this is due to the water curing methods. During the curing, the free chloride which is not bounded diffuse into the water. However, it can be seen clearly in Figure 5.8 (b) that the total amount of chloride left in the washed mortar samples increases with curing time for all the mixes and M2' has much higher chloride content than that in M1' and M3', while M3' has the lowest level of chloride bounded in the mortar matrix. It is worth to mention that there is a sharp increase of chloride content in the washed mortar of M2', which indicates the bound chloride increased dramatically. M3' has lower

bound chloride at early age, however, it is noticed that the chloride content left in washed mortar is almost the same as M1'.

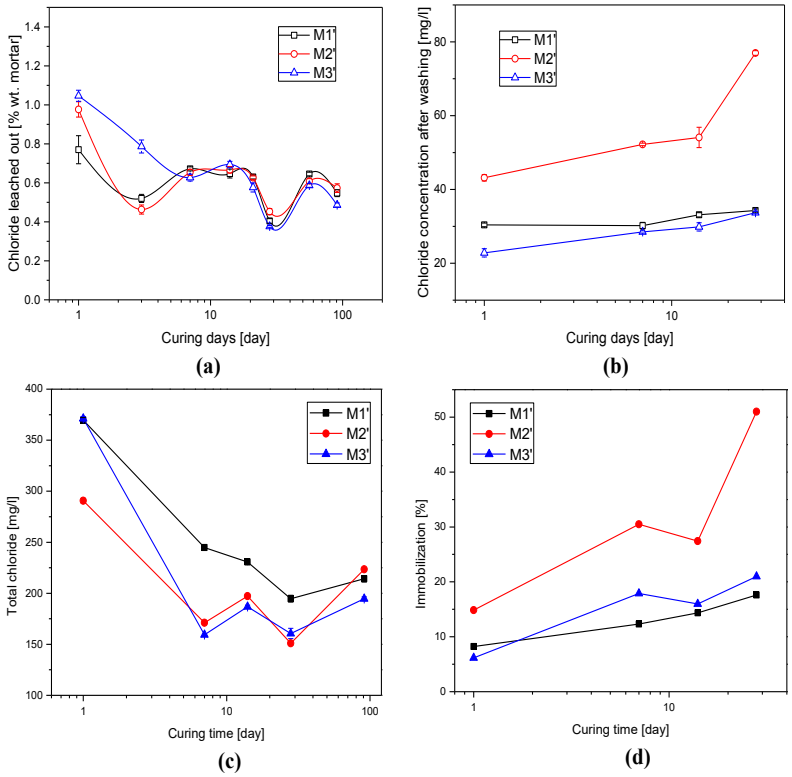

Figure 5.8: The (a) chloride leached out from crushed mortars after various curing ages and (b) the amount of chloride left in the washed mortars, and (c) the total chloride measured in the mortars before washing and (d) the calculated immobilized chloride percentage

Justnes (1998) summarized that the chloride binding is related to the content of C_3A and C_4AF regardless of types of chloride, and the chemically bound chloride is in Friedel's salt. The C-S-H gel content provides the main surface for free chloride absorption. Luo et al. (2003) stated that the GGBS can increase the chloride binding capacity dramatically, especially for chemically bound chloride, which is attributed to the formation of Friedel's salts. Song et al. (2008) used a similar test method on cement pastes mixed with a chloride solution. The results showed that at lower chloride contents, the chloride binding capacity of binders is higher than that at higher chloride content. The binding of chloride increases with the order of GGBS, pulverized fuel ash, OPC and silica fume, and has less relation with the pH of the pore solution.

For the tests performed in this study, the shaking test is performed on the crush mortar instead of milling the mortar into powder as described in others' research, hence, the

chloride bounded in the washed mortar includes the one chemically bound by the formation of Friedel's salts, one part absorbed on the surface of hydration products and one part entrapped into the matrix of the mortar.

5.6 Mortars with blended binders, F-BA and MF-BA

5.6.1 Strength development of mortars

The strength of the mortar with 100% sand replacement by fine MSWI bottom ash is shown in Figure 5.9. The flexural strengths of mortar did not have significant differences based on the binder types. Their compressive strengths have a similar trend, the mortar with GGBS obtaining the highest value.

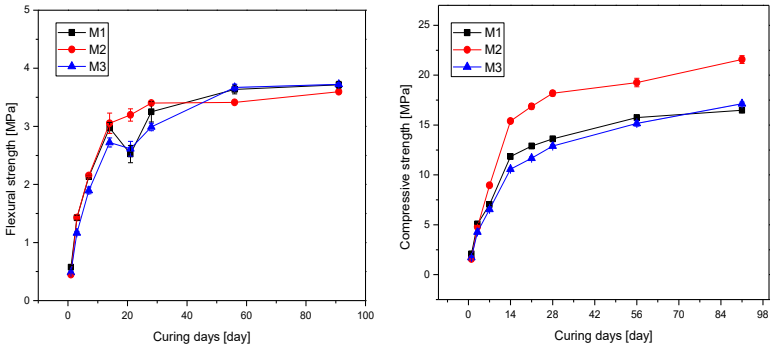

(a) (b)

Figure 5.9: The (a) flexural and (b) compressive strength of mortars with F-BAM as 100% sand replacement in mortars with blended binders

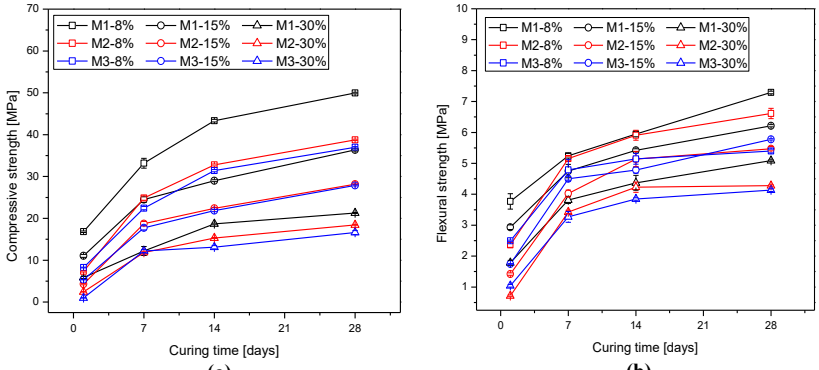

(a) (b)

Figure 5.10: The flexural and compressive strength of mortars with MF-BAM replacement level of 8%, 15% and 30%

Figure 5.10 shows the strengths of the mortars with binder replacement by milled F-BAM (MF-BAM) by 8%, 15% and 30% by mass, where number 1, 2 and 3 represent OPC, OPC blended with GGBS, and OPC blended with coal fly ash, respectively.

The strengths of mortars decrease when the replacement ratio of binders by MF-BAM increases, and the mortar with OPC blended with MF-BAM has the highest strength at each curing age, followed by mortars with GGBS blended binder and fly ash blended binder. The strengths of mortar with blended binders being replacement by MF-BAM did not show similar trend as the mortars with NaCl addition or mortars with F-BAM as sand, which need to be studied in future.

5.6.2 Leaching behaviours evaluation of mortar containing bottom ashes

The leaching of chloride from the mortar containing F-BAM as 100% sand replacement (Figure 5.11) shows a similar profile as the mortar with NaCl addition, but, it takes 14 days for mortar with F-BAM to have a stable chloride leaching. It seems that the chloride leaching from M2 is slightly higher than that from M1, while M3 has lower leaching of chloride than M1. The difference between the chloride leaching from M1, M2, and M3 is not very notable. The leaching of sulphate from mortars with F-BAM has a roughly increasing trend with age, while this trend is more obvious for sample M2.

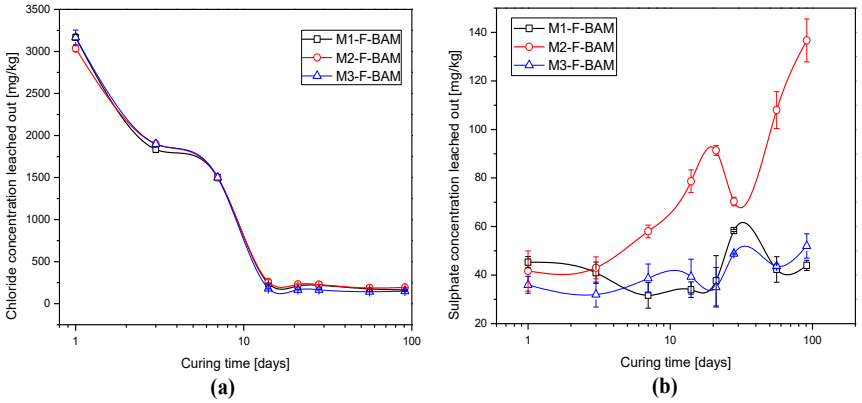

Figure 5.11：The leaching concentration of (a) chloride and (b) sulphate from mortar with 100% F-BAM as sand replacement

The leaching of antimony from mortars with F-BAM does not show a very clear trend related to curing age and binder types (Figure 5.12 (a)). The leaching of copper from mortars shows an increasing trend along with curing time (Figure 5.12 (b)). It seems that the copper leaching from M1 is lower than that from M2 and M3 after 56 days' curing, and M3 mostly has a lower amount of copper leached out than M2. However, after 91 days, the copper leaching from M1 increased, while it decreased from M2 and M3, and is lower than that from M1. Firstly, the increasing trend of copper leaching from mortar can be resulted from the increase of pH in the mortar along with curing time. The binder hydration produces $Ca(OH)_2$ which generates an alkaline environment of the pore water (Alonso et al., 2007). It is reported that the copper leaching in the MSWI bottom ash is significantly

influenced by the pH: it has an increasing amount of copper leached out when the pH is above 10 (Dijkstra et al., 2006).

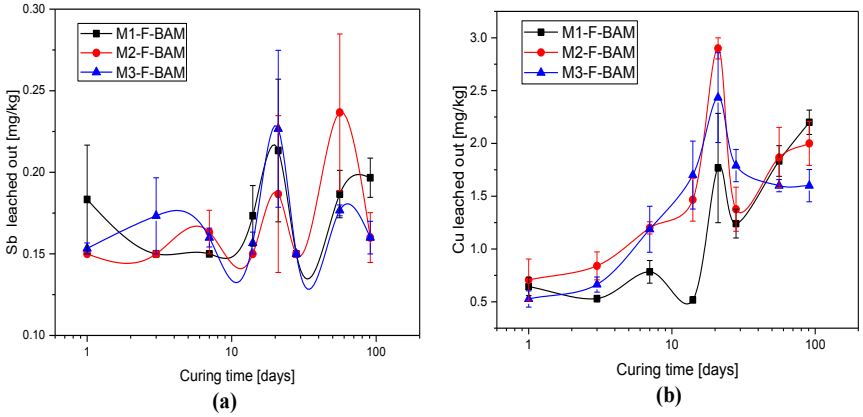

Figure 5.12: The leaching concentration of (a) antimony and (b) copper from mortar with F-BAM as 100% sand replacement

5.7 Conclusions

(1) The washing treatment shows that the increase of liquid to solid ratio (L/S) results in an increased leaching of the investigated salts and heavy metals. After the reduction of particle size by milling, the leaching of investigated heavy metals shows a lower leaching concentration, except Sb. The chloride leaching is not influenced by the reduction of particle size due to its highly solubility.

(2) The addition of NaCl promotes the hydration of blended binder by accelerating the reaction of C_3S/C_3A indirectly and the acceleration effect is more effective on the OPC and GGBS blends. The formation of Friedel's salt (Fs)/Hydrocalumite (Hc) in the samples with NaCl was observed. The waste water from the washing of BAM has a retarding effect on the hydration of blended binders, which results from the cumulative effect of heavy metals, sulphate and chloride content, and organic matter washed out from BAM and the pH of the leachate.

(3) The strengths of mortar with GGBS and NaCl are the highest, and the shaking test shows that the chloride leached out from the crushed mortars has a decreasing trend over curing time. The chloride leaching concentration starts to be stable after 7 days. The chloride left in the washed mortar samples demonstrates that the mortar with GGBS blended cement can immobilize a relatively higher amount of chloride than the other two binders.

(4) The use of fine MSWI bottom ash and milled fine bottom ash in mortar as sand and binder replacement respectively reduces the strength of mortar. The leaching of chloride from mortar with bottom ashes shows a similar trend as mortar with NaCl addition. Sulphate leaching slightly increases and mortar with GGBS has a higher

sulphate leaching than the other mortars. The Sb and Cu have an increasing leaching trend over curing time which is due the dissolving of heavy metals salts at high pH over time. Therefore, other application methods should be considered for fine MSWI bottom ashes, which is shown in the next chapter.

Chapter 6

6 Employing cold bonded pelletization to recycle incineration fine bottom ash*

6.1 Introduction

The fine incineration bottom ash (0-2 mm, F-BA) without any treatment can only be used when the material is isolated and monitored during the application period due to its leaching of Sb, Cu, chloride and sulphate as shown in previous chapters. Moreover, it contains metals which can lead to cracks when used in mortar or concrete, and then damage the strength and decrease the durability of the concrete (Müller & Rübner, 2006). The F-BA can also end up in landfills (Bosmans et al., 2013); however, due to the decreasing available space and increasing cost for landfilling, this is not a preferable option and will not be allowed by Dutch legislation in the future.

In Chapter 4, treatments which can remove the fine dust on the fine bottom ash particles and then the use of the treated bottom ash as binder substitute are presented. However, the cost may be too high compared with its application value. In Chapter 5, the use of F-BA as sand and binder supplementary in mortar with blended binders showed that the mortar strengths were decreased. In one of our previous work (Yu et al., 2014), the washed bottom ash was used in concrete as sand replacement; however, the metallic Al was still a problem. So far, the recycling and reuse of municipal solid waste incineration (MSWI) F-BA remains an issue to be solved in practice. The integral recycling or reuse of F-BA without treatments and consequent minimization of the deleterious effect of F-BA on the final products would be more suitable for F-BA management.

The cold bonded pelletizing technique is a method to agglomerate the powdered materials into bigger roundish particles with the assistance of a disc pelletizer and gluing agents, such as water, binder, chemical activators, etc. The produced aggregates can be further used as aggregates in concrete. Nowadays, the cold bonded pelletizing technique is widely used to recycle industrial waste powders for producing artificial aggregates, and the raw materials (powder level) used are extended to various waste powders in recent years, such as iron ore fines, coal fly ash and bottom ash, granulated blast furnace slag, quarry dust, etc. (Dutta et al., 1997; Ferone et al., 2013; Geetha & Ramamurthy, 2010a; Gesoğlu et al., 2007, 2012; Thomas & Harilal, 2015). The widespread research on the production of artificial aggregates using waste powders through cold bonding technique proposes a positive view on the investigation of producing artificial aggregate using F-BA, which is rarely studied. This could be a method for the integral purposes of immobilizing the contaminants of F-

*Content of this chapter was published elsewhere [Tang, P., Florea, M.V.A., and Brouwers, H.J.H., (2017) J. Clean. Prod. 165, 1371–1384]

BA by cementitious materials, producing an artificial aggregate which can be used in concrete, and in this way transfer F-BA from waste to value.

Regarding the recycling of industrial waste powdered materials by the cold bonded pelletizing technique, there are several aspects which have been investigated from literature (Baykal & Doven, 2000; Bui et al., 2012; Cioffi et al., 2011; Colangelo et al., 2015; Dutta et al., 1992 & 1997, Geetha & Ramamurthy, 2010a, 2013, Gesoğlu et al., 2004, 2007, 2012, 2014; Güneyisi et al., 2015a; Manikandan & Ramamurthy, 2008; Thomas & Harilal, 2015) and need to be considered for the design of pelletization, as listed below:

- ***Types of waste powders to be recycled as raw materials for pelletization***

The most used solid waste is coal fly ash (FA), which accounts for over 50% of the total solids used for pelletization. In most studies, the cold bonded pelletization is considered as an efficient method to manage the coal fly ash (Colangelo et al., 2015; Thomas & Harilal, 2015). However, among all these recycled solid materials, the particle sizes are rather small (<125 μm) compared to the corresponding pellets they produced (> 4 mm). The use of relatively bigger particles (>125 μm) rather than only powders has rarely been reported. Moreover, the inherent characteristics of the raw materials have a significant influence on the properties of the produced lightweight aggregates.

- ***Binder/chemical activator***

To guarantee the strength of the produced lightweight aggregates, a certain amount of ordinary Portland cement (OPC) is added, which normally accounts for 5-10% of the total solid mass (Dutta et al., 1997; Gesoğlu et al., 2004, 2014). Another binder system is an alkali-activated binder (geopolymer), which consists of a chemical activator and slag or fly ash (Bui et al., 2012; Geetha & Ramamurthy, 2013). Using this binder system for pelletization, the chemical activator in liquid form is generally sprayed on the powder as gluing agent instead of water, to promote the formation of granulates at the very early age of pelletization and later activate the slag or fly ash to provide strength to the pellets.

- ***Additives***

There is research which shows that the addition of CaO or $Ca(OH)_2$ contributes positively to the pelletization efficiency and the strength of the produced pellets (Cioffi et al., 2011; Geetha & Ramamurthy, 2010a). Ground-granulated blast-furnace slag (GGBS) from the steel industry and rice husk ash (RHA) from the combustion of rice hulls were also used to improve the properties of the lightweight aggregates due to their contribution to cement hydration, or their own chemical activation (Bui et al., 2012).

- ***Curing methods***

Several curing methods were applied in other studies, including water curing, moisture curing, steam curing at different temperatures, autoclave curing, etc. (Manikandan &

Ramamurthy, 2008). In most of the studies, moisture curing is performed by sealing the freshly produced aggregated in bags or buckets until the testing date, this is also possible in large scale production. The other three types of curing can promote the strength development of the aggregates; however, their efficiency depends on the properties of the raw materials and the available conditions in practice.

- ***Pelletizing parameters***

The pelletizing parameters include the diameter of the pan, its angle and speed, and the feeding speed of raw materials. The effect of the pelletizing parameters on the properties of the pellets depends on the pelletizer used and the other procedure parameters. The disc pelletizer used in literature had a diameter between 40-80 cm, and the rotating angle and speed were 45-55º and 35-55 rpm, respectively.

The applying of cold bonded pelletizing technique to recycle the F-BA involves the above-mentioned parameters, and the compatibility of the F-BA during the pelletization is not known. Hence, the main purpose in this chapter is to investigate the potential and compatibility of recycling the MSWI fine bottom ash from Moerdijk (0-2 mm, F-BAM) through the pelletizing technique to produce cold bonded lightweight aggregate. The properties of the artificial aggregate produced (such as density, pellet strength, crushing resistance, water absorption, etc.) are evaluated and compared with the ones produced by other raw materials. The leaching properties of the F-BA and the aggregate are determined and compared with the legislation. The practical application of this artificial aggregate in concrete is also studied.

6.2 Materials and methods

6.2.1 Materials

The wet bottom ash fine particles fraction (F-BAM, 0-2 mm) is selected from the Moerdijk MSWI plant for the investigation in this chapter. These bottom ash fine particles (F-BAM) were obtained by sieving and sealed in a bag before use to avoid the variation of moisture content (around 1000 kg was collected and stored at once to reduce sample variety). Three other industrial powder wastes, which are facing similar reuse/recycling issue as F-BAM in the Netherlands, were also used in this study. These powders are coal fly ash (FA) from a Dutch power plant, paper sludge ash (PSA) from a Dutch paper recycling company, and washing aggregate sludge (WAS) from a gravel washing factory (Smals, the Netherlands). An Ordinary Portland Cement (OPC) CEM I 42.5N (ENCI, the Netherlands) is used as binder. Figure 6.1 shows the raw materials used and the artificial aggregate produced.

The chemical compositions, crystalline phases, PSDs, and specific densities of the used materials are determined as described in Section 3.2.2. Isothermal calorimetry is employed to investigate the hydration development of the blended binders. The influence of the PSA and FA on the cement hydration are studied by replacing the cement by different

proportions of each respective material. The interaction between PSA, FA and cement is studied as well.

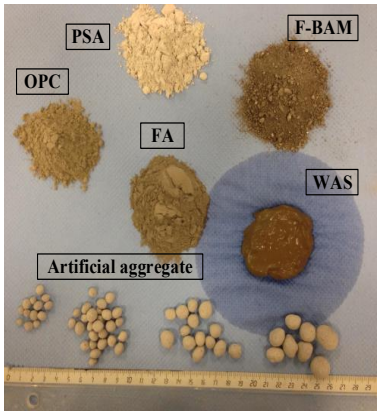

Figure 6.1: The raw materials applied and produced artificial aggregate

The proportions of the raw materials used (based on total dried mass) are 10% OPC, 40%-75% F-BAM (with a water content (ω) of around 22% wt.), 5% WAS (with a water content (ω) of 53% wt.), while FA and PSA fill up the remaining part. The determination of the recipe will be discussed in Section 6.3.1.

6.2.2 Cold bonded lightweight aggregate (CBLA) manufacture and characterization

- **Pelletizing procedure**

The size of the disc pelletizer and parameters for the pelletization used in the literature varies as summarized in Section 6.1; hence, the chosen pelletizing parameters are determined based on the information from literature and the practical experience acquired during the utilization of the disc pelletizer in this chapter.

The disc pelletizer used for the pelletization process has a diameter of 100 cm and collar height of 15 cm in this chapter. The angle of the disc is fixed at 45° and the speed is 15 rpm following practical laboratory experience and suggestion from literature (Gesoğlu et al., 2007). The pelletizing procedure is shown in Figure 6.3. The raw materials used for the aggregate are firstly mixed homogeneously and then around 10 kg of the mixed materials are put on the running disc (Zone 1 in Figure 6.2 (a)). After around 5 minutes running, about 2 kg of water is sprayed continuously on to the materials in the pan and then running again for 10 minutes. The next running cycle starts with the addition of another 10 kg of mixed materials to the running pan (Zone 1), and the rounded artificial aggregates from the last round will drop off automatically from the left lower corner of the pan (Zone 2 Figure

6.2 (a)). Around 100 kg of granulates was produced and the freshly produced aggregates are sealed in plastic bags for further use and tests.

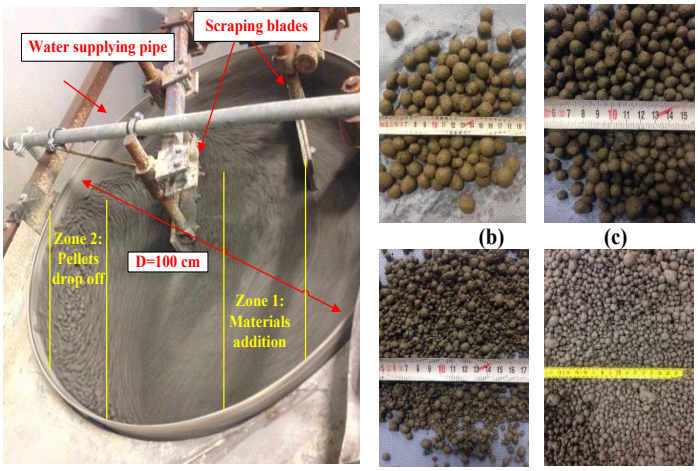

Figure 6.2: (a) The device and (b)-(e) produced aggregates ((b) pellets collected from zone 2; (c) pellets collected between zone 1-2; (d) pellets collected in zone 1; (e) pellets collected for further use

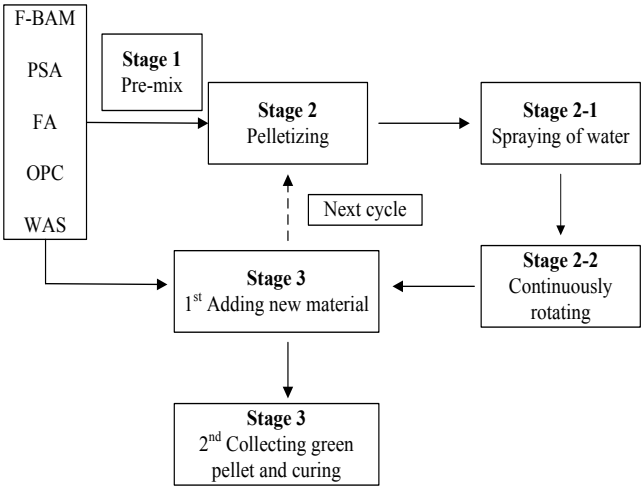

Figure 6.3: The pelletizing procedure

- **Characterization of produced aggregates**

After a certain curing time, a batch of aggregate is collected for relevant tests. The bulk density of the aggregates is determined following EN 1097-3 (1998) and the water absorption of the aggregate is measured following the EN 1097-6 (2013); the value is equal to the average of three tested values.

The individual pellet strength is tested using a similar test method to the one described and used in (Gesoğlu et al., 2007, 2012) (Figure 6.4 (a)); 45 pellets are chosen to be tested for each curing age. The crushing resistance of the aggregates is also evaluated after different days of curing following EN 13055-1 (Annex A, procedure 1) (2002) to describe the strength of the produced aggregates and three samples are tested for each value (Figure 6.4 (b)). Optical microscopy and scanning electron microscopy (SEM, Quanta 650 FEG, FEI) are used to observe the cross section of the pellet.

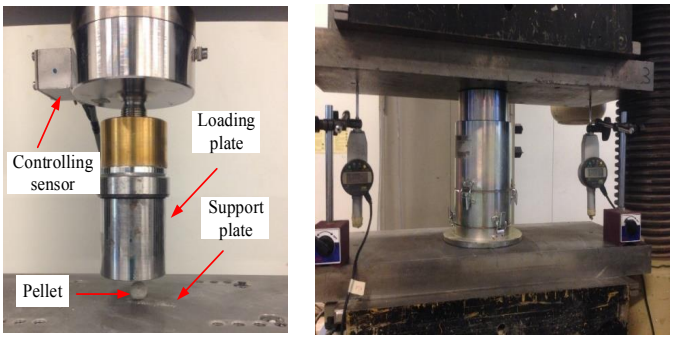

Figure 6.4: The device for (a) individual pellet strength and (b) crushing resistance

- **Application of artificial aggregates in concrete**

The produced aggregate is used in concrete as aggregates with a proportion of 50% and 100% replacement by volume of the natural quartz aggregate (2-8 mm). Concrete cubes with artificial aggregates (150 × 150 ×150 mm^3) are produced; the proportions used are: cement 280 kg/m^3, sand (0-4 mm) 830 kg/m^3, and the gravel (2-8 mm) 1248 kg/m^3. The water to cement ratio is 0.5 for samples with 50% gravel replacement, and 0.6 for samples with 100% gravel replacement in order to get a similar flowability. The compressive strengths of the cubes are determined after 28 days.

- **Leaching property evaluation**

The environmental impact of the F-BAM and the generated aggregate was evaluated using column leaching tests according to Dutch standard NEN 7383 (2004) as described in Section 3.2.2. The column leaching test is also performed on the crushed concrete cubes to observe the leaching properties of recycled concrete. The concrete cubes are crushed under 4 mm and then column leaching as described above is conducted.

6.3 Results and discussion

6.3.1 Integral recycling of F-BA by cold bonded pelletization

Considering the recycling of F-BAM using the cold bonded pelletizing technique, the influencing parameters summarized in Section 6.1 need to be considered and determined.

Due to the fact that F-BAM has a particle size between 0-2 mm which is coarser than the powders generally used for pelletization, it might be necessary to add other powdered materials to make sure there are enough fines to fill the space between bigger particles and then to glue all the particles together in a spherical shape when water is added. The powdered materials chosen are expected: (1) to act as filler to condense the microstructure of pellets which can significantly affect the pellet properties, and to have a good compatibility with other materials during the pelletizing process; (2) to have pozzolanic or hydraulic characteristics which will contribute to the binder hydration, and eventually enhance the pellet properties; (3) the use of these chosen powdered materials can be eco- and environmental friendly, such as using wastes from industrial fields. In this way, the recycling of BAF by the pelletizing technique is further valorised.

In literature, the pelletization of FA to produce cold bonded lightweight aggregates (CBLAs) has been widely studied and the technique is improved from both the mechanical and economic points of view (Baykal & Döven, 2000; Gesoğlu et al., 2014). Secondly, it is reported that FA could be used as filler, additive, or pozzolanic material in concrete, having a positive influence (Berryman et al., 2005). Hence, coal fly ash (FA) is chosen as one of the powder ingredients in this chapter. According to research (Cioffi et al., 2011; Geetha & Ramamurthy, 2010b), the addition of $Ca(OH)_2$ or lime can increase the pelletizing efficiency, and improve the hydration of the binder, which improves the pellet properties indirectly. It is known from literature that paper sludge ash (PSA) is a solid waste from the paper recycling industry, which mainly contains of free lime and calcite. It could be used as a hydraulic binder (Bin Mohd Sani et al., 2011; Wong et al., 2015), or raw material for eco-cement (Yen et al., 2011) for concrete. Therefore, the PSA which is available in the Netherlands is recycled and reused as a powder ingredient in this study from both the technical and economic points of view. To obtain the granulate during the pelletizing, particularly during the early stage, the moisture content and the plasticity of the raw materials are very important. Washing aggregate sludge (WAS) is a water-solids mixture (most of the solid particles are under 63 μm) collected from the aggregate washing plant, which needs to be settled in the clarifier before further use or deposit. This procedure is time consuming and not economically friendly. In other studies, this sludge is used to produce artificial aggregate by sintering (González-Corrochano et al., 2009; Volland & Brötz, 2015). The sludge normally contains 45%-55% liquid, which need to be drained out in normal treatment procedure; however, when being used for pelletization, the sludge mixture could be directly used without any other treatment (settling or draining). This is due to the fact that firstly the dried sludge is generally agglomerated and needs to be crushed or milled before use; secondly, during the pelletizing of raw material in this study, a certain amount of water is needed. Hence, the utilization of washing aggregate sludge (WAS) as one ingredient in pelletizing is a more cost-effective way to recycle it, which can avoid the pre-treatment of the sludge and decrease the consuming of water during the pelletizing process. In this way, the waste materials are directly used as raw resources for

new products without additional treatments, which combine the reduction, recycle and reuse of the waste materials at the same time.

Therefore, in this chapter, the F-BAM is one of the main solid wastes which need to be reused or recycled soon instead of being disposed in landfills according to the circular development plan in the Netherlands (Greendeals, GD 076, 2010). Meanwhile, FA, PSA, and WAS are chosen as raw materials to produce the CBLAs, those materials are also solid wastes which need to be applied in consideration of environmental and economic aspects.

It is also noticed in nowadays research that generally the cement dosage is around 10% of the total mass, and it can be 4% - 6% when the binder is finer (Dutta et al., 1997). Hence, as a trial study the amount of the binder is controlled at 10% of the total solid mass in order to compare the results to others in literature. This binder dosage can be increased or decreased depending on the requirement of aggregate strength and cost in practical conditions. The proportions of the other raw materials for the artificial aggregates production are determined after the evaluation of their physical and chemical properties which is shown in the following section.

- **Properties of raw materials and determination of proportions for pelletization**

Table 6.1 shows the chemical compositions of the raw materials. It can be seen that F-BAM has high amounts of SiO_2 and Fe_2O_3, and a low amount of CaO; paper sludge ash (PSA) contains a quite high amount of CaO and a lower amount of SiO_2. Combustion fly ash (FA) has high amounts of SiO_2 and Al_2O_3, and a low amount of CaO. Washing aggregate sludge (WAS) is mainly composed of SiO_2 and Al_2O_3.

Table 6.1: The chemical compositions and specific density of the raw materials

Composition [% wt.]	OPC	PSA	FA	WAS	F-BAM
CaO	67.9	54.9	6.2	1.5	18.6
SiO_2	14.9	13.6	45.2	73.3	39.1
Al_2O_3	3.6	8.6	27.5	11.3	7.6
Fe_2O_3	3.3	1.0	6.6	6.0	12.9
K_2O	0.8	0.5	2.2	1.9	1.1
Na_2O	0.0	0.0	1.0	0.6	1.0
MgO	1.6	2.1	1.4	0.9	1.9
CuO	0.0	0.1	0.0	0.0	0.4
ZnO	0.1	0.1	0.1	0.0	0.7
Cl	0.1	2.2	0.0	0.0	0.3
SO_3	4.5	1.0	1.7	0.2	4.3
P_2O_5	0.4	0.3	0.8	0.1	0.9
TiO_2	0.3	0.7	1.5	0.4	1.1
Others	0.4	0.2	2.1	0.6	1.9
LOI	2.2	14.6	5.3	3.6	9.2
Specific density [g/cm^3]	3.1	2.7	2.3	2.7	2.7

It is also shown that F-BAM, PSA and WAS have very similar specific densities, intermediate between OPC and FA. The particle size distribution of the powders (OPC, WAS, PSA, FA) used are very similar, as shown in Figure 6.5 (a).

Figure 6.5 (b) shows that the main crystalline phases in F-BAM are quartz, anhydrite, calcite and hematite. PSA mainly consists of calcite, calcium hydroxide, a small amount of quartz. The main crystalline phase in WAS is quartz, and FA contains quartz and calcite as well. It is noticed during experiments that the initial water contents of the mixed raw materials are important for the growth of the new pellet, and is normally controlled at 21%-31% (Gesoğlu et al., 2007, 2012, Güneyisi et al., 2013a, 2015a; Manikandan & Ramamurthy, 2008). Therefore, the total amount of the dried WAS that can be used is controlled to less than 5% of the total solid mass (due to the fact that its water content (ω) is around 45%-55%). Hence, the influence of the WAS amount on the cement hydration is not further studied.

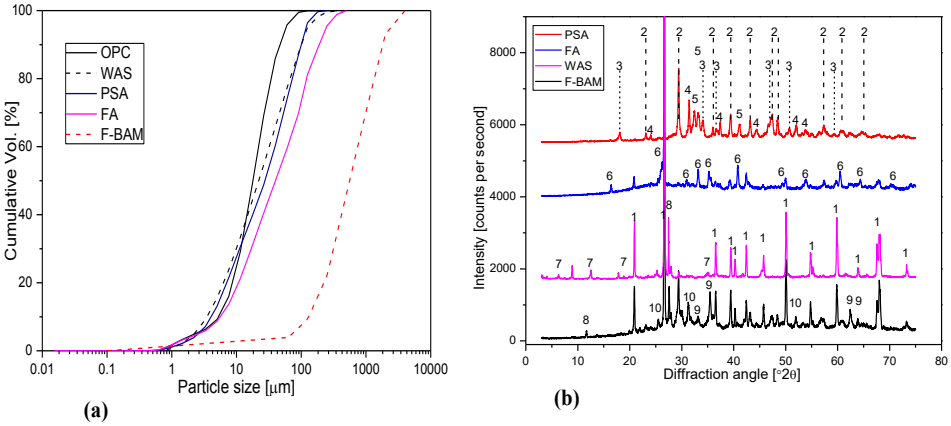

Figure 6.5: The (a) particle size distribution of raw materials and (b) the XRD pattern of the waste raw materials (1: Quartz; 2: Calcite; 3: Portlandite; 4: Gehlenite; 5: Calcium silicate; 6: Mullite; 7: Chlorite; 8: Feldspar; 9: Hematite; 10: Anhydrite)

The isothermal calorimetry results show the heat release of tested samples due to chemical reactions. The higher heat released from the mixed sample than plain cement samples means there is extra heat released from the chemical reaction when the material is mixed with cement. Figure 6.6 shows the heat development of OPC and PSA mixture.

The heat flow peak occurred after 12 hours of plain cement hydration (peak 2 in Figure 6.6 (a)) happens earlier when PSA is added (peak 1). The more PSA is added, the earlier the peaks appears. The height of this peak increases with the increasing amount of PSA. This peak in plain cement hydration represents the reaction of C_3S (tricalcium silicate) with the production of calcium silicate hydrate (C-S-H) gel phase and calcium hydroxide. It can be concluded that the addition of PSA accelerates the cement hydration. Figure 6.6 (b) shows that the total heat released from samples with 10-20% PSA is higher than that of plain

cement (from 104.6% to 101.1%, compared to 100% plain cement), and for samples with 30-60% PSA it is lower than that of plain cement (from 99.3% to 86.7%), which demonstrates that the PSA contributes to the chemical reaction of the mixed samples. Hence, the addition of a certain amount of PSA for the pelletization is expected to increase the strength of the pellets.

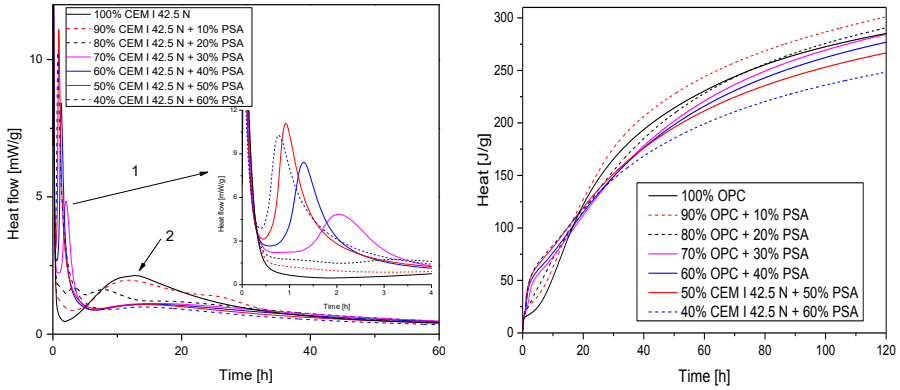

Figure 6.6: The (a) heat evolution and (b) cumulative heat of OPC with PSA relative to total powder

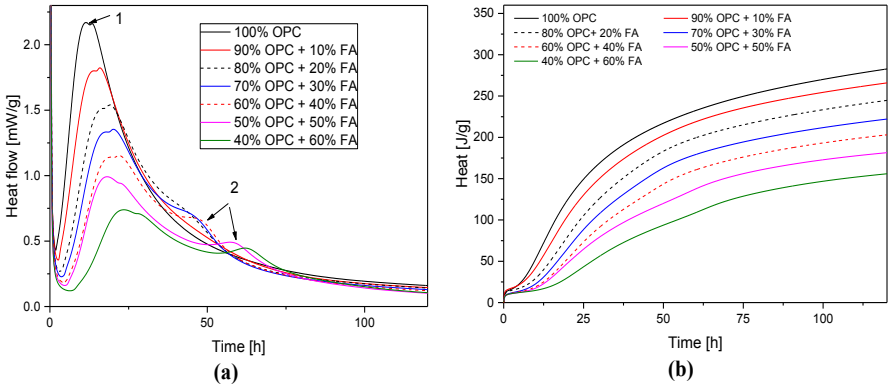

Figure 6.7: The (a) heat evolution and (b) cumulative heat of OPC with FA relative to total powder

Figure 6.7 (a) shows that the height of the main hydration peak (peak 1) at around 20 hours decreases with the increasing amount of FA; the duration of this peak of samples with FA is longer than that for the plain cement sample. There is a pozzolanic reaction after around 45-50 hours (peak 2), which contributes to the additional hydration peak. The total heat released decreases with the increase of FA, and it is always lower than the plain cement sample (Figure 6.7 (b)). However, the decrease of the total heat is lower than the replacement ratio of FA. For instance, after 120 hours, the total heat released from the solid mixtures decreases from 283 J/g (100% OPC) to 156 J/g, and its reduction is 45% (when

60% FA is used as OPC replacement) compared with plain OPC. This indicates that the 60% FA addition contributes 15% of the heat release. It can be stated that the FA may have a slight contribution to the cement hydration at early age, even though it is much less compared to that of PSA.

From the above shown calorimetric results, it can be assumed that at early ages of aggregates curing, the strength of the pellets is mainly influenced by cement and PSA, while the use of FA can have positive effects on the pellet strength after long term curing, due to its slow pozzolanic properties (De Weerdt et al., 2011).

To achieve a good combination of these two wastes, the relative proportions of FA and PSA should be determined when the cement amount is fixed at 10% for pelletization. Figure 6.8 shows the interaction between the PSA and the FA in the cement system. It can be seen that, with a fixed amount of cement (10% wt.), the addition of PSA accelerates the cement hydration, and when PSA and FA are mixed with a proportion 1:1, the total heat released is the closest to that of the plain cement sample. Therefore, the mix proportion of PSA and FA is 1:1 wt. of total PSA and FA for artificial aggregate production based on the calorimetric study.

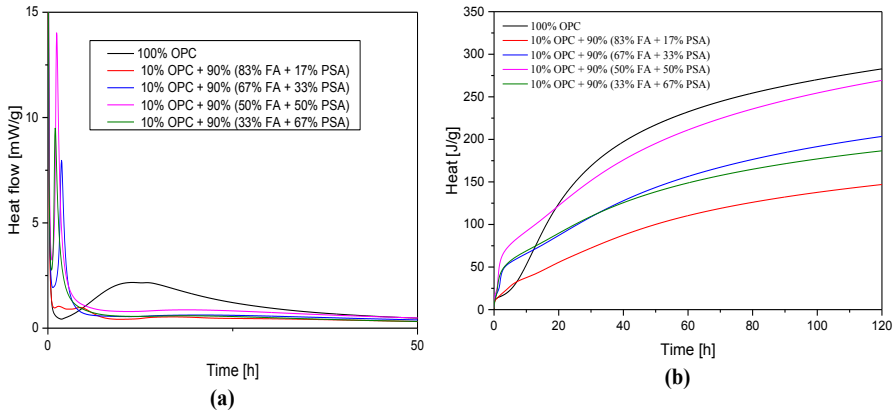

Figure 6.8: The (a) heat evolution and (b) cumulative heat of OPC with PSA and FA relative to total powder

The amount of F-BAM in this study is chosen based on its leaching properties, as well as the consideration of economic factors from the company. Due to the fact that the F-BAM properties could differ from plant to plant, the design of the recipe will change. In this study on the production of CBLAs using F-BAM, the amount of F-BAM is in the range of 10-75% of the total solids mass).

To summarize shortly, in the current study the proportions of the raw materials used are 10% cement, 40%-75% F-BAM, 5% WAS and the amounts of PSA and FA make up the rest of the total solid content as shown in Section 6.2.

6.3.2 Aggregate characteristics

- **Artificial aggregate (CBLA) properties**

The particle size distribution (PSD) of the produced artificial aggregate is shown in Figure 6.9, and it can be seen that its particles are mainly between 2-8 mm. The PSDs of the 28-days sample and 1 day sample are very similar, and the 28-dasy sample has slightly higher amount of small particles (< 2 mm, 1% more) and a bit lower amount of coarse particles (> 8 mm, 3% less) compared with the 1 days samples. This could be due to the shrinkage of the pellets and the metallic Al in the F-BAM which may cause the cracking and break down of some pellets. Meanwhile, the powders on the pellets surface may be removed due to the fraction between particles when the pellets are dried.

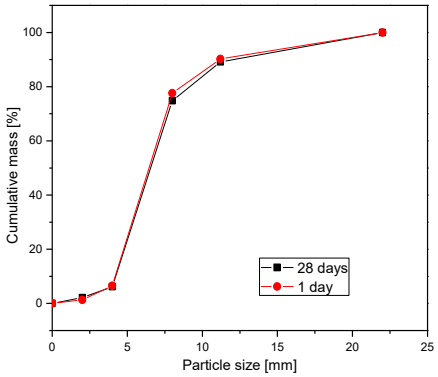

Figure 6.9: The particle distribution of produced aggregates after 1 day and 28-days curing

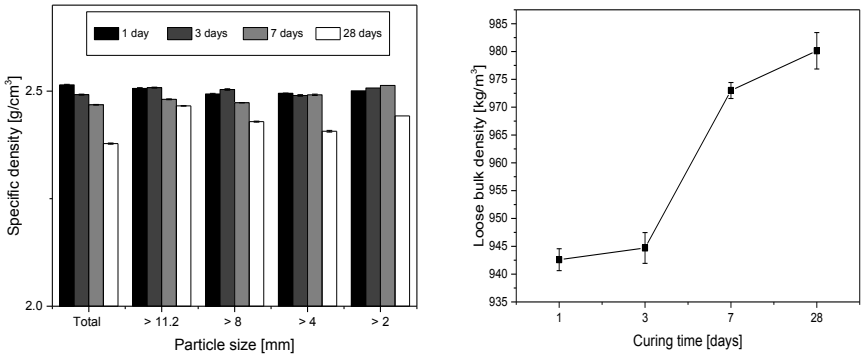

(a) **(b)**

Figure 6.10: The (a) specific density and (b) bulk density of the artificial aggregate after different curing ages

Figure 6.10 shows the specific densities of the artificial aggregate fractions and the loose bulk density of the investigated fraction (fraction 4-16 mm was chosen according to EN 1097-3 (1998). The specific density (Figure 6.10 (a)) of the aggregates produced is around

2.50 g/cm^3, which is slightly lower than that of natural quartz aggregates (2.65 g/cm^3), and the specific density of the fractions are very similar, which indicates the homogeneity of the produced aggregates. It can be noticed as well that the specific densities are decreasing slightly with the curing time; this could be attributed to the hydration of cement, the hydration product of which fills the pores inside the aggregate, and eventually decreases the porosity of the aggregates and finally their shrinkage. This could be further confirmed by the loose bulk density of the aggregates above 4 mm, which shows an increasing trend along with the curing days (Figure 6.10 (b)). The loose bulk density of the aggregates above 4 mm is around 985 g/cm^3 after 28-days curing, which is lower than 1200 kg/m^3; hence, this aggregate fraction can be defined as lightweight aggregate according to standards EN 13055-1 (2002). The apparent density of the produced aggregate is 2323-2358 kg/m^3; its oven dried particle density is 1709-1730 kg/m^3, and the saturated and surface-dried particle density is 1975-1988 kg/m^3.

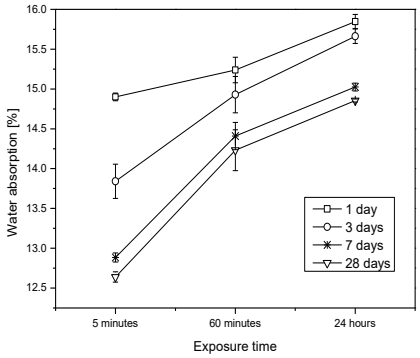

Figure 6.11: The water absorption of the artificial aggregate after different curing ages

Figure 6.11 shows the water absorption of the produced cold bonded lightweight aggregates (CBLAs) above 4 mm. The 24 hours' water absorption after 28 days curing is around 14.9%, which is lower compared with the CBLAs produced by fly ash in literature which is 21.2% (Güneyisi et al., 2015a) and 18.7-21.2% (Thomas & Harilal, 2015). It can be seen that the water absorption has a decreasing trend along with the curing time, and the difference between 7 and 28 days cured samples is small. Moreover, the water absorption increases significantly during the first hour. After 5 minutes, the water absorption already reaches 94% of the 24 hours' water absorption for the 1-day cured sample, and this value is decreasing with the curing days (from 88% to 85% for 3-days and 28-days cured samples, respectively). After 1 hour, the water absorption of all the samples reach around 95-96% of their 24 hours' water absorption, respectively. It can be concluded that, the porosity of the CBLA is decreasing along with the curing time, which also indicates the hydration of the binder. The water absorption reflects the porosity of the aggregate, which is related to

its strength. For the artificial aggregate, it also reflects the compaction of the pellets during the pelletizing procedure.

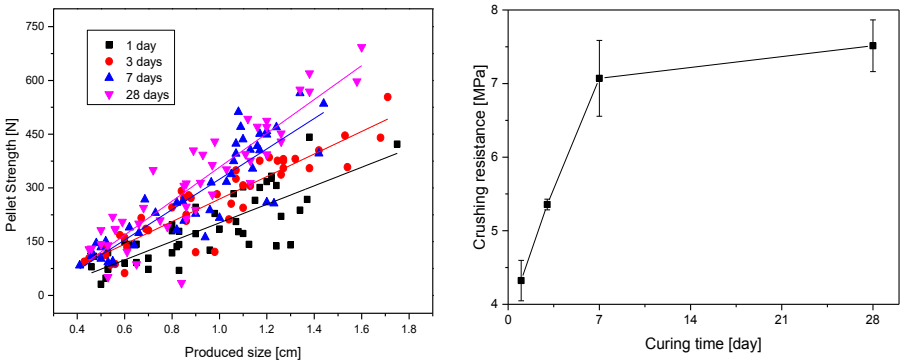

Figure 6.12: The strength development of the produced pellets (a) individual pellet strength and (b) crushing resistance of the CBLA

The strength of the pellets depends on the binder dosage and the microstructure of the pellet (void ratio/porosity of the pellet). It can be seen in Figure 6.12 (a) that the strength of the individual pellets increases with the curing age, and after 7 days the pellet strength is around 84% of its 28-day pellet strength; the pellet strength also increases with the particle size (around 125 N to 650 N for pellet size from 4 to 16 mm); these findings are in agreement with the results in (Gesoğlu et al., 2007, 2012). However, the results of the individual pellets strength are quite dispersing, as this test would be influenced significantly by the chosen pellets. Therefore, the crushing resistance of the aggregate according to EN 13055-1 (2002) was also evaluated to demonstrate the strength of the produced CBLAs. The result is shown in Figure 6.12 (b). It can be seen that the crushing resistance increases steeply during the first 7 days of curing; after that there is only a small increase. The crushing resistance of 7 days-cured samples achieves 94% of the 28 days-cured samples (around 7.5 MPa). This result suggests that after 7 days, the artificial CBLAs can be ready for use or for delivery in practical conditions.

- **Comparison with other artificial aggregates**

In literature (Baykal & Doven, 2000; Bui et al., 2012; Cioffi et al., 2011; Colangelo et al., 2015; Dutta et al., 1992, 1997, Geetha & Ramamurthy, 2010a, 2013, Gesoğlu et al., 2012, 2014, 2004, 2007; Güneyisi et al., 2015a; Manikandan & Ramamurthy, 2008; Thomas & Harilal, 2015), the particle size of the cold bonded lightweight aggregates (CBLAs) was below 20 mm and their bulk density was between 800-1600 kg/m^3. The water absorption of the pellets was between 14-27%. Gesoğlu et al. (2007) applied the cold bonded pelletizing technique to recycle fly ash from a thermal power plant, in which the cement/fly ash ratio was 0.1 by weight and the pelletizing duration was 20 minutes in total (compared

to 15 minutes in the present study). The produced CBLA had a particle size between 4-14 mm, its water absorption was around 32%, and individual particle crushing strength after 28-days curing was around 70-310 N for particle sizes from 6 to 14 mm (125-650 N for 4-16 mm in this study). Güneyisi et al. (2013b) produced a CBLA from a mix of powders of class F fly ash and Portland cement (9:1 of wt.) using the same device and pelletizer as described in (Gesoğlu et al., 2007). The particle size of the produced CBLA was 4-16 mm with a water absorption of around 18%, and its maximum pellet strength for pellets between 4-8 mm was 127 N. Colangelo et al. (2015) used OPC, hydrated lime and coal fly ash as binding materials to recycle MSWI fly ash, and the binder accounted for around 30-50% of the total solid mass. The produced aggregate was surface treated using a cement/coal fly ash mixture (1:1 by mass), and the total cement used for the pelletization accounted for around 14% of the total mass. The produced CBLAs had a particle size of 4-18 mm, and their crushing resistance was 2-6 MPa (7.5 MPa in the present study) and their maximum water absorption was 15%. Comparing with other CBLAs, the one produced in this study has a slightly lower water absorption, and higher pellet or crushing strength. Hence, it can be concluded that the production of the artificial lightweight aggregate using MSWI F-BAM together with other industrial solid powders is possible and F-BAM has good compatibility with other industrial powdered materials during the pelletization. The properties of the pellets are comparable or even better than the artificial aggregate reported in literature. The benefits of integral recycling F-BAM with other industrial solid wastes through cold bonded pelletizing technique are summarized below.

- **Mechanical benefits of F-BAM in cold bonded aggregate**

Figure 6.13 demonstrates the pellet microstructure produced with only powdered materials (Figure 6.13 (a)) and with MSWI F-BAM (Figure 6.13 (b)).

The higher crushing resistance of the artificial CBLA produced in this chapter with F-BAM particles compared with the others may be attributed to the following reasons: (1) the F-BAM particles in the pellet can act as a skeleton of the single pellet, which has the similar role as the aggregate acts in the concrete, resulting in the enhancement of the pellet strength compared with pellets produced with only powders. In another study (Cioffi et al., 2011), the incineration bottom ash was milled into powder for artificial aggregates production, which on one hand increased the production cost; while on the other hand, disrupted the contribution of bottom ash particles as skeleton to increase the pellet strength. Hence, the direct use of F-BAM for pelletization in this study is more beneficial; (2) the angular particle shape of F-BAM enhances the interlocking force and bonding between the powder matrix and the F-BAM particles, which increase the failure force of the pellet; (3) comparing the use of F-BAM with the use of only powder materials for producing artificial aggregate, with a fixed amount of binder and pellet size, the F-BAM has lower specific surface area than powder particles. This means less binder is needed for binding all the particles together and the pellet shape will be more stable (less powder will be removed

from the surface of the pellets), similar to the statement in (Kim et al., 2016). Hence, with the same amount of binder, higher strength can be obtained for pellets with F-BAM than pellets with only powders.

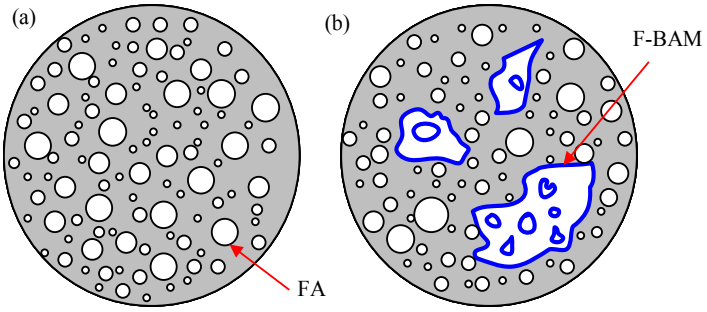

Figure 6.13: Schematic representation of cross section of pellets produced with (a) only powders and (b) with addition of F-BAM

- **Valorisation of F-BAM by pelletization**

Figure 6.14 shows the cross section of the pellets with F-BAM under optical and scanning electron microscope, where the distribution of F-BAM particles, WAS and PSA can be seen clearly, and the F-BAM particles are well embedded into the matrix (Figure 6.14 (a)).

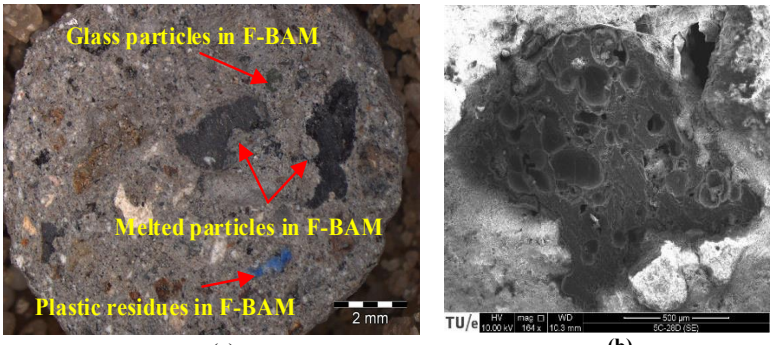

(a) **(b)**

Figure 6.14: The cross surface of a produced pellet (a) under optical microscope and a F-BAM particle (b) under scanning electron microscope

It can be seen in Figure 6.14 (b) that the F-BAM particle is porous and has an irregular shape. Moreover, there are pores inside the F-BAM particles which contribute to the slightly lower specific density and lower loose bulk density of the produced aggregates as the results shown in Figure 6.10. In general, the F-BAM has an angular particle shape and the surface of the particles is covered by dust, which contributes to the high water absorption during its application in mortar or concrete. However, these disadvantages of F-BAM in concrete can be positive factors during the pelletizing process in this study.

The F-BAM used in this work is collected from the MSWI bottom ash by sieving and it has a moisture content (ω) around 22% because of the water cooling of the bottom ash after the combustion. When the wet F-BAM is mixed with the powders, some powder particles are firstly agglomerated on the F-BAM particles due to their moisture content, which can shorten the pelletization duration to save energy consumption on a large-scale industrial production. When extra water is added, more fine powders are coated on the F-BAM particles, also the fine powders themselves start to agglomerate. Moreover, due to the bigger particle size compared to powder materials (such as fly ash) and rough surface structure, the compaction of the pellets during the pelletizing procedure is more efficient. The powder materials can easily absorb water on their surfaces, which generates a water layer, contributing to a longer compaction duration or a porous microstructure of the dried pellets. The agglomeration of powder and particles, and the compaction of the pellets happen during the whole pelletizing process.

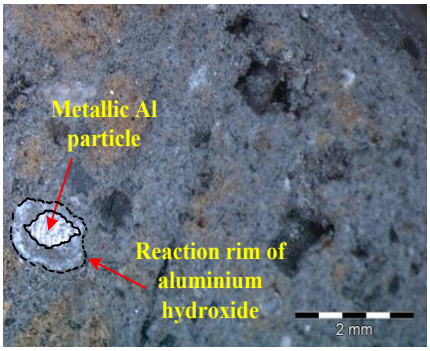

Figure 6.15: The cross surface of a pellet where a metallic Al particle was found

It is observed during the tests that there are pellets which have cracks on their surface before crushing test or application. This could be attributed to the metallic Al in the F-BAM which reacts with alkalis and then generates H_2, leading to the cracking of the pellet before any external force is applied. Figure 6.15 shows the cross section of a pellet and there is a piece of metallic Al found. Around the metallic Al piece there is a white trace observed, which might be the reaction rim of aluminium hydroxide due to the reaction of metallic Al with the alkaline surroundings during curing (Müller & Rübner, 2006). When the F-BAM is directly used in concrete, this gas formation could lead to the damage of the concrete like cracking and spalling. The same phenomenon takes place in the pellets. However, this does not mean that the crushing resistance of the whole pellet fraction will be decreased dramatically, because few pellets will undergo cracking (as shown in Figure 6.9, the difference between the particle size distribution of samples after 1 day and 28 days curing is around 1-3%). Meanwhile, this reaction can take place during the curing of the pellets, which means there will be less risk due to the metallic Al when the aggregates are later

used in concrete. Hence, in the application of artificial aggregate with F-BAM, the metallic Al is less of a problem.

Compared with traditional cold bonded artificial aggregate, the use of F-BAM is of more beneficial considering both the properties of produced pellets and the recycling of F-BAM. Therefore, the cold bonding technique is a good way to recycle the F-BAM for producing lightweight cold bonded aggregate together with other industrial waste powders.

6.3.3 Concrete properties with CBLAs

The 28-days compressive strength of the concrete with this artificial aggregate decreases with the increasing amount of aggregate replacement, from 37.1 MPa to 27.7 MPa when the replacement ratio increases from 50% to 100%. This is attributed to the low strength of the artificial aggregate, similar to (Colangelo et al., 2015; Güneyisi et al., 2015a, 2015b; Thomas & Harilal, 2015).

Table 6.2: Literature summary of cold bonded aggregate application

Reference	Water to binder ratio	Cement [kg/m^3]	Diameter [mm]	Replacement ratio [%]	Compressive strength [MPa]
This study	0.5 0.6	280	2-8	50 100	37.1 27.7
(Thomas & Harilal, 2015)	0.45	250 350 450	10-20	100	20-28 21-30 21-30
(Cioffi et al., 2011)	0.5	345	5-20	100	12.8-25.8
(Güneyisi et al., 2015a)	0.4	440	0.25-4	50 100	37 21
(Gesoğlu et al., 2004)	0.55	400	4-9.5	30 45 60	22 27 21
(Güneyisi et al., 2013b)	0.55	400	4-16	100	29
(Gesoğlu et al., 2006)	0.55	400	4-9.5	100	23.2-37.8
(Gesoğlu et al., 2013)	0.55	350	4-16	100	27.5

It can be seen from Table 6.2 that, with a similar water to binder ratio, comparable particle size and replacement ratio of artificial aggregate, the compressive strength of concrete in this study with much less amount of cement, is higher than that in literature (Cioffi et al., 2011; Gesoğlu et al., 2006, 2013, Güneyisi et al., 2013b, 2015a; Thomas & Harilal, 2015). It is reported in (Güneyisi et al., 2015a) that the concrete strength is decreased by 43.2% when the replacement ratio increased by 50% (from 50% to 100%), and in (Güneyisi et al., 2015b) the concrete strength decreased by 18.5% after the replacement ratio increased from 30% to 45%. It can be concluded that the concrete strength decrease is higher than the replacement ratio of the aggregate, which indicates the adding of the artificial aggregate could not contribute to the concrete strength properly. However, in this study, the compressive strength of the concrete decreased by 25% when the replacement ratio increased by 50% (from 50% to 100%), which means the artificial aggregates contribute to the concrete strength. This could be attributed to the higher crushing strength of the

artificial aggregate produced in this study than others. Therefore, it can be concluded that the application of artificial aggregate in concrete produced in this study has better results than other artificial aggregates.

There are several factors that influence the application of this kind of artificial aggregates in concrete: aggregate strength which relates to the concrete strength directly; water absorption which influence the fresh properties of concrete and aggregate density which is related to the concrete density. Figure 6.16 shows the relationship between the water absorption, crushing resistance and loose bulk density of the artificial aggregate produced in this study. It can be seen that both the crushing resistance and loose bulk density of the aggregate has a linear relation with its water absorption.

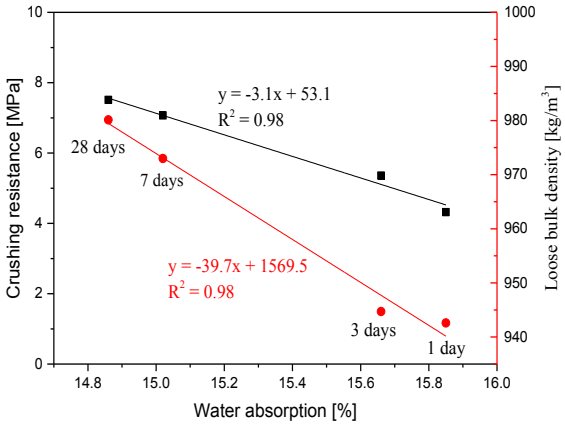

Figure 6.16: The relation between water absorption, crushing resistance, and loose bulk density of the artificial aggregate

A lower water absorption value means lower porosity of the aggregate. The loose bulk density of artificial aggregate is influenced by raw material density and aggregate porosity. The lower density of raw materials or higher porosity of aggregate results into lower loose bulk density. The crushing resistance in this study is related to the pellet strength (which is porosity related), packing of the sample during test, etc. Therefore, by adjusting the porosity of the artificial aggregate to determine its application in concrete where the concrete strength is more focused or the density of concrete, is more important. Moreover, a lower porosity of the aggregate will also lead to decreased contaminant leaching.

6.3.4 Leaching behaviour evaluation of CBLAs

The F-BAM contains high amounts of Cu - around 3100 mg/kg of dry solid (d.m.), chloride (2100 mg/kg d.m.) and sulphate (22900 mg/kg d.m.), and also Sb (83 mg/kg d.m.) and Mo (19 mg/kg d.m.) (Table 5.2). The leachability of the elements is calculated by dividing their leached-out amount from the tested samples (F-BAM or artificial aggregate) by the total amount of the elements in the F-BAM according to Eq. (3.8), respectively. The column

leaching results of the Sb, Cu, Mo, chloride and sulphate of the F-BAM, the produced aggregate and crushed concrete with 50% vol. of produced aggregate. The leaching level shows that chloride and sulphate in F-BAM has quite high leachability during the column test (around 45.2% of the total chloride and 48% of the total sulphate from the F-BAM is leached out, respectively).

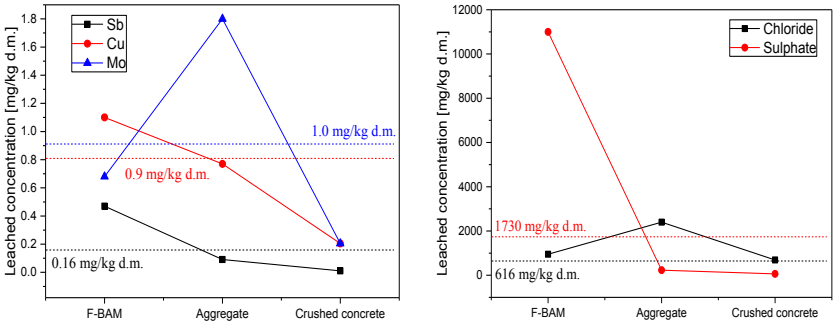

Figure 6.17: Comparison of leaching values of F-BAM, artificial aggregate, crushed concrete with 50% aggregate replacement and the leaching limit value for non-shaped materials in legislation (SQD, 2013) (dash - straight line)

The leaching of the artificial aggregate after 28 days curing shows that the Mo and chloride leaching still exceed the limit value for non-shaped materials in the Dutch legislation (SQD, 2013), while the leaching of the other investigated elements is well under this limit value. The leachability of Cu and Mo in the artificial aggregate increase compared with that of the F-BAM, especially for Mo which increases more than 3 times (Meima et al., 2002). The leachability of Sb and sulphate in the artificial aggregate decreases compared with that of the F-BAM and the sulphate leaching decreased dramatically, which demonstrates the immobilization effect of cementitious materials differ from dilution effect. For chloride, the total amount in the artificial aggregate is 0.3% (test value), and the leached-out amount is 0.24%, indicating that the chloride in the artificial aggregate is highly leachable.

Considering the binding capacity of these elements, it seems that Sb and sulphate are well bound, for the others the leaching capacity is increased. This is mostly attributed to the influence of the pH (Meima et al., 2002). The sulphate leaching is improved significantly in the artificial aggregate; this could be attributed to the fact that the sulphate in the F-BAM could contribute to the cement hydration. For the leaching of chloride, the high amount of PSA (2%, Table 6.1) contributes to the higher leaching of chloride compared with calculated leaching based on the F-BAM only.

The column leaching test on the crushed concrete samples (demolished samples) with 50% aggregate replacement (Figure 6.17) shows that its leaching concentrations of Sb, Cu, Mo and sulphate are far below their limit values according to SQD (2013), which means this

crushed concrete can be used as recycled aggregate again after its useful service life and the leaching of heavy metals would not be a problem. The leaching of chloride in the concrete is slightly higher than its limit value, which may limit its application in reinforced concrete. On the other hand, the binder amount of the concrete may influence the immobilization of contaminants; in general, more binder can reduce the leaching of heavy metals. Hence, for environmental considerations, the amount of produced aggregates applied in concrete can be modified according to the binder content in practice.

Due to the fact that the leaching properties of the F-BAM will vary between plants, and also the leaching legislation on the F-BAM and aggregate with F-BAM are different between countries, the leaching properties can be adjusted by changing the amount of F-BAM or binder used according to specific requirements. Additionally, the produced aggregate can be used as aggregate replacement in concrete, even if its leaching properties does not meet all requirements for non-shaped materials, by controlling its replacement ratio to guarantee the leaching of the final shaped concrete products comply with the environmental legislation (SQD, 2013). In this way, the concrete with artificial aggregate, the leaching of which is under the limit value, will be the final product available for further application, considering the environmental legislation. Therefore, it is of interest to study the properties of concrete with this artificial aggregate from the mechanical point of view, which is relevant to its applications in the construction field (which is shown in Chapters 7 and 8). The binding capacity of cementitious materials on contaminants from F-BAM when used to produce artificial aggregates is summarized in Chapter 9.

6.4 Conclusions

This chapter presents the recycling of MSWI bottom ash fine particles (F-BAM, 0-2 mm) through a cold bonding technique to produce lightweight aggregate, together with other waste powders. From the results obtained in this paper the following conclusions can be drawn:

(1) The cold bonded pelletizing technique, which is widely used to recycle the fly ash, slag, or quarry dust, can also be used to recycle MSWI F-BAM successfully.
(2) The strength properties of the lightweight aggregate produced in this study are comparable to, or even better, than other artificial aggregates reported in literature. The use of F-BAM instead of powders only for pelletization has a positive effect on the properties of the artificial aggregate.
(3) The F-BAM particles act as skeleton in the pellets, playing a similar role as aggregates in concrete and the angular F-BAM particle shape improves the interlocking force and bounding between the F-BAM particles and the powder matrix in the pellets, which contributes to a higher crushing resistance of the produced lightweight aggregates.

(4) Less cement is needed for producing artificial lightweight aggregate with similar crushing resistance using F-BAM than using only powders, due to the lower specific surface area of F-BAM comparing with powders.
(5) The leachability of sulphate and antimony in the artificial aggregate is decreased, while for copper it is increased due to the influence of pH. The leaching of the sulphate, copper and antimony of the produced artificial aggregate is well under the limit value for the non-shaped material according to the Dutch legislation, while that of Mo and chloride not. The leaching of Mo and chloride can be further decreased in the final concrete samples by using a lower replacement ratio in case the requirements for non-shaped produces are not met.
(6) Compared with concrete with other artificial aggregates, higher compressive strength of concrete with artificial aggregate produced from F-BAM can be obtained due to the higher aggregate crushing resistance compared with other artificial aggregates. The leaching of heavy metals and salts from concrete with artificial aggregates is below the limit values according to the Dutch legislation, which indicates that the recycle and reuse of these concretes after their service life will comply with the current environmental legislation.

In this chapter, the use of F-BAM to produce cold bonded lightweight aggregates (CBLAs) shows positive results; however, the properties of the raw materials, such as binder types and contents, additives properties, proportions of raw materials, etc., have significant influence on the properties of CBLAs. Hence, it is necessary to optimize the combination of raw materials for producing CBLAs with good properties based on the characteristics of the raw materials applied, which is investigated in the next chapter.

Chapter 7

7 Influence of raw material combinations on CBLA properties*

7.1 Introduction

The study in Chapter 6 showed that the application of fine MSWI bottom ash to produce cold bonded lightweight aggregate (CBLA) by pelletization is possible with the integral combination of the chosen industrial powders; moreover, the properties of the obtained aggregate are comparable with the ones in literature and it can be used as aggregate replacement in concrete. However, it is also noticed that the strength of the pellets has a remarkable influence on its application in concrete (Colangelo et al., 2015; Güneyisi et al., 2015b; Thomas & Harilal, 2015), by decreasing the concrete strength due to its lower strength compared with natural aggregates, which limits the amount of artificial aggregate that can be used. In addition, the leaching of the produced artificial aggregates in Chapter 6 did not comply with the Dutch legislation completely. Hence, the investigation of methods to improve the properties of the cold bonded lightweight aggregate by integrated recycling of industrial powder wastes and F-BAM is the focus of this chapter, and the influence of the raw materials combination on the aggregate properties are studied as well.

In current research, the general methods for improving the pellet strength are mainly adjusting the pelletizing parameters (Baykal & Doven, 2000; Harikrishnan & Ramamurthy, 2006), changing the raw materials' properties (Baykal & Doven, 2000; Dutta et al., 1997; Manikandan & Ramamurthy, 2007; Thomas & Harilal, 2015) and curing conditions (Gomathi & Sivakumar, 2015; Manikandan & Ramamurthy, 2008). In the present chapter, the investigated parameters are binder amount, proper powder materials as additives, various F-BAM amounts, polypropylene fibres, and nano-silica addition. The influences of these parameters on the properties of the produced cold bonded aggregates are evaluated and the corresponding mechanisms are discussed.

7.2 Materials and methodology

The raw materials used in this chapter are the same as described in Section 6.2.1. In addition, ground granulated blast furnace slag (Gao et al., 2015) (GGBS, ENCI, the Netherlands) and nano-silica (nS) produced from olivine dissolution (Lázaro García, 2014; Quercia Bianchi, 2014) are used as OPC alternatives for the aggregate productions. Polypropylene fibre (PPF) with a length of 3 mm, density of 0.91 kg/m^3 provided by FBG (the Netherlands) and Bonar (England) is used as reinforcing fibre (Figure 7.1).

*Content of this chapter was published elsewhere [Tang, P., and Brouwers, H.J.H., (2017) Waste Manag. 62, 125–138].

The chemical compositions, crystalline phases, PSDs, densities, of the raw materials are present in Table 6.1 and Figure 6.5. The pelletizing procedure, the determination of the properties of the obtained artificial aggregates and the evaluation of material leaching properties are as described in Section 6.2.2. The proportions of solid materials of the mixtures for the aggregate productions are shown in Table 7.1 and sample Ref. is used as reference.

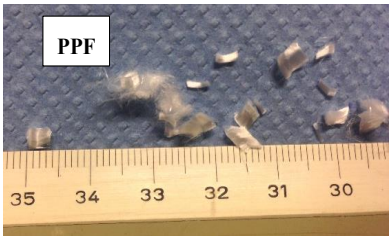

Figure 7.1: The raw materials used and aggregate produced

Table 7.1: The recipe design for artificial aggregate production (proportions of dried solid materials).

Samples	Binder	Alternatives				Coarser particles	Glue agent	Reinforcement
	OPC	nS	GGBS	FA	PSA	F-BAM*	WAS	PPF
	[% total solid]	[% OPC]	[% OPC]	[% total FA+PSA]		[% total solid]	[% total solid]	[% vol.]
Ref.	10	0	0	100	0	10-40	5	0
5C	5	0	0	50	50	40-75	5	0
10C	10	0	0					
15C	15							
6C	6		67					
No PSA	10	0	0	100	0	40-75	5	0
No WAS				50	50		0	
0.5% PPF	10	0	0	50	50	40-75	5	0.5
1.0% PPF								1.0
2.5% PPF								2.5
4.5% PPF								4.5
0.4 nS	9.6	4	0	50	50	40-75	5	0
0.8 nS	9.2	8						

*The amount of F-BAM is fixed and the exact value is in the range shown in the table.
The OPC, FA, PSA, F-BAM, and WAS are the same as used in Chapter 6, and the GGBS is the same as used in Chapter 5).

7.3 Results and discussion

7.3.1 Aggregate properties improvement

- **Particle size distributions**

For all the samples, there is very small amount of pellets above 16 mm, and these big pellets are not well compacted having an irregular shape and weak pellet strength. These fractions generally account for less than 5% of the total pellets produced in this chapter, therefore, this fraction is sieved out (as performed in the pilot plant of Attero & Smals).

During the pelletizing procedure, it is observed that the generation and growth of pellets in the samples with nS is earlier and faster than other samples, as well as in reference sample (Ref.); while samples with PPF take longer time to grow. The generation speed of pellets during the pelletization follows the order of: (0.8 or 0.4) nS > Ref. > 10C (5C, 6C, 15C) > No WAS (No PSA) > samples with PPF. However, this difference is minor. It can be concluded that increasing the F-BAM amount and adding PPF decrease slightly the generation speed of the pellets, while adding PSA or WAS result in a shorter time needed for the generation of pellets during pelletization. Finer particle sizes of the raw materials can shorten the granulation time.

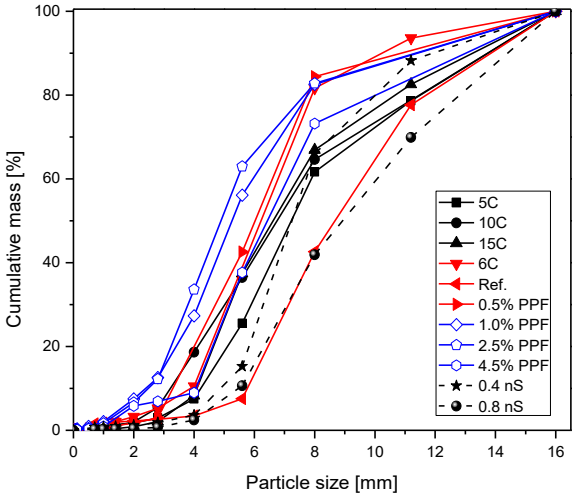

Figure 7.2: The particle size distributions of the produced lightweight aggregates

The particle size distributions of all the aggregates under 16 mm produced are shown in Figure 7.2. The particle size of Ref. is mainly between 2-16 mm, of which particles between 4-16 mm account for around 96% wt. It can be seen that pellets below 2 mm accounts for approximately less than 7% of the total for all the mixtures, and the pellets produced with PPF have a slightly higher amount of particles under 2 mm than other samples. The samples Ref., 0.4 nS and 0.8 nS have coarser particle size than other mixtures, while the samples with PPF have finer particle sizes. This can be explained by the following reasons: firstly, Ref. has a higher powder/F-BAM ratio, which means more water layers will be formed on the small particles; this water layer will make the pellets grow fast, hence, the pellets are bigger than other samples within the same pelletizing duration. It is also noticed that Ref. has some particles which are irregular, similar as shown in other work (Colangelo et al., 2015); while the particles of the samples except Ref. in this study are more rounded. This may indicate that the pellets containing only powder materials are more difficult to be compacted during the pelletizing procedure than the ones with more F-BAM. For aggregates produced with nS, it was observed that the particles are more rounded than the

other samples and slightly coarser particle sizes were obtained, which is due to the finer particle size of nano-silica. For the samples with PPF, the hydraulic property of the fibre influences its compatibility with all the solids, and the PPF needs more powder to compact them together which may result in pores in the pellets.

From the above shown results, it can be concluded that the use of nano-silica, PSA or WAS can shorten the growth time of pellets, the decreasing of F-BAM content can also benefit the growth of the pellets; however, the freshly produced pellets are more difficult to be compacted, thus, the pellets' shape is more irregular. The aggregates produced with higher powder/F-BAM ratios achieve larger particle sizes than others and the addition of PPF slightly disturbs the growth of pellets.

- **Bulk density and water absorption**

The bulk density and water absorption are essential parameters for evaluating the cold-bonding lightweight aggregates (CBLAs), which has a significant influence on its application. It can be seen in Figure 7.3 that the pellets of all the samples have a bulk density around 835-927 kg/m^3, which is below 1200 kg/m^3 and they all can be categorized as lightweight aggregates according to EN 13055-1 (2002). The CBLAs produced in this chapter have a water absorption of 17-25%, which is similar with the one produced in literature using powders (Cioffi et al., 2011; Colangelo et al., 2015; Ferone et al., 2013). Furthermore, it is shown that the bulk density and water absorption of these aggregates has an inverse relationship; a similar result is reported (Bernhardt et al., 2013).

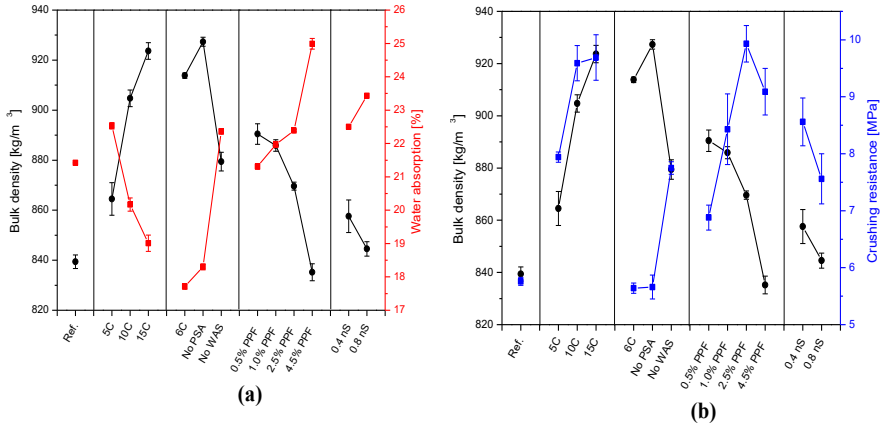

Figure 7.3: The relationship between bulk density, (a) water absorption and (b) crushing resistance of the produced CBLAs after 28 days curing

The comparison between samples 5C, 10C and 15C demonstrates the influence of binder amounts on the CBLA properties. It can be seen in Figure 7.3 that the bulk density increases with the increase of binder amount, while water absorption has a decreasing trend. This can be attributed to the fact that the higher binder amount mostly contributes to a lower

porosity (Manikandan & Ramamurthy, 2008) and denser microstructure of the pellets; also, cement has a higher density than the other raw materials, which increases the total density when its amount is increased. Similar results were observed in a previous study (Thomas & Harilal, 2015). For samples with PPF, the bulk densities decrease with the increase of PPF content while their water absorption increases. This is due to the fact that the PPF is not very easy to be glued and compacted in the pellets, hence the microstructure of the pellets is not as dense as the other samples; in addition, the PPF has very low density compared with OPC or F-BAM.

Comparison of sample Ref. and No PSA shows the influence of F-BAM content on the CBLA properties. Sample Ref. has a lower bulk density and higher water absorption than sample No PSA, which indicates that the increasing F-BAM amount can result in a lower porosity of the produced aggregates. The higher surface area of the powders than F-BAM results in a higher amount of water absorbed on their surface during pelletization, which may form a water layer force between particles. Subsequently, the compaction of the pellets is more difficult than the sample with F-BAM. Moreover, after the evaporation of the water, higher amounts of capillary pores are left, which results in a higher porosity. Thus, the sample with a higher powder/F-BAM ratio has a lower bulk density. When nS is used as cement replacement, the bulk density of the CBLAs decrease compared with sample 10C; and a higher content of nS results in lower bulk density and then higher water absorption. The higher surface area of nS particles than OPC and subsequently a thicker water layer (Quercia Bianchi, 2014) contributes to a porous microstructure.

Sample 6C shows an increased bulk density and decreased water absorption compared with sample 10C, while sample No WAS shows the opposite trend. The WAS can enhance the gluing of the particles, and also its finer particle size may contribute to a slightly denser microstructure.

It can be briefly summarized that increasing the binder amount (comparison of 5C, 10C and 15C), F-BAM content (Ref. and No PSA) and PSA (10C and No PSA) amount can result in the decrease of the porosity of the produced lightweight aggregates while the use of PPF and nS results in the increase of aggregate porosity.

- **Crushing resistance**

The cold bonded aggregates produced with similar methods as reported in (Cioffi et al., 2011; Colangelo et al., 2015; Ferone et al., 2013) have a bulk density around 1200-1600 kg/m^3 and water absorption about 8-20%, and the crushing resistance is between 2-6 MPa. Hence, it is observed that the aggregate Ref. has a lower bulk density and higher water absorption, which indicates that Ref. has higher porosity; while it has a higher crushing resistance compared with others products, this may be attributed to the addition of MSWI bottom ash fines (F-BAM) instead of powders only. The mechanism of the contribution from F-BAM can be explained by the following hypothesis (as described in Chapter 6):

firstly, the F-BAM can act as 'aggregates' in the pellets which enhance the skeleton strength of pellets, and F-BAM has an irregular particle shape which can contribute to a better bonding strength with the paste; secondly, F-BAM has smaller surface area compared with powdered materials with same volume, which means less binder is needed to bind the particles. Hence, Ref. can reach a higher crushing resistance with same binder amount, although it has a higher porosity.

The 28-day crushing resistance (CR) of the samples produced in this study is around 5.64-9.93 MPa (Figures 7.3 and 7.4). Figure 7.4 shows the CR development along with curing time. The CR of all the samples is increasing with the curing time and this increase is more dramatic at the early age (around 70-85% can be reached). The crushing resistance of Ref. is increasing with the curing time and this increase is relatively slow after 7 days curing.

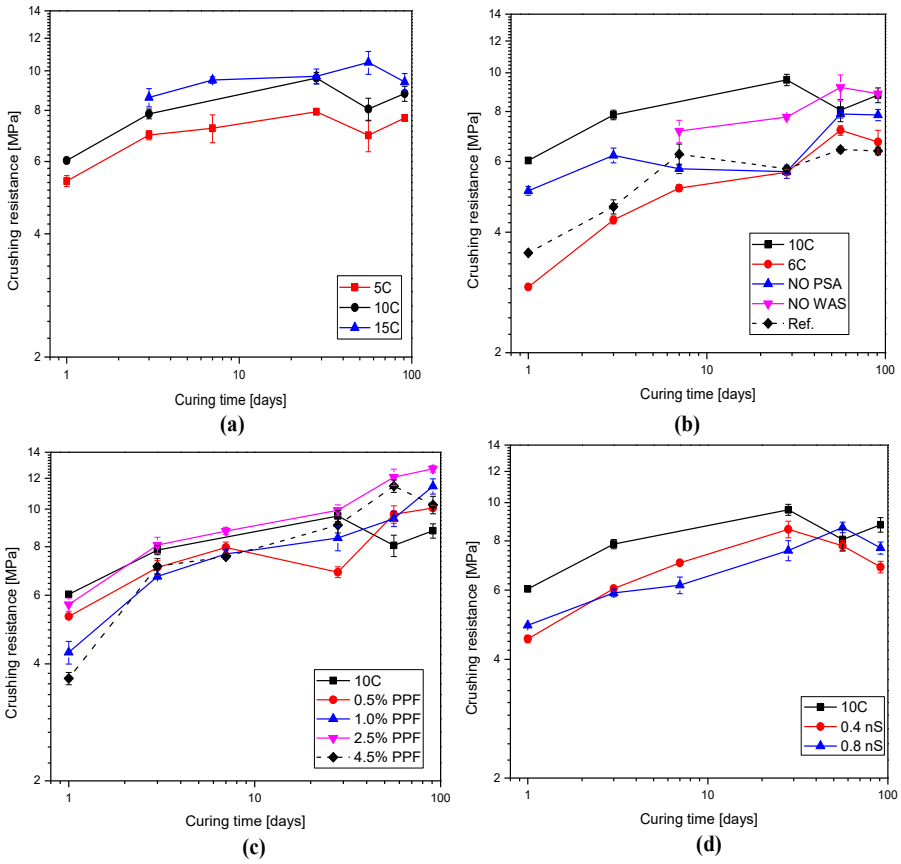

Figure 7.4: The crushing resistance of the aggregates after different curing ages

Figure 7.4 (a) shows that the CR has an increasing trend with the order of sample 5C, 10C and 15C during the whole curing time. After 91 days, the CR of 10C and 15C is higher than 5C by 14.7% and 22.5%, respectively. The binder amount has an influence on the CR

and a higher amount of binder results in higher CR, and Figure 7.3 (b) shows that the bulk density of these samples has a positive correlation with the binder amount. This is due to a denser microstructure and better bonding strength between particles and matrix. Similar results were obtained in other research regarding artificial aggregates produced from only powder materials (Colangelo et al., 2015; Thomas & Harilal, 2015). It can be seen in Figure 7.5 (a) and (b) that the hydration products grow well around the particles, and the F-BAM particle is well embedded in the matrix and surrounded by the binder hydrates and fly ash particles, which contribute to the pellet strength.

The CR comparison of sample No PSA and 10C (Figure 7.4 (b)) shows that the addition of paper sludge ash (PSA) has a positive effect on the CR: sample 10C containing PSA obtains around 12% higher CR than sample No PSA after 91 days curing. In addition, Figure 7.3 (b) shows that sample No PSA has a higher bulk density than 10C which indicates a good compaction of aggregate, while its CR is lower compared to sample 10C. This is due to the fact that, firstly, PSA contains calcium silicate and portlandite (as shown in Figures 6.5-6.8) and contributes to cement hydration which manifest after longer curing times (Ferrándiz-Mas et al., 2014), while FA is reported to have pozzolanic properties (Bentz et al., 2011). Therefore, the early strength which is necessary for keeping the aggregates shape can be improved by adding PSA, while the longer time strength can be increased by FA. Hence, the combination of FA and PSA is beneficial for the aggregates properties.

Sample No WAS and 10C has very similar CR (slightly higher after 91 days), and the addition of washing aggregate sludge (WAS) slightly decreases the CR of pellets. The WAS is an inert material which does not contribute to the cement hydration, however, the production of the pellet can be shortened due to its fine particle size and high water absorption. Sample 6C has lower CR compared with 10C and comparable to sample 5C and its CR is increasing steadily. It is reported that the ground granulated blast furnace slag (GGBS) can result in higher strength and lower porosity of concrete due to its pozzolanic property (Oner & Akyuz, 2007), however, this is not observed in the produced aggregates. The possible reasons can be that the pozzolanic reaction needs a longer time and higher pH in order to make a significant contribution.

Samples with nS have a lower crushing resistance compared with 10C (Figure 7.4 (d)) when nS is used as OPC replacement, which is in contrast to the phenomenon in concrete (Quercia Bianchi, 2014), which is due to the porous microstructure of the pellet with nS.

Comparing samples Ref. and No PSA, the amount of F-BAM is increased by around 25% wt. Sample Ref. has a lower CR and after 91-days sample No PSA has a CR higher than Ref. by 23%. Moreover, as addressed in Section 7.3, Ref. has a higher CR than other cold bonded lightweight aggregates which were produced with only powders (Baykal & Doven, 2000). This demonstrates that the addition of F-BAM contributes to a higher CR. This can

be comprehensively explained from two aspects: firstly, when more F-BAM is added to replace coal fly ash, the amount of binder needed to bind them decreases as the surface area of the F-BAM is lower than the powder coal fly ash. Hence, sample with more F-BAM has higher CR when the binder amount is the same. Secondly, the F-BAM can act as 'aggregate' in the pellet to support the pellet strength and the irregular shape of the F-BAM also increases the bonding strength between the matrix and F-BAM, also the F-BAM is stronger than the matrix to support the loading. Therefore, the addition of F-BAM can improve the artificial aggregate strength, which is in line with the findings in Chapter 6. Additionally, in this way the F-BAM can be used as a suitable material for producing aggregates, instead of as aggregate use directly, when the F-BAM only has a detrimental influence (Müller & Rübner, 2006; Yu et al., 2014) or being disposed as waste material in landfill areas. Furthermore, the F-BAM particles are mostly very porous, hence, the use of F-BAM instead of powders would not increase the bulk density of the pellets, or even a lower bulk density of pellets can be achieved.

Hence, the combination of these solid wastes with various proportions for producing lightweight aggregates is an efficient way to recycle them, because they can be used to improve the pellet properties based on their special characteristics. In future studies, other waste fine fractions can also be added to modify the properties of the artificial aggregates, such as sludge, finer bottom ashes, recycled concrete fines, etc.

The comparison of samples 10C, 0.5%-4.5% PPF demonstrates the influence of PPF on the CR. The addition of the PPF contributes to comparable CR or even higher than 10C, while achieving lower bulk densities; the more PPF is added, the higher CR can be reached. Hereby, the functions of the PPF are similar to the fibres used in concrete (Bernhardt et al., 2014; Bonakdar et al., 2013; Lee et al., 2010). Under the individual pellet test, the pellets without PPF are broken into two hemispheres, while the pellets with PPF were still held together after the crack almost penetrated the whole pellet (as shown in Figure 7.5 (c)); also the PPF embedded in the matrix goes through the voids (Figure 7.5 (d)), which in general are the weak part of the pellets. It is observed that along the crack after loading, some fibres were broken, some of them were pulled out, which means the PPF bear the force during the loading procedure. However, the CR of samples with PPF at early stage is lower than 10C, and the higher amount of PPF the sample contains, the lower CR it will have at early age. This may attribute to the fact that these samples have high porosity and the hydration of the binders is still ongoing, which leads to a lower capacity to bind the fibre into the matrix. Hence, when the aggregates are under loading, most fibres are pulled out easily, and do not play a significant role as reinforcement. The CR increase of samples with 0.5%, 1.0%, 2.5% and 4.5% vol. PPF after 91 days is about 14.4%, 30.2%, 44.4% and 16.6% compared with 10C, respectively. It can be seen that when the PPF amount is 4.5%, the CR is lower than the sample with 2.5% PPF. Firstly, when the amount of the PPF exceeds a certain level, the pellets are more difficult to compact during the pelletizing

procedure, which results in a higher porosity of the pellets. Secondly, higher amounts of PPF need more binder to provide a good bonding strength between the PPF and the matrix. Hence, the amount of PPF should be controlled and 2.5% vol. seems to be an optimized dosage. It is worth to mention that, regarding the fibre that can be used to increase the pellet strength, also waste fibres can be considered, such as waste wood fibres, waste PPF (García et al., 2014), etc. which cannot be used directly in the concrete and do not contribute too much to the concrete strength.

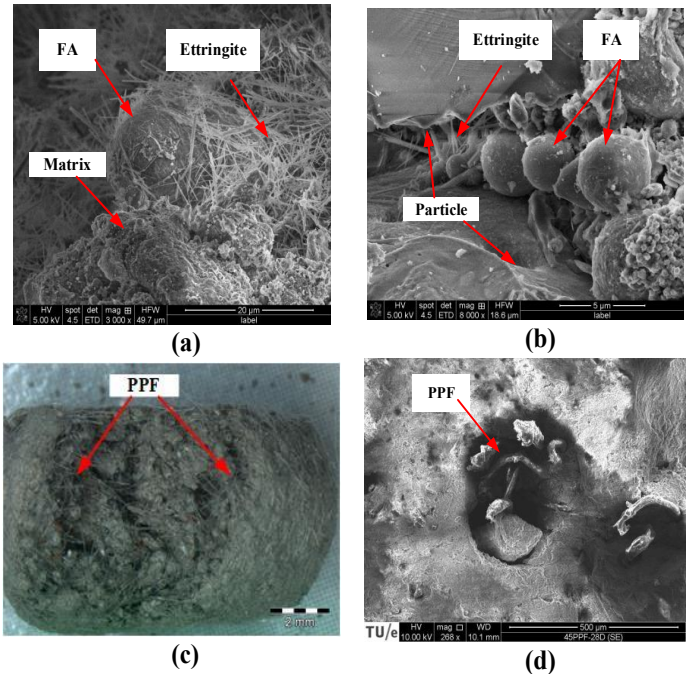

Figure 7.5: The optical microscopy and scanning electron microscopy (SEM) graphs of the pellets ((a): sample Ref.; (b): sample 10C; (c): sample 2.5% PPF; (d): sample 4.5% PPF)

It is shown in Figure 7.4 that some test values are lower than previous values, which may be due to the inhomogeneity of samples and variation of testing operation. Additionally, F-BAM has a certain amount of metallic aluminium (around 0.4% wt.) which may lead to the cracking of some pellets when it reacts with alkalis, and could be also a reason why the pellet strength of some samples decreases. Further research is needed to investigate and quantify this influence.

In literature, there were several special methods used to increase the pellet strength, such as lime addition (Geetha & Ramamurthy, 2010b; Vasugi & Ramamurthy, 2014), milling of bottom ash fraction into powder (Cioffi et al., 2011), two-step pelletizing (Colangelo et al., 2015), and surface treatment (Gesoğlu et al., 2007). However, by milling the bottom ash into powder the cost is increased and more binder is needed to obtain similar strengths

due to the increasing surface area of raw materials. In this study, the F-BAM is used as received without further treatment, and better results are obtained. Considering two-step pelletization and aggregate surface treatment, the increase of the pellet strength is not so substantial considering the binder amount added. This is due to the fact that the microstructure of the pellet, which influences the pellet strength, is not densified by these two methods (only the shell layer of the pellets is strengthened, but the core of the pellet is still weak), even though the binder amount is quite high (almost 14% wt.). In the present study, the F-BAM and other industrial powders are mixed homogenously and the F-BAM is acting as 'aggregates' to support the pellet strength and this can decrease the amount of binder used and increase pellet strength, which is one of the benefits of combining the use of F-BAM with other wastes. Polypropylene fibres are introduced into the pelletizing process to produce cold bonded lightweight aggregates for the first time, and the aggregates produced have lower bulk density while achieving higher crushing resistance compared with normal cold bonded lightweight aggregates.

It can be summarized that, to increase the crushing strength of the cold-bonding lightweight aggregates, the binder amount, F-BAM addition, and applying appropriate waste powders as additives can be considered. For decreasing the bulk density and increasing the crushing strength of the lightweight aggregates, the addition of 2.5% vol. PPF can be an option.

7.3.2 Leaching behaviour evaluation of CBLAs

The total amount of investigated heavy metals and salts in raw materials for CBLAs and their leaching concentrations in F-BAM are shown in Table 7.2.

Table 7.2：The total amount of chlorides, sulphates, antimony, copper and molybdenum in raw materials and their leaching concentrations during the column test, and the limit level of their leaching specified in Dutch legislation-SQD (2013) [mg/kg d.m.]

	Sb	Cu	Mo	Chloride	Sulphate
Total amount F-BAM	83	3100	19	2100	22900
FA	110	99	28	200	10300
PSA	11	22	<1.0	18300	6200
WAS	42	450	3.9	<100	1100
Column leaching F-BAM	0.47	1.1	0.68	950	11000
Leachability F-BAM (%)	0.57	0.035	3.58	45.24	48.03
SQD limit	0.32	0.9	1.0	616	1730

The leaching concentration of antimony (Sb), copper (Cu), molybdenum (Mo), chloride and sulphate of the aggregate samples after 28 days and 91 days curing is shown in Figure

7.10. The amount of F-BAM used for aggregates production is much higher than the other materials (FA, PSA, WAS), and the total content of Sb, Cu and Mo in F-BAM is almost 2-10 times of that in the chosen industrial powders (Table 7.2). The leaching of the heavy metals in aggregates is supposed to be mainly influenced by the F-BAM properties. Hence, the leaching of the F-BAM is tested only. The total amount of heavy metals and salts in the produced CBLAs after 28 days and 91 days curing are tested and summarized in Table 7.3. The total amount of the investigated heavy metals and salts vary in CBLAs with the different proportions of raw materials. Therefore, their leachabilities in CBLAs after 91 days curing are also calculated according to Eq. (3.8) and compared.

Table 7.3: The total content of heavy metals, chloride and sulphate in the produced CBLAs

Total content	Sb		Cu		Mo		Chloride		Sulphate	
[mg/kg d.m.]	28d	91d	28d	91d	28d	91d	28d	91d	28d	91d
Ref.	66	64	950	810	20	21	1400	1600	15000	14700
5C	70	70	1700	1700	15	15	5000	5800	17000	17000
10C	52	60	1300	1200	13	13	3900	4800	13700	18700
15C	66	54	1600	1400	14	15	4600	5200	16300	17400
6C		64		1400		13		4000		13500
No PSA		76		1500		20		3100		16200
No WAS		67		1500		16		6800		17500
0.5% PPF	*	64	*	1500	*	16	*	5400	*	16200
1.0% PPF		70		1600		14		8200		20000
2.5% PPF		71		1500		15		6700		16000
4.5% PPF		71		1300		15		7900		20900
0.4 nS	76	66	1600	1600	15	17	4800	5800	16000	17600
0.8 nS	66	64	1800	1600	15	15	4800	4900	15900	18200

*not tested

- **The leaching behaviour of antimony (Sb)**

Figure 7.6 (a) shows that the Sb leaching concentrations of all the samples are well under the limit value (0.32 mg/kg d.m.) according to legislation SQD (2013).

Comparing samples 5C, 10C and 15C, the leaching concentrations of Sb are decreasing with the increase of the binder amount. The Sb leaching of sample 15C decreased by around 23% compared with sample 5C, which indicates that a higher amount of binder is beneficial to the immobilization of Sb in the aggregates. In general, the immobilization of the contaminants is positively related to the binder dosage, which produces more hydrates to absorb the contaminants on the surface, or provide precipitation surface, or for the ion-exchange during the hydration process (Batchelor, 2006). In this study, as shown in Figures 7.6-7.10, the leaching of heavy metals (Sb, Mo and Cu), chloride and sulphate mostly decreases with the cement amount. The leachability of Sb decreases from 0.26% to 0.13% when the binder amount increases from 5% to 10% (5C and 10C after 91 days curing). With very similar total amount of Sb, the decreased Sb leachability of CBLAs demonstrates

that this is due to the binding property of binder, instead of dilution effect of total Sb content in the CBLAs. In case of dilution effect, the Sb leachability of CBLAs will be the same as that of F-BAM.

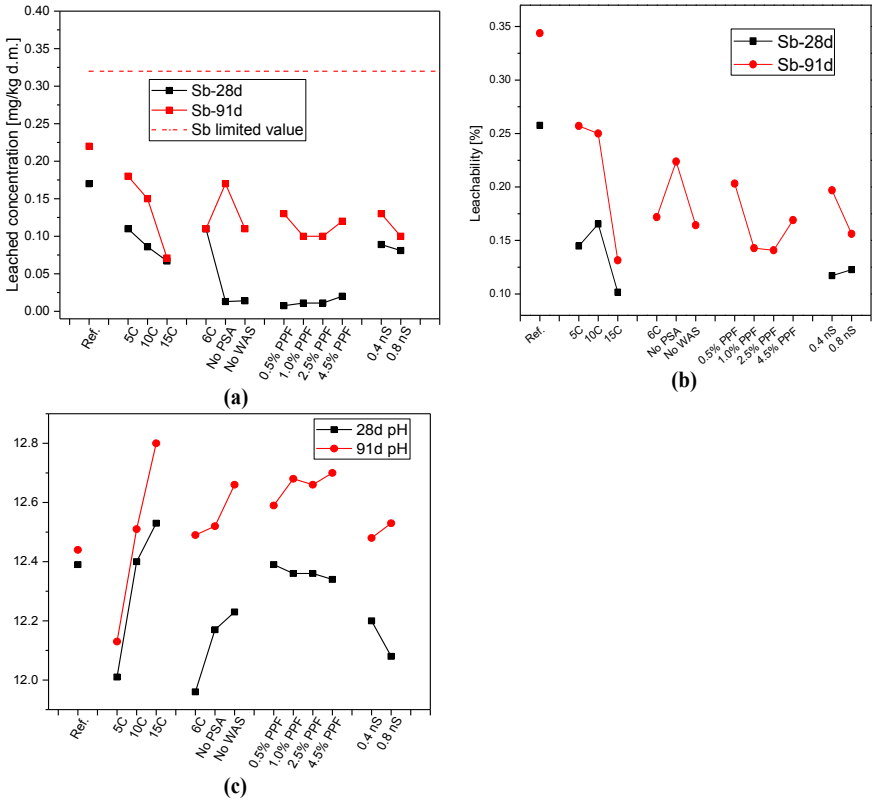

Figure 7.6: The (a) leaching concentration and (b) leachability of Sb, and (c) pH of CBLAs

Sample 6C has a similar leaching concentration after 28 and 91 days curing and it has lower leaching of Sb after 91 days compared with sample 10C when the OPC amount is 40% less. The Sb leachability of sample 6C after 91 days is 0.17%, which is 68% of that from sample 10C. It is reported that ground granulated blast furnace slag (GGBS) has an excellent immobilization capacity on contaminants (Laforest & Duchesne, 2005; Müllauer et al., 2015). It is also stated that the addition of GGBS contributes to lower hydration speed, less portlandite and generation of C-S-H with lower Ca/Si ratio compared with OPC, which results in lower pH and maybe a negative charge surface of calcium silicate hydrate (C-S-H) (Laforest & Duchesne, 2005; Müllauer et al., 2015). Eventually, the solubility of the metal-bearing phases is lower at the resulted pH and they are more favourable to be situated on the surface of the C-S-H. Hence, the samples with GGBS has a lower pH (Figure 7.6 (c)) and has lower leaching of contaminates as shown in this study compared with 10C, even though it has lower crushing resistance. The Sb leaching of samples with nS is lower

than sample 10C and higher nS content results in lower leaching concentration and leachability. Similar results are reported in (Li et al., 2014).

Sample 10C has a higher leaching of Sb than sample No PSA after 28 days curing, while it is lower than sample No PSA after 91 days curing. The Sb leachability after 91 days of sample No PSA is 0.22%, and is slightly lower than sample 10C. This can be explained by the fact that the addition of paper sludge ash (PSA) provides a calcium oxide resource which has a significant immobilization influence on Sb as reported (Van Caneghem et al., 2016). Moreover, the PSA contains calcium silicate which contributes to the generation of more hydrates for immobilization. Sample No WAS has a similar Sb leaching to sample 10C and the Sb leaching of samples with PPF did not show a significant influence considering the amount of PPF added.

It is also noticed that the Sb leaching concentrations of samples after 91 days curing are higher than the samples which are cured for 28 days, and the pH of the samples has a similar trend (Figure 7.6 (c)). Similar Sb leaching behaviour is reported by Cornelis et al. (2012). The cement hydrates can immobilize the Sb ions and then reduce its leaching, however, the Sb leaching of the F-BAM is influenced by pH (Cornelis et al., 2012) and the leaching of the Sb from F-BAM or FA can happen during the whole hydration procedure. Simultaneously, the released Sb ions are immobilized by the cement hydrates. Hence, it can be assumed that the hydration rate of binders after longer time curing is much slower than the leaching of the Sb from the waste solids, which contribute to the higher leaching of Sb after 91 days curing.

For Sb leaching in the produced aggregates in the present work, the addition of additives with calcium oxide which can contribute to hydrates, decreasing amounts of FA and F-BAM, the addition of GGBS or nano-silica and increased binder amounts, will decrease the leaching concentration of produced aggregates in case the leaching of Sb exceeds the limit value.

- **The leaching behaviour of copper (Cu)**

Sample Ref. contains the lowest amount of F-BAM and has the lowest leaching of Cu content among all the samples. Most likely, the leaching of copper decreases with the curing age (Figure 7.7 (a)).

The leaching of copper mostly exceeds the limit value, while samples Ref. and 6C are very close to the limit value. Samples 5C, 10C and 15C after 91 days curing show that the leaching of copper has a roughly decreasing trend when the amount of binder increases and sample No PSA has a higher Cu leaching than sample 10C, indicating the contribution of PSA on the Cu immobilization.

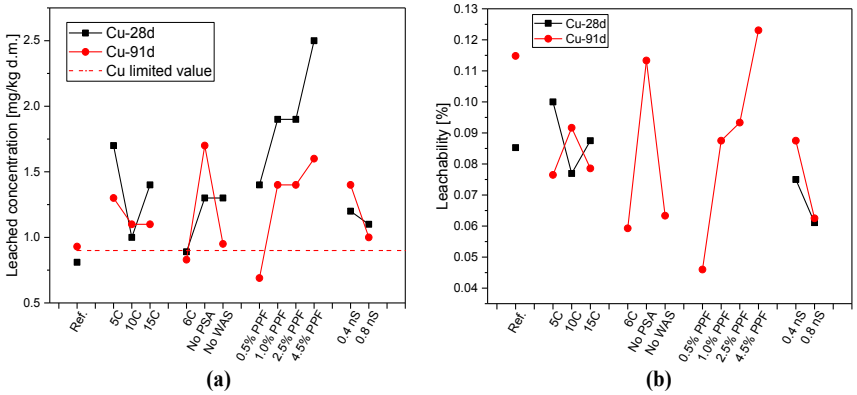

Figure 7.7: The (a) leaching concentration and (b) leachability of Cu of CBLAs

According to Zomeren & Comans (2009), the leaching of copper in F-BAM is related to its dissolved organic carbon content, and other research shows that the copper leaching has an increasing trend when the pH is higher than 10 (Keulen et al., 2015). Therefore, during the cement hydration the leaching of the copper from F-BAM will be increased due to the high pH environment; meanwhile the Cu ions are bound by the cement hydrates. As also concluded by Li et al. (2001), the leaching of heavy metals in cement based system is controlled by pH and the solubility of the related metal hydroxides. This explains the low Cu leaching of sample 6C, which has lower pH and slower hydration speed compared with sample 10C. However, compared with the Sb leaching, the leaching of Cu did not show a clear trend related to the curing time. The Cu leaching of samples with PPF shows an increasing trend when the PPF content is increased, and the leaching of Cu after 91 days is decreased compared with samples after 28 days curing. This might be attributed to the high porosity of pellets with PPF, which increases the ability of water to contract with cement hydrated during the leaching process; eventually more hydrates can be dissolved and release Cu ions. The leachability of Cu of the CBLAs is between 0.06%-0.12%, which is higher than the Cu leachability of F-BAM (0.035%), as shown in Table 7.2.

Hence, decreasing the F-BAM amount, increasing the binder content and adding GGBS or nano-silica can lower the Cu leaching of the produced aggregates when the Cu leaching concentration is required during application.

- **The leaching behaviour of molybdenum (Mo)**

The Mo leaching of the samples mostly exceed the limit value, which is 1.0 mg/kg d.m. and there is no clear relation between Mo leaching and pH (Santos et al., 2013). It seems that the Mo leachability (Figure 7.8 (b)) decreases with the curing age and the addition of nano-silica shows good ability to decrease the Mo leachability.

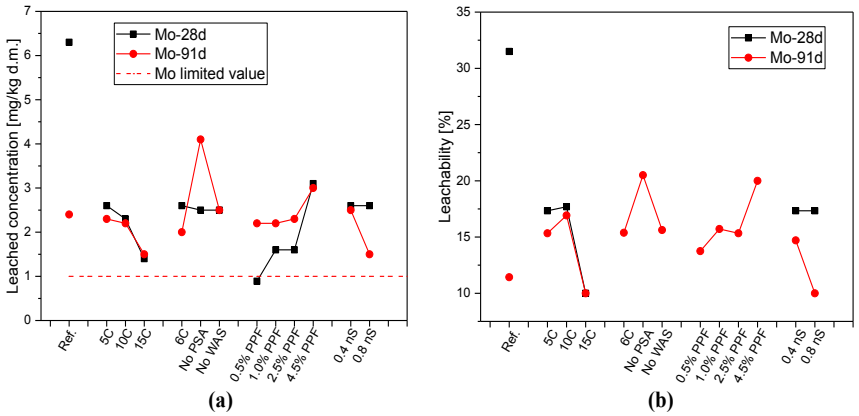

Figure 7.8: The (a) leaching concentration and (b) leachability of Mo of CBLAs

Samples 5C, 10C, and 15C has a decreasing leaching amount of Mo when the binder amount is increased. The replacement of cement by GGBS slightly decreased the Mo leachability when comparing sample 6C to 10C. Samples with nS shows lower leaching concentration than sample 10C, as well as lower Mo leachability. Sample No PSA has the highest Mo leaching after 91 days and the Mo leaching concentration decreases when PSA is added (sample 10C). The sample with PPF has a lower leaching of Mo after 28 days compared with sample 10C, the leaching concentration is increasing with the PPF addition. While after 91 days curing the leaching of the Mo is similar to sample 10C and the samples with PPF have a very close leaching concentration of Mo related to the amount of PPF. From the obtained leaching results, it can be seen that increasing the binder amount and using GGBS and nano-silica can reduce the Mo leaching and leachability significantly.

- **The leaching behaviour of chloride**

It can be seen that the leaching of chloride exceeds the limit value and that is not significantly influenced by the curing time (Figure 7.9 (a)). Table 7.2 shows that the chloride content in the aggregates is mainly influenced by the F-BAM and PSA amounts.

Sample Ref. has the lowest chloride leaching due to the fact that the total chloride in this sample is mainly influences by the amount of the F-BAM, which exceeds the leaching limit slightly. Sample No PSA has a higher chloride leaching when the F-BAM amount is increased by 25%. The leaching of chloride decreased with the increasing amount of OPC, sample 6C features a lower chloride leaching than 10C, and very similar to sample 15C. Samples with PPF has an increasing chloride trend with the increase of PPF amount which is explained due to the high porosity of the pellets.

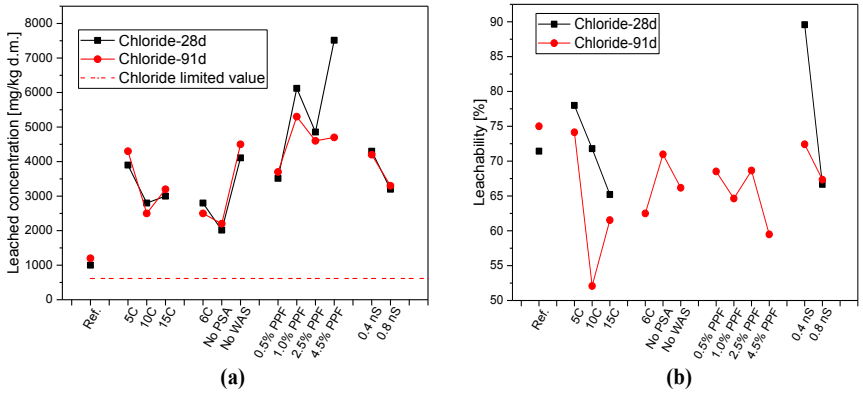

Figure 7.9: The (a) leaching concentration and (b) leachability of chloride of CBLAs

The chloride leachability of the CBLAs is in the range of 52%-75%, and the chloride leaching after longer time curing did not show a large difference, which indicates that the immobilization of the chloride by hydration is limited and the chloride in the aggregates is highly soluble. Hence, the immobilization of chloride cannot be easily achieved by increasing the binder content. Moreover, the amount of the produced aggregates should be controlled when the chloride leaching is restricted during the application.

- **The leaching behaviour of sulphate**

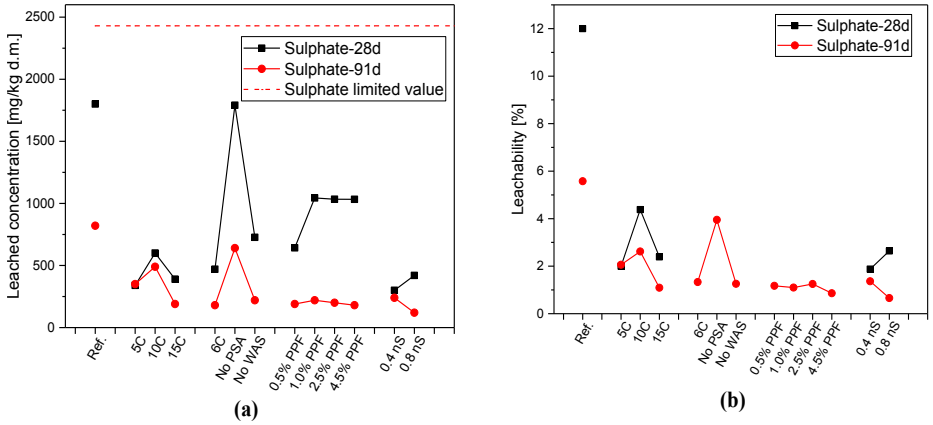

Figure 7.10: The (a) leaching concentration and (b) leachability of sulphate of CBLAs

The leaching of sulphate for all the samples decreased after longer curing times and is well under the limit. Samples 5C, 10C and 15C show that the leaching of sulphate is increased when binder is increasing; while the leaching of sulphate in 10C is higher than 5C and 15C. Sample 6C shows a lower leaching of sulphate than sample 10C, and similar to sample 15C. Sample No PSA and Ref. have much higher amounts of sulphate leaching than other

samples compared with sample 10C. The leaching of sulphate is not influenced by the amount of PPF. The leachability of sulphate decreases when PSA is added for CBLAs (samples Ref., 10C and No PSA), and it increases with curing age. In the cement based system used here, the sulphate is mainly provided from OPC and F-BAM, which participates in the hydration to form AFt/AFm, hence its leaching is significantly reduced along with the hydration time of cement.

- **Summary**

To summarize shortly, the leaching of Cu, Mo, and chloride of most of the aggregates produced, based on the current recipes still exceed their leaching limit according to the Dutch legislation, and the leaching of Sb and sulphate can comply with the legislation (SQD, 2013). However, when they are used in concrete, the leaching of the concrete in general will comply with the legislation. In this case, the concrete with the addition of these aggregates can be employed as a final product in market.

In summary, the aggregates properties, especially crushing resistance, which influence the application of cold bonded lightweight aggregates, are improved by both chemical (increasing binder amount) and physical methods (PPF addition). The leaching concentration of some contaminants (Mo and chloride), which exceed the limited values according to Dutch legislation (SQD, 2013) can be reduced by adjusting the proportions of the raw materials. Moreover, these aggregates can be used in shaped materials, such as concrete blocks, the leaching of which will be reduced significantly and will comply with the environmental legislation. Furthermore, the application of the aggregates can be adjusted according to the mechanical (crushing resistance, density), economic (binder amount, wastes proportions) and environmental (leaching properties) points of view.

7.4 Conclusions

To improve the properties of the cold bonded lightweight aggregates (CBLAs), several methods are investigated in this chapter. It is concluded that:

(1) The increase of binder amount results in the increase of crushing resistance (CR) and bulk density of the aggregates; the addition of paper sludge ash increases the CR due to its contribution to cement hydration; the addition of F-BAM increases the CR which is attributed to the fact that F-BAM can act as ‘aggregate’ in the pellet to strengthen the skeleton of the pellets, as well as providing a smaller surface area; the addition of polypropylene fibre (PPF) increases the CR dramatically, and the amount of fibre should be controlled to have a maximum CR increase.

(2) For the produced lightweight aggregates, the leaching of the Sb and sulphate are all well under the limit value due to the immobilization by binder hydrates. Increasing the binder amount reduces the leaching of Sb, Cu, Mo, chloride and sulphate.

(3) The immobilization of contaminants by cementitious materials is mainly related to the parameters: the pH, the hydration products, and the properties of the

contaminants (stability, complexation, etc.). For the aggregates produced by F-BAM and industrial wastes in this study, the Sb can be immobilized successfully by increasing the binder amount, GGBS, nano-silica and PSA addition, which all results in more hydration by-products. The leaching of Cu is mainly influenced by the behaviour of organic matter in F-BAM, which can be immobilized by binder addition, use of GGBS and nano-silica. The binding of Mo shows a good correlation with binder content and its hydration. Sulphate leaching are well under the limit value owing to its participation in cement hydration. The chloride in the aggregates is highly soluble, and can partially be immobilized. Furthermore, the immobilization procedure in the pellets is a combination of ions leaching from the solid wastes and their stabilization by cement hydrates. Therefore, to modify the leaching of ions, especially heavy metals, their leaching behaviour at high pH, and the stabilization mechanism by cement is suggested to be determined individually before the combination of solid wastes.

(4) The produced cold-bonding lightweight aggregates can be used as aggregate replacement, and the amount of these aggregates can be controlled when the leaching properties of the concrete is required. Further research can focus on the integrated recycling of other wastes, durability and life cycle of the produced artificial aggregates and comprehensive study on their application in concrete which is studied in the next chapter.

The properties of the CBLAs can be modified through controlling the chosen combinations of raw materials and their proportions, as well as changing pelletizing parameters. The use of CBLAs in concrete has significant influence on the concrete properties, which is studied in the next chapter.

Chapter 8

8 The environmental properties and durability of concrete incorporating CBLAs*

8.1 Introduction

In this chapter, three types of CBLAs are produced with consideration of improving their strength, including the use of F-BAM, nano-silica from olivine dissolution and polypropylene fibre. The properties of these CBLAs are evaluated and compared with the ones produced by others in literature. These CBLAs are used in self-compacting concrete to replace natural gravels, and the fresh and hardened properties of the concretes are tested. The durability properties of the concretes are studied through the water penetration and freeze-thaw tests. Finally, the environmental impact of the concretes with artificial aggregates are evaluated and results are compared with the Dutch legislation.

8.2 Materials and experimental methods

8.2.1 Production of CBLAs and their properties

In this chapter, three recipes used to produce CBLAs in Chapter 7 are selected for further study, and then three types of CBLAs were produced.

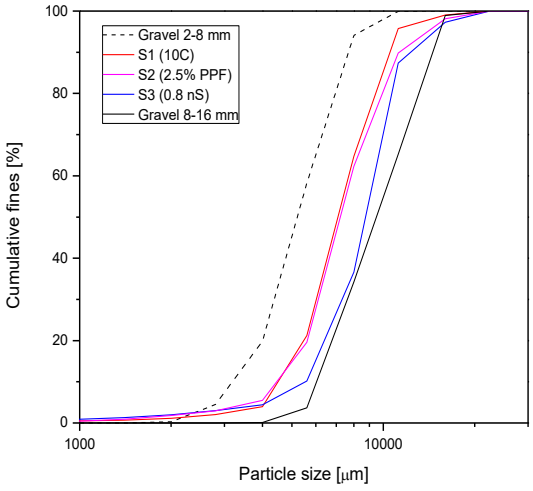

Figure 8.1: The particle size distributions of the gravels and the produced CBLAs used for concrete

The raw materials used for CBLA sample 1 (S1) are OPC (10%), F-BAM (a value between 40-75%), WAS (5%), PSA and FA (around 10-45% in total) based on total dry mass, the

*Content of this chapter was submitted to Journal and now under review.

same as sample 10C in Chapter 7. For sample 2 (S2), around 2.5% vol. polypropylene fibre (PPF) is added to the mixture of the raw materials (the sample as sample 2.5% PPF in Chapter 7), the other proportion of the raw materials are the same as S1. For sample 3 (S3, the same as sample 0.8 nS in Chapter 7), around 0.8% of the cement is replaced by nano-silica, and the amount of the other materials are kept the same as S1.

The PSDs of the produced aggregates and gravels are shown in Figure 8.1. The bulk density (BD) of S1, S2 and S3 is approximately 923 kg/m^3, 870 kg/m^3, and 844 kg/m^3, respectively. The water absorption (WA) and crushing resistance (CR) of S1, S2 and S3 are 19% and 9.6 MPa, 22.4% and 9.9 MPa, and 23% and 7.56 MPa, respectively. Figure 8.1 depicts that the particle sizes of the produced aggregates are mainly between 4-12 mm, and the sample S3 has coarser particles than S1 and S2, while samples S1 and S2 have very similar particle size distribution.

8.2.2 Concrete mixture design and test

A self-compacting concrete (SCC) is designed; the materials used are OPC, coal fly ash, sand with a particle size under 4 mm, crushed gravel with a particle size between 2-8 mm, and gravel with a particle size between 8-16 mm. The proportions of materials for each concrete mixture are listed in Table 8.1. A superplasticizer (SP, Glenium 51 (BASF)) is used to adjust the flowability of concrete and its amount is fixed at 5.89% of the OPC for all the concrete mixtures.

Table 8.1: The design for concrete mixtures

Materials	Ref.	Mix 1		Mix 2		Mix 3	
		30% vol.	60% vol.	30% vol.	60% vol.	30% vol.	60% vol.
	[kg/m^3]						
CEM I 42.5 N	310						
Coal fly ash (FA)	179						
Sand 0-4 mm	572.9						
Gravel 2-8 mm	697.8	566.52	435.24	577.07	456.33	667.05	558.38
Artificial aggregates	0	241.43 (S1)	483.00 (S1)	234.29 (S2)	468.71 (S2)	236.14 (S3)	472.14 (S3)
Gravel 8-16 mm	376	249.57	123.13	239.02	102.04	149.04	0
Water	139.5	139.5	139.5	139.5	139.5	139.5	139.5
SP	5.89						

The gravels (2-8 mm and 8-16 mm) in the concrete are replaced by the produced artificial aggregates (S1, S2, S3) with 30% and 60% by volume. The amount of each aggregates in concrete mixtures is calculated based on the idea that the particle size distribution of all the aggregates for the concrete should be similar to that of the reference concrete. Before

mixing, the artificial aggregates are immersed in water for 24 hours and then dried in open air for 2 hours to avoid their absorption of water during concrete mixing.

The slump-flow of the freshly mixed concrete is tested following the procedure described in EN 12350-8 (2010), the largest diameters of the flow spread on the two vertical dimensions are recorded and their average value is presented as the slump-flow (S-F) of the concrete. During this test, the time used for the concrete to first reach the 500mm circle on the testing plat after the cone is lifted is recorded and presented as t_{500}. The V-funnel test is performed on the fresh concrete according to the procedure defined in EN 12350-9 (2010), and the time used for the concrete finishing flow out of the V-funnel is recorded as t_v. The bulk density of the fresh concrete is tested according to EN 12350-6 (2009). The fresh concrete is filled in cubic moulds (150×150×150 mm^3) and prism moulds (100×100×500 mm^3) and demoulded after 1 day, then sealed in plastic buckets until testing date. The compressive strength tests are performed on the concrete cubes and two-point loading flexural strength tests (Figure 8.2 (a)) are conducted on the concrete prisms after 28 and 56 days' curing according to EN 12390-4 (2000) and EN 12390-5 (2009), respectively.

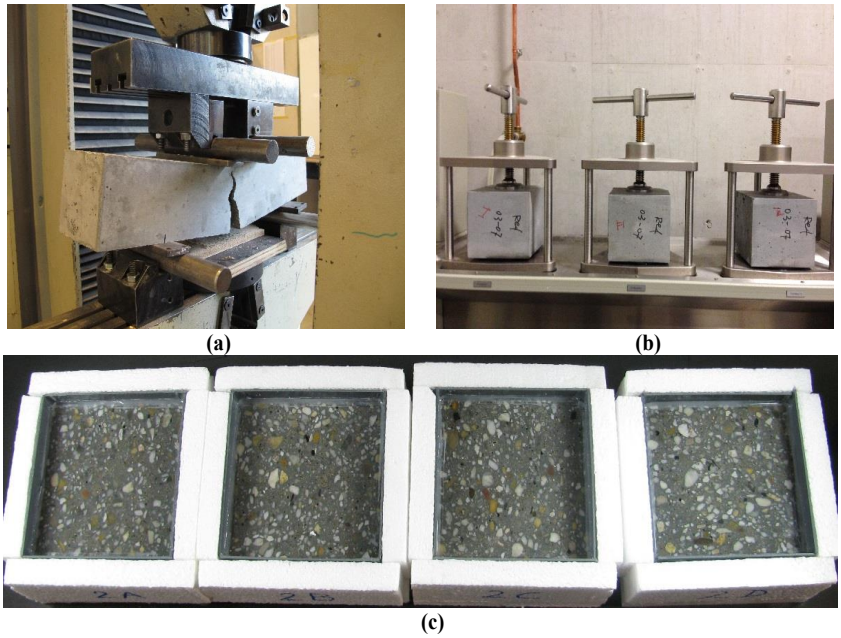

Figure 8.2: The device for (a) flexural strength test, (b) water penetration test and (c) prepared samples for freeze thaw test

The water penetration tests on the hardened concrete cubes under pressure are performed following the procedure described in EN 12390-8 (2009) and the device used is shown in Figure 8.2 (b). The freeze-thaw resistance of the hardened concretes is evaluated by

performing the freeze-thaw attack with de-icing salt on the concrete slabs sawn from concrete cubes (Figure 8.2 (c)) according to NPR-CEN/TS 12390-9 (part 5) (2006), the mass loss of the tested samples after each testing cycling (7, 14, 28, 42 and 56 cycles) is recorded.

8.2.3 Leaching behaviour evaluation of F-BA, CBLAs and concrete

The leaching properties of the F-BAM, artificial aggregates and crushed concrete containing artificial aggregates were evaluated using the column leaching method described in Section 3.2.2.

The hardened concrete cubes were sent for diffusion test according to NEN 7375 (2004). The dried concrete samples were merged in demineralised water for specified time, and then the leachate was renewed by new demineralised water. The volume ratio of liquid to tested sample was 2. The pH and concentration (ε) of components in the changed leachate were determined using ICP as described in Section 3.2.2. The time to renew the water is 6 hours after the samples were merged in water, and then 1, 2.25, 4, 9, 16, 36 and 64 days. The cumulative leaching concentration of a component after 64 days (ε_{64}) was a sum of its concentration in each renewed leachate. The derived cumulative leaching of a component was also calculated separately in each of the test periods. For each concrete mixture, duplicate samples were tested.

To determine the leaching mechanism of components during diffusion test, the slop (rc) of the linear regression line between the log (ε) and log (hour) was determined and used to determine if the leaching of component is diffusion controlled or due to other leaching mechanisms. As specified in NEN 7375 (2004), for the fully diffusion controlled leaching, the rc is 0.5, when rc of the tested sample is between 0.35-0.65, then the leaching of this sample is diffusion controlled (Table 8.2).

Table 8.2: The significance of rc in NEN 7375

Increment	rc		
	≤0.35	>0.35 and ≤0.65	>0.65
2-7	Surface wash-off	Diffusion	Dissolution
5-8	Depletion	Diffusion	Dissolution
4-7	Depletion	Diffusion	Dissolution
3-6	Depletion	Diffusion	Dissolution
2-5	Depletion	Diffusion	Dissolution
1-4	Surface wash-off	Diffusion	Delayed diffusion or dissolution

8.3 Results and discussions

8.3.1 Properties of fresh concrete

- **Slump flow**

Figure 8.3 shows the slump flow (S-F) diameter of the fresh mixed concrete with and without CBLAs. The reference concrete (Ref.) has a S-F diameter around 753 mm, which belong to class SF2 according to EN 206-9 (2007).

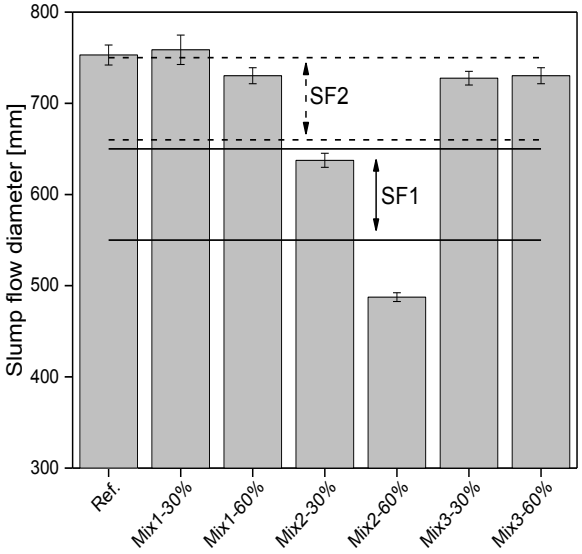

Figure 8.3: The slump flow diameter of the fresh concrete mixtures

For concrete mixture 1, its S-F diameter has a slight increase (0.7% increase) compared to the reference when 30% vol. of artificial aggregates (S1) is added to replace natural aggregates, while a decrease of S-F diameter is observed when 60% vol. of aggregate is replaced by S1 (around 3% reduction). The S-F diameter of concrete mixture 1 with artificial aggregates (S1) with 30% and 60% vol. replacement still belongs to class SF2 according to EN 206-9 (2007). Concrete mixtures with CBLAs-S2 (Mix 2) shows a decrease of S-F diameter, and this diameter decreases with the increase of the S2 replacement level. The S-F diameter decreases by 15% when 30% vol. of S2 is used compared to the reference, and it belongs to SF1. Around 35% reduction of the S-F diameter of the concrete with 60% vol. of S2 is observed. For concrete with CBLAs-S3 (Mix 3), its S-F diameter has a slight decrease (about 3%) compared to the reference for both mixtures with 30% and 60% vol. of S3, which belongs to SF2 according to EN 206-9 (2007). The increased use of S3 to replace natural aggregates does not show a significant influence on the SF diameter.

The slump flow diameter indicates the flowability and filling ability of the fresh self-compacting concrete (SCC). The above shown results demonstrate that the addition of artificial aggregates S1 and S3 up to 60% vol. will not influence the flowability of SCC dramatically. As reported by other researchers (Gesoğlu et al., 2013), the round shape of CBLAs promotes the flowability due to less friction between particles and matrix, hence, the use of chemical admixtures for increased flowability can be reduced. In this study, the dosage of SP for all the mixtures is kept the same, which contributes to less viscosity of the concrete when CBLAs are added. Furthermore, the CBLAs are lighter than the natural gravel. Due to the above-mentioned reasons, the S-F diameter of concrete with CBLAs is lower than that of the reference.

The addition of S2 to SCC reduces notably its S-F diameter, which is contrary to the phenomena reported in some of the research related to the application of artificial aggregates (Gesoğlu et al., 2012; Güneyisi et al., 2015a). For CBLAs-S2, PPF is used to increase the pellet strength. During the pelletization, part of the fibres is embedded inside the pellets completely, to support the pellet strength as reinforcement. However, there are also some fibres which are just partially embedded inside the pellets as shown in Figure 8.4. During the concrete mixing, these fibres will increase the cohesive force between the artificial aggregates and the matrix, similar to the influence of PPF in concrete (Yu et al., 2014). Hence, the flowability of the fresh concrete (Mix 2) is decreased dramatically compared to Mix 1 and Mix 3.

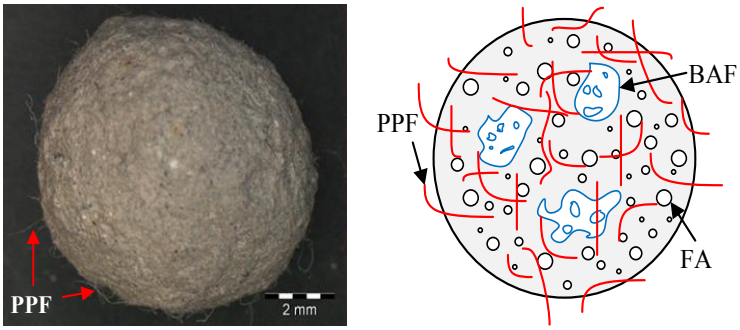

Figure 8.4: The artificial aggregate pellet with PPF addition (a) under optical microscope and (b) the schematic representation of the pellet cross section

- **t_{500} time**

During the slump-flow test, the time used by the concrete to flow to a diameter of 500 mm is recorded and the results are displayed in Figure 8.5. The designed SCC reference has a t_{500} of around 8 second, which is in the range of viscosity class VS3 according to EN 206-9 (2007).

For the concrete mixture with CBLAs-S1 (Mix 1), the t_{500} of Mix 1 with 30% vol. of S1 is around 2% less than the reference, while Mix1 with 60% vol. of S1 has a t_{500} about 1% longer than the reference. The t_{500} of Mix 2 with 30% vol. of S2 is around 8% longer than the reference, while it is almost 13% higher than the reference when 60% vol. of S2 is used. The t_{500} of Mix 1 and Mix 2 with 30% and 60% vol. of CBLAs indicates that their viscosity class belongs to VS3 according to EN 206-9 (2007), the same as the reference. The t_{500} of the concrete mixture with CBLAs-S3 (Mix 3) decreases significantly compared with the reference: the reduction for Mix 3 with 30% and 60% vol. of S3 is around 48% and 54%, respectively. The viscosity class of Mix 3 belongs to VS2 according to EN 206-9 (2007).

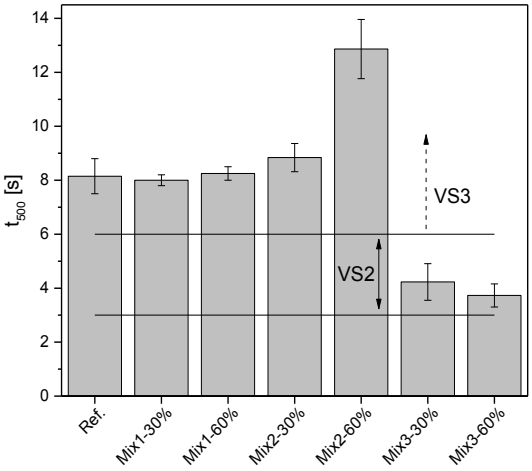

Figure 8.5: The t_{500} time of the fresh concrete mixtures

The t_{500} of concretes with S1 are not dramatically affected by the CBLAs' replacement level, while the t_{500} has a notable increase when more S2 aggregates are applied to replace natural aggregates, which is due to the blocking effect of fibres on the surface of the pellets as explained above. The reduction of t_{500} for concrete Mix 3 may be due to the following reasons: the sample S3 has a coarser particle size than S1 and S2, and it can be seen from Table 8.1 that all the coarser gravels are replaced by S3 in order to keep a similar total particle size distribution of aggregates; in this way there is much less friction between the mortar matrix and the coarse aggregates, which indirectly decreases the viscosity of the matrix; thus less time is needed to reach the 500 mm spread.

- **V-funnel test**

Figure 8.6 shows the time used for the V-funnel test on the fresh mixed concrete samples. It takes around 23 seconds for the reference concrete to flow out of the V-funnel, and this demonstrates that the viscosity class of reference concrete is VF2 according to EN 206-9 (2007).

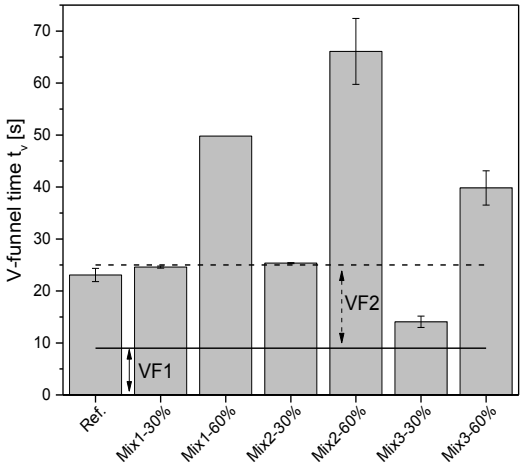

Figure 8.6: The V-funnel time of the fresh concrete mixtures

The t_v of Mix 1 with 30% vol. of S1 increases with around 7% compared with the reference concrete, while it takes more than 2 times longer for Mix 1 with 60% vol. of S1 in the V-funnel test. Mix 2 with 30% vol. of S2 has a longer t_v than the reference by approximately 10%, and when 60% vol. of S2 is applied its t_v is almost 3 times longer than the reference. The use of 30% vol. of S3 in Mix 3 results in a 40% reduction of t_v, while 60% vol. of S3 application in concrete causes a t_v around 1.7 times longer. The t_v for all the concrete mixtures with CBLAs increases with the increasing amount of aggregate replacing level. During the tests, it was observed that the artificial aggregates were pushed up and accumulated on top of the tested samples due to their roundish particle shape and less viscosity with the mortar matrix. They did not fell out of the V-funnel bottom until the mortar matrix finishing flowing out, which is believed to result in the much longer t_v during test when 60% vol. of CBLAs are used. The small viscosity of concrete may lead to segregation. Therefore, with the artificial aggregates replacement, the V-funnel test cannot demonstrate the viscosity of the concrete mixture accurately in case the sample tends to have segregation.

- **Bulk density of fresh concrete mixtures**

Figure 8.7 indicates the influence of artificial aggregates replacement on the fresh density of concrete mixtures. It can be seen that the use of S1, S2 and S3 leads to the reduction of the fresh density of the concrete, and the higher their replacement level, the lower the fresh density of concrete. The fresh density of concrete with S3 is the lowest compared with concrete with the same content of S1 or S2. The bulk density of sample S1 is higher than the other two, and S3 has the lowest bulk density. The fresh density of the concrete is related closely to the bulk density of the materials used for mixing; the results obtained in this study are consistent with literature (Güneyisi et al., 2015a).

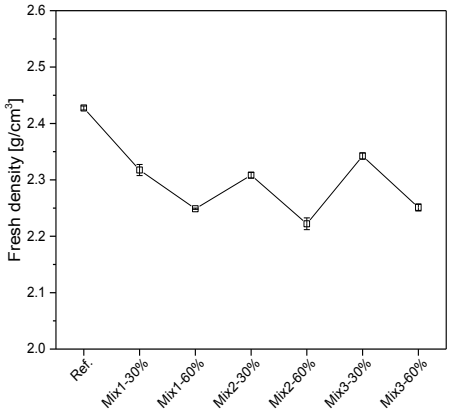

Figure 8.7: The density of the fresh concrete mixtures

It can be shortly summarized that the use of cold bonded artificial aggregates (S1and S2) does not influence the slump flow of the concrete, while the use of S2 decreases the slump flow due to the blocking effect of PPF. The use of CBLAs (S1 and S3) can reduce the viscosity of concrete due to their roundish particle shape, hence, the dosage to modify the water requirement can be reduced. The use of CBLAs in concrete furthermore reduces the bulk density of fresh concrete.

8.3.2 Properties of hardened concrete

Figure 8.8 displays the flexural strength of all the hardened concretes with and without aggregates replacement.

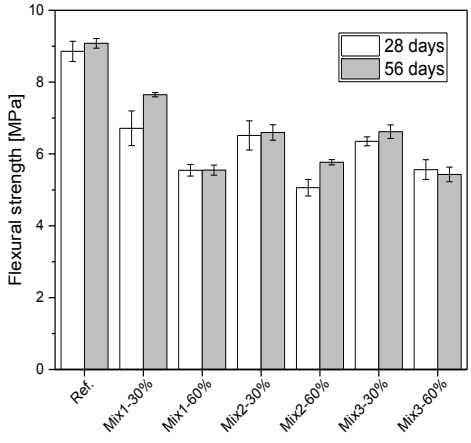

Figure 8.8: The flexural strength of concrete after 28 and 56 days

It can be observed that the use of CBLAs decreases the flexural strength of concrete, and the increasing replacement level of aggregates contributes to a higher reduction of flexural

strength. For all the concrete mixtures after 56 days curing, the reduction of flexural strength is around 16%-27% of the reference value when 30% aggregates are replaced by CBLAs, while this reduction is around 36-40% when 60% vol. of artificial aggregates are used.

Figure 8.9 (a) shows the compressive strength of hardened concretes after 28 and 56 days curing. It indicates that the addition of CBLAs decreases the compressive strength of concrete, and this reduction increases with the increasing replacement level. This is similar as reported by other researchers (Gesoglu et al., 2015).

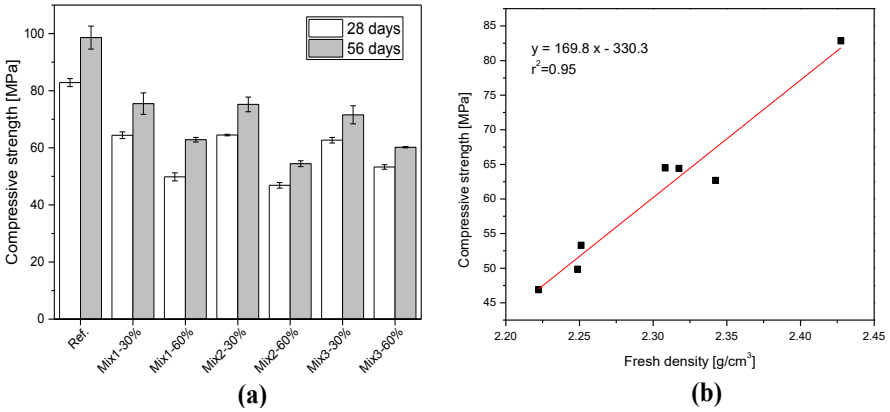

Figure 8.9: (a) The compressive strength of concrete cubes after 28 and 56 days curing and (b) the relation between 28-days compressive strength and fresh density of concrete mixtures

The compressive strength after 56 days curing has a 23-45% decrease compared to the reference, and higher replacement levels result in higher reductions. According to EN 206-1, the concretes with CBLAs have the compressive strength class between C35/45-C50/60. The higher crushing resistance of artificial aggregates does not give a high strength of the concrete as expected. Figure 8.9 (b) shows that the compressive strength and the fresh density of the concrete have a linear relationship. It seems that when 30% vol. of CBLAs is applied, the flexural and compressive strength has linear correlation with the crushing resistance of the CBLAs; while when 60% vol. of CBLAs is used, there is no clear trend anymore between the concrete strength and the CR of CBLAs. The above presented results and phenomena can be due to the following reasons: as observed during the test and the results from the fresh properties of the concrete, it is known that the use of CBLAs reduces the viscosity of concrete, which subsequently affects the strength of concrete. The slump flow diameter and the V-funnel time of the concrete is more influenced when 60% vol. of CBLAs is used, as shown in Section 8.3.2. Therefore, the influencing factors of concrete strength includes the CR of CBLAs and the other parameters of the concrete (such as porosity, etc.).

8.3.3 Durability properties of hardened concrete

- **Water penetration**

Figure 8.10 indicates the water depth measured after the water penetration test on the hardened concrete cubes.

The measured water depths of all the concrete mixtures with artificial aggregates are higher than that of the reference, and a higher level of aggregates used causes a higher water penetration depth. It is also noticed that the water depths of concrete with aggregates S3 are much higher than those of Mix 1 and Mix 2. It is reported that the use of artificial aggregate causes the increase of gas permeability (Güneyisi et al., 2015a). Figure 8.11 shows the cross section of the concrete cube with 60% vol. of S2. The distribution of the artificial aggregates is much denser near the edge of the concrete sample; a similar situation was observed during the moulding of the concrete. Moreover, it can be seen that the artificial aggregates are very porous, and some particles have voids inside. The water penetration depth in concrete with CBLAs consists of the penetration in the cementitious matrix in concrete, and the penetration in the CBLAs, while in normal concrete, it only includes the former. Therefore, the water penetration depth with CBLAs is higher than that of the reference concrete.

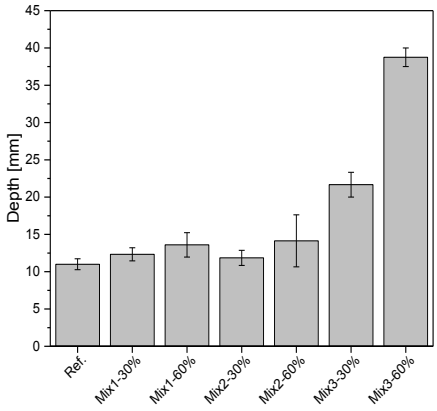

Figure 8.10: The water penetration depth in hardened concretes after 56 days' curing

The water penetration depth reflects the porosity of concrete, and the results obtained demonstrate that concrete Mix 3 is more porous than the other two with CBLAs. This is due to the following reasons: (1) CBLA S3 is more porous than S1 and S2, which can be seen from its higher water absorption and lower crushing resistance in Section 8.3.1; (2) the use of S3 reduces the viscosity of concrete significantly, as shown by the t_{500} and t_v, which subsequently influences the concrete microstructure.

Figure 8.11: The cross section of the concrete cube with 60% Vol. (S2) aggregate replacement

- **Freeze-thaw test**

Figure 8.12 shows the cumulative mass loss (CML) of concrete slab samples under freeze-thaw cycles with the presence of a de-icing agent according to standard.

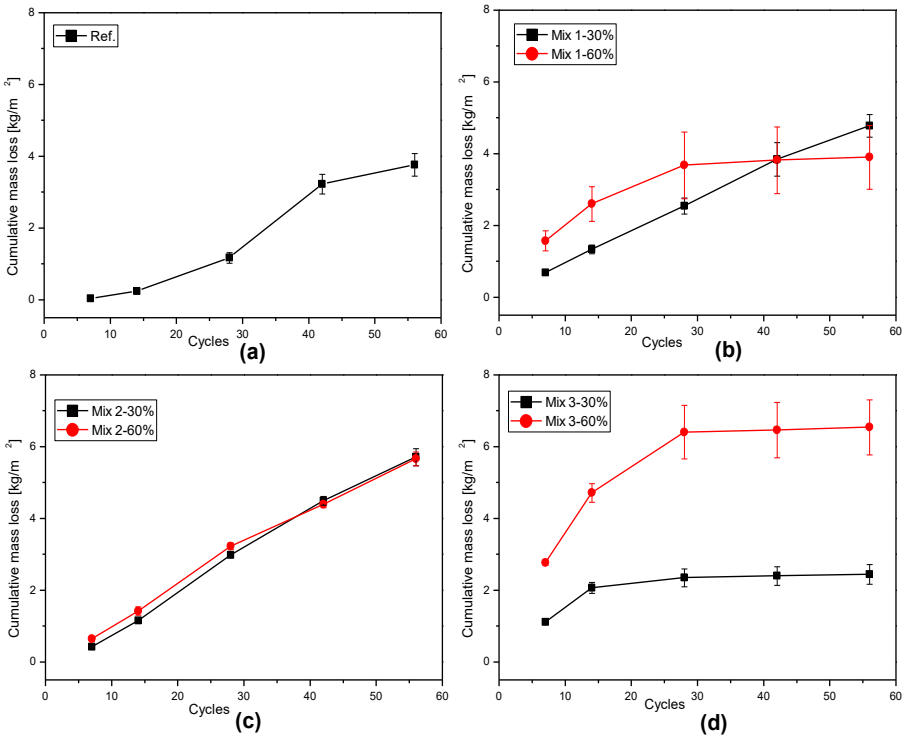

Figure 8.12: The cumulative mass loss of hardened concrete samples after freeze thaw cycles

The CML of reference concrete increases slowly in the first 28 cycles, after which there is a sharp increase. The CML of Mix 1 with 30% vol. of S1 is increasing linearly, and it is

27% higher than that of the reference after 56 cycles. When 60% vol. of S1 is used, the CML of concrete increases during the first 28 cycles and is higher than that of the reference; after this, it is almost steady and it is nearly the same as the reference after 56 cycles. The CML of Mix 2 shows a linearly increasing trend during the test cycles, which is higher than the reference. Moreover, the increasing amount of artificial aggregates S2 does not lead to a significant difference in the CML profile. The CML of Mix 3 with 30% vol. of S3 is almost stable after 14 cycles, and it is 35% lower than of the reference after 56 cycles. When 60% S3 is used, its CML is the highest among all the tested samples in this study, and it is stable after 28 cycles. According to EN 206-1, the recommended mixing proportions for concretes exposed to freeze-thaw attack at a defined level of XF1 are: maximum water to cement ratio of 0.55, minimum strength class of C30/37, minimum and cement content of 300 kg/m^3; the designed self-compacting concrete with CBLAs has a water to cement ratio of 0.45, cement content of 310 kg/m^3 and strength class of C35/45-C50/60. Hence, the self-compacting concretes complies the freeze-thaw exposure class of XF1, which means moderate water saturation without de-icing agent, such as vertical concrete surface exposed to rain and freezing.

For normal concrete, the CML under freeze-thaw condition is due to: (1) the loss of cementitious matrix; (2) the loss of natural aggregates due to less binding by the matrix (Medina et al., 2013b). For the concrete with artificial aggregates, which have a higher porosity compared with natural aggregates, the CML of concrete also includes the mass loss of artificial aggregates due to expansion of water inside the saturated aggregates. This is one of the main reasons for the higher CML of Mix 1, Mix 2 and Mix 3 at early freeze-thaw cycles (Medina et al., 2013b). The higher CML of concretes with higher artificial aggregates confirms this finding. The addition of PPF in aggregates S2 results in a slightly lower CML of concretes, which was also reported in (Roustaei et al., 2015) during soil treatment. This may be attributed to the gradual mass loss of concrete during the freeze-thaw test. For concrete with aggregates S3, the fast stability of CML could be resulting from the addition of nano-silica. Researchers have figured out that the use of a certain amount of silica in concrete could increase the freeze-thaw resistance of concrete (Alkaysi et al., 2016). Hence, the addition of silica in aggregates production results in the higher freezing-thaw resistance of concrete with S3. Another possible reason is the higher porosity of Mix 3 with 30% vol. of S3, which is reflected in the water penetration depth. The porosity of concrete leaves space for the expansion of water, which results in less damage during freeze-thaw tests. However, Mix 3 with 60% vol. of S3 achieves the highest mass loss; this may result from the lower bonding strength of the highly porous cementitious matrix; hence, the detaching of the mortar matrix is much easier during the freeze-thaw test.

The above results indicate the different influences of artificial aggregates on the freeze-thaw resistance of concretes. It seems that, in the present study, the cumulative mass loss

of concretes with artificial aggregates has two types of profiles: linearly increasing and a two-stage type (firstly increase and then reaching a stable level). The correlation between the artificial aggregates properties (porosity, strength, etc.) and the freeze-thaw resistance profile needs to be investigated in a future study.

8.3.4 Leaching behaviour evaluation of hardened concrete

- **Column leaching on the crushed hardened concrete**

Figure 8.13 (a) shows the total amount of heavy metals (Sb, Cu and Mo) and salts (chloride and sulphate) in the crushed concrete samples with and without artificial aggregates by mass. The amount of these elements in concrete increases when the artificial aggregates are used and a higher replacement level leads to a higher concentration of these elements compared to the reference. Figure 8.13 (b) shows the leaching concentrations of the investigated elements from the crushed concretes. It demonstrates that the leaching concentrations of these elements are all under the limit value according to the Dutch legislation and their leaching concentration increase with the increasing amount of artificial aggregates (SQD, 2013). The leaching of Sb is lower than 0.004 mg/kg d.m. and below the detectable level, therefore they are not shown in the graph. This leaching result means that these concretes can be recycled and reused as secondary building materials as non-shaped materials according to SQD (2013), in case recycling of these concretes is required when they finish their service life.

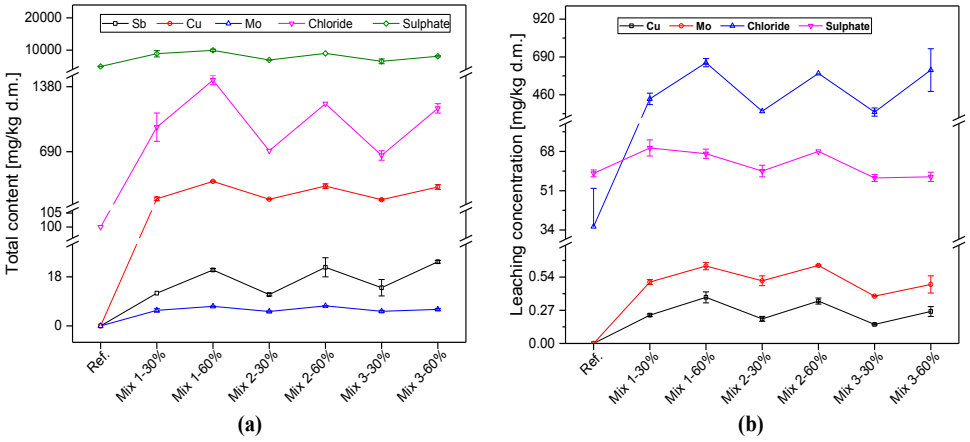

Figure 8.13: The total concentration (a) and (b) the leaching concentration of Sb, Cu, Mo, chloride and sulphate in the concrete mixtures

The leaching of Sb for the CBLAs is around 0.1-0.15 mg/kg d.m., which is under the limit value. The leaching concentration of Cu and Mo of the produced CBLAs is 1-1.4 and 1.5-2.3 mg/kg d.m., and exceed the limit values, respectively. The leaching of chloride is about 2500-4600 mg/kg d.m. and exceeds the limit value, while the leaching of sulphate (120-

499 mg/kg d.m.) is well under the limit value. Due to the fact that the total amount of the investigated elements is influenced by the amount of artificial aggregates applied, the leachability of the concretes is calculated based on their total amount and leached out amount of elements following Eq. (3.8). Figure 8.14 shows the leachability of Cu, Mo, chloride and sulphate of CBLAs and the concretes containing CBLAs. It shows that the sample S3 has a lower leachability of Sb, Cu, Mo and sulphate, while it has higher chloride leachability compared with sample S1. This demonstrates that the addition of nano-silica could promote the immobilization of the above-mentioned elements. For chloride, it seems that the use of PPF and nS have a negative influence on its immobilization, which may be explained by the higher porosity of S2 and S3, giving the highly soluble chloride more chance to be washed out.

The Cu leachability of concrete decreases with the increasing amount of artificial aggregates for all the concrete mixtures and concrete Mix 3 has the lowest Cu leachability compared with Mix 1 and Mix 2. The leachability of chloride has an increasing trend from reference to Mix 3, and a higher aggregates replacement level results in a lower leachability of chloride for each concrete mixture. The sulphate leachability of concrete with artificial aggregates is lower than that of the reference, and higher levels of aggregates being replaced contribute to a lower leachability of sulphates.

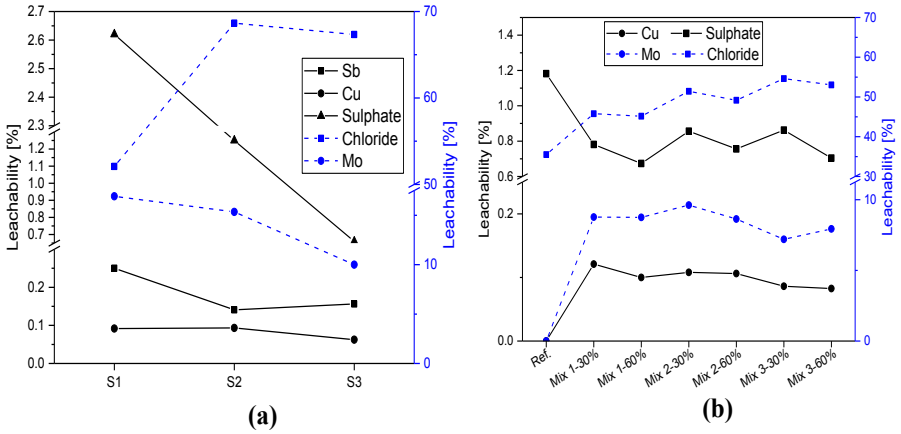

Figure 8.14: The leachability of Cu, Mo, chloride and sulphate from the concretes

It seems that the concretes containing aggregates S3 have a better immobilization of heavy metals compared with the ones with S1 and S2. This may be due to the addition of nano-silica in the aggregates production which is reported to decrease the pH of the cementitious matrix in concrete (Byfors, 1987).

As shown in Figure 8.15, the pH of the tested leachate from the crushed concrete shows that the addition of artificial aggregates (S1 and S2) results in a higher pH of the leachate,

while the pH of leachate from Mix 3 (with S3) is lower than that of the other samples; this also proves that the addition of nano-silica to the cementitious matrix leads to a lower pH. Moreover, the leaching behaviour of heavy metals in MSWI residues is highly related to the pH (Zhang et al., 2016). The use of nano-silica to produced CBLAs did not increase the crushing resistance of the aggregates, but it improves the leaching of the aggregates and the concrete with these aggregates.

The leaching of the concrete with the produced CBLAs in this study complies with the Dutch legislation, which means the recycling of these concrete as secondary building materials is environmental friendly after they finish their service life. Considering the leaching of concrete with CBLAs, the amount of CBLAs can be increased when additives are applied in concrete, such as fly ash, silica fume, ground granulate blast furnace slag, etc. which are reported to reduce the pH of the concrete (Byfors, 1987). Moreover, these additives can also be applied to be used as raw materials for CBLAs production when the leaching of the aggregates is critical.

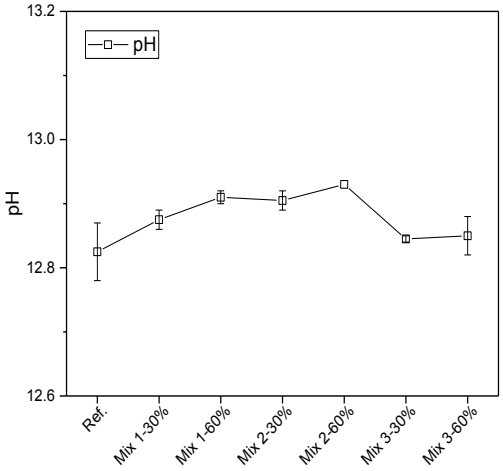

Figure 8.15: The pH of the crushed concrete samples with and without aggregate replacement

- **Diffusion test on the hardened concrete**

The diffusion tests on the hardened concrete containing 30% and 60% vol. CBLAs were performed, and the cumulative concentration (ε_{64}) of components leached out from the concrete cube were shown in Table 8.3 and compared with the limit value for shaped materials according to SQD (2013). It shows that the ε_{64} of all the components is far below the limit value in SQD, which demonstrate the non-hazardous of these concrete to environment.

Table 8.3: The cumulative emission of components from hardened concrete containing CBLAs and the leaching limit for shaped materials according to SQD (2013)

Components	limit for shaped materials ε_{64} [mg/m^2]	Cumulative emission ε_{64} [mg/m^2]					
		Mix1-30%	Mix1-60%	Mix2-30%	Mix2-60%	Mix3-30%	Mix3-60%
Sb	8.7	0.19±0.01	0.19±0.01	0.17±0.0	0.17±0.0	0.25±0.02	0.2±0.01
Cu	98	2.0±0.0	2.0±0.0	2.0±0.0	2.0±0.0	2.0±0.0	2.0±0.0
Mo	144	0.62±0.05	1.4±1.1	0.53±0.01	0.52±0.02	1.3±0.28	1.1±0.15
Cl^-	110000	665±78	3750±2192	960±57	1400±0.0	1750±71	2400±283
SO_4^{2-}	165000	825±21	1480±877	880±42	865±21	1300±141	1020±113

According to NEN 7375 (Table 8.2), when the slope (rc) of the linear regression line of log ε versus log t of each increment (increment 2-7, 5-8, 4-7, 3-6, 2-5, and 1-4) is between 0.35 and 0.65, then the leaching mechanism can be defined as diffusion control, when the rc of increments 5-8, 4-7, 3-6, and 2-5 is below 0.35, then it is depletion and for increment 2-7 and 1-4, it is surface wash-off.

Table 8.4 shows the rc of Mix1-60% as an example. The rc of all the investigated components of the diffusion tests on the concrete cubes in our study are mostly between 0.35 and 0.65 for increment 2-7, which demonstrates the diffusion control; the rc for chloride and Mo show high chance to dropped in the range of 0.35-0.65 for increment 2-5. While, for the other increments of investigated components, their rc are mostly below 0.35, which means the depletion mechanism.

Table 8.4: The rc of the increment according to NEN 7375 (Mix1-60% is shown as example)

Components	rc2-7	rc5-8	rc4-7	rc3-6	rc2-5	rc1-4
Sb	0.1	0.38	-0.09	0.07	0.2	0.5
Cu	0.1	0.07	-0.09	0.07	0.2	0.5
Mo	0.3	-0.13	-0.13	0.43	0.67	0.55
Cl^-	0.12	0.29	0.23	0.3	0.55	0.63
SO_4^{2-}	0.17	0.23	0.05	0.07	0.2	0.5

Figure 8.16 shows the pH of the leachate obtained at each testing time, which is above 11 and has an increasing trend with time. It was reported that the leaching of some heavy metals in MSWI bottom ash is pH dependent (Chimenos et al., 2000; Dijkstra et al., 2006; Malviya & Chaudhary, 2006; Meima & Comans, 1999), the leachability of most heavy metals increases when the pH is higher than 10. However, the leaching of investigated components in concrete did not follow a linear increasing trend, which may due to the combined effect of immobilization of binder and the low concentration of components.

Hence, it can be concluded that there seems to be two stages regarding the leaching mechanisms of the investigated components in the concrete containing CBLAs: at the first stage, it is diffusion controlled; afterwards, it seems to be depletion controlled. However, the leaching of investigated components complies with the leaching limit according to SQD (2013). Therefore, the use of these concrete containing CBLAs produced from fine MSWI bottom ash and other industrial solid wastes are environmental non-hazardous.

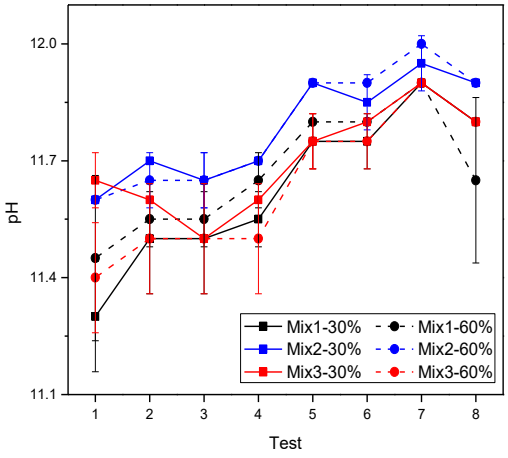

Figure 8.16: The pH of the obtained leachate at each testing moment

The column and tank leaching tests on the crushed and cubic concretes containing the three types of CBLAs produced from mixtures of industrial solid wastes show that these crushed and cubic concretes can be classified as non-hazardous materials, even though the CBLAs cannot comply with the leaching limit completely and then not allowed to be treated as building materials directly. These concretes containing CBLAs will be the final products which could be used in construction fields, in which around 13%-27% industrial solid wastes due to the use of CBLAs are additionally recycled.

To summarize, the use of these concrete containing CBLAs produced from fine MSWI bottom ash and other industrial solid wastes are environmental non-hazardous according to legislation and they can be used directly. It can be concluded that, the pelletizing technique is successfully applied to produce artificial aggregates from integrated industrial solid wastes, and the concrete produced with these artificial aggregates is non-hazardous to environment. In this way, the environmental burden related to disposal of industrial solid wastes and consumption of natural resource in construction field could be reduced. Moreover, the leaching of the crushed concretes complies the limits in legislation, which means after service life, they can be recycled and then reused again. Thus, a closed recycling circulation of several industrial solid wastes can be achieved.

8.4 Conclusions

In this study, the mixed industrial solid wastes are integrally recycled and innovative methods are used to improve the properties of the produced artificial cold bonded lightweight aggregates (CBLA). Three types of aggregates are produced and used as aggregates in self-compacting concretes, and their influence on the concrete properties is studied. The following conclusions can be drawn:

(1) Three types of CBLAs are produced from combined industrial solid wastes, including municipal solid waste incineration (MSWI) bottom ash fines (F-BAM, 0-2 mm), paper sludge ash (PSA), coal fly ash (FA), and washing aggregates sludge (WAS), with ordinary Portland cement as binder. The F-BAM, polypropylene fibre (PPF) and nano-silica from olivine dissolution were used to improve the properties of the artificial aggregates, such as crushing resistance, bulk density, etc.

(2) The produced CBLAs were used as natural aggregate in designed self-compacting concrete. It was found that the addition of CBLAs produced without (S1) and with (S3) nano-silica do not have a significant influence on the slump flow diameter, while the one with aggregates produced with the addition of PPF (S2) had a smaller slump flow diameter due to the blocking function of PPF. The t_{500} of concrete mixtures with S1 and S2 is slightly influenced, while the addition of S3 results in shorter t_{500} time. It is observed during the V-funnel test that the round shape of the artificial aggregates had a 'ball effect', which makes the artificial aggregate particles to be pushed on the top layer of the sample.

(3) The compressive and flexural strength of the concrete is decreased with the increasing amount of artificial aggregates. The concrete strength has a positive linear correlation with the crushing resistance of the CBLAs when 30% Vol. aggregates is replaced, while this relationship is not found for the samples with 60% vol. aggregates replacement, due to the significant influence of CBLAs on the fresh properties of concrete (such as viscosity). The compressive strength of the concrete containing CBLAs has linear relation with its fresh bulk density.

(4) The water penetration depth (WPD) of concretes shows that the use of CBLAs increases the water WPD, and the concrete with aggregates S3 has a much higher WPD, which is attributed to the influence of concrete viscosity. Less water or chemical admixtures for modifying the water requirement is recommended when CBLAs are used.

(5) There are two cumulative mass loss (CML) profiles of concrete with CBLAs during freeze-thaw tests obtained in this study: one linearly increases with the test cycles, another one is a two-stage profile (increasing stage and stable stage). The use of aggregates S2 which contains PPF results in a linear increase of CML, and there is a marginal difference when the amount of S2 is increased from 30% to 60% vol.

The concrete with aggregates S3 has a two-stage CML profile, which is assumed to be influenced by the nano-silica in aggregates and the porosity of the concrete.

(6) The leaching of the investigated metals (Cu, Sb, Mo) and anions (chloride and sulphate) from the crushed concretes with CBLAs complies with the Dutch environmental legislation, which demonstrates these concretes are environmental friendly to be recycled and reused after they finish their service life. The diffusion tests on the concretes containing CBLAs show that the leaching of components is diffusion controlled at early age and then depletion controlled. In addition, the cumulative leaching concentration after 64 days of these investigated components complies with the leaching limit for shaped materials in SQD.

Chapter 9

9 Leachability study of F-BA and cementitious immobilization

9.1 Introduction

In the previous Chapters (Chapters 4, 5, 6, 7 and 8), the leaching behaviour of the heavy metals and salts from the fine MSWI bottom ashes (F-BA) in the column leaching tests or shaking tests was shown. Meanwhile, the corresponding leaching behaviour during the application of the F-BA in the presence of cementitious materials was also tested.

The aim of this chapter is to study the relationship between the leaching of F-BA and the leaching of mortar or concrete with F-BA, to assess the immobilization capacity of cementitious materials on the investigated components existing in F-BA during application and to distinguish binding effect of cementitious materials on the contaminants from dilution effect during the application of solid wastes. This, in turn, can be used as an indicator for the cementitious stabilization of F-BA as a treatment, related to its application purpose or potential.

In this chapter, the leaching behaviour of heavy metals and salts from F-BA or mortar and concrete containing F-BA is summarized, and the leachability of these investigated components in F-BA or in mortar and concrete is calculated and compared. The cementitious immobilization as a treatment to reduce the leaching of components regarding application method (as binder substitute, sand application, or as ingredient for aggregate production) is evaluated. This is divided into several aspects, namely:

(1) The influence of thermal treatment on the leachability of heavy metals and salts, and the leachability of these components in mortar when the treated F-BA is used as binder substitutes;
(2) Leachability profile of investigated components during shaking test related to the particle size of F-BA (milled and not milled), and in the mortar when used as sand replacement with blended binders;
(3) Influence of binders on the leachability profile of the investigated components existing in F-BA when being used in the form of artificial cold bonded lightweight aggregates (CBLAs);
(4) Leachability study of concrete with by-products containing F-BA (CBLAs).

9.2 Leachability related to treatment and application purpose

9.2.1 Thermal treatment and binder substitute

The leaching data used in this analysis has been presented in detail in Chapter 4. The leachability of Sb, Cu, Mo, chloride and sulphate in the treated MF-BAW is calculated according to Eq. (3.8). The total contents of heavy metals and salts in mortars containing

treated MF-BAW were not tested, hence, these were calculated based on their total contents in the treated MF-BAW and the amount of treated MF-BAW used in mortar samples. The mass ratios of the materials for mortar preparation is 1 cement: 3 sand: 0.5 water, the mass of mortar used for calculation is between the one with and without water content, due to the participation of part water into cement hydration and release of free water. Hence, the total content of components is calculated and showed in the range as:

$$C_t = (C \times \frac{r \times 450}{450 + 1350 + 225} \sim C \times \frac{r \times 450}{450 + 1350}) \quad (9.1)$$

Where C_t is the range of calculated total content of components (mg/kg) in mortar, C is the total content of components (mg/kg) in treated MF-BAW (Table 4.4), and r is the replacement ratio of cement by treated MF-BAW, which is 30% in Chapter 4. Table 9.1 summarizes the leachabilities of MF-BAW and mortars. If the leachability of contaminants in mortar samples is the same as the relevant leachability of the treated MF-BAW, this means the lower leaching concentration of the contaminants from mortars is due to the dilution effect; if the leachability of mortars is lower than that of treated MF-BAW, this means the leaching of contaminants from mortar is reduced due to the binding ability of the cementitious materials; if the leachability of mortars is higher than that of threated MF-BAW, this means there are other influencing parameters promote the leaching of contaminants from MF-BAW.

Table 9.1: The leachability of Sb, Cu, Mo, chloride and sulphate in treated MF-BAW (according to Eq. 3.8) and mortar containing treated MF-BAW (according to Eq. 9.1) in column leaching test

Leachability [%]	Treated F-BAW samples			Mortar samples		
	MF-BAW	5TM	5TMS	MF-BAW	5TM	5TMS
Sb	1.05	0.04	0.02	< 0.14-0.16	< 0.08-0.09	< 0.10-0.11
Cu	0.12	0.00	0.01	0.07	< 0.02	0.02-0.03
Mo	6.1	14.0	21.7	9.8-11.1	13.2-14.8	9.2-10.4
Chloride	115.8	62.3	71.7	110.5-124.3	65.7-73.9	58.0-66.0
Sulphate	88.0	83.3	50.3	11.9-13.4	9-10.1	7.1-8

The Sb leachability after thermal treatment decreases dramatically, as well as Cu leachability, which demonstrates the efficiency of the thermal treatment in removing Cu and Sb. The Mo increases after thermal treatment by around 2 times, and sample 5TMS has the highest Mo leachability. The chloride leachability of MF-BAW exceeds 100% due to sample variation, which shows its quite high leachability. Samples 5TM and 5TMS have slightly lower chloride leachability. The sulphate leachability is also quite high in F-BAW, and it decreases slightly after thermal treatment; sample 5TMS has the lowest leachability of sulphate.

For mortar with MF-BAW, the leachabilities of Sb and Cu decrease by around 90% and 42% compared to those of MF-BAW, respectively. This can be attributed to the

immobilization ability of cement in the mortar instead of dilution effect. The leachability of Mo has a slight increase, and there is no significant change for chloride leachability; the sulphate leachability is reduced by more than 80%. Similar changes of these leachabilities are observed for mortar samples containing 5TM. For mortar containing 5TMS, compared to 5TMS, the Mo and sulphate leachabilities decreased by more than 50% and 80%, respectively. The leachability of chloride has a marginal reduction, by around 18%.

It seems that the leachability of components in mortar with 5TMS is reduced more than that of samples with MF-BAW and 5TM. This is consistent with the hydration study in Section 4.3.2, and demonstrates that a better binder hydration results in a higher immobilization of investigated components, such as chloride and sulphate. However, there is no clear trend for the immobilization of Sb, Cu and Mo. It seems that their immobilization in mortar with treated MF-BAW used as binder substitute is related to their total amount, their initial properties in the treated MF-BAW and the binder hydration.

9.2.2 Washing treatment and sand replacement with blended binders

- **Washing treatment**

The leachability of F-BAM is calculated using the Eq. (3.8), and the data used is the same as shown in (Table 5.2). Table 9.2 shows that the leachability of F-BAM of chloride and sulphate is more than 40% during the column leaching test, which is lower than that of F-BAW in shaking test at L/S 10. The leachability of Mo, Sb and Cu of F-BAM is also lower than that of F-BAW in shaking test by around 40-70%.

Table 9.2：The total amount of investigated salts and heavy metals in F-BAM and their leaching concentrations during the column test and their leachability

Parameters	Sb	Cu	Mo	Chloride	Sulphate
Total amount [mg/kg d.m.]	83	3100	19	2100	22900
Column leaching [mg/kg d.m.]	0.47	1.1	0.68	950	11000
Leachability [%]	0.57	0.035	3.6	45	48

As shown in Figure 9.1, the leachability of chloride of F-BAM in shaking is around 55% when L/S is 10, and it is around 50% for MF-BAM, it seems independent to the L/S ratio. The sulphate leachability is around 50% for F-BAM and MF-BAM, which is lightly higher than the column leaching result, and increases with the L/S ratio. For both chloride and sulphate, the leachability decreases slightly after milling of the sample. The Cu leachability of F-BAM in the shaking test is much higher (by 1.4 times) than that of the column leaching test at L/S 10, while it is lower after the milling of F-BAM. The Cu leachability of F-BAM is strongly L/S ratio dependent, while for the MF-BAM, it is much less dependent. The Sb

leachability for both F-BAM and MF-BAM is L/S ratio dependent and the milling treatment increases Sb leachability.

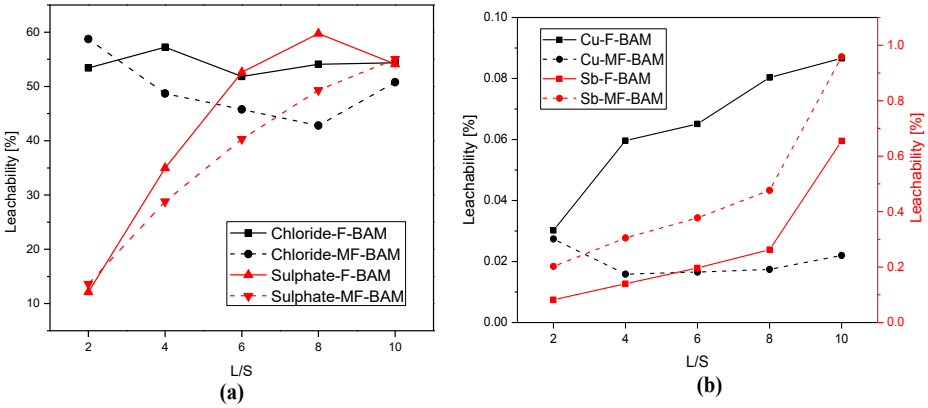

Figure 9.1: The leachability of chloride, sulphate, Cu and Sb of F-BAM and MF-BAM (Figure 5.2)

- ***Mortar with NaCl addition***

Figure 9.2 shows the chloride leaching profile in the shaking test from mortars with blended binders with the addition of NaCl and the immobilization efficiency of chloride in all mortar samples; the leaching data used is the same as Figure 5.8.

The amount of chloride immobilized in the mortar samples after shaking test increases with curing age, and samples M1' and M3' have a very similar amount of chloride immobilized. Sample M2' has the highest immobilized chloride, which is around 50% after 28 days.

According to Luo et al. (2003), around 80% chloride can be bound by OPC mortar, and 91% bound by mortar with 70% GGBS to replace OPC when 1% wt. of binder NaCl was added; the test on plain binder without sand showed similar chloride binding capability. It was also reported that the chemical bound chloride in OPC paste and mortar after 28-days curing was around 62% and 33% of the total bound chloride, respectively; for OPC and GGBS blended paste and mortar, it was 78% and 51%, respectively. The reason for the higher chloride binding in OPC and GGBS blended samples were mainly attributed to chemical chloride binding capability, which was demonstrated by the higher amount of Friedel's salt found in blended samples. The chloride amount left in the washed sample is lower compared with the reported results (Luo et al., 2003). Kayali et al. (2012) reported that the magnesia in GGBS resulted in the formation of hydrotalcite, and this product contributes significantly to the excellent chloride binding capacity of GGBS blended binders. In this study, the MgO content in GGBS is around 9% (Table 5.1), and hydrotalcite was detected in the hydrated samples with GGBS and OPC blended (Figure 5.5). Therefore, the founding in this study is consistent with the other studies.

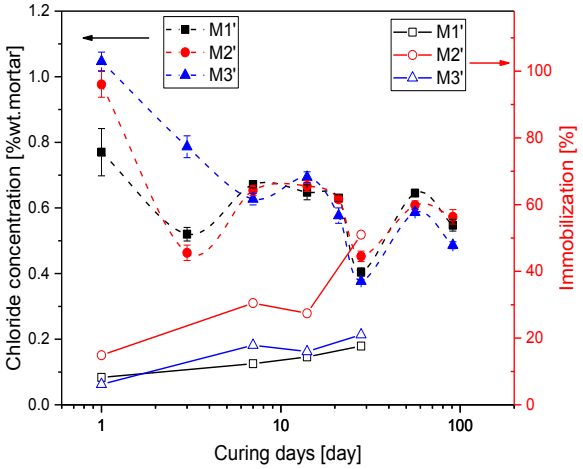

Figure 9.2: The chloride leached out from crushed mortars after various curing ages and the immobilized chloride in mortar with NaCl (Figure 5.8)

The shaking test is performed on the crushed mortar; therefore, it could be possible that some free chloride or physically bounded chloride is trapped in the mortar particles, which does not come in contact with water. However, it is also possible that the free and physical bound chloride is washed out, and maybe part of the chemical bound chloride. Additionally, the total chloride in the mortar samples decreases with the curing ages, which may attribute to the diffusion of chloride into the water during the early hydration age due to the water curing. This is consistent with the high amount of chloride leached out after shaking during the first day curing (Figure 5.8). The current results demonstrate that OPC blended with GGBS can immobilize high amounts of chloride, and OPC blended with FA has similar immobilization efficiency compared with plain OPC.

Hence, the obtained results in this chapter can be used to demonstrate the chloride binding of mortar with blended binders in shaking tests only, and are suitable for estimating the leaching of chloride under cementitious solidification/stability treatment of wastes.

- **Mortar with F-BAM as 100% sand replacement**

Figures 9.3 and 9.4 show the leachability of chloride, sulphate, Sb and Cu from blended mortars during shaking test when F-BAM is used as sand replacement. The total amount is calculated based on their content in F-BAM and the proportion of this F-BAM in mortar (the leaching data used is the same as in Figures 5.11 and 5.12). It can be seen that the chloride leachability has a similar trend as the mortar with addition of NaCl, and calculated chloride leachability at early ages is over 100%, which is due to the fact that binders also contain a certain amount of chloride, which is not included into the total chloride content. After around 14 days curing, the chloride leachability is already stable, which is around 17%, 19% and 13% for mortar with OPC, OPC blended with GGBS and OPC blended with

FA, respectively; after 91 days, the corresponding chloride leachability is around 11%, 13% and 10%, respectively. Hence, about 80-90% of chloride is bound in the mortar after 14 days. For mortars with additions of NaCl, the chloride leachability is stable after 7 days curing, and the bound chloride is around 12%, 30% and 18%, respectively.

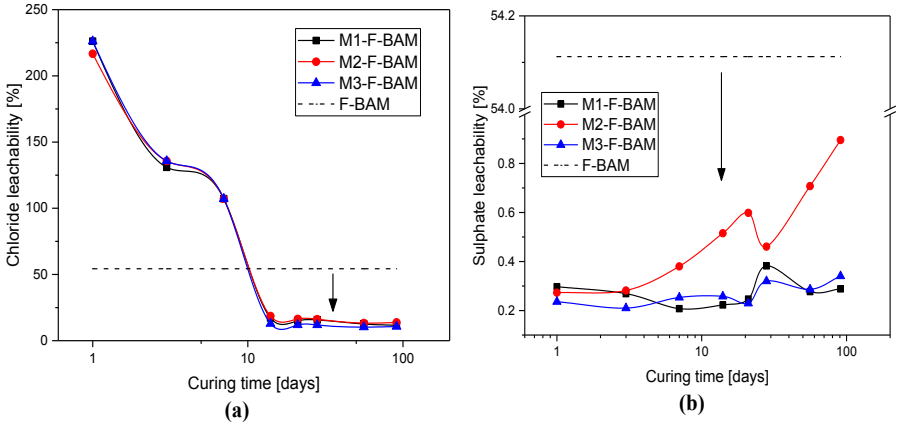

Figure 9.3：The leachability of (a) chloride and (b) sulphate from mortars with F-BAM their leachability of F-BAM in shaking test with L/S 10 (Figure 5.11)

It seems that the chloride binding in mortar with F-BAM has a slower rate and is higher than that of mortar with addition of NaCl, and the difference between blended binder is marginal. Several reasons could be responsible for this phenomenon: (1) the total chloride content is different with the same amount of binders. In mortars with NaCl, the chloride content is around 5% by mass of binder; while in mortar with F-BAM, it is around 1%. As reported in (Tang & Nilsson, 1993), higher free chloride content resulted in higher bound chloride; (2) The calorimetry study shows that the addition of bottom ash or the waste water from washing bottom ash has a retardation effect on the binder hydration, subsequently influencing the binding capacity of chloride in mortar with F-BAM; (3) different from NaCl addition, the chloride in mortar F-BAM will firstly dissolve or be released from F-BAM into the pore solution and then bound by the binder hydrates; even though the chloride in F-BAM is highly soluble, this will slow down the chloride binding. This delay of available free chloride for participating in the binder hydration may influence the amount of chemically bound chloride, which then reduces the chloride immobilization during the shaking test.

Hence, it is of interest to investigate the chloride binding capacity of blended binders when the chloride source is provided from the wastes during their application life.

The leachability of sulphate has a slight increasing trend with the curing age, and mortar with blended OPC and GGBS has higher sulphate leachability. The sulphate leachability is very low, around 99% of sulphate is stable, similar to the founding in (Lampris et al.,

2011). Müllauer et al. (2015) reported that the concrete with GGBS as cement replacement showed higher sulphate leaching than OPC or OPC blended with FA, which is due to the dissolution of AFt and AFm.

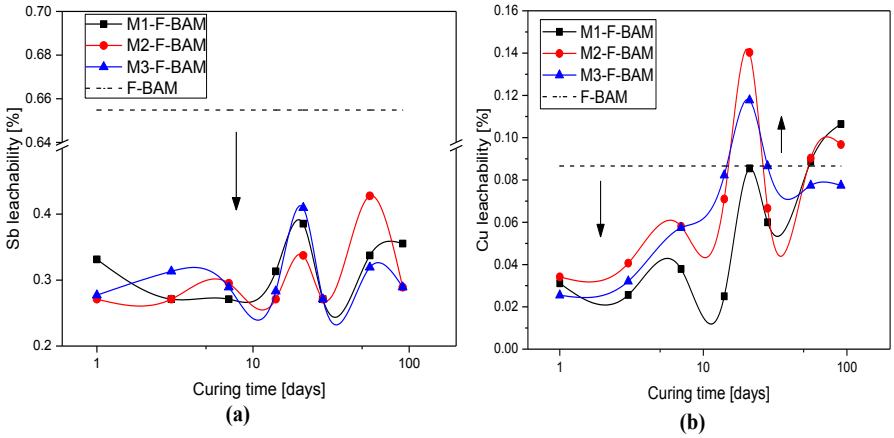

Figure 9.4: The leachability of (a) antimony and (b) copper from mortars with F-BAM and their leachability of F-BAM in shaking test with L/S 10 (Figure 5.12)

The leachability of Sb from mortars containing F-BAM as sand is around 0.27%-0.4%, which is lower than that of F-BAM (around 0.65% at L/S 10 in shaking test). The Cu leachability is between 0.02%-0.11%, it increases with the curing time, and is higher than that of F-BAM (around 0.09% at L/S 10 in shaking test) after around 21 days curing. The relation of Sb and Cu leachability with the blended binders cannot be clearly distinguished.

The leachability of the mortars with blended binders containing F-BAM as sand replacement shows that with the use of binders, the leachability of chloride, sulphate and Sb decreases compared with that of F-BAM. This demonstrates the contribution of binders on the immobilization of these components. However, the Cu leachability shows an increasing trend along with mortar curing time, and tends to exceed the leachability of F-BAM.

Regarding cementitious stabilization as a treatment on MSWI bottom ash during its application, it was reported that this was a promising method to immobilize the heavy metals and salts. However, during the application there are several factors that need to be considered:

(1) The leaching behavior of the components in MSWI bottom ash various under different conditions, such as pH, leaching methods, etc. (Arickx et al., 2008; Chimenos et al., 2003; Cornelis et al., 2012; Lampris et al., 2011; Olsson et al., 2009). The high pH in mortar due to binder hydration may result in the dissolution of some stable metal-bearing phases, consequently, leading to the high leaching of these metals. For instance, it was reported that Sb is low pH stable, hence, the

mortar with high pH may result in higher Sb leaching during application (Cornelis et al., 2012). The leaching of Cu in MSWI bottom ash was reported as pH depended (Meima et al., 1999; Solpuker et al., 2014), also as shown in this study. Hence, when the pH of the mortar increases with curing age, the leaching of Cu also increases.

(2) The hydration of the binders can immobilize the leached components chemically and physically. For instance, it was reported the Cu may replace the Ca to form CSH and then being immobilized (Hashem et al., 2011). However, it is also learned in this study by calorimeter results that the waste materials can retard the binder hydration due to the organic matters or heavy metals. This obstruction directly reduces the immobilization capacity of the binders, which may partially explain why there is no clear relation between the leachability of components and the blended binders.

(3) In mortars with F-BAM, the immobilization and dissolution of components happen simultaneously. The binder hydration immobilizes the leached components, meanwhile, providing alkaline surroundings which leads to the dissolution of more corresponding components. Once the dissolution speed and amount is higher that the immobilization rate and capacity, the leaching of components increases with curing age. Especially in the long term, the binder hydration gradually decreases and is almost fully finished, while the dissolution of the components is continuing.

9.2.3 Aggregate production with blended binders/cementitious materials

Figure 9.5 shows the leachability of components from artificial lightweight aggregates using F-BAM under column test, and compared with that of F-BAM.

It can be seen that the leachability of Sb and sulphate is lower than that of F-BAM, which confirms that the cementitious stabilization benefits Sb and sulphate immobilization effectively. Sb leachability shows an increasing trend with curing time, while Cu and Mo has a slight decrease after longer curing, which is attributed to the stability of metal-bearing phases with the pH increase. Compared to mortar containing F-BAM, the leachability obtained during the column leaching on CBLAs is higher than that of mortar obtained from the shaking test. Several reasons may contribute to this result: (1) as showed from column and shaking leaching test on F-BAM, the leachability of components in shaking leaching is higher than that from column leaching; (2) the CBLAs contains higher amount of F-BAM while lower amount of binders compared with mortar, (5-10% of binders in CBLAs while 33% of binders in mortars), higher binders result in high immobilized components.

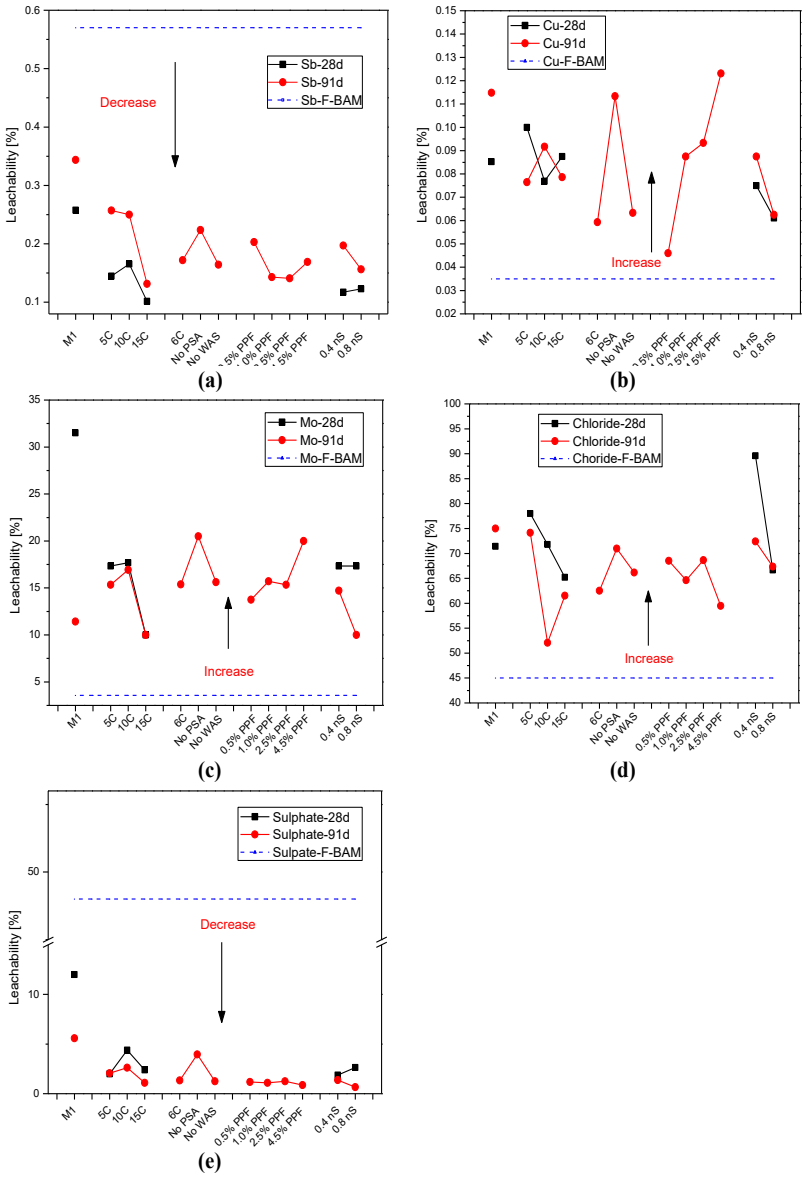

Figure 9.5: The leachability of Sb, Cu, Mo, chloride and sulphate from F-BAM and CBLAs containing F-BAM after 28 and 91-days curing, respectively (Figures 7.6-7.10)

9.2.4 Application in concrete in the form of CBLAs

Figure 9.6 depicts the leachability of components in CBLAs and that of concrete containing CBLAs. It can be seen that the CBLAs produced with PPF and nano-silica have lower Sb, Cu, Mo, and sulphate leachabilities, while higher chloride leachability. The concrete containing 30% and 60% vol. of CBLAs has a decreased leachability of Sb, Mo, chloride

and sulphate, while increased Cu leachability. In the concrete, the cement accounts for 18% of the total solids and the binder amount including cement and FA accounts for 28% of the total solids; 8% more cement is used in concrete compared to the amount used to produced CBLAs. The trend of the leachability in concrete is very similar to that of the CBLAs, which demonstrates that the properties of the CBLAs are corresponding to the leaching of the concrete, when they are used in concrete.

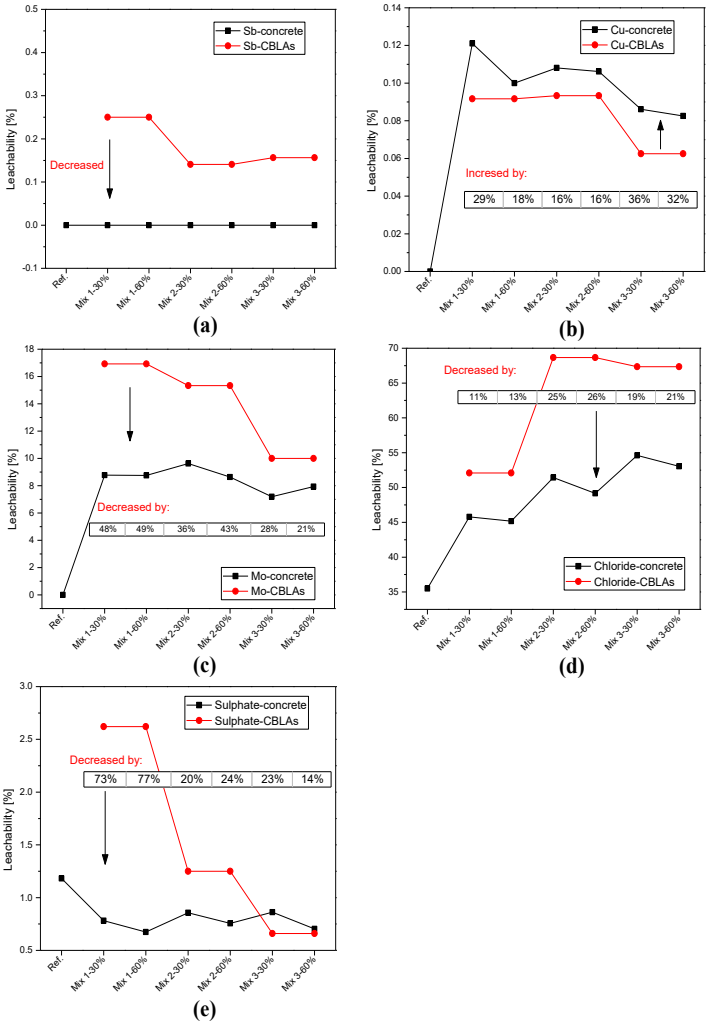

Figure 9.6: The leachability of Cu, Mo, chloride and sulphate from the CBLAs and concretes containing CBLAs after 28-days hardening (Figure 8.14)

The Sb leaching of concretes is below detection level, which demonstrates that the Sb immobilization is enhanced when CBLAs are used in concrete. The Cu leachability of concrete is higher than that of CBLAs and the increment for each concrete is shown in

Figure 9.6. The higher cement amount does not contribute to a lower, but a higher Cu leaching, which is similar as observed in mortar with F-BAM. The concretes with CBLAs have lower Mo leachability than the corresponding CBLAs, and chloride and sulphate leachability decreases by 11-26% and 14-77%, respectively.

It can be summarized that the higher binder content results in lower leachability of Sb, Mo, chloride and sulphate, while increases the leachability of Cu.

9.3 Conclusions

The leachability of Sb, Cu, Mo, chloride and sulphate regarding the treatments and application methods is evaluated and compared with that of F-BA. The following conclusions can be drawn:

(1) The thermal treatment on F-BAW can reduce the leachability of Sb and Cu significantly, while it results in a higher Mo leachability. The chloride leachability after thermal treatment decrease slightly, as well as sulphate leachability. The mortar with thermally treated F-BAW as binder substitute has lower Sb, Mo, chloride and sulphate leachability compared with treated F-BAW, while it has a higher Cu leachability.

(2) The leachability of Sb, Cu and sulphate in F-BAM during washing increases with the L/S ratio, and lower leachability of MF-BAM was observed than F-BAM, except for Sb. The chloride and Cu leachabilities are less dependent on the L/S ratio. The leachability of heavy metals are L/S and particle size related.

(3) The mortar with NaCl addition shows a decreasing trend of chloride leaching during the shaking test, and the chloride concentration leached out is stable after around 7 days curing. The immobilized chloride in the mortars with blended binder increases with the curing time, and the binder blended with cement and GGBS obtains the highest amount of bound chloride, which is around 50%, and attributed to the formation of Friedel's salt and hydrotalcite.

(4) The mortars with F-BAM as sand replacement show a similar chloride leaching profile and lower chloride leachability. The chloride leaching is stable after around 21 days curing. This can be the result of less chloride amount in F-BAM, and the later participation of chloride into the cement hydration. The Sb leachability is lower than that of F-BAM, which demonstrates the immobilization of Sb in mortar instead of dilution effect. The Cu leachability shows an increasing trend with curing age and exceeds the leachability of F-BAM after around 21 days. This is due to, firstly, the increasing pH of mortar which changes the stability of the Cu-bearing phases and secondly the dissolving of Cu-bearing phases, which is faster than the binding of cement hydrates, especially in later stages of cement hydration.

(5) When F-BAM is used to produce artificial aggregates with binders, the leachability of Sb and sulphate is lower than that of F-BAM indicating the binding effect from

cementitious materials than the dilution effect, while the ones of Cu, Mo and chloride are higher. The concretes containing artificial aggregates have lower Sb, Mo, chloride and sulphate leachability compared to the relevant artificial aggregates used which results from the immobilization of binders in concrete, while they have higher Cu leachability than the artificial aggregates.

(6) Regarding the cementitious immobilization of contaminants in MSWI fine bottom ash, the leachability of Sb, Mo and sulphate can be significantly decreased with 5-10% of binder content, while Cu leachability will increase with binder content or increasing pH. The chloride leachability can be slightly decreased by increasing binder amount. During the application life of MSWI fine bottom ash with cementitious binders, the hydration of binders with the ability to immobilize contaminants and the dissolving of metal-bearing phases in alkaline environment proceed simultaneously. Hence, the quantification of immobilization capacity of binders in the application process of MSWI bottom ash should consider both processes.

Chapter 10

10 Conclusions and recommendations

10.1 Conclusions

The Waste-to-Energy (WtE) technique is a relatively efficient way to manage the municipal solid waste, coupled with the generation of energy in the form of heat or electricity. However, there are combustion by-products generated at different points of the WtE procedure, which need to be further handled.

In the Netherlands, the WtE technique is well developed nowadays. The way to manage the combustion by-products is dominantly landfilling and application as road base. However, due to the potential risk of lack of land space and resource, as well as the sustainable circular economy development, the Dutch government is encouraging the alternative management of these solid by-products-maximizing their recycling and reuse and avoiding landfill. Therefore, a systematic investigation on the MSWI residues is in demand in the Netherlands.

As a combustion solid waste, the MSWI bottom ash is quite heterogenous and its properties varies depending on its source, combustion procedure, etc. Hence, this study starts with the evaluation of the stability of the MSWI bottom ashes from two WtE plants in the Netherlands. The analysis is based on the historical experimental data on the MSWI bottom ash properties over 7 years. Subsequently, the application potential of the MSWI bottom ash is evaluated based on its characteristics by using it in mortar and concrete and then comparing with normal ingredients of building materials.

The treatments on fine MSWI bottom ash are conducted with the purpose of improving its properties for better application in the construction field.

Finally, the integral recycling of MSWI bottom ash are proposed, combining the treatment and application purposes. Moreover, the final products containing MSWI bottom ash are assessed regarding their mechanical and environmental properties.

The main conclusions are further summarized in detail and shown below.

10.1.1 Stability of MSWI bottom ash properties

The properties of the MSWI bottom ashes provided by Attero in the Netherlands from two WtE plants (located in Moerdijk and Wijster) are evaluated by summarizing the historical experimental data.

The MSWI bottom ashes have a particle size under 31.5 mm, and the particle size distributions of these two bottom ashes are very similar to each other and relatively stable over time. Their water content varies between 12-23%, depending on the quenching

process and open-air storage. They have a rather high water absorption than recycled aggregates, and bottom ash from one of the WtE plants has a higher water absorption than the other. The losses on ignition (LOI) of the bottom ashes are stable over time as well, in the range of 2-5% wt. The metal content in bottom ash is quite stable over time and the bottom ash from Moerdijk plant contains higher ferrous metals and loose metallic iron than that from Wijster.

The leaching characteristics of the MSWI bottom ashes show that the leaching behaviour of the two bottom ashes are quite stable over time and the investigated bottom ashes can be classified as IMC materials according to the Dutch legislation, which means they can be used when an isolation layer and monitoring of the leaching behaviour during their service life will be performed. To be used as non-shaped materials (such as aggregates, etc.), the main leaching issue is the exceeding leaching concentration of antimony (Sb), copper (Cu), chloride and sulphate for both bottom ashes, even though they are produced in different plants and procedures.

10.1.2 Application potential of F-BA

The application potential of fine MSWI bottom ash fraction (F-BA, 0-2 mm) which contains higher amounts of contaminants and is more difficult to be cleaned or recycled using general industrial methodology and techniques, is investigated experimentally in this study.

The dominant chemical components in the whole bottom ash and their fractions are SiO_2, CaO, Al_2O_3, Fe_2O_3, etc. and the main crystalline phases are SiO_2, $CaCO_3$, Fe_2O_3, etc. Moreover, the finer bottom ash fraction has a higher amount of CaO and a lower content of SiO_2 than the coarser fractions. The fine MSWI bottom ash fraction (0-2 mm) has a similar particle size distribution as standard sand.

The chemical components of F-BA suggest the possibility for its re-use as raw material for cement clinker production. Three parameters used to evaluate the properties for clinker production, namely hydraulic ratio, silica ratio, alumina ratio and lime saturation factor are calculated based on the oxide compositions of F-BAs. The results show that the F-BAs are not preferable to be used for clinker production, but can be applied as correction materials in the raw mix design for clinker.

The use of F-BA in mortar as sand replacement results in the decrease of the flexural and compressive strengths, and the more F-BA is added in mortar, the lower the strengths will be. This can be due to the inclusion of metallic aluminum, which reacts with the alkalis provided by the binder hydration and then generates hydrogen.

The milled F-BAMs have a retarding influence on the cement hydration, and a much lower hydraulic reactivity. The sulphate content in the milled F-BAs may participate in the binder

hydration and leads to more ettringite generation. Hence, improvement of milled F-BAM properties is necessary to increase its contribution to the binder hydration.

10.1.3 Treatments on F-BA

Based on the characterization of MSWI bottom ash and the investigation of its application potential as F-BA, it is noticed that treatments to improve the reactivity and leaching properties of bottom ash are necessary.

In this study, a thermal treatment at different temperatures is applied on F-BAW or milled F-BAW (MF-BAW), accompanied by the reduction of particle size. The MF-BAW treated under 550 ˚C can decomposed the organic matter, subsequently reducing the retarding effect on binder hydration when the treated F-BAW is milled and then used as cement replacement. The comparison of thermal treatment before and after milling of F-BAW shows that the thermal treatment on the initial F-BAW is more effective than on the milled F-BAW. The thermally treated MF-BAW contributes to extra formation of AFt or AFm due to the participation of sulphate content in MF-BAW into cement hydration. The slow speed milling on the thermally treated F-BAW combined with sieving can separate the dust agglomerated on the surface of F-BAW particles. This dust is found to contain a relatively higher amount of heavy metals and salts than the cleaned particles. Moreover, after sieving, the fine dust contains a lower amount of metallic aluminium than the coarse cleaned particles. The dust removed from the thermally treated MF-BAW can be utilized as binder substitute in mortar and contributes to 15% of the compressive strength.

The thermal treatment reduces the leaching of Sb and Cu of MF-BAW, due to the decomposition of organic matter, while the chloride leaching is not significantly influenced. The leaching of the crushed mortars containing MF-BAW with and without thermal treatment can well comply with the limit value according to the Dutch legislation - Soil Quality Decree (SQD).

Washing treatment and size reduction of the F-BAM are also studied. The size reduction can reduce the leaching of most metals during the washing test with various liquid to solid (L/S) ratios, except Sb. For most investigated elements, the increase of L/S ratio results in an increasing leaching concentration, while the chloride leaching is not influenced due to the high solubility of chloride.

To investigate the immobilization capacity of chloride and heavy metals, blended binders are used. The study on the hydration of the blended binders with NaCl through isothermal calorimetric experiments shows that the hydration of binders is accelerated, especially for binders blended by Ordinary Portland cement and 40% ground granulated blast furnace slag (GGBS). The generation of Friedel’s salts and hydrotalcite is detected in the hydrated samples with NaCl.

10.1.4 Integral recycling of F-BA

The fine MSWI bottom ash is integrally recycled as a raw material together with the other industrial solid wastes to produce artificial aggregates applying the cold bonded pelletizing technique. This is a way to combine the treatment and application of the F-BAM instead of only focusing on the treatment of the F-BAM without considering its final application purpose.

The compatibility of the chosen industrial solid wastes and F-BAM in pelletization is experimentally studied, and a type of lightweight aggregates is obtained with a bulk density of around 980 g/cm^3, and a crushing resistance of around 7.5 MPa, which has comparable properties to artificial aggregates produced using similar methods.

To improve the properties of the artificial aggregates using F-BAM through pelletization, several methods are applied, namely increasing the binder content, using the F-BAM contribution and by reinforcement of polypropylene fibres (PPF).

The curing duration of the artificial aggregate did not influence its properties. It was found that the strength of the aggregates is mainly developed at early age (it can reach 70-85% of its 28-day strength). Increasing the binder content results in the increase of crushing strength of the aggregates, and the PPF can behave as reinforcement to benefit the aggregate strength. Meanwhile, the used of industrial wastes which have pozzolanic properties can be beneficial for the properties of the aggregates.

The environmental impact of the artificial aggregates evaluated using the column leaching tests shows that the Sb and sulphate leaching are well under the limit value of SQD, and the Cu, Mo and chloride leaching can be reduced by modifying the content of F-BAM used.

The study of concrete with three types of artificial aggregates shows that the use of the produced aggregates decreases the concrete strength due to their lower strength and the density of concrete decreases with the addition of artificial aggregates, and the compressive strength of the concrete has linear relation with its fresh density.

10.1.5 Contaminant leachability of F-BA regarding treatments and application

The leachability of Sb, Mo, Cu, chloride and sulphate, which are the contaminants in F-BA in this study according to Dutch legislation, is evaluated regarding the treatments (such as thermal and washing treatments) and the application methods (such as binder and sand replacement, for artificial aggregate production and use of artificial aggregates in concrete).

The thermal treatment on F-BA results in significant decrease of Sb and Cu leachability, while the Mo leachability is increased around 2 times. The application of treated F-BA in mortars as binder replacement shows that the Sb and sulphate leachability is decreased by more than 80%, and the Mo and chloride leachability is related to the binder hydration significantly. After application of treated F-BA in mortar, the Sb, Cu and sulphate leaching was reduced due to the binding effect of binders instead of dilution effect.

Dynamic washing by shaking on F-BA and milled F-BA shows that the leachability of the investigated components during column leaching is lower than shaking leaching. The leachability of investigated contaminants, except chloride, is directly related to the L/S ratio used during the shaking test. After milling, the MF-BA shows lower leachability than that of F-BA, except for Sb.

The addition of NaCl in mortars with blended binders shows a decreasing amount of chloride leaching, while the immobilized chloride in mortar increases with the curing age. The mortars with blended cement and GGBS achieve the highest bound chloride, while the mortars with cement and cement blended with FA have similar amounts of bound chloride. The higher amount of bound chloride can be attributed to the formation of Friedel's salt and hydrotalcite.

The mortar with F-BA as sand replacement shows a lower leachability of chloride, sulphate and Sb compared with F-BA indicating the immobilization effect of binders rather than dilution effect. However, the Cu leachability increases with the curing time and then exceeds that of F-BA after around 21 days curing.

The leachability of investigated components in artificial aggregates produced from F-BA is higher than that of F-BA, except Sb and sulphate; while when the artificial aggregates are used in concrete, the leachability of contaminants in concretes is lower than the artificial aggregates, except for Cu. This demonstrates the excellent binding effect of cementitious materials on Sb and sulphate, while for Cu, Mo and chloride, higher amount of binders may be necessary. The diffusion test on concrete incorporating artificial aggregates shows that the chloride leaching is diffusion controlled while the leaching of Cu, Sb, Mo and sulphate are more depletion influenced. However, their leaching concentrations are all under the limit value for shaped materials specified in the SQD.

To be summarized, the leachability of Sb, Mo, and sulphate can be reduced significantly with the use of cementitious binders, while Cu shows an increasing leachability with the use of binder. The immobilization of contaminants in F-BA during its application by cementitious binder is accompanied by the dissolving of metal-bearing phases in the alkaline environment provided by the binder hydration.

10.2 Recommendations for future research

This thesis addresses the systematic study on the municipal solid waste incineration (MSWI) bottom ashes from two Dutch Waste-to-Energy (WtE) plants, including characterization, treatments, integral recycling and application as building materials. The obtained results can provide information and guidance for the management of MSWI residues, however, further research is still in demand for the remaining issues, which are listed as follows:

(1) In this study, the thermal treatment combined with low speed milling can reduce the negative influence of bottom ash on cement hydration and remove the metallic

aluminium. The removal of metallic aluminium from fine bottom ash by changing the shape of metals due to their good ductility is supposed to be realized by impact milling methods. However, the efficiency of metal recycling on fine MSWI bottom ash and the application of the treated fine bottom ash by impact milling need to be further studied. Furthermore, to reduce the leaching of the fine MSWI bottom ash, avoiding the fine dust layer accumulated on the surface of bottom ash particles can be a promising way, and methods to realize it need to be further investigated, such as dry cooling of fresh MSWI bottom ash.

(2) The leaching behaviour study on MSWI fine bottom ash related to the reduction of particle size by milling shows the different leaching profiles before and after milling; the relations between the particle size and the leaching parameters need to be observed, and can be used as indicating information for the milled fine bottom ash by impact milling methods as mentioned above. The immobilization of heavy metals and salts in fine MSWI bottom ash by blended binders, before and after its reduction of particle size, regarding different application methods also needs further research to figure out the optimized immobilizing mixtures for the fine MSWI bottom ash when it is used in powder or particle shape.

(3) The integral recycling of industrial solid wastes based on their inherent properties and the final products can be extended to more formats, such as pavement blocks, partition wall, isolation element, etc.

(4) The production of artificial lightweight aggregates using the cold bonded pelletizing technique can be further improved, including the combination of other new solid wastes, such as incinerated sewage sludge ash, etc., further improving the artificial aggregate properties according to their application requirements. Additionally, the comparison of artificial aggregates with commercial lightweight aggregates produced mostly under high temperature available at the market should be performed to assess their economic and environmental profit.

(5) The artificial aggregates produced in this study were applied in concrete as normal aggregates replacement, it is recommended to apply CBLA in lightweight concretes. Therefore, it is necessary to study the application behaviour of these artificial aggregates in lightweight aggregate (LWA) concrete and evaluate their influence on the properties of the LWA concrete. Meanwhile, the correlation between the LWA concrete properties and the artificial aggregates characteristics should be figured out to provide guidance for further application in practice.

(6) The leachability of contaminants in MSWI bottom ash during its application life with the use of cementitious binders should be investigated regarding the dissolving of metal-bearing phases. A study on the immobilization of contaminants can be performed to evaluate the binder immobilization capacity during the application of solid wastes.

(7) In this study, treatments and applications of fine MSWI bottom ash are presented. However, the possibility to realize them with acceptable profit in practice or industrial scale need to be analysed. The life cycle analysis (LCA) is essential for the evaluation of the systematic treatment and application of fine bottom ash based on its final utilization purpose. Furthermore, the LCA can be used to optimize the management of fine MSWI bottom ash, which can maximize its recycling.

(8) The study presented in this thesis is conducted on lab scale and the obtained results are not transferred and checked in real scale application. Hence, large scale tests of the treatments, production of lightweight aggregates, etc. can be executed, which can be applied to further develop the sustainable management of MSWI bottom ash.

Bibliography

Abd Kadir, S.A.S., Yin, C.-Y., Rosli Sulaiman, M., Chen, X., & El-Harbawi, M. (2013). Incineration of municipal solid waste in Malaysia: Salient issues, policies and waste-to-energy initiatives. Renew. Sustain. Energy Rev. 24, 181–186.

Al-Rawas, A.A., Wahid Hago, A., Taha, R., & Al-Kharousi, K. (2005). Use of incinerator ash as a replacement for cement and sand in cement mortars. Build. Environ. 40, 1261–1266.

Alam, Q., Florea, M.V.A., Schollbach, K., & Brouwers, H.J.H. (2017). A two-stage treatment for Municipal Solid Waste Incineration (MSWI) bottom ash to remove agglomerated fine particles and leachable contaminants. Waste Manag. 67, 181-192.

Alkaysi, M., El-Tawil, S., Liu, Z., & Hansen, W. (2016). Effects of silica powder and cement type on durability of ultra high performance concrete (UHPC). Cem. Concr. Compos. 66, 47–56.

Allegrini, E., Maresca, A., Olsson, M.E., Holtze, M.S., Boldrin, A., & Astrup, T.F. (2014). Quantification of the resource recovery potential of municipal solid waste incineration bottom ashes. Waste Manag. 34, 1627–1636.

Alonso, M.C., Luco, L.F., García, J.L., Hidalgo, A., & Huertas, F. (2007). Low-pH Cementitious Materials Design and Characterisation. 12th Int. Congr. Chem. Cem. Canada.

Amutha Rani, D., Boccaccini, A.R., Deegan, D., & Cheeseman, C.R. (2008). Air pollution control residues from waste incineration: Current UK situation and assessment of alternative technologies. Waste Manag. 28, 2279–2292.

Anastasiou, E., Georgiadis Filikas, K., & Stefanidou, M. (2014). Utilization of fine recycled aggregates in concrete with fly ash and steel slag. Constr. Build. Mater. 50, 154–161.

Antoni, M., Rossen, J., Martirena, F., & Scrivener, K. (2012). Cement substitution by a combination of metakaolin and limestone. Cem. Concr. Res. 42, 1579–1589.

Arickx, S., Van Gerven, T., & Vandecasteele, C. (2006). Accelerated carbonation for treatment of MSWI bottom ash. J. Hazard. Mater. 137, 235–243.

Arickx, S., Van Gerven, T., Knaepkens, T., Hindrix, K., Evens, R., & Vandecasteele, C. (2007). Influence of treatment techniques on Cu leaching and different organic fractions in MSWI bottom ash leachate. Waste Manag. 27, 1422–1427.

Arickx, S., Van Gerven, T., Boydens, E., L'hoëst, P., Blanpain, B., & Vandecasteele, C. (2008). Speciation of Cu in MSWI bottom ash and its relation to Cu leaching. Appl. Geochemistry 23, 3642–3650.

Arickx, S., De Borger, V., Van Gerven, T., & Vandecasteele, C. (2010). Effect of carbonation on the leaching of organic carbon and of copper from MSWI bottom ash. Waste Manag. 30, 1296–1302.

Attero, b.v., (2015). Private communication from Attero b.v.

Baciocchi, R., Costa, G., Lategano, E., Marini, C., Polettini, A., Pomi, R., Postorino, P., & Rocca, S. (2010). Accelerated carbonation of different size fractions of bottom ash from RDF incineration. Waste Manag. 30, 1310–1317.

Batchelor, B. (2006). Overview of waste stabilization with cement. Waste Manag. 26, 689–698.

Baur, I., Keller, P., Mavrocordatos, D., Wehrli, B., & Johnson, C.A. (2004). Dissolution-precipitation behaviour of ettringite, monosulfate, and calcium silicate hydrate. Cem. Concr. Res. 34, 341–348.

Baykal, G., & Döven, A.G (2000). Utilization of fly ash by pelletization process ; theory, application areas and research results. Resour. Conserv. Recycl. 30, 59–77.

Bayuseno, A.P., & Schmahl, W.W. (2010). Understanding the chemical and mineralogical properties of the inorganic portion of MSWI bottom ash. Waste Manag. 30, 1509–1520.

Bentz, D.P., Hansen, A.S., & Guynn, J.M. (2011). Optimization of cement and fly ash particle sizes to produce sustainable concretes. Cem. Concr. Compos. 33, 824–831.

Bernhardt, M., Tellesbø, H., Justnes, H., & Wiik, K. (2013). Mechanical properties of lightweight aggregates. J. Eur. Ceram. Soc. 33, 2731–2743.

Bernhardt, M., Tellesbø, H., Justnes, H., & Wiik, K. (2014). Fibre reinforced lightweight aggregates. J. Eur. Ceram. Soc. 34, 1341–1351.

Berryman, C., Zhu, J., Jensen, W., & Tadros, M. (2005). High-percentage replacement of cement with fly ash for reinforced concrete pipe. Cem. Concr. Res. 35, 1088–1091.

Biganzoli, L., & Grosso, M. (2013). Alumninium recovery from waste incineration bottom ash and its oxidation level. Waste Manag. Res. 31, 954-959.

Biganzoli, L., Gorla, L., Nessi, S., & Grosso, M. (2012). Volatilisation and oxidation of aluminium scraps fed into incineration furnaces. Waste Manag. 32, 2266–2272.

Biganzoli, L., Ilyas, A., Praagh, M.V., Persson, K.M., & Grosso, M. (2013). Aluminium recovery vs. hydrogen production as resource recovery options for fine MSWI bottom ash fraction. Waste Manag. 33, 1174–1181.

Biganzoli, L., Grosso, M., & Forte, F. (2014). Aluminium Mass Balance in Waste Incineration and Recovery Potential From the Bottom Ash: A Case Study. Waste and Biomass Valor. 5, 139-145.

Bin Mohd Sani, M.S.H., Bt Muftah, F., & Ab Rahman, M. (2011). Properties of Waste Paper Sludge Ash (WPSA) as cement replacement in mortar to support green technology material. 3rd ISESEE -Int. Symp. Exhib. Sustain. Energy Environ., 94-99.

Bonakdar, A., Babbitt, F., & Mobasher, B. (2013). Physical and mechanical characterization of Fiber-Reinforced Aerated Concrete (FRAC). Cem. Concr. Compos. 38, 82–91.

Born, J.G.P., & Veelenturf, R.A.L. (1997). MSWI residues in the Netherlands putting policy into practice. Studies in Environment Science 71, 841-850.

Bosmans, A., Vanderreydt, I., Geysen, D., & Helsen, L. (2013). The crucial role of Waste-to-Energy technologies in enhanced landfill mining: a technology review. J. Clean. Prod. 55, 10–23.

Brunner, P.H., & Rechberger, H. (2015). Waste to energy - key element for sustainable waste management. Waste Manag. 37, 3–12.

Bui, L.A., Hwang, C., Chen, C., Lin, K., & Hsieh, M. (2012). Manufacture and performance of cold bonded lightweight aggregate using alkaline activators for high performance concrete. Constr. Build. Mater. 35, 1056–1062.

Bullard, J.W., Jennings, H.M., Livingston, R.A., Nonat, A., Scherer, G.W., Schweitzer, J.S., Scrivener, K.L., & Thomas, J.J. (2011). Mechanisms of cement hydration. Cem. Concr. Res. 41, 1208–1223.

Byfors, K. (1987). Influence of silica fume and flyash on chloride diffusion and pH values in cement paste. Cem. Concr. Res. 17, 115–130.

Calder, G.V., & Stark, T.D. (2010). Aluminum Reactions and Problems in Municipal Solid Waste Landfills. Practice Periodical of Harzardous, Toxic, and Ratioactive Waste Manag. 14, 258-265.

Chen, C.H., & Chiou, I.J. (2007). Distribution of chloride ion in MSWI bottom ash and de-chlorination performance. J. Hazard. Mater. 148, 346–352.

Chen, H., & Wang, Q. (2006). The behaviour of organic matter in the process of soft soil stabilization using cement. Bull. Eng. Geol. Env. 65, 445–448.

Chen, M.Z., Lin, J.T., Wu, S.P., & Liu, C.H. (2011). Utilization of recycled brick powder as alternative filler in asphalt mixture. Constr. Build. Mater. 25, 1532–1536.

Chen, Q.Y., Hills, C.D., Tyrer, M., Slipper, I., Shen, H.G., & Brough, A. (2007). Characterisation of products of tricalcium silicate hydration in the presence of heavy metals. J. Hazard. Mater. 147, 817–825.

Cheng, A. (2012). Effect of incinerator bottom ash properties on mechanical and pore size of blended cement mortars. Mater. Des. 36, 859–864.

Chimenos, J.M., Segarra, M., Fernández, M.A., & Espiell, F. (1999). Characterization of the bottom ash in municipal solid waste incinerator. J. Hazard. Mater. 64, 211–222.

Chimenos, J.M., Fernández, A.I., Nadal, R., & Espiell, F. (2000). Short-term natural weathering of MSWI bottom ash. J. Hazard. Mater. 79, 287–299.

Chimenos, J.M., Fernández, A.I., Miralles, L., Segarra, M., & Espiell, F. (2003). Short-term natural weathering of MSWI bottom ash as a function of particle size. Waste Manag. 23, 887–895.

Cimpan, C., & Wenzel, H. (2013). Energy implications of mechanical and mechanical-biological treatment compared to direct waste-to-energy. Waste Manag. 33, 1648–1658.

Cioffi, R., Colangelo, F., Montagnaro, F., & Santoro, L. (2011). Manufacture of artificial aggregate using MSWI bottom ash. Waste Manag. 31, 281–288.

Colangelo, F., Messina, F., & Cioffi, R. (2015). Recycling of MSWI fly ash by means of cementitious double step cold bonding pelletization: Technological assessment for the production of lightweight artificial aggregates. J. Hazard. Mater. 299, 181–191.

Cornelis, G., Van Gerven, T., & Vandecasteele, C. (2006). Antimony leaching from uncarbonated and carbonated MSWI bottom ash. J. Hazard. Mater. 137, 1284–1292.

Cornelis, G., Van Gerven, T., & Vandecasteele, C. (2012). Antimony leaching from MSWI bottom ash: modelling of the effect of pH and carbonation. Waste Manag. 32, 278–286.

Cossu, R., Lai, T., & Pivnenko, K. (2012). Waste washing pre-treatment of municipal and special waste. J. Hazard. Mater. 207–208, 65–72.

Crannell, B.S., Eighmy, T.T., Krzanowski, J.E., Eusden, J.D., Shaw, E.L., & Francis, C.A. (2000). Heavy metal stabilization in municipal solid waste combustion bottom ash using soluble phosphate. Waste Manag. 20, 135–148.

Dabo, D., Badreddine, R., De Windt, L., & Drouadaine, I. (2009). Ten-year chemical evolution of leachate and municipal solid waste incineration bottom ash used in a test road site. J. Hazard. Mater. 172, 904–913.

Del Valle-Zermeño, R., Formosa, J., Chimenos, J.M., Martínez, M., & Fernández, A.I. (2013). Aggregate material formulated with MSWI bottom ash and APC fly ash for use as secondary building material. Waste Manag. 33, 621–627.

De Vries, W., Rem, P., & Berkhout, P. (2009). ADR : A New Method For Dry Classification. Preoceeding of the ISWA Internation Conference. 12, 103-113.

De Weerdt, K., Ben Haha, M., Le Saout, G., Kjellsen, K.O., Justnes, H., & Lothenbach, B. (2011). Hydration mechanisms of ternary Portland cements containing limestone powder and fly ash. Cem. Concr. Res. 41, 279–291.

Deschner, F., Lothenbach, B., Winnefeld, F., & Neubauer, J. (2013). Effect of temperature on the hydration of Portland cement blended with siliceous fly ash. Cem. Concr. Res. 52, 169–181.

Dijkstra, J.J., Van Der Sloot, H.A., & Comans, R.N.J. (2006). The leaching of major and trace elements from MSWI bottom ash as a function of pH and time. Appl. Geochemistry 21, 335–351.

Dutta, D.K., Bordoloi, D., Gupta, S., Borthakur, P.C., Srinivasan, T.M., & J.B. Patil (1992). Investigation on cold bonded pelletization of iron ore fines using Indian slag-cement. Int. J. Miner. Process. 34, 149–159.

Dutta, D.K., Bordoloi, D., & Borthakur, P.C. (1997). Investigation on reduction of cement binder in cold bonded pelletization of iron ore fines. Int. J. Miner. Process. 49, 97–105.

EBA (2017). European Biogas Association. http://european-biogas.eu/

Ecke, H., Sakanakura, H., Matsuto, T., Tanaka, N., & Lagerkvist, A. (2000). State-of-the-art treatment processes for municipal solid waste incineration residues in Japan. Waste Manag. Res. 18, 41–51.

EPA (2017). United States Environmental Protection Agency-Environmental Topics.

EEA (2013). European Environment Agency-Managing municipal solid waste - a review of achievements in 32 European counties.

EN 196-1, (2005). Methods of testing cement - Part 1: Determination of strength.

EN 206-1, (2000). Concrete - Part 1: Specification, performance, production and conformity.

EN 206-9, (2007). Concrete Part 9: Additional rules for self-compacting concrete (SCC).

EN 933-1, (1997). Tests for geometrical properties of aggregates - Part 1: Determination of particle size distribution- Sieving method.

EN 1015-3, (2007). Methods of test for mortar for masonry - Part 3: Determination of consistence of fresh mortar (by flow table).

EN 1097-3, (1998). Test for mechanical and physical properties of aggregates - Part 3: Determination of loose bulk density and voids.

EN 1097-5, (1999). Tests for mechanical and physcial properties of aggregates - Part 5: Determination of the water content by drying in a ventilated oven.

EN 1097-6, (2013). Tests for mechanical and physical properties of aggregates - Part 6: Determination of particle density and water absorption.

EN 12390-4, (2000). Testing hardened concrete - Part 4: Compressive strength-Specification for testing machines.

EN 12390-5, (2009). Testing hardened concrete - Part 5: Flexural strength of test specimens.

EN 12350-6, (2009). Testing fresh concrete - Part 6: Density.

EN 12350-8, (2010). Testing fresh concrete - Part 8: Self-compacting concrete-Slump-flow test.

EN 12350-9, (2010). Testing fresh concrete - Part 9: Self-compacting concrete – V-funnel test.

EN 12390-8, (2009). Testing hardened concrete - Part 8: Depth of penetration of water under pressure.

EN 12620, (2002). Aggregates for concrete.

EN 13055-1, (2002). Lightweight aggregates - Part 1: Lightweight aggregates for concrete, mortar and grout.

Eurostat, (2017). Statistical office of the European Union Situated in Luxembourg (statistic on Municipal waste statistics in Europe checked in 2017)

Ferone, C., Colangelo, F., Messina, F., Iucolano, F., Liguori, B., & Cioffi, R. (2013). Coal combustion wastes reuse in low energy artificial aggregates manufacturing.

Materials. 6, 5000–5015.

Ferrándiz-Mas, V., Bond, T., García-Alcocel, E., & Cheeseman, C.R. (2014). Lightweight mortars containing expanded polystyrene and paper sludge ash. Constr. Build. Mater. 61, 285–292.

Ferraris, M., Salvo, M., Ventrella, A., Buzzi, L., & Veglia, M. (2009). Use of vitrified MSWI bottom ashes for concrete production. Waste Manag. 29, 1041–1047.

Filipponi, P., Polettini, A., Pomi, R., & Sirini, P. (2003). Physical and mechanical properties of cement-based products containing incineration bottom ash. Waste Manag. 23, 145–156.

Fléhoc, C., Girard, J.-P., Piantone, P., & Bodénan, F. (2006). Stable isotope evidence for the atmospheric origin of CO2 involved in carbonation of MSWI bottom ash. Appl. Geochemistry 21, 2037–2048.

Florea, M.V.A., Ning, Z., & Brouwers, H.J.H. (2014). Activation of liberated concrete fines and their application in mortars. Constr. Build. Mater. 50, 1–12.

Forteza, R., Far, M., Seguí, C., & Cerdá, V. (2004). Characterization of bottom ash in municipal solid waste incinerators for its use in road base. Waste Manag. 24, 899–909.

Freyssinet, P., Piantone, P., Azaroual, M., Itard, Y., Clozel-Leloup, B., Guyonnet, D., & Baubron, J.C. (2002). Chemical changes and leachate mass balance of municipal solid waste bottom ash submitted to weathering. Waste Manag. 22, 159–172.

Gabrovšek, R., Vuk, T., & Kaučič, V. (2006). Evaluation of the hydration of Portland cement containing various carbonates by means of thermal analysis. Acta Chim. Slov. 53, 159–165.

Gao, X., Yu, Q.L., & Brouwers, H.J.H. (2015). Properties of alkali activated slag–fly ash blends with limestone addition. Cem. Concr. Compos. 59, 119–128.

García, D., Vegas, I., & Cacho, I. (2014). Mechanical recycling of GFRP waste as short-fiber reinforcements in microconcrete. Constr. Build. Mater. 64, 293–300.

Garcia-Lodeiro, I., Carcelen-Taboada, V., Fernández-Jiménez, A., & Palomo, A. (2016). Manufacture of hybrid cements with fly ash and bottom ash from a municipal solid waste incinerator. Constr. Build. Mater. 105, 218–226.

Geetha, S., & Ramamurthy, K. (2010a). Environmental friendly technology of cold-bonded bottom ash aggregate manufacture through chemical activation. J. Clean. Prod. 18, 1563–1569.

Geetha, S., & Ramamurthy, K. (2010b). Reuse potential of low-calcium bottom ash as aggregate through pelletization. Waste Manag. 30, 1528–1535.

Geetha, S., & Ramamurthy, K. (2013). Properties of geopolymerised low-calcium bottom ash aggregate cured at ambient temperature. Cem. Concr. Compos. 43, 20–30.

Gesoglu, M., Güneyisi, E., Ozturan, T., Oz, H.O., & Asaad, D.S. (2015). Shear thickening intensity of self-compacting concretes containing rounded lightweight aggregates.

Constr. Build. Mater. 79, 40–47.

Gesoğlu, M., Özturan, T., & Güneyisi, E. (2004). Shrinkage cracking of lightweight concrete made with cold-bonded fly ash aggregates. Cem. Concr. Res. 34, 1121–1130.

Gesoğlu, M., Özturan, T., & Güneyisi, E. (2006). Effects of cold-bonded fly ash aggregate properties on the shrinkage cracking of lightweight concretes. Cem. Concr. Compos. 28, 598–605.

Gesoğlu, M., Özturan, T., & Güneyisi, E. (2007). Effects of fly ash properties on characteristics of cold-bonded fly ash lightweight aggregates. Constr. Build. Mater. 21, 1869–1878.

Gesoğlu, M., Güneyisi, E., Mahmood, S.F., Öz, H.Ö., & Mermerdaş, K. (2012). Recycling ground granulated blast furnace slag as cold bonded artificial aggregate partially used in self-compacting concrete. J. Hazard. Mater. 235–236, 352–358.

Gesoğlu, M., Güneyisi, E., Alzeebaree, R., & Mermerdaş, K. (2013). Effect of silica fume and steel fiber on the mechanical properties of the concretes produced with cold bonded fly ash aggregates. Constr. Build. Mater. 40, 982–990.

Gesoğlu, M., Güneyisi, E., Özturan, T., Öz, H.Ö., & Asaad, D.S. (2014). Self-consolidating characteristics of concrete composites including rounded fine and coarse fly ash lightweight aggregates. Compos. Part B Eng. 60, 757–763.

Gesoğlu, M., Güneyisi, E., Mahmood, S.F., öz, H. öznur, & Mermerdaş, K. (2012). Recycling ground granulated blast furnace slag as cold bonded artificial aggregate partially used in self-compacting concrete. J. Hazard. Mater. 235–236, 352–358.

Gesoğlu, M., Güneyisi, E., Ali, B., & Mermerdaş, K. (2013). Strength and transport properties of steam cured and water cured lightweight aggregate concretes. Constr. Build. Mater. 49, 417–424.

Ginés, O., Chimenos, J.M., Vizcarro, A., Formosa, J., & Rosell, J.R. (2009). Combined use of MSWI bottom ash and fly ash as aggregate in concrete formulation: Environmental and mechanical considerations. J. Hazard. Mater. 169, 643–650.

Gineys, N., Aouad, G., & Damidot, D. (2010). Managing trace elements in Portland cement – Part I: Interactions between cement paste and heavy metals added during mixing as soluble salts. Cem. Concr. Compos. 32, 563–570.

Gomathi, P., & Sivakumar, A. (2015). Accelerated curing effects on the mechanical performance of cold bonded and sintered fly ash aggregate concrete. Constr. Build. Mater. 77, 276–287.

González-Corrochano, B., Alonso-Azcárate, J., & Rodas, M. (2009). Characterization of lightweight aggregates manufactured from washing aggregate sludge and fly ash. Resour. Conserv. Recycl. 53, 571–581.

GovHK (2015). The Government of the Hong Kong Special Administative Region-Waste & Recycling - Municipal Solid Waste.

Greendeals GD 076, (2010). Sustainable useful application of WtE bottom ash, Dutch

ministry of Infrastructure and Environment.

Grosso, M., Biganzoli, L., & Rigamonti, L. (2011). A quantitative estimate of potential aluminium recovery from incineration bottom ashes. Resour. Conserv. Recycl. 55, 1178–1184.

Guimaraes, A.L., Okuda, T., Nishijima, W., & Okada, M. (2005). Chemical extraction of organic carbon to reduce the leaching potential risk from MSWI bottom ash. J. Hazard. Mater. 125, 141–146.

Guimaraes, A.L., Okuda, T., Nishijima, W., & Okada, M. (2006). Organic carbon leaching behavior from incinerator bottom ash. J. Hazard. Mater. 137, 1096–1101.

Gundupalli, S.P., Hait, S., & Thakur, A. (2017). A review on automated sorting of source-separated municipal solid waste for recycling. Waste Manag. 60, 56–74.

Güneyisi, E., Gesoğlu, M., & İpek, S. (2013a). Effect of steel fiber addition and aspect ratio on bond strength of cold-bonded fly ash lightweight aggregate concretes. Constr. Build. Mater. 47, 358–365.

Güneyisi, E., Gesoğlu, M., Pürsünlü, Ö., & Mermerdaş, K. (2013b). Durability aspect of concretes composed of cold bonded and sintered fly ash lightweight aggregates. Compos. Part B Eng. 53, 258–266.

Güneyisi, E., Gesoğlu, M., Altan, İ., & Öz, H.Ö. (2015a). Utilization of cold bonded fly ash lightweight fine aggregates as a partial substitution of natural fine aggregate in self-compacting mortars. Constr. Build. Mater. 74, 9–16.

Güneyisi, E., Gesoğlu, M., & Booya, E. (2015b). Strength and permeability properties of self-compacting concrete with cold bonded fly ash lightweight aggregate. Constr. Build. Mater. 74, 17–24.

Harikrishnan, K.I., & Ramamurthy, K. (2006). Influence of pelletization process on the properties of fly ash aggregates. Waste Manag. 26, 846–852.

Hashem, F.S., Amin, M.S., & Hekal, E.E. (2011). Stabilization of Cu (II) wastes by C_3S hydrated matrix. Constr. Build. Mater. 25, 3278–3282.

He, R., Wei, X.-M., Tian, B.-H., Su, Y., & Lu, Y.-L. (2015). Characterization of a joint recirculation of concentrated leachate and leachate to landfills with a microaerobic bioreactor for leachate treatment. Waste Manag. 46, 380–388.

Hendrik G. van Oss (2015). Cement - Mineral Commodity Summaries. U.S. Geol. Surv. 703, 648-7712.

Hjelmar, O., Holm, J., & Crillesen, K. (2007). Utilisation of MSWI bottom ash as sub-base in road construction: first results from a large-scale test site. J. Hazard. Mater. 139, 471–480.

Holm, O., & Simon, F.G. (2016). Innovative treatment trains of bottom ash (BA) from municipal solid waste incineration (MSWI) in Germany. Waste Manag. 59, 229–236.

Hu, Y., Bakker, M.C.M., & De Heij, P.G. (2011). Recovery and distribution of incinerated

aluminum packaging waste. Waste Manag. 31, 2422–2430.

Hüsken, G. (2010). A multifunctional design approach for sustainable concrete: with application to concrete mass products, PhD Thesis. Eindhoven University of Technology, Eindhoven, The Netherlands.

Hyks, J., Nesterov, I., Mogensen, E., Jensen, P.A., & Astrup, T. (2011). Leaching from waste incineration bottom ashes treated in a rotary kiln. Waste Manag. Res. 29, 995–1007.

Izquierdo, M., Querol, X., Josa, A., Vazquez, E., & López-Soler, A. (2008). Comparison between laboratory and field leachability of MSWI bottom ash as a road material. Sci. Total Environ. 389, 10–19.

Jamkar, S.S., & Rao, C.B.K. (2004). Index of Aggregate Particle Shape and Texture of coarse aggregate as a parameter for concrete mix proportioning. Cem. Concr. Res. 34, 2021–2027.

Jansen, D., Goetz-Neunhoeffer, F., Lothenbach, B., & Neubauer, J. (2012). The early hydration of Ordinary Portland Cement (OPC): An approach comparing measured heat flow with calculated heat flow from QXRD. Cem. Concr. Res. 42, 134–138.

Juric, B., Hanzic, L., Ilić, R., & Samec, N. (2006). Utilization of municipal solid waste bottom ash and recycled aggregate in concrete. Waste Manag. 26, 1436–1442.

Justnes, H. (1998). A review of chloride binding in cementitious systems. Nord. Concr. Res. 21, 48-63

Karanjekar, R.V., Bhatt, A., Altouqui, S., Jangikhatoonabad, N., Durai, V., Sattler, M.L., Hossain, M.D.S., & Chen, V. (2015). Estimating methane emissions from landfills based on rainfall, ambient temperature, and waste composition: The CLEEN model. Waste Manag. 46, 389–398.

Kaya, M. (2016). Recovery of metals and nonmetals from electronic waste by physical and chemical recycling processes. Waste Manag. 57, 64–90.

Kayali, O., Khan, M.S.H., & Sharfuddin Ahmed, M. (2012). The role of hydrotalcite in chloride binding and corrosion protection in concretes with ground granulated blast furnace slag. Cem. Concr. Compos. 34, 936–945.

Keulen, A., Van Zomeren, A., Harpe, P., Aarnink, W., Simons, H.A.E., & Brouwers, H.J.H. (2015). High performance of treated and washed MSWI bottom ash granulates as natural aggregate replacement within earth-moist concrete. Waste Manag. 49, 83–95.

Kim, H.K., Ha, K.A., & Lee, H.K. (2016). Internal-curing efficiency of cold-bonded coal bottom ash aggregate for high-strength mortar. Constr. Build. Mater. 126, 1–8.

Klein, R., Baumann, T., Kahapka, E., & Niessner, R. (2001). Temperature development in a modern municipal solid waste incineration (MSWI) bottom ash landfill with regard to sustainable waste management. J. Hazard. Mater. 83, 265–280.

Kou, S.C., & Poon, C.S. (2012). Enhancing the durability properties of concrete prepared with coarse recycled aggregate. Constr. Build. Mater. 35, 69–76.

Kou, S.C., Poon, C.-S., & Etxeberria, M. (2011). Influence of recycled aggregates on long term mechanical properties and pore size distribution of concrete. Cem. Concr. Compos. 33, 286–291.

Kowalski, P.R., Kasina, M., & Michalik, M. (2016). Metallic Elements Fractionation in Municipal Solid Waste Incineration Residues. Energy Procedia 97, 31–36.

Kuo, N.-W., Ma, H.-W., Yang, Y.-M., Hsiao, T.-Y., & Huang, C.-M. (2007). An investigation on the potential of metal recovery from the municipal waste incinerator in Taiwan. Waste Manag. 27, 1673–1679.

Kuo, W.-T., Liu, C.-C., & Su, D.-S. (2013). Use of washed municipal solid waste incinerator bottom ash in pervious concrete. Cem. Concr. Compos. 37, 328–335.

Laforest, G., & Duchesne, J. (2005). Immobilization of chromium (VI) evaluated by binding isotherms for ground granulated blast furnace slag and ordinary Portland cement. Cem. Concr. Res. 35, 2322–2332.

Lam, C.H.K., Ip, A.W.M., Barford, J.P., & McKay, G. (2010). Use of incineration MSW ash: A review. Sustainability 2, 1943–1968.

Lampris, C., Stegemann, J.A., Pellizon-Birelli, M., Fowler, G.D., & Cheeseman, C.R. (2011). Metal leaching from monolithic stabilised/solidified air pollution control residues. J. Hazard. Mater. 185, 1115–1123.

Lázaro García, A. (2014). Nano-silica production at low temperatures from the dissolution of olivine, PhD Thesis. Eindhoven University of Technology, Eindhoven, the Netherlands.

Leckner, B. (2015). Process aspects in combustion and gasification Waste-to-Energy (WtE) units. Waste Manag. 37, 13-25

Lee, H.K., Kim, H.K., & Hwang, E.A (2010). Utilization of power plant bottom ash as aggregates in fiber-reinforced cellular concrete. Waste Manag. 30, 274–284.

Lee, T.-C., Chang, C.-J., Rao, M.-K., & Su, X.-W. (2011). Modified MSWI ash-mix slag for use in cement concrete. Constr. Build. Mater. 25, 1513–1520.

Li, M., Xiang, J., Hu, S., Sun, L.-S., Su, S., Li, P.-S., & Sun, X.-X. (2004). Characterization of solid residues from municipal solid waste incinerator. Fuel 83, 1397–1405.

Li, X., Chen, Q., Zhou, Y., Tyrer, M., & Yu, Y. (2014). Stabilization of heavy metals in MSWI fly ash using silica fume. Waste Manag. 34, 2494–2504.

Li, X.-G., Lv, Y., Ma, B.-G., Chen, Q.-B., Yin, X.-B., & Jian, S.-W. (2012). Utilization of municipal solid waste incineration bottom ash in blended cement. J. Clean. Prod. 32, 96–100.

Li, X.D., Poon, C.S., Sun, H., Lo, I.M.C., & Kirk, D.W. (2001). Heavy metal speciation and leaching behaviors in cement based solidified/stabilized waste materials. J. Hazard. Mater. 82, 215–230.

Li, Y., Zhao, X., Li, Y., & Li, X. (2015). Waste incineration industry and development policies in China. Waste Manag. 46, 234–241.

Lin, K.L., & Lin, D.F. (2006). Hydration characteristics of municipal solid waste incinerator bottom ash slag as a pozzolanic material for use in cement. Cem. Concr. Compos. 28, 817–823.

Lin, W.Y., Heng, K.S., Sun, X., & Wang, J.-Y. (2015). Influence of moisture content and temperature on degree of carbonation and the effect on Cu and Cr leaching from incineration bottom ash. Waste Manag. 43, 264–272.

Lin, Y.-C., Panchangam, S.C., Wu, C.-H., Hong, P.-K.A., & Lin, C.-F. (2011). Effects of water washing on removing organic residues in bottom ashes of municipal solid waste incinerators. Chemosphere 82, 502–506.

Liu, A., Ren, F., Lin, W.Y., & Wang, J.-Y. (2015). A review of municipal solid waste environmental standards with a focus on incinerator residues. Int. J. Sustain. Built Environ. 4, 165–188.

Liu, Y., Li, Y., Li, X., & Jiang, Y. (2008). Leaching behavior of heavy metals and PAHs from MSWI bottom ash in a long-term static immersing experiment. Waste Manag. 28, 1126–1136.

Luo, R., Cai, Y., Wang, C., & Huang, X. (2003). Study of chloride binding and diffusion in GGBS concrete. Cem. Concr. Res. 33, 1–7.

Malviya, R., & Chaudhary, R. (2006). Leaching behavior and immobilization of heavy metals in solidified/stabilized products. J. Hazard. Mater. 137, 207–217.

Manikandan, R., & Ramamurthy, K. (2007). Influence of fineness of fly ash on the aggregate pelletization process. Cem. Concr. Compos. 29, 456–464.

Manikandan, R., & Ramamurthy, K. (2008). Effect of curing method on characteristics of cold bonded fly ash aggregates. Cem. Concr. Compos. 30, 848–853.

Matschei, T., Lothenbach, B., & Glasser, F.P. (2007). The AFm phase in Portland cement. Cem. Concr. Res. 37, 118–130.

Medina, C., Banfill, P.F.G., Sánchez de Rojas, M.I., & Frías, M. (2013a). Rheological and calorimetric behaviour of cements blended with containing ceramic sanitary ware and construction/demolition waste. Constr. Build. Mater. 40, 822–831.

Medina, C., Sánchez de Rojas, M.I., & Frías, M. (2013b). Freeze-thaw durability of recycled concrete containing ceramic aggregate. J. Clean. Prod. 40, 151–160.

Meima, J.A., & Comans, R.N.J. (1999a). The leaching of trace elements from municipal solid waste incinerator bottom ash at different stages of weathering. Appl. Geochemistry 14, 159–171.

Meima, J.A., Van Zomeren, A., & Comans, R.N.J. (1999b). Complexation of Cu with Dissolved Organic Carbon in Municipal Solid Waste Incinerator Bottom Ash Leachates. Environ. Sci. Technol. 33, 1424–1429.

Meima, J.A., Van der Weijden, R.D., Eighmy, T.T., & Comans, R.N.J. (2002). Carbonation processes in municipal solid waste incinerator bottom ash and their effect on the leaching of copper and molybdenum. Appl. Geochemistry 17, 1503–1513.

Müllauer, W., Beddoe, R.E., & Heinz, D. (2015). Leaching behaviour of major and trace elements from concrete: Effect of fly ash and GGBS. Cem. Concr. Compos. 58, 129–139.

Müller, U., & Rübner, K. (2006). The microstructure of concrete made with municipal waste incinerator bottom ash as an aggregate component. Cem. Concr. Res. 36, 1434–1443.

Munuswamy, T. (2016). Internal chloride binding capacity of blended binders in mortar, Master Thesis. Eindhoven University of Technology, Eindhoven, the Netherlands.

NBS, (2015). National Bureau of Statistics of the People's republic of China.

NEN 6961, (2005). Environment – Digestion with nitric acid and hydrochloric acid (aqua regia) for the determination of selected elements in water, sediment, sludge, water contaning sludge, air dust, soil and building materials.

NEN 6966, (2005). Environment - Analysis of selected elements in water, eluates and destruates - atomic emission spectrometry with inductively coupled plasma.

NEN 7375, (2004). Leaching characteristics - Determination of the leaching of inorganic compoments from moulded or monolitic materials with a diffusion test - Soil earthy and stony materials.

NEN 7383, (2004). Leaching characteristics - Determination of the cumulative leaching of inorganic components from granular materials with a simiplified procedure of the column test - Solid earthy and stony materials.

NEN-EN-ISO 10304-2, (1996). Water quality - Determination of dissolved anions by liquid chromatography of ions - Part 2: Determination of bromide, chloride, nitrate, nitrite, orthophosphate and sulfate in waste water.

NEN-EN 1744-7, (2010). Determination of loss of ignition of Municipal Incinerator Bottom Ash Aggregate (MIBA Aggregate).

NPR-CEN/TS 12390-9, (2006). Testing hardened concrete - Part 9: Freeze- thaw resistance - Scaling.

NT BUILD 492, (1999). Concrete , Mortar and Cement-Based Repair Materials : chloride migration coefficient from non-steady-state migration experiments

Olsson, S., Kärrman, E., & Gustafsson, J.P. (2006). Environmental systems analysis of the use of bottom ash from incineration of municipal waste for road construction. Resour. Conserv. Recycl. 48, 26–40.

Olsson, S., Gustafsson, J.P., Kleja, D.B., Bendz, D., & Persson, I. (2009). Metal leaching from MSWI bottom ash as affected by salt or dissolved organic matter. Waste Manag. 29, 506–512.

Oner, A., & Akyuz, S. (2007). An experimental study on optimum usage of GGBS for the compressive strength of concrete. Cem. Concr. Compos. 29, 505–514.

Onori, R., Polettini, A., & Pomi, R. (2011). Mechanical properties and leaching modeling of activated incinerator bottom ash in Portland cement blends. Waste Manag. 31,

298–310.

Pan, J.R., Huang, C., Kuo, J.-J., & Lin, S.-H. (2008). Recycling MSWI bottom and fly ash as raw materials for Portland cement. Waste Manag. 28, 1113–1118.

Pera, J., Coutaz, L., Ambroise, J. & Chababbet, M., (1997). Use of incineratior bottom ash in concrete. Cem. Concr. Res. 27, 1–5.

Preda, C. (2007). Management of municipal solid waste in Europe. Report to Enviroment, Agriculture and Local and Reginal Affaris.

Pivnenko, K., Eriksson, E., & Astrup, T.F. (2015). Waste paper for recycling: Overview and identification of potentially critical substances. Waste Manag. 45, 134–142.

Pivnenko, K., Eriksen, M.K., Martín-Fernández, J.A., Eriksson, E., & Astrup, T.F. (2016). Recycling of plastic waste: Presence of phthalates in plastics from households and industry. Waste Manag. 54, 44–52.

Polettini, A., & Pomi, R. (2004). The leaching behavior of incinerator bottom ash as affected by accelerated ageing. J. Hazard. Mater. 113, 209–215.

Polettini, A., Pomi, R., & Fortuna, E. (2009). Chemical activation in view of MSWI bottom ash recycling in cement-based systems. J. Hazard. Mater. 162, 1292–1299.

Porciúncula, C.B., Marcilio, N.R., Tessaro, I.C., & Gerchmann, M. (2012). Production of hydrogen in the reaction between aluminum and water in the presence of NaOH and KOH. Braz. J. Chem. Eng. 29, 337–348.

Qiao, X.C., Tyrer, M., Poon, C.S., & Cheeseman, C.R. (2008a). Characterization of alkali-activated thermally treated incinerator bottom ash. Waste Manag. 28, 1955–1962.

Qiao, X.C., Tyrer, M., Poon, C.S., & Cheeseman, C.R. (2008b). Novel cementitious materials produced from incinerator bottom ash. Resour. Conserv. Recycl. 52, 496–510.

Qiao, X.C., Ng, B.R., Tyrer, M., Poon, C.S., & Cheeseman, C.R. (2008c). Production of lightweight concrete using incinerator bottom ash. Constr. Build. Mater. 22, 473–480.

Qiao, X.C., Cheeseman, C.R., & Poon, C.S. (2009). Influences of chemical activators on incinerator bottom ash. Waste Manag. 29, 544–549.

Quercia Bianchi, G. (2014). Application of nano-silica in concrete, PhD Thesis,. Eindhoven University of Technology, Einhoven, the Netherlands.

Rahman, M.A., & Bakker, M.C.M. (2013). Sensor-based control in eddy current separation of incinerator bottom ash. Waste Manag. 33, 1418–1424.

Rémond, S., Pimienta, P., & Bentz, D.P. (2002). Effects of the incorporation of Municipal Solid Waste Incineration fly ash in cement pastes and mortars I. Experimental study. Cem. Concr. Res. 32, 303–311.

Rendek, E., Ducom, G., & Germain, P. (2006). Carbon dioxide sequestration in municipal solid waste incinerator (MSWI) bottom ash. J. Hazard. Mater. 128, 73–79.

Roessler, J.G., Townsend, T.G., & Ferraro, C.C. (2015). Use of leaching tests to quantify trace element release from waste to energy bottom ash amended pavements. J. Hazard. Mater. 300, 830–837.

Roustaei, M., Eslami, A., & Ghazavi, M. (2015). Effects of freeze-thaw cycles on a fiber reinforced fine grained soil in relation to geotechnical parameters. Cold Reg. Sci. Technol. 120, 127–137.

Saffarzadeh, A., Shimaoka, T., Wei, Y., Gardner, K.H., & Musselman, C.N. (2011). Impacts of natural weathering on the transformation/neoformation processes in landfilled MSWI bottom ash: a geoenvironmental perspective. Waste Manag. 31, 2440–2454.

Saffarzadeh, A., Arumugam, N., & Shimaoka, T. (2016). Aluminum and aluminum alloys in municipal solid waste incineration (MSWI) bottom ash: A potential source for the production of hydrogen gas. Int. J. Hydrogen Energy 41, 820–831.

Saikia, N., Cornelis, G., Mertens, G., Elsen, J., Van Balen, K., Van Gerven, T., & Vandecasteele, C. (2008). Assessment of Pb-slag, MSWI bottom ash and boiler and fly ash for using as a fine aggregate in cement mortar. J. Hazard. Mater. 154, 766–777.

Sandor Popovics (1992). Concrete Materials: Properties, Specification, and Testing. (2nd Edition)

Saner, D., Blumer, Y.B., Lang, D.J., & Koehler, A. (2011). Scenarios for the implementation of EU waste legislation at national level and their consequences for emissions from municipal waste incineration. Resour. Conserv. Recycl. 57, 67–77.

Santos, R.M., Mertens, G., Salman, M., Cizer, O., & Van Gerven, T. (2013). Comparative study of ageing, heat treatment and accelerated carbonation for stabilization of municipal solid waste incineration bottom ash in view of reducing regulated heavy metal/metalloid leaching. J. Environ. Manage. 128, 807–821.

Schneider, M., Romer, M., Tschudin, M., & Bolio, H. (2011). Sustainable cement production—present and future. Cem. Concr. Res. 41, 642–650.

Settimo, F., Bevilacqua, P., & Rem, P. (2004). Eddy Current Separation of Fine Non-Ferrous Particles from Bulk Streams. Phys. Sep. Sci. Eng. 13, 15–23.

Sheen, Y.-N., Wang, H.-Y., Juang, Y.-P., & Le, D.-H. (2013). Assessment on the engineering properties of ready-mixed concrete using recycled aggregates. Constr. Build. Mater. 45, 298–305.

Shekdar, A. V. (2009). Sustainable solid waste management: An integrated approach for Asian countries. Waste Manag. 29, 1438–1448.

Shen, Y., Qian, J., & Zhang, Z. (2013). Investigations of anhydrite in CFBC fly ash as cement retarders. Constr. Build. Mater. 40, 672–678.

Shi, H.-S., & Kan, L.-L. (2009a). Leaching behavior of heavy metals from municipal solid wastes incineration (MSWI) fly ash used in concrete. J. Hazard. Mater. 164, 750–754.

Shi, H., & Kan, L. (2009b). Characteristics of municipal solid wastes incineration (MSWI) fly ash–cement matrices and effect of mineral admixtures on composite system. Constr. Build. Mater. 23, 2160–2166.

Siddique, R., & Bennacer, R. (2012). Use of iron and steel industry by-product (GGBS) in cement paste and mortar. Resour. Conserv. Recycl. 69, 29–34.

Singh, M., & Siddique, R. (2013). Effect of coal bottom ash as partial replacement of sand on properties of concrete. Resour. Conserv. Recycl. 72, 20–32.

Soares, M.A.R., Quina, M.J., Reis, M.S., & Quinta-Ferreira, R. (2016). Assessment of co-composting process with high load of an inorganic industrial waste. Waste Manag. 59, 80–89.

Soil Quality Decree, (2013). Regeling Bodemkwaliteit, VROM, Den Haag: Ruimte en Milieu, Ministerie van Volkshuisvesting, Ruimtelijke Ordeling en Milieubeheer.

Solpuker, U., Sheets, J., Kim, Y., & Schwartz, F.W. (2014). Leaching potential of pervious concrete and immobilization of Cu, Pb and Zn using pervious concrete. J. Contam. Hydrol. 161, 35–48.

Song, G.-J., Kim, K.-H., Seo, Y.-C., & Kim, S.-C. (2004). Characteristics of ashes from different locations at the MSW incinerator equipped with various air pollution control devices. Waste Manag. 24, 99–106.

Song, H.W., Lee, C.H., Jung, M.S., & Ann, K.Y. (2008). Development of chloride binding capacity in cement pastes and influence of the pH of hydration products. Can. J. Civ. Eng. 35, 1427–1434.

Sorlini, S., Abbà, A., & Collivignarelli, C. (2011). Recovery of MSWI and soil washing residues as concrete aggregates. Waste Manag. 31, 289–297.

Stehlík, P. (2009). Contribution to advances in waste-to-energy technologies. J. Clean. Prod. 17, 919–931.

Tam, V.W.Y., Gao, X.F., Tam, C.M., & Ng, K.M. (2009). Physio-chemical reactions in recycle aggregate concrete. J. Hazard. Mater. 163, 823–828.

Tang, L., & Nilsson, L.O. (1993). Chloride binding capacity and binding isotherms of OPC pastes and mortars. Cem. Concr. Res. 23, 247–253.

Tang, P., Florea, M.V.A., Spiesz, P., & Brouwers, H.J.H. (2015). Characteristics and application potential of municipal solid waste incineration (MSWI) bottom ashes from two waste-to-energy plants. Constr. Build. Mater. 83, 77–94.

Tang, P., Florea, M.V.., Spiesz, P., & Brouwers, H.J.H. (2016). Application of thermally activated municipal solid waste incineration (MSWI) bottom ash fines as binder substitute. Cem. Concr. Compos. 70, 194–205.

Tang, P., Munuswamy, T., Florea, M.V.A., & Brouwers, H.J.H. (2015). Internal chloride binding and leaching behaviour in mortars regarding to blended binders. In H.B. Fischer, K.A. Bode & C. Beutan (Eds.), The 19th International Conference on Building Materials (IBAUSIL), 2, pp. 493-498, Weimar, Germany: Bauhaus-University.

Tang, P., Florea, M.V.A., & Brouwers, H.J.H. (2017) Employing cold bonded pelletization to produce lightweight aggregates from incineration fine bottom ash, J. Clean. Prod. 165, 1371–1384.

Tang, P., & Brouwers, H.J.H. (2017) Integral recycling of municipal solid waste incineration (MSWI) bottom ash fines (0–2 mm) and industrial powder wastes by cold-bonding pelletization, Waste Manag. 62, 125–138.

Taylor, H.F.W. (1997). Cement chemistry (Thomas Telford Publishing).

Thomas, J., & Harilal, B. (2015). Properties of cold bonded quarry dust coarse aggregates and its use in concrete. Cem. Concr. Compos. 62, 67–75.

Tishmack, J., Olek, J., & Diamond, S. (1999). Characterization of High-Calcium Fly Ashes and Their Potential Influence on Ettringite Formation in Cementitious Systems. Cem. Concr. Aggregates 21, 82-92.

Tkaczewska, E., Mróz, R., & Łój, G. (2012). Coal-biomass fly ashes for cement production of CEM II/A-V 42.5R. Constr. Build. Mater. 28, 633–639.

Uwasu, M., Hara, K., & Yabar, H. (2014). World cement production and environmental implications. Environ. Dev. 10, 36–47.

Van der Sloot, H.A., Kosson, D.S., & Hjelmar, O. (2001). Characteristics, treatment and utilization of residues from municipal waste incineration. Waste Manag. 21, 753–765.

Vasugi, V., & Ramamurthy, K. (2014). Identification of design parameters influencing manufacture and properties of cold-bonded pond ash aggregate. Mater. Des. 54, 264–278.

Van Caneghem, J., Verbinnen, B., Cornelis, G., De Wijs, J., Mulder, R., Billen, P., & Vandecasteele, C. (2016). Immobilization of antimony in waste-to-energy bottom ash by addition of calcium and iron containing additives. Waste Manag. 54, 162–168.

Van Dr Wegen, G., Hofstra, U., & Speerstra, J. (2013). Upgraded MSWI bottom ash as aggregate in concrete. Waste and Biomass Valor 4, 737–743.

Van Gerven, T., Geysen, D., Stoffels, L., Jaspers, M., Wauters, G., & Vandecasteele, C. (2005). Management of incinerator residues in Flanders (Belgium) and in neighbouring countries. A comparison. Waste Manag. 25, 75–87.

Van Gerven, T., Cooreman, H., Imbrechts, K., Hindrix, K., & Vandecasteele, C. (2007). Extraction of heavy metals from municipal solid waste incinerator (MSWI) bottom ash with organic solutions. J. Hazard. Mater. 140, 376–381.

Van Zomeren, A., & Comans, R.N.J. (2004). Contribution of natural organic matter to copper leaching from municipal solid waste incinerator bottom ash. Environ. Sci. Technol. 38, 3927–3932.

Van Zomeren, A., & Comans, R.N.J. (2009). Carbon speciation in municipal solid waste incinerator (MSWI) bottom ash in relation to facilitated metal leaching. Waste Manag. 29, 2059–2064.

Vazquez, Y. V., & Barbosa, S.E. (2016). Recycling of mixed plastic waste from electrical and electronic equipment. Added value by compatibilization. Waste Manag. 53, 196–203.

Volland, S., & Brötz, J. (2015). Lightweight aggregates produced from sand sludge and zeolitic rocks. Constr. Build. Mater. 85, 22–29.

Wang, H., & Wang, C. (2013). Municipal solid waste management in Beijing: characteristics and challenges. Waste Manag. Res. 31, 67–72.

Weeks, C., Hand, R.J., & Sharp, J.H. (2008). Retardation of cement hydration caused by heavy metals present in ISF slag used as aggregate. Cem. Concr. Compos. 30, 970–978.

Wei, Y., Shimaoka, T., Saffarzadeh, A., & Takahashi, F. (2011). Mineralogical characterization of municipal solid waste incineration bottom ash with an emphasis on heavy metal-bearing phases. J. Hazard. Mater. 187, 534–543.

Wiles, C.C. (1996). Municipal solid waste combustion ash : State-of-the-knowledge. J. Hazard. Mater. 47, 325–344.

Wilson, A. (1993). Cement and Concrete : Environmental Considerations. Environ. Build. News. 2, 1-11

Wong, H.S., Barakat, R., Alhilali, A., Saleh, M., & Cheeseman, C.R. (2015). Hydrophobic concrete using waste paper sludge ash. Cem. Concr. Res. 70, 9–20.

Woon, K.S., & Lo, I.M.C. (2016). A proposed framework of food waste collection and recycling for renewable biogas fuel production in Hong Kong. Waste Manag. 47, 3–10.

Xia, Y., He, P., Shao, L., & Zhang, H. (2017). Metal distribution characteristic of MSWI bottom ash in view of metal recovery. J. Environ. Sci. 52, 178–189.

Xu, T., Galama, T., & Sathaye, J. (2013). Reducing carbon footprint in cement material making: Characterizing costs of conserved energy and reduced carbon emissions. Sustain. Cities Soc. 9, 54–61.

Yang, J., Du, Q., & Bao, Y. (2011). Concrete with recycled concrete aggregate and crushed clay bricks. Constr. Build. Mater. 25, 1935–1945.

Yang, R., Liao, W.-P., & Wu, P.-H. (2012). Basic characteristics of leachate produced by various washing processes for MSWI ashes in Taiwan. J. Environ. Manage. 104, 67–76.

Yang, S., Saffarzadeh, A., Shimaoka, T., & Kawano, T. (2013). Existence of Cl in municipal solid waste incineration bottom ash and dechlorination effect of thermal treatment. J. Hazard. Mater. 267, 214–220.

Yao, J., Li, W.-B., Kong, Q.-N., Wu, Y.-Y., He, R., & Shen, D.-S. (2010a). Content, mobility and transfer behavior of heavy metals in MSWI bottom ash in Zhejiang province, China. Fuel 89, 616–622.

Yao, J., Li, W.-B., Tang, M., Fang, C.-R., Feng, H.-J., & Shen, D.-S. (2010b). Effect of

weathering treatment on the fractionation and leaching behavior of copper in municipal solid waste incinerator bottom ash. Chemosphere 81, 571–576.

Yao, J., Kong, Q., Zhu, H., Long, Y., & Shen, D. (2013). Content and fractionation of Cu, Zn and Cd in size fractionated municipal solid waste incineration bottom ash. Ecotoxicol. Environ. Saf. 94, 131–137.

Yao, Q., Samad, N.B., Keller, B., Seah, X.S., Huang, L., & Lau, R. (2014). Mobility of heavy Metals and rare earth Elements in incineration bottom ash through particle size reduction. Chem. Eng. Sci. 118, 214-220

Yen, C.-L., Tseng, D.-H., & Lin, T.-T. (2011). Characterization of eco-cement paste produced from waste sludges. Chemosphere 84, 220–226.

Yu, R., Tang, P., Spiesz, P., & Brouwers, H.J.H. (2014). A study of multiple effects of nano-silica and hybrid fibres on the properties of Ultra-High Performance Fibre Reinforced Concrete (UHPFRC) incorporating waste b GovHK ottom ash (WBA). Constr. Build. Mater. 60, 98–110.

Yudovich, Y.E., & Ketris, M.P. (2006). Chlorine in coal: A review. Int. J. Coal Geol. 67, 127–144.

Zajac, M., Rossberg, A., Le Saout, G., & Lothenbach, B. (2014). Influence of limestone and anhydrite on the hydration of Portland cements. Cem. Concr. Compos. 46, 99–108.

Zhang, H., Schuchardt, F., Li, G., Yang, J., & Yang, Q. (2013). Emission of volatile sulfur compounds during composting of municipal solid waste (MSW). Waste Manag. 33, 957–963.

Zhang, Y., Cetin, B., Likos, W.J., & Edil, T.B. (2016). Impacts of pH on leaching potential of elements from MSW incineration fly ash. Fuel 184, 815–825.

Zhao, Z., Wang, S., Lu, L., & Gong, C. (2013). Evaluation of pre-coated recycled aggregate for concrete and mortar. Constr. Build. Mater. 43, 191–196.

List of abbreviations and symbols

Abbreviations

ADR	Advanced dry recovery
APC	Air pollution control
AR	Alumina ratio
ASR	Alkali-silica reaction
BA	Bottom ash
BD	Bulk density
BAM	Incineration bottom ash from Moerdijk
BAW	Incineration bottom ash from Wijster
CBLA	Cold bonded lightweight aggregate
CDW	Construction and demolition waste
CML	Cumulative mass loss
CR	Crushing resistance
DOC	Dissolved organic carbon
FA	Coal fly ash
F-BA	Fine incineration bottom ash below 2 mm
F-BAM	Fine incineration bottom ash (0-2 mm) from Moerdijk
F-BAW	Fine incineration bottom ash (0-2 mm) from Wijster
GGBS	Ground granulated blast furnace slag
HA	Humic acid
Hc	Hydrotalcite
HCFA	High calcium fly ash from coal combustion power plant
HPLC	High performance liquid chromatography
HR	Hydraulic ratio
IBA	Incineration bottom ash
IBC	Isoleren-Beheersen-Controleren
IC	Ion chromatography
ICP-AES	Inductively coupled plasma-atomic emission spectrometry
IFA	Incineration fly ash
IMC	Insulation, Management, Control
L	Liter
LCA	Life cycle analysis
LWA	Lightweight aggregate
LOI	Loss on ignition
LSF	Lime saturation factor
L/S	Liquid to solid ratio

MF-BA	Milled MSWI fine bottom ash
MF-BAW	Milled fine incineration bottom ash from Wijster
MF-BAM	Milled fine incineration bottom ash from Moerdijk
MHR	Maximum heat release rate
MSW	Municipal solid waste
MSWI	Municipal solid waste incineration
NA	Natural aggregate
nS	Nano-silica
OPC	Ordinary Portland cement
PFA	Pulverized fly ash
PPF	Polypropylene fiber
PSA	Paper sludge ash
PSD	Particle size distribution
RCA	Recycled concrete aggregate
RHA	Rice husk ash
SCC	Self-compacting concrete
SCMs	Supplementary cementing materials
SEM	Scanning electron microscope
SF	Sand fraction
S-F	Slump-flow
SMHR	Second maximum heat release rate
SP	Superplasticizer
SQD	Soil Quality Decree
SR	Silica ratio
TH	Total heat after 168 hours
3R	Reduce, Reuse and Recycle
WA	Water absorption
WAS	Washing aggregate sludge
WBA	Natural weathered incineration bottom ash
WPD	Water penetration depth
w/p	Water to powder ratio
WtE	Waste to Energy
XRD	X-ray diffraction
XRF	X-ray fluorescence

Symbols

C_t	The range of calculated total content of components in mortar	[mg/kg]
d.m.	Dry mass	
ε	Leaching concentration of components in the changed leachate during diffusion test	[mg/m^2]
ε_{64}	The cumulative leaching concentration of a component after 64 days diffusion test	[mg/m^2]
m_1	Initial mass of the sample before drying	[g]
m_2	Mass of sample after drying	[g]
m_d	Mass of sample after drying	[g]
m_{wet}	Mass of original tested sample after water absorption procedure	[g]
rc	The slop of the linear regression line between the log (ε) and log (hour)	
t_{500}	Slump flow time to reach diameter of 500 mm	[s]
t_v	V-funnel time	[s]
ω	Water content	[%]
W_{24}	Water absorption	[%]

Chemical abbreviation

AFm	Alumina, ferric oxide, mono-sulphate
AFt	Alumina, ferric oxide, tri-sulphate
B	Brownmillite
C	Calcite
C_3A	Tricalcium aluminate
C_4AF	Tetracalcium aluminoferrite
CH	Portlandite
Cl-LDH	Chloride layered double hydroxide
C-S-H	Calcium silicate hydrate
C_2S	Belite
C_3S	Alite
Fs	Friedel's salt
Ms	Monosulphate
Qz	Quartz

Chemical components

Al_2O_3	Aluminum oxide
$CaCl_2$	Calcium chloride
CaO	Calcium oxide
CO_2	Carbon dioxide
$CaSO_4$	Calcium sulphate
Fe_2O_3	Iron oxide
H_2	Hydrogen
KOH	Potassium hydroxide
NaCl	Sodium chloride
NaOH	Sodium hydroxide
SiO_2	Silica oxide

Minerals terminology

$Ca_2Al_2SiO_7$	Gehlenite
$CaCO_3$	Calcite
$Ca_3Si_3O_9$	Wollastonite
$CaSO_4$	Anhydrite
Fe_3O_4	Magnetite
Fe_2O_3	Hematite
SiO_2	Quartz
$Zn_2P_2O_7$	Zinc pyrophosphate

Appendix A

The amount of CaO, Al_2O_3, Fe_2O_3, CuO, SO_3, Cl in BAW and BAM fractions

(a)

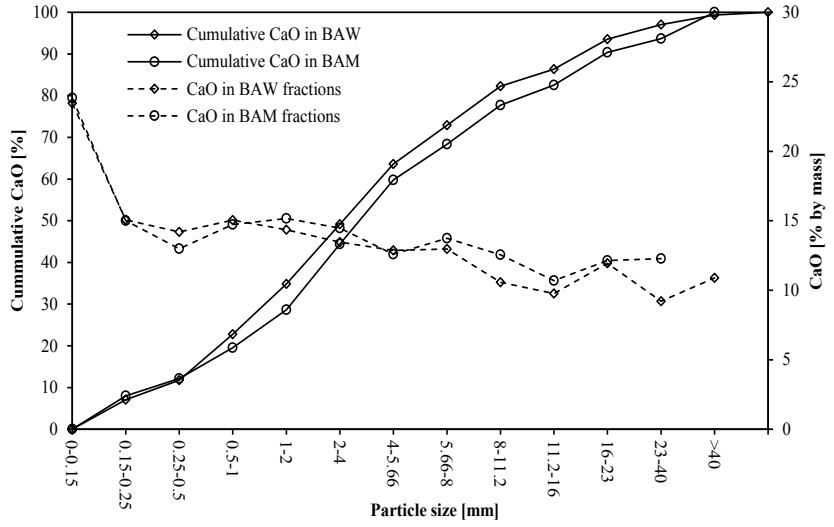

(b)

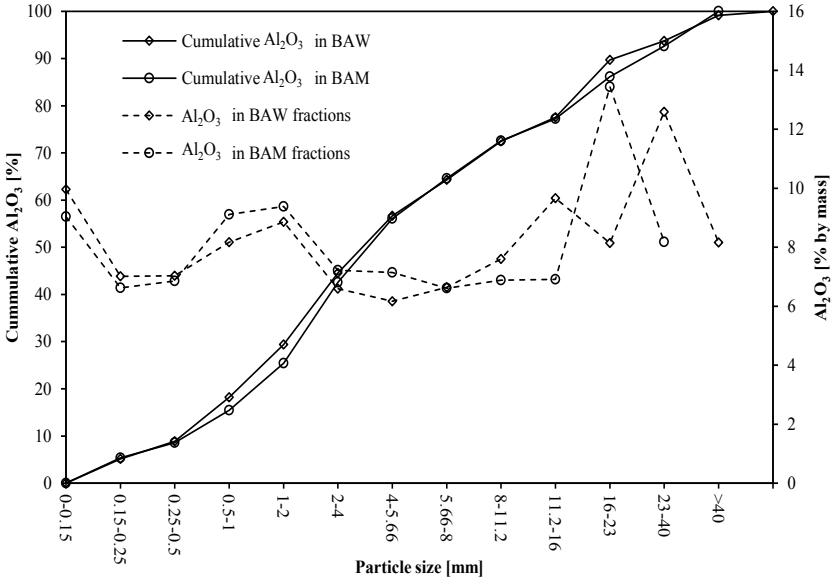

(c)

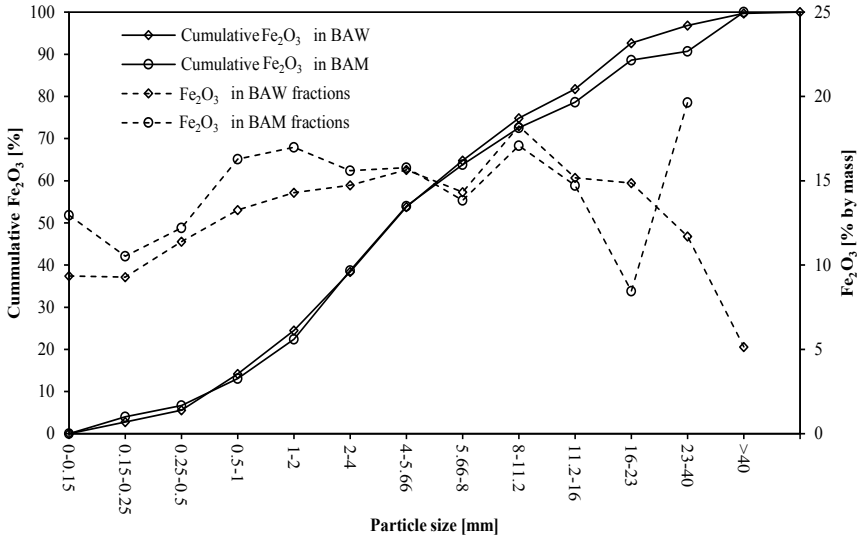
Cumulative Fe_2O_3 in BAW
Cumulative Fe_2O_3 in BAM
Fe_2O_3 in BAW fractions
Fe_2O_3 in BAM fractions
Cummulative Fe_2O_3 [%]
Fe_2O_3 [% by mass]
Particle size [mm]
0-0.15
0.15-0.25
0.25-0.5
0.5-1
1-2
2-4
4-5.66
5.66-8
8-11.2
11.2-16
16-23
23-40
>40

(d)

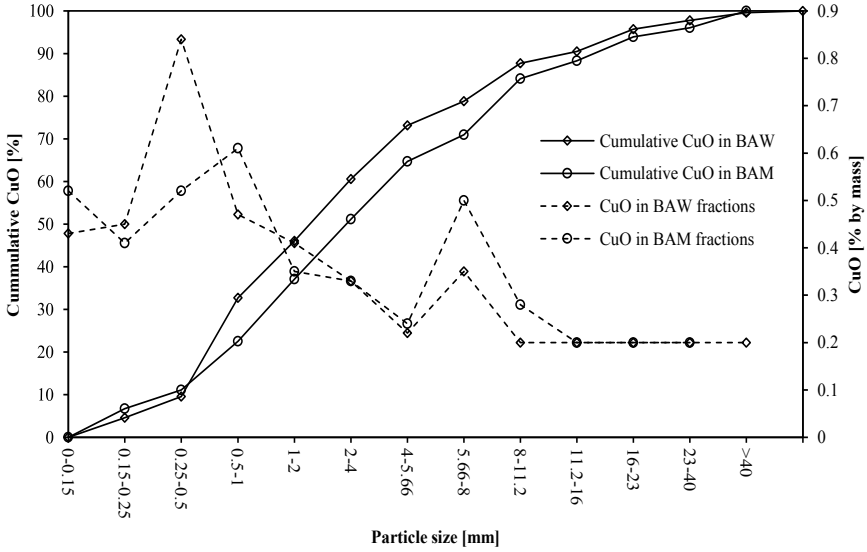
Cumulative CuO in BAW
Cumulative CuO in BAM
CuO in BAW fractions
CuO in BAM fractions
Cummulative CuO [%]
CuO [% by mass]
Particle size [mm]
0-0.15
0.15-0.25
0.25-0.5
0.5-1
1-2
2-4
4-5.66
5.66-8
8-11.2
11.2-16
16-23
23-40
>40

(e)

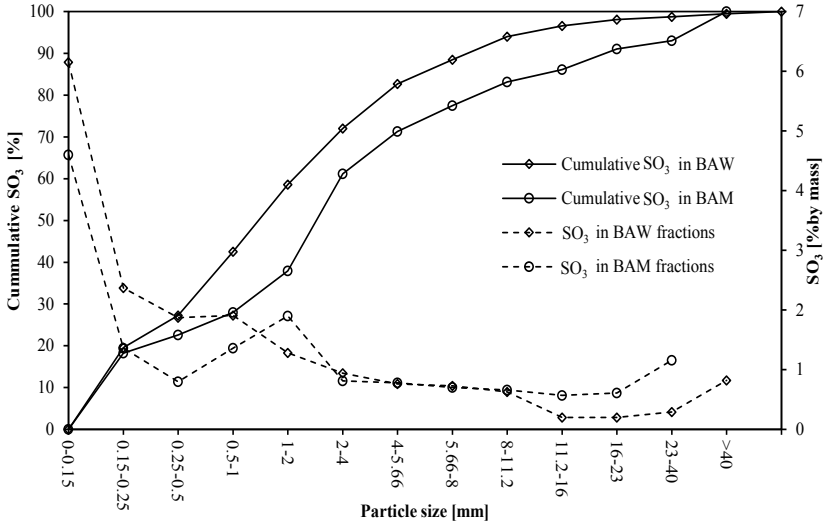
Cummulative SO_3 [%]
SO_3 [%by mass]
Cumulative SO_3 in BAW
Cumulative SO_3 in BAM
SO_3 in BAW fractions
SO_3 in BAM fractions
0-0.15
0.15-0.25
0.25-0.5
0.5-1
1-2
2-4
4-5.66
5.66-8
8-11.2
11.2-16
16-23
23-40
>40
Particle size [mm]

(f)

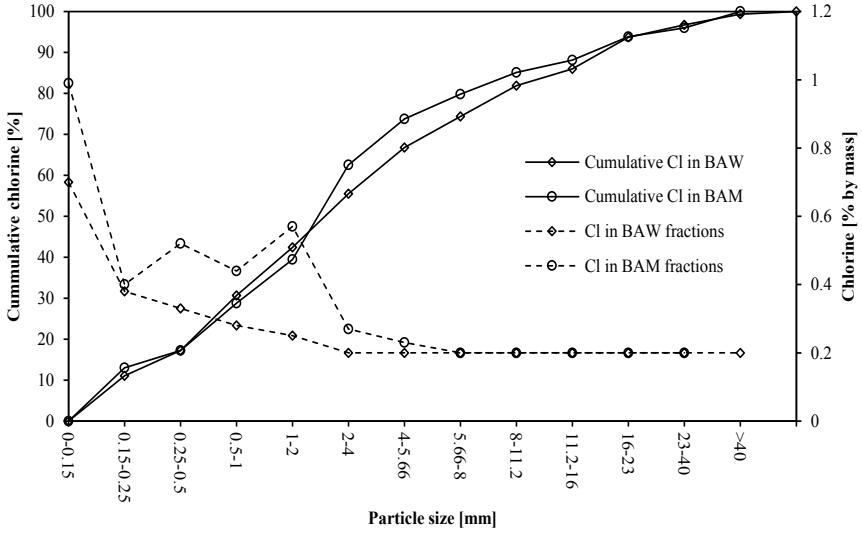
Cummulative chlorine [%]
Chlorine [% by mass]
Cumulative Cl in BAW
Cumulative Cl in BAM
Cl in BAW fractions
Cl in BAM fractions
0-0.15
0.15-0.25
0.25-0.5
0.5-1
1-2
2-4
4-5.66
5.66-8
8-11.2
11.2-16
16-23
23-40
>40
Particle size [mm]

Appendix B

H_2 volume calculation

$$2Al + 6H_2O \rightarrow 2Al(OH)_3 + 3H_2 \uparrow$$

Molar ratio	2	3
Molar mass	26.98	2.01

Mass	1 g	
↓		
Moles	1÷ 26.98	(1÷ 26.98)÷2×3

$$n\ (H_2) = (1 \div 26.98) \div 2 \times 3 \text{ mol}$$

Ideal gas law: $PV = nRT$

n	Amount of substance of the gas [moles]
P	Pressure of the gas [atm]
V	Volume of the gas [dm^3]
T	The absolute temperature of the gas [K]
R	Gas constant [atm dm^3/mol/K]

Therefore:

$V = nRT \div P$

$V\ (H_2) = [(1 \div 26.98) \div 2 \times 3] \times 0.082 \times 293 \div 1.0 = 1.336\ dm^3$

Summary

Municipal solid waste incineration (MSWI) bottom ash - from waste to value: Characterization, treatments and application

The waste-to-energy technique as a sufficient method to manage the municipal solid wastes in the way of incineration has been widely applied. However, the increasing amount of solid by-products (such as incineration bottom ash, fly ash and air pollution control residues) generated in the incineration becomes an issue, which need to be solved in consideration of the sustainable development of environment and economy. This thesis aims at investigating the potential applications of municipal solid waste incineration (MSWI) bottom ash as building materials, such as binder substitutes, sand and aggregate replacement.

The stability of the physical and chemical properties of the MSWI bottom ashes was assessed by analyzing the historic experimental data and shown in Chapter 3. It was figured out that the MSWI bottom ashes from two different incinerations in the Netherlands had very similar properties, and their properties were quite stable over time. Their environmental property was evaluated through column leaching test, and the leaching contaminants in both bottom ashes according to the Dutch legislation (Soil Quality Decree, SQD) were copper, antimony, molybdenum, chloride and sulphate. The use of fine bottom ashes (0-2 mm) as sand replacement or as cement replacement after milling showed that the metallic aluminum in the bottom ash cased crack in mortar and the milled fine bottom ash had low reactivity.

To improve the properties of the fine bottom ash, and make it suitable to be used as building materials, several treatments were investigated in Chapter 4 and Chapter 5. Thermal treatment plus slow speed milling process could reduce the antimony and copper leaching significantly, and the retardation effect of milled bottom ash on the cement hydration was reduced. The washing treatment on fine bottom ash can remove the chloride content by more than 50%. The use of fine bottom ash in mortar with blended binders showed that the Sb, chloride and sulphate in fine bottom ash could be well bound by the binders, while the Cu leaching showed an increasing treated with curing time.

To combine the treatment and application of the fine bottom ashes, integral recycle through cold bonded pelletization was introduced (Chapters 6, 7 and 8). Several industrial solid wastes, such as paper sludge ash, coal fly ash, washing aggregate sludge, fine bottom ash, etc. were chosen as raw materials and mixed with cementitious binders to produced artificial cold bonded lightweight aggregates (CBLAs). The properties of the CBLAs could be modified by changing the proportions of the raw materials, adding of polypropylene

fibers, etc. The leaching of antimony and sulphate of the produced CBLAs was well under the limit value according to SQD, while the leaching of copper, molybdenum and chloride can be decreased by reducing the use of fine bottom ash or increasing the binder content. The used of CBLAs in self-compacting concrete showed decrease of the concrete strength due to lower aggregate strength compared with natural aggregate, while the use of water can be decreased due to the rounded particle shape of the CBLAs. Moreover, the leaching concentration of contaminants from the concrete with CBLAs complied with the leaching limits due to the binding of the cementitious binders in concrete.

List of publications

Publication written within this PhD project are listed below:

Journals

[1] **P. Tang**, H.J.H. Brouwers, The durability and environmental properties of self-compacting concrete incorporating cold bonded lightweight aggregates produced from combined industrial solid wastes (under review)

[2] **P. Tang**, M.V.A. Florea, H.J.H. Brouwers, Employing cold bonded pelletization to produce lightweight aggregates from incineration fine bottom ash, J. Clean. Prod. 165 (2017) 1371–1384.

[3] **P. Tang**, H.J.H. Brouwers, Integral recycling of municipal solid waste incineration (MSWI) bottom ash fines (0–2 mm) and industrial powder wastes by cold-bonding pelletization, Waste Manag. 62 (2017) 125–138.

[4] **P. Tang**, M.V.A. Florea, P. Spiesz, H.J.H. Brouwers, Application of thermally activated municipal solid waste incineration (MSWI) bottom ash fines as binder substitute, Cem. Concr. Compos. 70 (2016) 194–205.

[5] **P. Tang**, M.V.A. Florea, P. Spiesz, H.J.H. Brouwers, Characteristics and application potential of municipal solid waste incineration (MSWI) bottom ashes from two waste-to-energy plants, Constr. Build. Mater. 83 (2015) 77–94.

[6] R. Yu, **P. Tang**, P. Spiesz, H.J.H. Brouwers, A study of multiple effects of nano-silica and hybrid fibres on the properties of Ultra-High Performance Fibre Reinforced Concrete (UHPFRC) incorporating waste bottom ash (WBA), Constr. Build. Mater. 60 (2014) 98–110.

Conference proceedings

[1] **P. Tang**, M.V.A. Florea, H.J.H. Brouwers, (2016) Production of Artificial Aggregate Using MSWI Bottom Ash Fines (0-2 mm) Applying The Cold Bonding Pelletizing Technique. In 4th International Conference on Sustainable Solid Waste Management, 23–25 June, Limassol, Cyprus.

[2] **P. Tang**, M.V.A. Florea, H.J.H. Brouwers, (2016) Recycling of waste materials as lightweight aggregate by cold bonding pelletizing technique. In 38th International Cement Microscopy Association (ICMA) conference, April 17-21, Lyon, France.

[3] **P. Tang,** T. Munuswamy, M.V.A. Florea, H.J.H. Brouwers, (2015). Internal chloride binding and leaching behaviour in mortars regarding to blended binders. In H.B. Fischer, K.A. Bode & C. Beutan (Eds.), Conference paper published at the 19th International Conference on Building Materials (IBAUSIL 2015), 16. bis 18. September, Weimar, Germany, (2, pp. 493-498). Weimar, Germany: Bauhaus-University.

[4] **P. Tang**, M.V.A. Florea, P. Spiesz, H.J.H. Brouwers, (2014). Thermal treatment on MSWI bottom ash fines. In V. Bilek & Z. Kersner (Eds.), Conference Paper: Proceedings of the International Conference of Non-Traditional Cement and Concrete (NTCC2014), June 16-19, 2014, Brno, Czech Republic, (pp. 305-306). Brno: NOVPRESS s.r.o.

[5] **P. Tang,** Q.L. Yu, R. Yu, H.J.H. Brouwers, (2013). The application of MSWI bottom ash fines in high performance concrete. 1st International Conference on the Chemistry of Construction Materials, 7-9 October 2013, Berlin, (pp. 435-438). Berlin.

[6] **P. Tang**, M.V.A. Florea, H.J.H. Brouwers, (2012). The characterization of MSWI bottom ash. In H.B. Fischer, K.A. Bode & C. Beutan (Eds.), 18th International Conference on Building Materials (IBAUSIL 2012), 12. bis 15. September, Weimar, Germany, (2, pp. 1192-1199). Weimar, Germany: Bauhaus-University.

Curriculum vitae

Personal data

Name: Pei Tang

Date of birth: 22nd December 1987

Place of birth: Henan, China

PhD research/work

2017-present The Hong Kong Polytechnic University (PolyU), Hong Kong, China
Department of Civil and Environmental Engineering
Associate researcher

2011–2016 Eindhoven University of Technology (Tu/e), Eindhoven, the Netherlands
Department of Built Environment
PhD student and researcher

Education

2009 – 2011 Master of Structural Engineering
Wuhan University of Technology (WUT), Wuhan, P. R. China
Thesis title:
Experimental Research on Mechanical Property of Reinforced Inorganic Polymer Concrete Beam
Participated project:
Application of geopolymer concrete in rapid repairing and construction in airport (supported by China Military)

2005 – 2009 Bachelor of Civil Engineering
Xuchang University, Xuchang, P. R. China
Graduation project:
Design of T-beam pre-stressed concrete bridge

Bouwstenen is een publikatiereeks van de Faculteit Bouwkunde, Technische Universiteit Eindhoven. Zij presenteert resultaten van onderzoek en andere aktiviteiten op het vakgebied der Bouwkunde, uitgevoerd in het kader van deze Faculteit.

Bouwstenen zijn telefonisch te bestellen op nummer
040 - 2472383

Kernredaktie
MTOZ

Reeds verschenen in de serie
Bouwstenen

nr 1
Elan: A Computer Model for Building Energy Design: Theory and Validation
Martin H. de Wit
H.H. Driessen
R.M.M. van der Velden

nr 2
Kwaliteit, Keuzevrijheid en Kosten: Evaluatie van Experiment Klarendal, Arnhem
J. Smeets
C. le Nobel
M. Broos
J. Frenken
A. v.d. Sanden

nr 3
Crooswijk: Van 'Bijzonder' naar 'Gewoon'
Vincent Smit
Kees Noort

nr 4
Staal in de Woningbouw
Edwin J.F. Delsing

nr 5
Mathematical Theory of Stressed Skin Action in Profiled Sheeting with Various Edge Conditions
Andre W.A.M.J. van den Bogaard

nr 6
Hoe Berekenbaar en Betrouwbaar is de Coëfficiënt k in x-ksigma en x-ks?
K.B. Lub
A.J. Bosch

nr 7
Het Typologisch Gereedschap: Een Verkennende Studie Omtrent Typologie en Omtrent de Aanpak van Typologisch Onderzoek
J.H. Luiten

nr 8
Informatievoorziening en Beheerprocessen
A. Nauta
Jos Smeets (red.)
Helga Fassbinder (projectleider)
Adrie Proveniers
J. v.d. Moosdijk

nr 9
Strukturering en Verwerking van Tijdgegevens voor de Uitvoering van Bouwwerken
ir. W.F. Schaefer
P.A. Erkelens

nr 10
Stedebouw en de Vorming van een Speciale Wetenschap
K. Doevendans

nr 11
Informatica en Ondersteuning van Ruimtelijke Besluitvorming
G.G. van der Meulen

nr 12
Staal in de Woningbouw, Korrosie-Bescherming van de Begane Grondvloer
Edwin J.F. Delsing

nr 13
Een Thermisch Model voor de Berekening van Staalplaatbetonvloeren onder Brandomstandigheden
A.F. Hamerlinck

nr 14
De Wijkgedachte in Nederland: Gemeenschapsstreven in een Stedebouwkundige Context
K. Doevendans
R. Stolzenburg

nr 15
Diaphragm Effect of Trapezoidally Profiled Steel Sheets: Experimental Research into the Influence of Force Application
Andre W.A.M.J. van den Bogaard

nr 16
Versterken met Spuit-Ferrocement: Het Mechanische Gedrag van met Spuit-Ferrocement Versterkte Gewapend Betonbalken
K.B. Lubir
M.C.G. van Wanroy

nr 17
De Tractaten van Jean Nicolas Louis Durand
G. van Zeyl

nr 18
Wonen onder een Plat Dak: Drie Opstellen over Enkele Vooronderstellingen van de Stedebouw
K. Doevendans

nr 19
Supporting Decision Making Processes: A Graphical and Interactive Analysis of Multivariate Data
W. Adams

nr 20
Self-Help Building Productivity: A Method for Improving House Building by Low-Income Groups Applied to Kenya 1990-2000
P. A. Erkelens

nr 21
De Verdeling van Woningen: Een Kwestie van Onderhandelen
Vincent Smit

nr 22
Flexibiliteit en Kosten in het Ontwerpproces: Een Besluitvormingondersteunend Model
M. Prins

nr 23
Spontane Nederzettingen Begeleid: Voorwaarden en Criteria in Sri Lanka
Po Hin Thung

nr 24
Fundamentals of the Design of Bamboo Structures
Oscar Arce-Villalobos

nr 25
Concepten van de Bouwkunde
M.F.Th. Bax (red.)
H.M.G.J. Trum (red.)

nr 26
Meaning of the Site
Xiaodong Li

nr 27
Het Woonmilieu op Begrip Gebracht: Een Speurtocht naar de Betekenis van het Begrip 'Woonmilieu'
Jaap Ketelaar

nr 28
Urban Environment in Developing Countries
editors: Peter A. Erkelens
George G. van der Meulen (red.)

nr 29
Stategische Plannen voor de Stad: Onderzoek en Planning in Drie Steden
prof.dr. H. Fassbinder (red.)
H. Rikhof (red.)

nr 30
Stedebouwkunde en Stadsbestuur
Piet Beekman

nr 31
De Architectuur van Djenné: Een Onderzoek naar de Historische Stad
P.C.M. Maas

nr 32
Conjoint Experiments and Retail Planning
Harmen Oppewal

nr 33
Strukturformen Indonesischer Bautechnik: Entwicklung Methodischer Grundlagen für eine 'Konstruktive Pattern Language' in Indonesien
Heinz Frick arch. SIA

nr 34
Styles of Architectural Designing: Empirical Research on Working Styles and Personality Dispositions
Anton P.M. van Bakel

nr 35
Conjoint Choice Models for Urban Tourism Planning and Marketing
Benedict Dellaert

nr 36
Stedelijke Planvorming als Co-Produktie
Helga Fassbinder (red.)

nr 37
Design Research in the Netherlands
editors: R.M. Oxman
M.F.Th. Bax
H.H. Achten

nr 38
Communication in the Building Industry
Bauke de Vries

nr 39
Optimaal Dimensioneren van Gelaste Plaatliggers
J.B.W. Stark
F. van Pelt
L.F.M. van Gorp
B.W.E.M. van Hove

nr 40
Huisvesting en Overwinning van Armoede
P.H. Thung
P. Beekman (red.)

nr 41
Urban Habitat: The Environment of Tomorrow
George G. van der Meulen
Peter A. Erkelens

nr 42
A Typology of Joints
John C.M. Olie

nr 43
Modeling Constraints-Based Choices for Leisure Mobility Planning
Marcus P. Stemerding

nr 44
Activity-Based Travel Demand Modeling
Dick Ettema

nr 45
Wind-Induced Pressure Fluctuations on Building Facades
Chris Geurts

nr 46
Generic Representations
Henri Achten

nr 47
Johann Santini Aichel: Architectuur en Ambiguiteit
Dirk De Meyer

nr 48
Concrete Behaviour in Multiaxial Compression
Erik van Geel

nr 49
Modelling Site Selection
Frank Witlox

nr 50
Ecolemma Model
Ferdinand Beetstra

nr 51
Conjoint Approaches to Developing Activity-Based Models
Donggen Wang

nr 52
On the Effectiveness of Ventilation
Ad Roos

nr 53
Conjoint Modeling Approaches for Residential Group preferences
Eric Molin

nr 54
Modelling Architectural Design Information by Features
Jos van Leeuwen

nr 55
A Spatial Decision Support System for the Planning of Retail and Service Facilities
Theo Arentze

nr 56
Integrated Lighting System Assistant
Ellie de Groot

nr 57
Ontwerpend Leren, Leren Ontwerpen
J.T. Boekholt

nr 58
Temporal Aspects of Theme Park Choice Behavior
Astrid Kemperman

nr 59
Ontwerp van een Geïndustrialiseerde Funderingswijze
Faas Moonen

nr 60
Merlin: A Decision Support System for Outdoor Leisure Planning
Manon van Middelkoop

nr 61
The Aura of Modernity
Jos Bosman

nr 62
Urban Form and Activity-Travel Patterns
Daniëlle Snellen

nr 63
Design Research in the Netherlands 2000
Henri Achten

nr 64
Computer Aided Dimensional Control in Building Construction
Rui Wu

nr 65
Beyond Sustainable Building
editors: Peter A. Erkelens
Sander de Jonge
August A.M. van Vliet
co-editor: Ruth J.G. Verhagen

nr 66
Das Globalrecyclingfähige Haus
Hans Löfflad

nr 67
Cool Schools for Hot Suburbs
René J. Dierkx

nr 68
A Bamboo Building Design Decision Support Tool
Fitri Mardjono

nr 69
Driving Rain on Building Envelopes
Fabien van Mook

nr 70
Heating Monumental Churches
Henk Schellen

nr 71
Van Woningverhuurder naar Aanbieder van Woongenot
Patrick Dogge

nr 72
Moisture Transfer Properties of Coated Gypsum
Emile Goossens

nr 73
Plybamboo Wall-Panels for Housing
Guillermo E. González-Beltrán

nr 74
The Future Site-Proceedings
Ger Maas
Frans van Gassel

nr 75
Radon transport in Autoclaved Aerated Concrete
Michel van der Pal

nr 76
The Reliability and Validity of Interactive Virtual Reality Computer Experiments
Amy Tan

nr 77
Measuring Housing Preferences Using Virtual Reality and Belief Networks
Maciej A. Orzechowski

nr 78
Computational Representations of Words and Associations in Architectural Design
Nicole Segers

nr 79
Measuring and Predicting Adaptation in Multidimensional Activity-Travel Patterns
Chang-Hyeon Joh

nr 80
Strategic Briefing
Fayez Al Hassan

nr 81
Well Being in Hospitals
Simona Di Cicco

nr 82
Solares Bauen: Implementierungs- und Umsetzungs-Aspekte in der Hochschulausbildung in Österreich
Gerhard Schuster

nr 83
Supporting Strategic Design of Workplace Environments with Case-Based Reasoning
Shauna Mallory-Hill

nr 84
ACCEL: A Tool for Supporting Concept Generation in the Early Design Phase
Maxim Ivashkov

nr 85
Brick-Mortar Interaction in Masonry under Compression
Ad Vermeltfoort

nr 86
Zelfredzaam Wonen
Guus van Vliet

nr 87
Een Ensemble met Grootstedelijke Allure
Jos Bosman
Hans Schippers

nr 88
On the Computation of Well-Structured Graphic Representations in Architectural Design
Henri Achten

nr 89
De Evolutie van een West-Afrikaanse Vernaculaire Architectuur
Wolf Schijns

nr 90
ROMBO Tactiek
Christoph Maria Ravesloot

nr 91
External Coupling between Building Energy Simulation and Computational Fluid Dynamics
Ery Djunaedy

nr 92
Design Research in the Netherlands 2005
editors: Henri Achten
Kees Dorst
Pieter Jan Stappers
Bauke de Vries

nr 93
Ein Modell zur Baulichen Transformation
Jalil H. Saber Zaimian

nr 94
Human Lighting Demands: Healthy Lighting in an Office Environment
Myriam Aries

nr 95
A Spatial Decision Support System for the Provision and Monitoring of Urban Greenspace
Claudia Pelizaro

nr 96
Leren Creëren
Adri Proveniers

nr 97
Simlandscape
Rob de Waard

nr 98
Design Team Communication
Ad den Otter

nr 99
Humaan-Ecologisch Georiënteerde Woningbouw
Juri Czabanowski

nr 100
Hambase
Martin de Wit

nr 101
Sound Transmission through Pipe Systems and into Building Structures
Susanne Bron-van der Jagt

nr 102
Het Bouwkundig Contrapunt
Jan Francis Boelen

nr 103
A Framework for a Multi-Agent Planning Support System
Dick Saarloos

nr 104
Bracing Steel Frames with Calcium Silicate Element Walls
Bright Mweene Ng'andu

nr 105
Naar een Nieuwe Houtskeletbouw
F.N.G. De Medts

nr 106 and 107
Niet gepubliceerd

nr 108
Geborgenheid
T.E.L. van Pinxteren

nr 109
Modelling Strategic Behaviour in Anticipation of Congestion
Qi Han

nr 110
Reflecties op het Woondomein
Fred Sanders

nr 111
On Assessment of Wind Comfort by Sand Erosion
Gábor Dezsö

nr 112
Bench Heating in Monumental Churches
Dionne Limpens-Neilen

nr 113
RE. Architecture
Ana Pereira Roders

nr 114
Toward Applicable Green Architecture
Usama El Fiky

nr 115
Knowledge Representation under Inherent Uncertainty in a Multi-Agent System for Land Use Planning
Liying Ma

nr 116
Integrated Heat Air and Moisture Modeling and Simulation
Jos van Schijndel

nr 117
Concrete Behaviour in Multiaxial Compression
J.P.W. Bongers

nr 118
The Image of the Urban Landscape
Ana Moya Pellitero

nr 119
The Self-Organizing City in Vietnam
Stephanie Geertman

nr 120
A Multi-Agent Planning Support System for Assessing Externalities of Urban Form Scenarios
Rachel Katoshevski-Cavari

nr 121
Den Schulbau Neu Denken, Fühlen und Wollen
Urs Christian Maurer-Dietrich

nr 122
Peter Eisenman Theories and Practices
Bernhard Kormoss

nr 123
User Simulation of Space Utilisation
Vincent Tabak

nr 125
In Search of a Complex System Model
Oswald Devisch

nr 126
Lighting at Work: Environmental Study of Direct Effects of Lighting Level and Spectrum on Psycho-Physiological Variables
Grazyna Górnicka

nr 127
Flanking Sound Transmission through Lightweight Framed Double Leaf Walls
Stefan Schoenwald

nr 128
Bounded Rationality and Spatio-Temporal Pedestrian Shopping Behavior
Wei Zhu

nr 129
Travel Information: Impact on Activity Travel Pattern
Zhongwei Sun

nr 130
Co-Simulation for Performance Prediction of Innovative Integrated Mechanical Energy Systems in Buildings
Marija Trčka

nr 131
Niet gepubliceerd

nr 132
Architectural Cue Model in Evacuation Simulation for Underground Space Design
Chengyu Sun

nr 133
Uncertainty and Sensitivity Analysis in Building Performance Simulation for Decision Support and Design Optimization
Christina Hopfe

nr 134
Facilitating Distributed Collaboration in the AEC/FM Sector Using Semantic Web Technologies
Jacob Beetz

nr 135
Circumferentially Adhesive Bonded Glass Panes for Bracing Steel Frame in Façades
Edwin Huveners

nr 136
Influence of Temperature on Concrete Beams Strengthened in Flexure with CFRP
Ernst-Lucas Klamer

nr 137
Sturen op Klantwaarde
Jos Smeets

nr 139
Lateral Behavior of Steel Frames with Discretely Connected Precast Concrete Infill Panels
Paul Teewen

nr 140
Integral Design Method in the Context of Sustainable Building Design
Perica Savanović

nr 141
Household Activity-Travel Behavior: Implementation of Within-Household Interactions
Renni Anggraini

nr 142
Design Research in the Netherlands 2010
Henri Achten

nr 143
Modelling Life Trajectories and Transport Mode Choice Using Bayesian Belief Networks
Marloes Verhoeven

nr 144
Assessing Construction Project Performance in Ghana
William Gyadu-Asiedu

nr 145
Empowering Seniors through Domotic Homes
Masi Mohammadi

nr 146
An Integral Design Concept for Ecological Self-Compacting Concrete
Martin Hunger

nr 147
Governing Multi-Actor Decision Processes in Dutch Industrial Area Redevelopment
Erik Blokhuis

nr 148
A Multifunctional Design Approach for Sustainable Concrete
Götz Hüsken

nr 149
Quality Monitoring in Infrastructural Design-Build Projects
Ruben Favié

nr 150
Assessment Matrix for Conservation of Valuable Timber Structures
Michael Abels

nr 151
Co-simulation of Building Energy Simulation and Computational Fluid Dynamics for Whole-Building Heat, Air and Moisture Engineering
Mohammad Mirsadeghi

nr 152
External Coupling of Building Energy Simulation and Building Element Heat, Air and Moisture Simulation
Daniel Cóstola

nr 153
Adaptive Decision Making In Multi-Stakeholder Retail Planning
Ingrid Janssen

nr 154
Landscape Generator
Kymo Slager

nr 155
Constraint Specification in Architecture
Remco Niemeijer

nr 156
A Need-Based Approach to Dynamic Activity Generation
Linda Nijland

nr 157
Modeling Office Firm Dynamics in an Agent-Based Micro Simulation Framework
Gustavo Garcia Manzato

nr 158
Lightweight Floor System for Vibration Comfort
Sander Zegers

nr 159
Aanpasbaarheid van de Draagstructuur
Roel Gijsbers

nr 160
'Village in the City' in Guangzhou, China
Yanliu Lin

nr 161
Climate Risk Assessment in Museums
Marco Martens

nr 162
Social Activity-Travel Patterns
Pauline van den Berg

nr 163
Sound Concentration Caused by Curved Surfaces
Martijn Vercammen

nr 164
Design of Environmentally Friendly Calcium Sulfate-Based Building Materials: Towards an Improved Indoor Air Quality
Qingliang Yu

nr 165
Beyond Uniform Thermal Comfort on the Effects of Non-Uniformity and Individual Physiology
Lisje Schellen

nr 166
Sustainable Residential Districts
Gaby Abdalla

nr 167
Towards a Performance Assessment Methodology using Computational Simulation for Air Distribution System Designs in Operating Rooms
Mônica do Amaral Melhado

nr 168
Strategic Decision Modeling in Brownfield Redevelopment
Brano Glumac

nr 169
Pamela: A Parking Analysis Model for Predicting Effects in Local Areas
Peter van der Waerden

nr 170
A Vision Driven Wayfinding Simulation-System Based on the Architectural Features Perceived in the Office Environment
Qunli Chen

nr 171
Measuring Mental Representations Underlying Activity-Travel Choices
Oliver Horeni

nr 172
Modelling the Effects of Social Networks on Activity and Travel Behaviour
Nicole Ronald

nr 173
Uncertainty Propagation and Sensitivity Analysis Techniques in Building Performance Simulation to Support Conceptual Building and System Design
Christian Struck

nr 174
Numerical Modeling of Micro-Scale Wind-Induced Pollutant Dispersion in the Built Environment
Pierre Gousseau

nr 175
Modeling Recreation Choices over the Family Lifecycle
Anna Beatriz Grigolon

nr 176
Experimental and Numerical Analysis of Mixing Ventilation at Laminar, Transitional and Turbulent Slot Reynolds Numbers
Twan van Hooff

nr 177
Collaborative Design Support: Workshops to Stimulate Interaction and Knowledge Exchange Between Practitioners
Emile M.C.J. Quanjel

nr 178
Future-Proof Platforms for Aging-in-Place
Michiel Brink

nr 179
Motivate: A Context-Aware Mobile Application for Physical Activity Promotion
Yuzhong Lin

nr 180
Experience the City: Analysis of Space-Time Behaviour and Spatial Learning
Anastasia Moiseeva

nr 181
Unbonded Post-Tensioned Shear Walls of Calcium Silicate Element Masonry
Lex van der Meer

nr 182
Construction and Demolition Waste Recycling into Innovative Building Materials for Sustainable Construction in Tanzania
Mwita M. Sabai

nr 183
Durability of Concrete with Emphasis on Chloride Migration
Przemysław Spiesz

nr 184
Computational Modeling of Urban Wind Flow and Natural Ventilation Potential of Buildings
Rubina Ramponi

nr 185
A Distributed Dynamic Simulation Mechanism for Buildings Automation and Control Systems
Azzedine Yahiaoui

nr 186
Modeling Cognitive Learning of Urban Networks in Daily Activity-Travel Behavior
Şehnaz Cenani Durmazoğlu

nr 187
Functionality and Adaptability of Design Solutions for Public Apartment Buildings in Ghana
Stephen Agyefi-Mensah

nr 188
A Construction Waste Generation Model for Developing Countries
Lilliana Abarca-Guerrero

nr 189
Synchronizing Networks: The Modeling of Supernetworks for Activity-Travel Behavior
Feixiong Liao

nr 190
Time and Money Allocation Decisions in Out-of-Home Leisure Activity Choices
Gamze Zeynep Dane

nr 191
How to Measure Added Value of CRE and Building Design
Rianne Appel-Meulenbroek

nr 192
Secondary Materials in Cement-Based Products: Treatment, Modeling and Environmental Interaction
Miruna Florea

nr 193
Concepts for the Robustness Improvement of Self-Compacting Concrete: Effects of Admixtures and Mixture Components on the Rheology and Early Hydration at Varying Temperatures
Wolfram Schmidt

nr 194
Modelling and Simulation of Virtual Natural Lighting Solutions in Buildings
Rizki A. Mangkuto

nr 195
Nano-Silica Production at Low Temperatures from the Dissolution of Olivine - Synthesis, Tailoring and Modelling
Alberto Lazaro Garcia

nr 196
Building Energy Simulation Based Assessment of Industrial Halls for Design Support
Bruno Lee

nr 197
Computational Performance Prediction of the Potential of Hybrid Adaptable Thermal Storage Concepts for Lightweight Low-Energy Houses
Pieter-Jan Hoes

nr 198
Application of Nano-Silica in Concrete
George Quercia Bianchi

nr 199
Dynamics of Social Networks and Activity Travel Behaviour
Fariya Sharmeen

nr 200
Building Structural Design Generation and Optimisation including Spatial Modification
Juan Manuel Davila Delgado

nr 201
Hydration and Thermal Decomposition of Cement/Calcium-Sulphate Based Materials
Ariën de Korte

nr 202
Republiek van Beelden:
De Politieke Werkingen van het Ontwerp in Regionale Planvorming
Bart de Zwart

nr 203
Effects of Energy Price Increases on Individual Activity-Travel Repertoires and Energy Consumption
Dujuan Yang

nr 204
Geometry and Ventilation:
Evaluation of the Leeward Sawtooth Roof Potential in the Natural Ventilation of Buildings
Jorge Isaac Perén Montero

nr 205
Computational Modelling of Evaporative Cooling as a Climate Change Adaptation Measure at the Spatial Scale of Buildings and Streets
Hamid Montazeri

nr 206
Local Buckling of Aluminium Beams in Fire Conditions
Ronald van der Meulen

nr 207
Historic Urban Landscapes:
Framing the Integration of Urban and Heritage Planning in Multilevel Governance
Loes Veldpaus

nr 208
Sustainable Transformation of the Cities:
Urban Design Pragmatics to Achieve a Sustainable City
Ernesto Antonio Zumelzu Scheel

nr 209
Development of Sustainable Protective Ultra-High Performance Fibre Reinforced Concrete (UHPFRC):
Design, Assessment and Modeling
Rui Yu

nr 210
Uncertainty in Modeling Activity-Travel Demand in Complex Uban Systems
Soora Rasouli

nr 211
Simulation-based Performance Assessment of Climate Adaptive Greenhouse Shells
Chul-sung Lee

nr 212
Green Cities:
Modelling the Spatial Transformation of the Urban Environment using Renewable Energy Technologies
Saleh Mohammadi

nr 213
A Bounded Rationality Model of Short and Long-Term Dynamics of Activity-Travel Behavior
Ifigeneia Psarra

nr 214
Effects of Pricing Strategies on Dynamic Repertoires of Activity-Travel Behaviour
Elaheh Khademi

nr 215
Handstorm Principles for Creative and Collaborative Working
Frans van Gassel

nr 216
Light Conditions in Nursing Homes: Visual Comfort and Visual Functioning of Residents
Marianne M. Sinoo

nr 217
Woonsporen: De Sociale en Ruimtelijke Biografie van een Stedelijk Bouwblok in de Amsterdamse Transvaalbuurt
Hüseyin Hüsnü Yegenoglu

nr 218
Studies on User Control in Ambient Intelligent Systems
Berent Willem Meerbeek

nr 219
Daily Livings in a Smart Home: Users' Living Preference Modeling of Smart Homes
Erfaneh Allameh

nr 220
Smart Home Design: Spatial Preference Modeling of Smart Homes
Mohammadali Heidari Jozam

nr 221
Wonen: Discoursen, Praktijken, Perspectieven
Jos Smeets

nr 222
Personal Control over Indoor Climate in Offices: Impact on Comfort, Health and Productivity
Atze Christiaan Boerstra

nr 223
Personalized Route Finding in Multimodal Transportation Networks
Jianwe Zhang

nr 224
The Design of an Adaptive Healing Room for Stroke Patients
Elke Daemen

nr 225
Experimental and Numerical Analysis of Climate Change Induced Risks to Historic Buildings and Collections
Zara Huijbregts

nr 226
Wind Flow Modeling in Urban Areas Through Experimental and Numerical Techniques
Alessio Ricci

nr 227
Clever Climate Control for Culture: Energy Efficient Indoor Climate Control Strategies for Museums Respecting Collection Preservation and Thermal Comfort of Visitors
Rick Kramer

nr 228
nog niet bekend / gepubliceerd

nr 229
nog niet bekend / gepubliceerd

nr 230
Environmental assessment of Building Integrated Photovoltaics: Numerical and Experimental Carrying Capacity Based Approach
Michiel Ritzen

nr 231
Design and Performance of Plasticizing Admixture and Secondary Minerals in Alkali Activated Concrete: Sustaining a Concrete Future
Arno Keulen

nr 232
nog niet bekend / gepubliceerd

nr 233
Stage Acoustics and Sound Exposure in Performance and Rehearsal Spaces for Orchestras:
Methods for Physical Measurements
Remy Wenmaekers

Pitem et fugia doluptam, si doluptatis accus.
Epresciatur, volorep udandebisque evernam aut optate etur magnime ndisime debitibus comnis debit harchic tem asimus alicab inciis doluptur am accaborepe occus velitium ut quiducim inullantium culluptaquae digentiae. Erchiti quassim illabo. Rovid moluptatur? Qui sequis ant et, vellatum quunt ipsam qui iunt, id qui iustia imod ut verferatem aditibus doluptatecces eos autemporibus re laboritia voluptae di conectint, nosam eum explita alibusdae voluptas magnate volupta dus utem laboreptate libus dolorerisque as rerae sitatur, occae voluptae aliquam, ipit doles miliquam que qui qui coreict otatur sunt eumquatat as et pa non repe nullupt atibusciasit rerio blantemquod ut accus si vendam quisqui to blaceaquia conseditint quam, suntore perspis ut quam labor saperum quaspe sitaepra sit as ma duciund elenimo luptatis soluptatemo blaudig nataque es es es sam ratus nonsentore eum qui ipsant volorepudi corumque endem fugita dusam estibusam non eum ilitius et alita corat.
Dolorat enimolo reptatempori ilicips anihicae porem aut es mi, quid quiatium hil iumetur aditatquis estrum sitist ea aut lant.
Ehendit laborem porepe inimoluptam soluptassin peres cus doloratur re simi, quatem que et que doluptur, aboriti aspedip iditece sectur? Quis excesti andundistia is postia et doluptiuntis etusam ditiae volut quae sim si nos doluptum vollabo. Officia tatium adipsum quunda si nit doluptus doloribusdae et lam, santem lam quosam faceris auda quo volutectis dolorumque prae nimet eturecto volum ex es de ipsam harum re veliquo comnia consequi corest, volorrum fuga. Onsed quunti dolesse quatur as eosam

F A C

B W H

E H I

/ Department of the Built Environment

TU/e Technische Universiteit **Eindhoven** University of Technology